

Integrated Analytical Systems
Series Editor: Radislav A. Potyrailo

Jin-Ming Lin *Editor*

Microfluidics for Single-Cell Analysis

 Springer

Integrated Analytical Systems

Series Editor

Radislav A. Potyrailo, Niskayuna, NY, USA

This comprehensive and interdisciplinary series offers the most recent advances in all key aspects of development and applications of modern instrumentation for chemical and biological analysis on the microscale.

These key aspects will include (1) innovations in sample introduction through micro- and nano-fluidic designs, (2) new types and methods of fabrication of physical transducers and ion detectors, (3) materials for sensors that became available due to the breakthroughs in combinatorial materials science and nanotechnology, and (4) innovative data processing and mining methodologies that provide dramatically reduced rates of false alarms.

Clearly, a true multidisciplinary effort is required to meet objectives for a system with previously unavailable capabilities. This cross-discipline fertilization is driven by the expanding need for chemical and biological detection and monitoring and leads to the creation of instruments with new capabilities for new demanding applications. Indeed, instruments with more sensitivity are required today to analyze ultra-trace levels of environmental pollutants, pathogens in water, and low vapor pressure energetic materials in air. Sensor devices with faster response times are desired to monitor transient in-vivo events and bedside patients. More selective instruments are wanted to analyze specific proteins in vitro and analyze ambient urban or battlefield air. For these and many other applications, new features of modern microanalytical instrumentation are urgently needed. This book series is a primary source of both fundamental and practical information on both the current state of the art and future directions for microanalytical instrumentation technologies. This book series is addressed to the rapidly growing number of active practitioners and developers and those who are interested in starting research in this direction, directors of industrial and government research centers, laboratory supervisors and managers, students and lecturers.

More information about this series at <http://www.springer.com/series/7427>

Jin-Ming Lin
Editor

Microfluidics for Single-Cell Analysis

 Springer

Editor
Jin-Ming Lin
Department of Chemistry
Tsinghua University
Beijing, China

ISSN 2196-4475

ISSN 2196-4483 (electronic)

Integrated Analytical Systems

ISBN 978-981-32-9728-9

ISBN 978-981-32-9729-6 (eBook)

<https://doi.org/10.1007/978-981-32-9729-6>

© Springer Nature Singapore Pte Ltd. 2019

This work is subject to copyright. All rights are reserved by the Publisher, whether the whole or part of the material is concerned, specifically the rights of translation, reprinting, reuse of illustrations, recitation, broadcasting, reproduction on microfilms or in any other physical way, and transmission or information storage and retrieval, electronic adaptation, computer software, or by similar or dissimilar methodology now known or hereafter developed.

The use of general descriptive names, registered names, trademarks, service marks, etc. in this publication does not imply, even in the absence of a specific statement, that such names are exempt from the relevant protective laws and regulations and therefore free for general use.

The publisher, the authors and the editors are safe to assume that the advice and information in this book are believed to be true and accurate at the date of publication. Neither the publisher nor the authors or the editors give a warranty, expressed or implied, with respect to the material contained herein or for any errors or omissions that may have been made. The publisher remains neutral with regard to jurisdictional claims in published maps and institutional affiliations.

This Springer imprint is published by the registered company Springer Nature Singapore Pte Ltd. The registered company address is: 152 Beach Road, #21-01/04 Gateway East, Singapore 189721, Singapore

Preface

Since the first observation of the structure of plant cells at the thin sheets of cork by Robert Hooke, a British scientist in 1665, the methods for the study of cellular biology are mainly from the employment of petri dishes as cell culture container even though there are million people using different types of dishes in all over the world. As we have described in our last book “Cell Analysis on Microfluidics” (Springer 2018), until now, after repeated optimization and modification, dishes are still utilized in every biochemical laboratory. The observation of cells culture in the dishes is also a challenge due to too big diameter of dish to be monitored by microscopy at all space. To develop a more advanced method for cell culture, observation, and metabolite analysis, with the grant supported by National Natural Science Foundation of China (Nos. 21435002 and 21727814), we innovated a new instrumentation of microchip combined with mass spectrometer and microscopy. This technique is commercialized by Shimadzu China in 2018 and started to be applied in the study of drug screening, environmental toxicology, basic medicine, and cell biology. However, during the cell culture study, we found that the same types of single cells often have the heterogeneities in morphology, functions, composition, and genetic performance of the seemingly identical cells. For understanding the heterogeneities of single cells, we tried to use the principles of surface tension, micro-flow force, and laminar for developing a new technique of single-cell analysis. We are lucky and successfully fabricated a microfluidic with two flow lines of “flow in” and “flow out” which can be used as live single-cell extractor. A number of research results concerning with microfluidics for single-cell analysis have been published in the recent years. In this book, we summarized in nine chapters of advances of single-cell analysis on microfluidics, microfluidic technology for single-cell capture and isolation, single-cell culture and analysis on microfluidics, microfluidic technology for single-cell manipulation, droplet-based microfluidics for single-cell encapsulation and analysis, microfluidics for single-cell genomics, microfluidics-mass spectrometry combination systems for single-cell analysis, micro/nano-fluidics-enabled single-cell biochemical analysis, and micro-fluidic chip-based live single-cell probes.

Although chapters in this book only provide a brief review of microfluidics for single-cell analysis and limited collection of its applications on cell biology, plenty of knowledge is included about almost every element to establish a microfluidic platform for single-cell analysis. And we hope this book can be helpful to those ardent researchers and students who wish to know more, explore more, and achieve more in the fields of microfluidics and cellular biology.

We would like to thank all the authors contributing to this book for their effort in helping us to put together this work. We also would like to thank Springer for inviting us to publish this book and all the support during its preparation. We are grateful to financial support to our research topics of cell analysis on microfluidics from National Key R&D Program of China (No. 2017YFC0906800) and National Natural Science Foundation of China (Nos. 21435002, 21727814, and 21621003).

Beijing, China

Jin-Ming Lin

Contents

1 Advances of Single-Cell Analysis on Microfluidics	1
Qiushi Huang and Jin-Ming Lin	
2 Microfluidic Technology for Single-Cell Capture and Isolation	27
Jing Wu and Jin-Ming Lin	
3 Single-Cell Culture and Analysis on Microfluidics	53
Weiwei Li and Jin-Ming Lin	
4 Microfluidic Technology for Single-Cell Manipulation	85
Weifei Zhang, Nan Li and Jin-Ming Lin	
5 Droplet-Based Microfluidics for Single-Cell Encapsulation and Analysis	119
Qiushui Chen and Jin-Ming Lin	
6 Microfluidics for Single-Cell Genomics	143
Mashooq Khan and Jin-Ming Lin	
7 Microfluidics-Mass Spectrometry Combination Systems for Single-Cell Analysis	163
Dan Gao, Chao Song and Jin-Ming Lin	
8 Micro/Nano fluidics Enabled Single-Cell Biochemical Analysis	197
Ling Lin	
9 Microfluidic Chip-Based Live Single-Cell Probes	217
Sifeng Mao and Jin-Ming Lin	
Index	257

Chapter 1

Advances of Single-Cell Analysis on Microfluidics



Qiushi Huang and Jin-Ming Lin

Abstract The advances of microfluidic technologies have promoted researchers to study the inherent heterogeneity of single cells in cell populations. This will be helpful in the acknowledgment of major disease and invention of personalized medicine. Different microfluidic approaches provide varieties of functions in the process of single-cell analysis. In this chapter, we introduce decades of the history in single-cell analysis and give an outline of the mechanisms of various microfluidic-based approaches for cell sorting, single-cell isolation, and single-cell lysis.

Keywords Microfluidics development · Single-cell analysis · Mechanisms

1.1 Introduction

Cells, as the basic unit of life, are the cornerstone of biology. Analysis of life's most basic units is able to provide insides into some of the most fundamental processes in life sciences. This is so-called single-cell analysis which cross-links analytical chemistry, classical cell biology, genomics, and proteomics. More and more scientists have focused on the single-cell analysis. As the demand for studying single cells expands, they will require delicate analytical tools to obtain and account for the results. Just as the development of cell theory powered advances in biology, it is clear that single-cell analysis will open new prospects for scientists to explore.

Q. Huang · J.-M. Lin (✉)
Department of Chemistry, Tsinghua University, Beijing 100084,
People's Republic of China
e-mail: jmlin@mail.tsinghua.edu.cn

© Springer Nature Singapore Pte Ltd. 2019
J.-M. Lin (ed.), *Microfluidics for Single-Cell Analysis*,
Integrated Analytical Systems, https://doi.org/10.1007/978-981-32-9729-6_1

1.1.1 The Origin of Single-Cell Analysis

The advance of new technologies promotes discovery of new biological knowledge. Till now, the advanced tools help to acquire increasingly refined information of abundant biomolecules within cells which lead to rapid growth of molecular and cellular assays. However, the assay results of average signals from many cells are difficult to explain in many fields such as hematology, stem cell biology, tissue engineering, and cancer biology. This can be attributed to different time dynamics of a sample and population heterogeneity within cells. Thus, measures of the cell population shall be misleading which necessitates single-cell methods in molecular biology.

Single-cell heterogeneity in a population is a common focus in single-cell analysis and differs from the traditional assays of average levels of molecules within the population. Commonly, technologies for molecular-level information from a cell population are not suitable for complex and heterogeneous cell samples. Therefore, it is important to apply the right tool for better data collection. In a standard molecular assay, all cells are disposed under the same condition and then analyzed with a substantive test. The steps can be accessible but may mistakenly result in the average distribution of behavior among all the cells in the sample. For instance, time-response signals of a single cell shall be covered up under cell populations due to the different time period of each cell (Fig. 1.1a). These signals are important because cells even with identical genes respond dynamical differently to stimuli due to epigenetic differences and randomness of intracellular signaling [1]. Besides, informational cells in complex samples are often among cell populations. In this case, informational cells' response to stimuli will be mixed with other cells' response which is weak and scarce. Such a measuring result cannot represent informational cells at single-cell resolution (Fig. 1.1b). Considering bimodal expression levels when cells respond dynamically to extracellular conditions [2], a bulk measurement of this population will output an average value that is not representative of either subpopulation (Fig. 1.1c). Another case is those cells of interest are a small percentage of the population; a bulk measurement of this population will lose the key information from cells of interest (Fig. 1.1d). As a result, only by measuring the character of single cells will the real heterogeneity and behavior of the population be analyzed.

Cell heterogeneity in population has promoted understanding in the fields of systems biology, stem cell biology, and cancer biology. Since the development of single-cell analysis techniques, these fields above have been benefited at the same time [3]. The heterogeneity of tumors has already been known in cancer biology [4]. And it is possible to infer tumor progression from genomic heterogeneity [5]. This condition has gained immense interest and insights. Using single-cell techniques, dynamic proteomics has been applied to measure the single-cell response to drug stimuli [6]. Besides, single-cell gene expression techniques have been developed for the studies of stem cells [7]. Using single-cell transcriptome analysis,

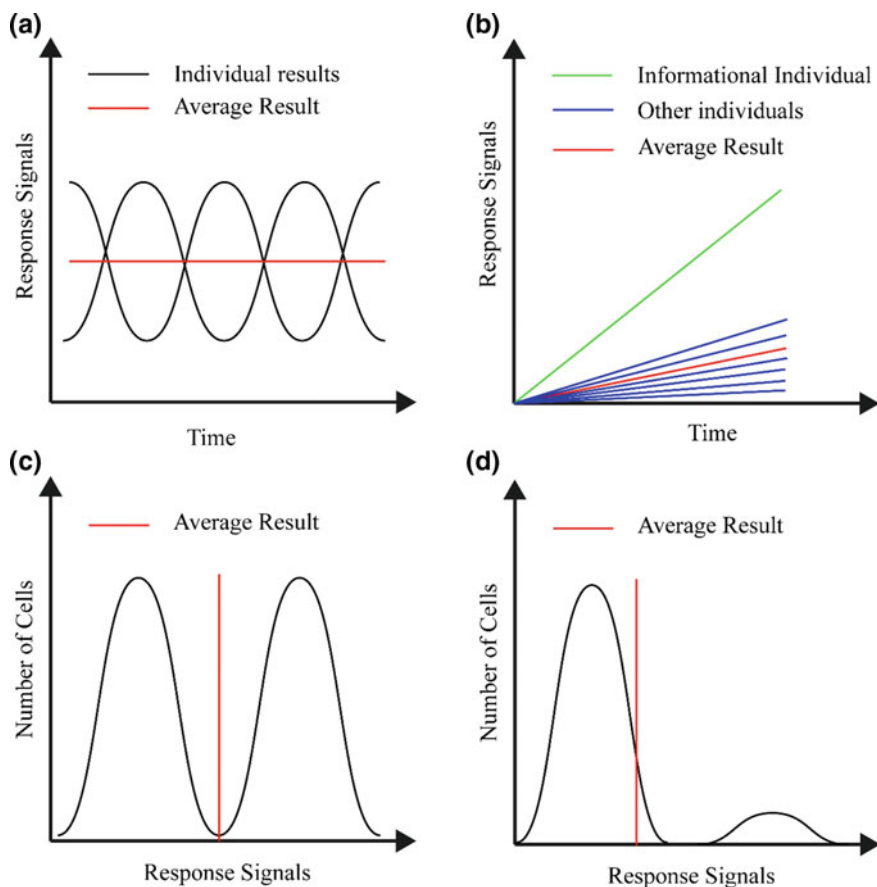


Fig. 1.1 Cell heterogeneity in population. **a** Time-response signals of single cells. **b** Informational cells' respond to stimuli mix with other cells' respond which is weak and scarce. **c** Subpopulations in bimodal expressions. **d** Rare cell populations are not accurately expressed by average assays

highly heterogeneous genetic expression profiles can be observed which is hardly to achieve by normal approaches.

Invention of the microfluidic technique has greatly promoted single-cell analysis. Traditional detection systems on multi-cells can be applied at single-cell resolution through this technique as well as isolating single populations from complex samples. Due to the development of microfabrication techniques, traditional analysis platforms have been miniaturized into micrometer scale which is so-called microfluidic lab-on-a-chip platforms. These tools support precise control of mechanical and chemical access [8] and are able to collect highly quantifiable single-cell data from high-throughput assays [9]. These miniaturized systems focus on evaluating of cell-cell interactions [10] and cell-substrates interactions [11]. Conventional macroscale platforms cannot achieve simulation in vivo microscale environments,

which microfluidic techniques can easily realize [12]. To analyze practical samples with complex components such as blood and cancer tissue, the high-throughput method is needed. Microfluidic meets the requirement of assigning precise positions in arrays or positioning in flow. Single-cell manipulation such as mechanical trapping [13], inertial isolation [14], dielectric isolation [15], and acoustic isolation [16] has been developed well suited for the single-cell analysis.

1.1.2 Development of Single-Cell Approaches

Single-cell analysis can be traced back to the year 1965, (Table 1.1) when Matioli et al. [17] firstly reported the isolation and direct observation of hemoglobin in single erythrocytes. Then, quantities of conventional techniques have been developed such as microthin layer chromatography (mTLC), gas chromatography–mass spectrometry (GC-MS), high-performance liquid chromatography–electrochemical (HPLC-EC) detection, and radioactive labeling [18–21]. However, these techniques are commonly not sensitive enough or limited in multiple components test thus have not been widely developed. mTLC requires several cells for sufficient result which is not strictly single-cell resolution. GC-MS is only applied for volatile compounds analysis. While target molecules are nonvolatile, derivatization will be required which limits the application. Results from HPLC-EC are highly related to

Table 1.1 Important works in the development of single-cell analysis

Year	Research	Reference
1965	Isolation and direct observation of haemoglobin in single erythrocytes	Matioli GT et al. Science 150(3705):1824–1826
1976	Patch clamping	Neher E et al. Nature 260(5554):799–802
1987	Open tubular liquid chromatography for the electrochemical analysis of single neurons	Kennedy RT et al. Mikrochimica Acta 2(1–3):37–4
1988	Single-cell capillary zone electrophoresis	Wallingford RA et al. Analytical Chemistry 60(18):1972–1975
2000	Single-cell proteomics	Zhang Z et al. Analytical Chemistry 72(2):318–322
	Valves	Unger MA et al. Science 288(5463):113–116
2005	Droplets	Utada AS et al. Science 308(5721):537–541
2009	Live single-cell MS	Masujima T. Analytical Sciences the International Journal of the Japan Society for Analytical Chemistry, 2009, 25(8):953
2015	Single-cell MALDI-MS	Ong TH et al. Analytical Chemistry 87(14):7036–7042
2018	Live single-cell extractor	Mao S et al. Angewandte Chemie International Edition 57(1):236–240

the cell size and concentration of the determinant which is hardly to control. Radioactive labeling is limited for one kind of compound detection at one time, and the unknown compound is not suitable. The development of flow cytometry has been widely applied in cytobiology [22]. When the sample is complex that contains multiple populations of cells, flow cytometry is able to detect the physical and chemical parameters of single cells. Parameters such as size, volume, quantity, and even the content of proteins and nucleic acids can be collected at high throughput. However, the flow cytometry also has limitations in the single-cell analysis that limits the universality, such as expensive instrument costs, complex cell surface markers, increased sample pre-treatment time and reduced cell viability, as well as sample contamination risk. Patch clamping was developed by Neher and Sakmann in 1976 [23]. This technique was applied for the discovering of the function of single ion channels in cells which has won the Nobel Prize in Physiology or Medicine in 1991. The high sensitivity and high spatial resolution of the patch clamping have great potential for the study of the rapid reaction kinetics in the ultra-microenvironment of single-cell organisms.

Single-cell analysis meets the formidable challenge that requires methods that are more sensitive, more selective, more quantitative, more informative, and can detect more analytes at the same time.

In 1987, Kennedy et al. [24] firstly developed open-tubular liquid chromatography for the electrochemical analysis of single neurons. In this approach, individual neurons from the subesophageal ganglia of *Helix aspersa* were analyzed. The putative neurotransmitters, dopamine and serotonin, and their precursor amino acids, tyrosine and tryptophan, were identified and quantified. However, the device and micro-operation techniques in this method are complex, and it is difficult to analyze small single cells. Subsequent development of this technique has been restricted.

Capillary electrophoresis (CE) can meet the requirements of single-cell analysis on small volume sampling, high sensitivity, good selectivity, multi-component analysis, and fast response. Ewing's group [25] has developed single-cell capillary zone electrophoresis (CZE) by *in vivo* analysis dopamine from a single nerve cell. Miniaturization works of the device were still demanded for the feasibility of mammalian cells which are much smaller than neurons.

Sweedler's group [26–29] has conducted research in single-cell analysis and focus on the development of analytical methods for assaying complex microenvironments, including CE, laser-based detectors, and MALDI sampling techniques. Their utilizing of MALDI-MS has achieved the detection of the spatial distribution of neuropeptide in different parts of nerve cells. Other studies include the metabolism, dynamic release of neuropeptides and classical transmitters in a cell-specific manner.

Dovich's group has proposed single-cell proteomics in 2000 [30]. They are trying to develop the tools for studying the proteome with two-dimensional CE, coupled with either laser-induced fluorescence (LIF), or MS for detection. It seems the group's long-term goal is to study protein expression in single cells and to determine how protein expression changes across a cellular population during cancer progression and during the development of an embryo. Till now, they have

acquired important achievements [31–33]. However, for the project of single-cell proteomics, it is still the beginning.

Microfluidic technologies in the single-cell analysis have been widely developed since the twenty-first century [34–36]. The microstructure of the microfluidic chip can be matched well with the single-cell volume, which is a promising single-cell analysis technology. The advantages of microfluidic techniques are listed as below:

- (1) The manipulation, transmission, sampling, positioning, dissolution, reaction, separation, and detection of cells can be integrated in one microfluidic chip. The control system of micropump and microvalve can be adopted to realize the integration and automation.
- (2) Microfluidic techniques supply high-throughput analysis of single cells which achieve high-speed studies of cell metabolism, gene expression, and drug screening.
- (3) The reagent consumption is significantly reduced. The sample required of the microfluidic chip is measured by nL– μ L, which greatly reduces the cost of experiments.
- (4) High temporal resolution of microfluidic devices can be used for continuous monitoring of stimulated release of living cells and cellular molecular response processes.
- (5) Closed operation environment helps to reduce the risk of sample contamination and improves cells' viability.

Zare's group has done excellent work in single-cell analysis on microfluidic [37–39]. In their previous work [40], they have developed multilayer microfluidic chips for the analysis of single cells. The microfluidic channels enabled the passive and gentle isolation of a single cell from the complex cell suspension, and integrated valves and pumps enabled the precise delivery of nanoliter volumes of reagents to the cell. Various applications were demonstrated such as cell viability analysis, ionophore-mediated intracellular Ca^{2+} flux measurements, and multistep receptor-mediated Ca^{2+} measurements. The experiments had significant improvements in reagent consumption, analysis time, and temporal resolution compared with macroscale assays.

Ramsey's group [41–43] has been devoted to the development of microfluidic technology. They are known for their pioneering efforts in demonstrating micro-fabricated chemical measurement devices. These devices have improved conventional laboratory measurements in microscale experiments of several orders of magnitude. The technology is presently followed by a number of research institutions and corporations around the world and is possible to be a general model for chemical and biochemical experimentation.

Our group has focused on this field as well in recent years. For cell sorting, two-dimensional ordered polystyrene microspheres based microwell arrays [44] has been developed for high-throughput single-cell analysis. In this work, rounded bottom microwell arrays (Fig. 1.2a) in poly(dimethylsiloxane) were fabricated by molding a monolayer of ordered polystyrene microspheres. Sizes of microwell were tunable in the 10–20 μm ranges which were able to capture adherent or

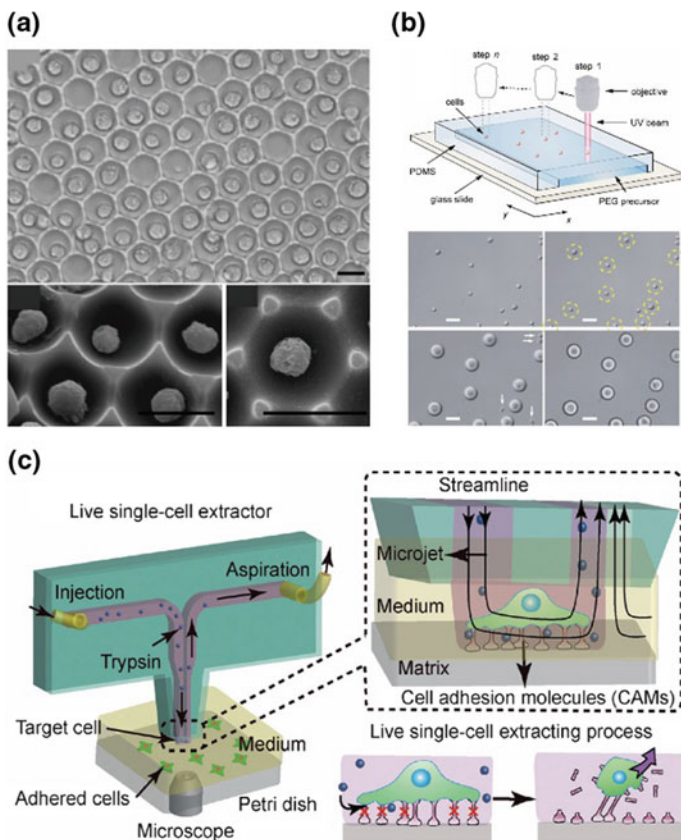


Fig. 1.2 Microfluidic enabled single-cell analysis. **a** Cell arrays on the microwells. Reprinted with permission from Ref. [44]. **b** Controlled encapsulation of single cells inside hydrogel microstructures. Reprinted with permission from Ref. [46]. **c** Microfluidic chip-based live single-cell extractor. Reprinted with permission from Ref. [11]

non-adherent cells with high efficiency. Further, designed microwell structures enable us to launch strong interactions of the target cell surface with biomolecules [45]. By coating DNA aptamer on the 3D-structured microwell, a satisfactory single-cell occupancy could be obtained.

For single-cell encapsulation, a microfluidic approach to generate hydrogel microstructures inside microchannels for controlled encapsulation of single cells was developed [46]. This approach has the capability to immobilize different phenotypes of cells inside hydrogel microstructures with different morphologies for identification (Fig. 1.2b). Recently, we reported a live single-cell extractor (Fig. 1.2c) to extract a single adhered cell in tissue culture for understanding cell heterogeneity and the connection of various single-cell behaviors [11]. By using this technique, the connection between cell adhesion strength and cell morphologies as well as that between cell adhesion strength and intracellular metabolites was explored.

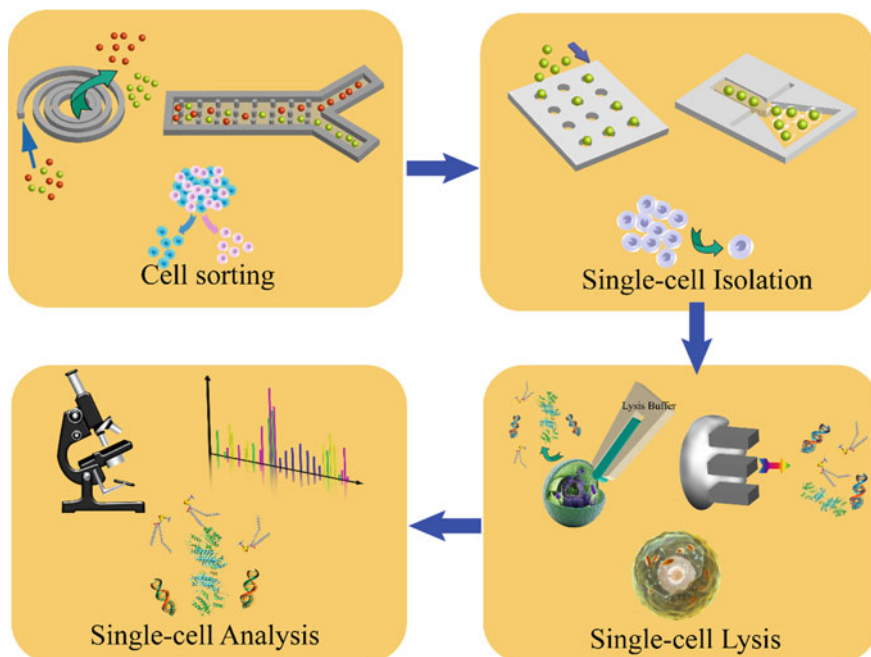


Fig. 1.3 Microfluidic enabled workflow of single-cell analysis

1.2 Mechanisms of Microfluidic Technologies in Single-Cell Analysis

As is discussed above, microfluidic devices have opened new avenues for point-of-care diagnostics due to the characteristic of fitted approximately to the size of an individual thus provided fascinating solutions to many issues in single-cell analysis. Microfluidic platforms have the advantages of portability, parallel processing, automation, and a large surface-to-volume ratio. This enables the integration of multiple liquid operating processes, such as pumping, metering, sampling, dispensing, sequential loading, and washing. These advantages make microfluidic technology more compatible and greatly reduce the labor compared with traditional laboratory technology. This part describes the various microfluidic-based approaches used for single-cell analysis which follows the workflow as shown in Fig. 1.3. Cell sorting, single-cell isolation, and single-cell lysis are involved. Up-to-date mechanisms of techniques and the pros and cons of these methods are discussed in detail. This section will be of great interest for researchers who will work in the same field and an informative tool for researchers from other fields and beginners.

1.2.1 Cell Sorting

Compared with traditional methods, microfluidic devices have inherent advantages in the cell sorting platform. Miniaturized devices reduce reagent consumption to a certain extent and increase portability. The production cost of the devices can be decreased by introducing soft lithography for standard microfabrication. The flowing cells can be controlled spatiotemporally by laminar fluid dynamics, which achieves passive and label-free cell separation. Commonly, cell sorting is achieved continuously in an enclosed microfluidic device, which minimizes the risk of sample contamination. However, several drawbacks exist as the immaturity of this technology. The throughput is a major research focus to improve compared with commercial flow cytometry. Besides, cell adhesion and clogging problems occur frequently which limit the life of the device. Till now, there are several excellent works [47–51] in the field regarding microfluidic enabled cell sorting. Here, we

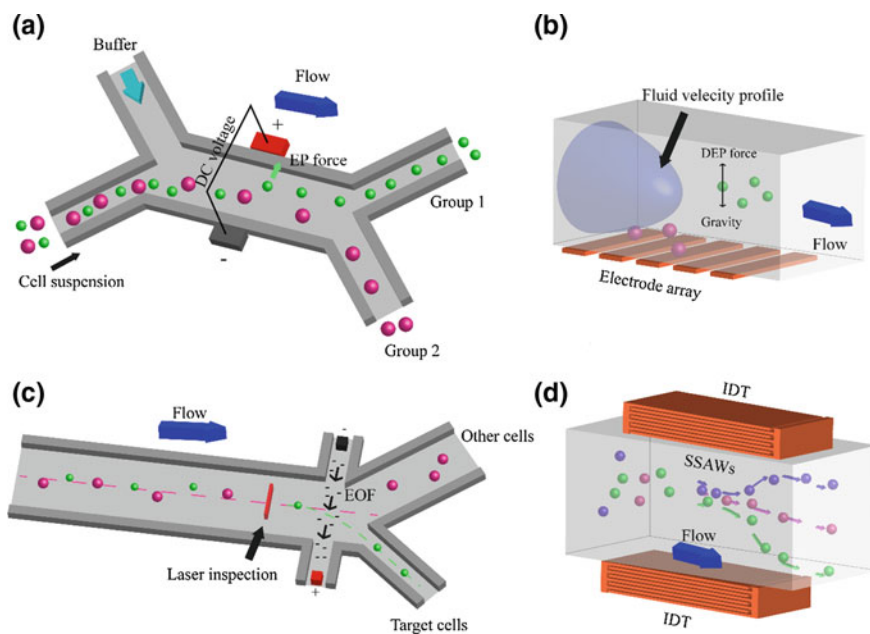


Fig. 1.4 Different microfluidic cell sorting techniques. **a** Mechanism of microfluidic cell sorting integrated with EP. A uniform electric field induces a Coulomb force on negatively charged cells, resulting in a net force toward the positive electrode. The target cells are then separated. **b** Mechanism of microfluidic cell sorting integrated with DEP. DEP force and gravity force together position different cell types at individual regions of different flow velocity, leading to different retention time for each cell type. **c** Mechanism of microfluidic cell sorting integrated with EOF. Solvated negative ions migrate toward the positive electrode, inducing fluid flow and cell separation. The electrode charge is controlled by the signal from laser interrogation. **d** Mechanism of microfluidic cell sorting integrated with SSAWs. The standing surface acoustic waves, generated by interdigital transducers, separate cells at distinct streamlines, and the cells are separated via different outlets

introduce existing cell sorting technologies integrated on microfluidic chips that specific relevance to single-cell analysis. Different sorting mechanisms suit for different cell type's properties.

1.2.1.1 Electrical

Most cells present negative charges on the surface at the condition of neutral pH. Once a constant electric field is added (Fig. 1.4a), cells will move toward the positive electrode [52]. In cell suspension, cells are mainly driven by two forces as the Coulomb and drag forces. Different quantities of force induce different velocity of movement. Therefore, different cell types with different charge or size can be separated under this constant electric field, which is called electrophoresis (EP) sorting [53].

Dielectrophoresis (DEP) approaches [53] are used more frequently for cell sorting due to its higher specificity in dielectric properties among cell types. In DEP [54], a complex mixture of cell suspension flows through a channel while the integrated electrodes at the bottom of channel generate an upward DEP force that balances the gravity force (Fig. 1.4b). Different cell type stabilizes at an individual height in the channel. Due to the parabolic velocity profile, they will have different flow velocity for the separation. Using this technology, an alternating current will polarize the cell instead cells' inherent surface charge. Therefore, cells are not required to present surface charge and move toward or away from the area of highest electric field density. An alternating electric field is required to inflict a force on the polarized cell and the move direction is due to the electrical permeability of the cells. Under the condition that the fluid has higher permeability than cells, negative dielectrophoresis (nDEP) will drive cells moving away from the field maxima and positive dielectrophoresis (pDEP) will drive cells moving toward the field maxima. Compared to EP sorting, DEP approaches have larger cell sorting specificity, and utilizing of alternating current prevents electrochemical reactions at the electrodes and decreases detriment to cell viability.

Similar to the EP and DEP sorting mechanisms, electroosmotic enabled separation also utilizes an electric field. Electroosmotic flow (EOF) is defined as fluid flow by inducing solvated ions movement under an electric field. Then particles in the solution will accompany the fluid flow induced by migrating solvated ions. Using this technique, target cells can be picked up actively from the complex sample (Fig. 1.4c). The advantage of EOF is the accurate control of volume in microfluidics which enables precise control of small volumes of reagents and size-based cell sorting. However, electrophoretic cell movement can influence the accuracy of electroosmotic driven in this approach.

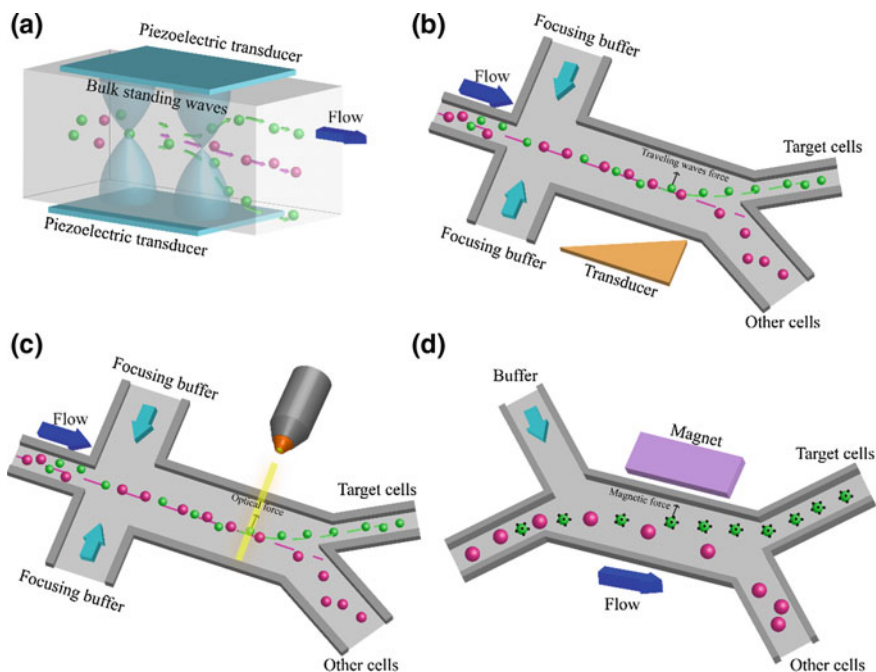


Fig. 1.5 Different microfluidic cell sorting techniques. **a** Mechanism of microfluidic cell sorting integrated with bulk standing waves. Cells separate to the wave node or antinode depending on their acoustic contrast factor. **b** Mechanism of microfluidic cell sorting integrated with traveling acoustic waves. **c** Mechanism of microfluidic cell sorting integrated with optical tweezers. A laser emitter is integrated on the microfluidic chip and the cells are deflected by the laser beam toward different outlet. **d** Mechanism of microfluidic cell sorting integrated with magnet. The device is operated under the magnetic field and the magnetic particle labeled cells are collected from different outlet with normal cells

1.2.1.2 Acoustic

Acoustic enabled cell sorting has no impact on cell viability which appears recently [55]. Acoustic separation works by inducing cell migration response to acoustically generated pressure waves. Currently, three kinds of acoustic cell sorting exist classified on the wave type as: standing surface acoustic waves, bulk standing waves, and traveling waves [47].

Standing surface acoustic waves (SSAW) form along the bottom of microfluidic channels when integrating interdigital transducers (IDTs). The IDTs are patterned on a piezoelectric substrate on the microfluidic chip which produces a longitudinal wave from the substrate and these longitudinal waves create pressure nodes for the particle separation (Fig. 1.4d). SSAWs are able to deflect particles in fluid flow independently which are flexible in separating cell populations [56].

Bulk standing waves are generated by a piezoelectric transducer in microfluidic channels when the acoustic wavelength matches the channel dimension. In this

approach, cells flowing through the channel will respond differently to the standing wave by the acoustic contrast factor, which is dependent on cell density and compressibility (Fig. 1.5a). Cells with a positive acoustic contrast factor will migrate toward the wave node, and cells with negative acoustic contrast factors will migrate toward the wave antinodes. Thus, cell sorting will be achieved by cell separation to different outlets.

Traveling waves can be used for cell sorting as well. Standing waves require wavelengths comparable to microfluidic channel width, and therefore, the sorting rate cannot be increased because the wavelengths are limited. Traveling waves overcome this limitation where acoustic waves are as a drive force similar to the electric sorting (Fig. 1.5b). The acoustic wave is generated by a transducer and the wave travels in the direction perpendicular to the flow direction, thereby deflecting cells from the fluid streamlines into the appropriate outlet channel.

Acoustic enabled cell sorting mitigates cell viability decrease which improves time and cost economy. However, similar to electrically enabled cell sorting, acoustic cell sorting requires integrated transducers. This makes fabrication and operation more complex. Examples of this technique are available from recent reviews [57, 58] for further discussion.

1.2.1.3 Optical

Light-driven particle movements can be found in 1970 when it was discovered that a focused laser could propel microparticles in a liquid [59]. Then, stable particles' trapping via a tightly focused laser was achieved [60] which was the foundation of "optical tweezers." In this technique, the optical forces form from momentum exchange between incident photons and the irradiated object. When the light rays into an object, the light's direction and magnitude will be changed due to the difference of refractive index between object and surrounding. Then, the photons' momentum will be changed associated. The particles' movements depend on their different refractive index. They will move toward the area of highest light intensity when the refractive index is higher than the surrounding fluid. In contrast, while the refractive index is lower, the particles will move to the opposite direction. Here are some reviews [61, 62] for more discussions on the light-induced forces. Optical manipulation has been utilized for cell sorting and manipulation on microfluidic chips (Fig. 1.5c). This approach has the advantage of minimally detrimental to cell viability, compared to sorting methods discussed above.

1.2.1.4 Magnetic

In magnetic enabled cell sorting, magnetic particles can be biologically combined with the target cells via a cell-specific antibody. Therefore, the target cells can be separated from the complex sample by flow through a microfluidic channel possessing a magnetic field (Fig. 1.5d). The advantages of this approach are the

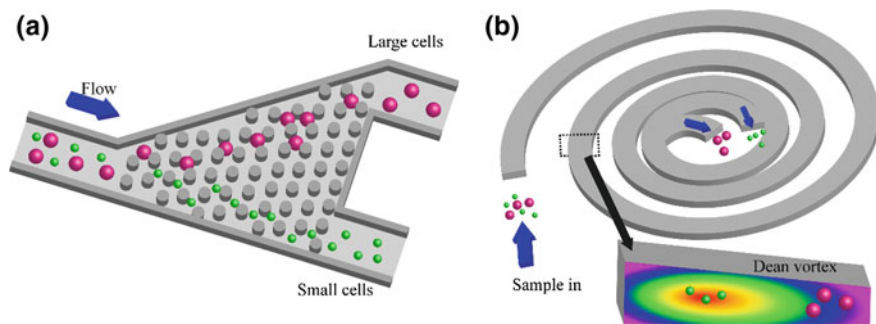


Fig. 1.6 Different microfluidic cell sorting techniques. **a** Mechanism of microfluidic cell sorting integrated with micropillars array. An array of micropillars induces cells with different radius toward different outlet. **b** Mechanism of microfluidic cell sorting based on inertial effect. A spiral channel is designed to form the vortex (Dean flow) perpendicular to the primary flow. Cells with different sizes, densities, or shapes are positioned at the vortex and the cells are separated from different outlets

simplicity and non-touching separation. The magnetic field can be induced via an integrated permanent magnet or an electromagnet for a low cost. However, applying magnetic sorting requires antibody labeling of magnetic particles on cells. This can be a drawback for several reasons. Labeling may negatively impact cells' endogenous genetic expression and is difficult to achieve in specific cells that lack of surface markers. Besides, labeling is not desirable in clinical concerns, and antibodies are quite expensive. Till now, microfluidic magnetic enabled cell sorting has been applied in many fields, and the reader can refer to several reviews [63–65].

1.2.1.5 Array of Micropillars

Here is a passive microfluidic cell sorting that uses a pillar array to induce cells' migration based on cell size. In this method, there is a critical cell size to separate different cells which are depending on the pillar design [66]. Cells with a smaller size than the critical radius flow in the direction of primary fluid. In contrast, cells bigger than the critical radius are deflected for the separation (Fig. 1.6a). This passive cell sorting approach can be advantageous due to the gentle and label-free separation. Besides, the fabrication of the device can be relatively simple. However, the limitation is that the target cells must differ from the others in size or shape, which greatly restricts its application. Readers can refer to a review for more research on this technique [67].

1.2.1.6 Inertial

When the microfluidic channel is at a suitable dimension and flow velocities, inertial effects will show up and can be utilized for cell sorting. In the curve channel, there is a typical inertial effect called Dean flow [68] which can form vortex perpendicular to the primary flow. Cells which have different size, density, or shape will respond differently to the inertial effects and have individual streamlines (Fig. 1.6b). Then, cell sorting is achieved by collecting cells from different outlets. This approach has the advantage of label-free separation and little influence on the cell viability. This can be attractive for the minimized costs, wide applicability, and maintaining most endogenous expression. Besides, this method conducts in continuous flow therefore increase the throughput of cell sorting. However, the disadvantage is obvious that the samples require to be diluted due to the cell interactions influence at high cell concentrations. Here are some reviews [69, 70] that discuss about the physics of inertial microfluidics. Our group has done relative work in this field that utilizes this principle combining with mass spectrometry, which realizes high-throughput single-cell MS analysis [71].

1.2.2 *Single-Cell Isolation*

Microfluidic devices offer many advantages to single-cell isolation [72]. In this technique, single-cell compartments can be miniaturized to reduce lysate dilution which is important for the analysis of low-abundance biomolecules in a single cell. Consumption of reagent volumes is minimized which decreases the costs. Most microfluidic chips are automatic and closed systems, decreasing contamination risk. In this section, a variety of microfluidic enabled single-cell isolation is introduced. The basic mechanisms of the involved methods are as the focus to discuss.

1.2.2.1 Valves

Valves can be utilized to trap objects in the microscopical pipes, which provide an easy conversion into microscale for the single-cell trapping. In microchannels, valves can be utilized to regulate fluid flow and control flow direction. Quake's group [73, 74] have developed valve on microfluidic that is so-called Quake valves, which is commonly used later in other researches. The common examples of Quake valves in microfluidic are two-layer pneumatic valves. The top layer integrated channels for the pneumatic valves. When gas passes through the channel, the barometric pressure will force the channels in the bottom layer to close, where single cells are trapped (Fig. 1.7a). The valves commonly utilize computer-controlled programs which simplify the operation but complicate device fabrication and increase the cost. The throughput of this approach is limited for the requirement of microscopy to confirm single-cell trapping. Perhaps, the combination of automatic

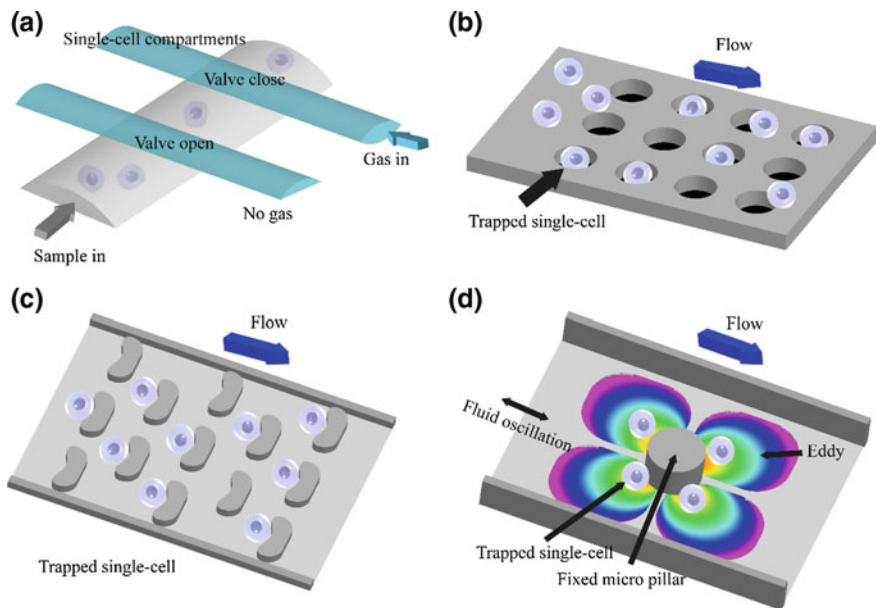


Fig. 1.7 Different microfluidic enabled single-cell isolation techniques. **a** Quake valves integrated microfluidic chip for single-cell isolation. **b** Schematic diagram of single-cell isolation based on microwells. **c** Schematic diagram of single-cell isolation based on microdams. **d** Schematic diagram of hydrodynamic single-cell isolation. An oscillating flow around a micropillar generates four surrounding eddies. Single cells are trapped at the center of eddies

feedback-controlled valves and microscopy will enable hands-off single-cell isolation and increase the throughput.

1.2.2.2 Microwells and Microdams

Single-cell isolation utilizing physical boundaries can be easily achieved by microfluidic chips. From the concept of multi-well plates for the isolating of cell groups, microwells can be used as a tool for the single-cell isolation. In this approach, microwells with suitable sizes are generated on the bottom of the channel. Single cells are trapped into individual microwells by gravity, and redundant cells will be flushed away (Fig. 1.7b). The size and shape of microwell can be adjusted to increase single-cell isolation efficiency. And the quantities of isolated single cells are depending on the scale of the microfluidic chip. However, the molecular analysis of single-cell studies is not suitable for this approach due to the non-isolated single-cell lysates. For more information about this technique, readers can refer to the previous reviews [75, 76].

Another single-cell isolation method uses physical boundaries is called microdams such as U-shaped cups to physically isolate single cells on chip (Fig. 1.7c).

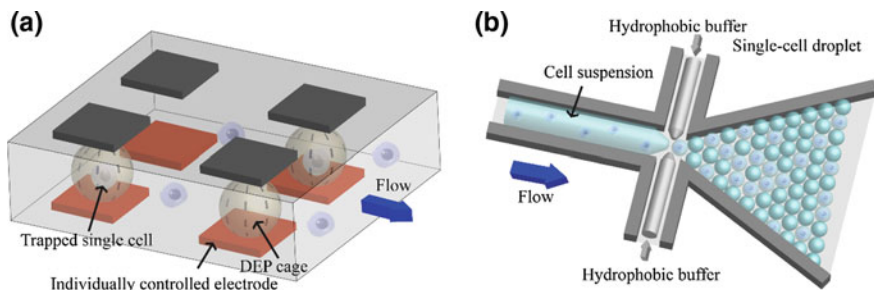


Fig. 1.8 Different microfluidic enabled single-cell isolation techniques. **a** Schematic diagram of single-cell isolation based on DEP. Individually controlled electrodes generate DEP cages to trap single cells. **b** Schematic diagram of droplets enabled single-cell isolation

The microdam is required to have cutaways allowing fluid flow through an unoccupied trap, thereby preventing clogging. This approach is beneficial because of the passive isolation and applicability for various cell sizes and shapes. However, most applications of this approach are used for single-cell culturing and transient imaging analysis, rather than single-cell lysate analysis.

1.2.2.3 Hydrodynamic

Single-cell isolation can be achieved passively by hydrodynamic mechanisms. This approach does not require complex fabrication systems thus attracting researchers to follow. In this approach, recirculating fluid flow is generated in the microfluidic channel for the cell trapping which is called eddies or vortices. It has been reported [77] that four surrounding eddies generated from an acoustic induced fluid oscillation around a micropillar can be applied to trap single cells (Fig. 1.7d). This approach is advantageous because of the passive isolation and applicability for various cell sizes and shapes. However, most application of this approach is used for single-cell culturing and transient imaging analysis, rather than single-cell lysate analysis due to the non-isolated single-cell lysates. For further discussion of hydrodynamic enabled single-cell isolation, readers can refer to the previous review [78].

1.2.2.4 Dielectrophoretic

Single-cell isolation by dielectrophoretic methods has been developed with great success. In this approach, a pair of electrodes enabling single-cell trapping is integrated into a microfluidic chip which is called DEP cage. A dielectrophoretic-based single-cell isolation system consists of a disposable cartridge which is an array of individually controllable DEP cages (Fig. 1.8a). After the process of trapping, cells are identified under a microscope and manipulated to other traps or isolated off the chip. The approach can be applied for isolating rare cancer cells from real blood

samples. However, the limitations of the approach are low throughput, inapplicability to smaller samples, and large labor costs. Besides, single cells are not strictly compartmentalized on a chip, which turns down the applicability for single-cell lysates analysis.

1.2.2.5 Droplets

Droplets recently have become a popular method in single-cell analysis. Just as its name implies, droplets are created by the incision of two immiscible fluids and can be utilized for cell encapsulation and isolation (Fig. 1.8b) [79]. This approach is especially suitable for molecular analysis from single-cell lysates. In this approach, each droplet functions as an individual chemical reactor and has no interchange of material with the others. The fabrication of systems is also simplified for easy operation. Droplet generation is achieved in a continuous flow which induces high-throughput single-cell encapsulation. Besides, the volume of each drop can be minimized into picoliter or even femtoliter. This greatly reduces the dilution of cell lysates for single-cell analysis. The single-cell capture rate is principally based on Poisson distribution, which cannot reach a hundred percent. Increasing this can be achieved by prefocusing or postsorting steps. Droplets have become a powerful platform for single-cell analysis. More discussion can be found in several focused reviews [80, 81].

1.2.3 Single-Cell Lysis

Microfluidic technology provides an ideal platform for single-cell lysis. Channels of microfluidic devices can be fabricated with special geometries and fluid flow can be controlled precisely, which allow accuracy control of single-cell lysis. The dimensions can be directly matched with the scale of single cells, which minimize the lysate dilution for better sensitivity. Most microfluidic devices are optically transparent, increasing the applicability with fluorescence detection. Close environment minimizes contamination of the sample. Till now, several approaches of microfluidic enabled single-cell lysis have been developed. Researchers often choose a suitable approach for the desired result. In this section, several popular models of microfluidic enabled single-cell lysis are discussed. And for further discussion, readers can refer to the later chapters or focused reviews [82, 83].

1.2.3.1 Chemical

Chemical lysis of cells is achieved by lysis buffer containing surfactants to solubilize lipids and proteins in the cell membrane. This process creates pores on the cell membrane and gradually induces fracture of an intact cell [84–86]. Microfluidic

devices are advantageous because of their precise control of fluid flow. Minimized lysis buffer can be consumed for the single-cell lysis which minimizes dilution (Fig. 1.9a). Although this is a simple and convenient approach in single-cell lysis, the limitation is obvious that the chemical reagent in the lysis buffer will contaminate the sample, which should be removed.

1.2.3.2 Mechanical

Mechanical lysis of cells can be achieved by tearing or puncturing cell membranes utilizing mechanical forces [87–89], such as shear stress, friction forces, or compressive stress. This approach directly breaks the cell structure and releases the target intracellular molecules (Fig. 1.9b). Mechanical enabled single-cell lysis can relatively minimize the protein damage, which is quite disturbing in other approaches. However, the cell's fragment produced by mechanical lysis makes the subsequent isolation complex.

1.2.3.3 Electrical

Electrical methods for single-cell lysis are common for generating pores on cell membranes to break the cell which are called electroporation lysis [90, 91]. In this approach, cells are disposed under an external electric field, where the potential is

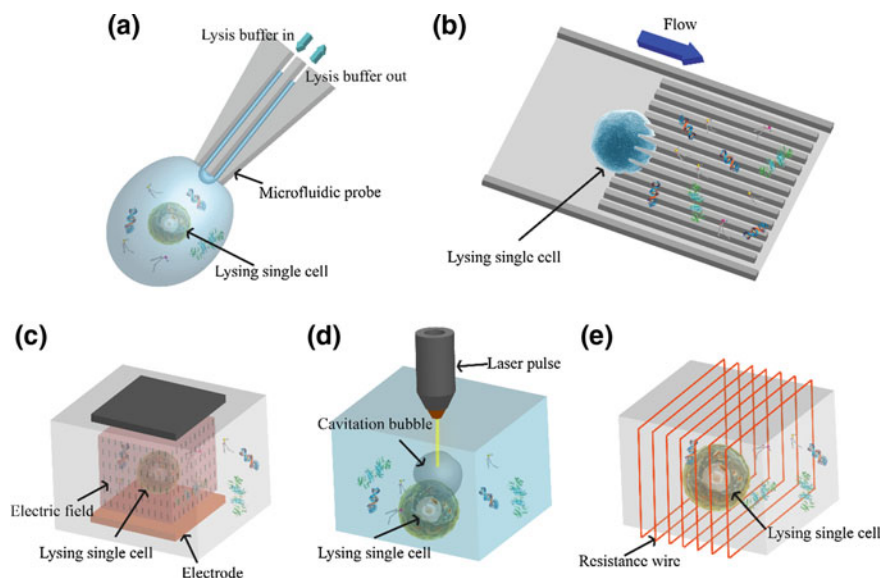


Fig. 1.9 Different microfluidic enabled single-cell lysis techniques. **a** Chemical. **b** Mechanical. **c** Electrical. **d** Optical. **e** Thermal

created through the cell membrane (also known as the transmembrane potential). Pores can be created on the cell membrane when the potential reaches a certain threshold at about 0.2-1.0 V [92]. The pores can be reversible under a mild electric field. However, while the electric field reaches to a high enough extent, the pores will become permanent and achieve complete lysis of cells (Fig. 1.9c) [93]. Commonly, reversible electroporation is utilized for small molecules' detection, and permanent electroporation is more suitable for macromolecules such DNA and proteins. Electrical enabled single-cell lysis is advantageous due to the ultra-high lysing efficiency on a millisecond level and better selectivity for different membranes by adjusting the electric field [94, 95]. However, the limitation is that the accuracy control of electrical field leads to a relatively complex operation process. And a short lifetime of electrode should be noted for the application.

1.2.3.4 Optical

Optical methods for single-cell lysis can be interpreted as the cell broken induced by fluid motion produced by a focused laser [96–98]. In this approach, a laser pulse is focused at a buffer interface around the surface of a cell. The high-energy laser will produce a localized cavitation bubble whose expansion and movement together with the induced fluid dynamic forces will help to break the cell membrane (Fig. 1.9d) [99]. Optical single-cell lysis has the advantages of high selectivity, high efficiency, and localized lysis region, which has destruction to the intracellular components [100]. Integrating the laser pulse into microfluidic chips also provides convenience controlling the time and location of the cell lysis. Besides, microchannels will restrain the over-expansion of the cavitation bubble, which is useful to control the volume [101]. However, the limitation is obvious that the complex integration of optical system greatly increases the experimental cost.

1.2.3.5 Thermal

Thermal methods for single-cell lysis can be interpreted as utilizing high temperature to denature the proteins on cell membranes which result in cell damaging for the intracellular components (Fig. 1.9e) [102, 103]. Thermal lysis is advantageous for high lysing intensity and simplicity. However, the temperature should be set carefully and controlled precisely for the existing of many heat-sensitive molecules in cells. Therefore, thermal single-cell lysis is most frequently used for parallel, on-chip PCR analysis instead of protein analysis [104, 105].

1.3 Conclusion and Outlook

Single-cell analysis is now a rapidly developing field. Various applications and future concerns will be discovered. Invention of novel microfluidic platforms will give a major push to single-cell biology. In this chapter, we have discussed the development and the mechanisms of single-cell analysis and microfluidic devices for cell sorting, single-cell isolation, and single-cell lysis.

Microfluidic enabled single-cell analysis now is a complete research field. Researchers continue to innovate and develop new techniques, which will be discussed in the later chapter. Microfabricated systems are advantageous due to little sample consumption, high cell viability, and low costs. However, the limited throughput compared with conventional flow cytometry prevents the wider adoption of microfluidic. Besides, microfluidics is not easily reusable due to clogging and cell adhesion. We expect the field of microfluidic single-cell analysis to continue growing for the widely commercialized application.

The modern science of single-cell biology is particularly fascinating. The development of detection techniques has allowed researchers to study cells in depth which are the basic units of life. Novel concepts in this field have been well established such as single-cell genomics, single-cell proteomics, and single-cell immunology which are a paradigm shift in biology. Currently, existing work in single-cell analysis always removes cells from their native environment for more convenient operation. This will lose the impact of native tissue and change cells' behavior. As such, new works often focus on the cells' original spatial context which has profound implications [106–108]. Nevertheless, these remarkable works only indicate the beginning of a new era, when revolutionary single-cell omics and innovative microfluidic approaches befall to the world.

References

1. Elowitz MB, Levine AJ, Siggia ED, Swain PS (2002) Stochastic gene expression in a single cell. *Science* 297(5584):1183–1186. <https://doi.org/10.1126/science.1070919>
2. Fiering S, Northrop JP, Nolan GP, Mattila PS, Crabtree GR, Herzenberg LA (1990) Single cell assay of a transcription factor reveals a threshold in transcription activated by signals emanating from the T-cell antigen receptor. *Genes Dev* 4(10):1823–1834
3. Hosis S, Murthy SK, Koppes AN (2016) Microfluidic sample preparation for single cell analysis. *Anal Chem* 88:354–380. <https://doi.org/10.1021/acs.analchem.5b04077>
4. Dexter DL, Kowalski HM, Blazar BA, Fligiel Z, Vogel R, Heppner GH (1978) Heterogeneity of tumor cells from a single mouse mammary tumor. *Cancer Res* 38(10):3174–3181
5. Navin N, Krasnitz A, Rodgers L, Cook K, Meth J, Kendall J, Riggs M, Eberling Y, Troge J, Grubor V, Levy D, Lundin P, Maner S, Zetterberg A, Hicks J, Wigler M (2010) Inferring tumor progression from genomic heterogeneity. *Genome Res* 20(1):68–80. <https://doi.org/10.1101/gr.099622.109>

6. Cohen AA, Geva-Zatorsky N, Eden E, Frenkel-Morgenstern M, Issaeva I, Sigal A, Milo R, Cohen-Saidon C, Liron Y, Kam Z, Cohen L, Danon T, Perzov N, Alon U (2008) Dynamic proteomics of individual cancer cells in response to a drug. *Science* 322(5907):1511–1516. <https://doi.org/10.1126/science.1160165>
7. Zhong JF, Chen Y, Marcus JS, Scherer A, Quake SR, Taylor CR, Weiner LP (2008) A microfluidic processor for gene expression profiling of single human embryonic stem cells. *Lab Chip* 8:68–74. <https://doi.org/10.1039/b712116d>
8. Murphy TW, Zhang Q, Naler LB, Ma S, Lu C (2018) Recent advances in the use of microfluidic technologies for single cell analysis. *Analyst* 143(1):60–80. <https://doi.org/10.1039/c7an01346a>
9. Huang Q, Mao S, Khan M, Lin JM (2019) Single-cell assay on microfluidic devices. *Analyst* 144:808–823. <https://doi.org/10.1039/c8an01079j>
10. Chen QS, Wu J, Zhuang QC, Lin XX, Zhang J, Lin JM (2013) Microfluidic isolation of highly pure embryonic stem cells using feeder-separated co-culture system. *Sci Rep* 3:2433. <https://doi.org/10.1038/srep02433>
11. Mao S, Zhang W, Huang Q, Khan M, Li H, Uchiyama K, Lin JM (2018) In Situ scatheless cell detachment reveals correlation between adhesion strength and viability at single-cell resolution. *Angew Chem Int Ed* 57(1):236–240
12. Lin L, Lin X, Lin L, Feng Q, Kitamori T, Lin JM, Sun J (2017) Integrated microfluidic platform with multiple functions to probe tumor–endothelial cell interaction. *Anal Chem* 89(18):10037–10044
13. Rettig JR, Folch A (2005) Large-scale single-cell trapping and imaging using microwell arrays. *Anal Chem* 77:5628–5634. <https://doi.org/10.1021/ac0505977>
14. Di Carlo D, Edd JF, Irimia D, Tompkins RG, Toner M (2008) Equilibrium separation and filtration of particles using differential inertial focusing. *Anal Chem* 80:2204–2211
15. Wang XB, Yang J, Huang Y, Vykoukal J, Becker FF, Gascoyne PR (2000) Cell separation by dielectrophoretic field-flow-fractionation. *Anal Chem* 72:832–839
16. Evander M, Johansson L, Lilliehorn T, Piskur J, Lindvall M, Johansson S, Almqvist M, Laurell T, Nilsson J (2007) Noninvasive acoustic cell trapping in a microfluidic perfusion system for online bioassays. *Anal Chem* 79(7):2984–2991. <https://doi.org/10.1021/ac061576v>
17. Matioli GT, Niewisch HB (1965) Electrophoresis of hemoglobin in single erythrocytes. *Science* 150(3705):1824–1826
18. Osborne NN, Szczepaniak AC, Neuhoff V (1973) Amines and amino acids in identified neurons of *Helix pomatia*. *Int J Neurosci* 5(3):125–131
19. McADOO DJ (1978) The Retzius cell of the leech *hirudo medicinalis*. In: Osborne NN (ed) *Biochemistry of Characterised Neurons*. Elsevier, Amsterdam
20. Lent CM, Mueller RL, Haycock DA (1983) Chromatographic and histochemical identification of dopamine within an identified neuron in the leech nervous-system. *J Neurochem* 41(2):481–490. <https://doi.org/10.1111/j.1471-4159.1983.tb04766.x>
21. McCaman RE, Weinreich D, Borys H (1973) Endogenous levels of acetylcholine and choline in individual neurons of *Aplysia*. *J Neurochem* 21(2):473–476
22. Melamed MR, Lindmo T, Mendelsohn ML, Bigler RD (1991) Flow cytometry and sorting. *Am J Clin Oncol* 14(1):90
23. Neher E, Sakmann B (1976) Single-channel currents recorded from membrane of denervated frog muscle fibres. *Nature* 260(5554):799–802
24. Kennedy RT, Stclair RL, White JG, Jorgenson JW (1987) Chemical-analysis of single neurons by open tubular liquid-chromatography. *Mikrochim Acta* 2(1–3):37–45
25. Wallingford RA, Ewing AG (1988) Capillary zone electrophoresis with electrochemical detection in 12.7-Mu-M diameter columns. *Anal Chem* 60(18):1972–1975. <https://doi.org/10.1021/ac00169a027>

26. Croushore CA, Supharoek SA, Lee CY, Jakmunee J, Sweedler JV (2012) Microfluidic device for the selective chemical stimulation of neurons and characterization of peptide release with mass spectrometry. *Anal Chem* 84(21):9446–9452. <https://doi.org/10.1021/ac302283u>
27. Rubakhin SS, Lanni EJ, Sweedler JV (2013) Progress toward single cell metabolomics. *Curr Opin Biotechnol* 24(1):95–104. <https://doi.org/10.1016/j.copbio.2012.10.021>
28. Comi TJ, Do TD, Rubakhin SS, Sweedler JV (2017) Categorizing cells on the basis of their chemical profiles: progress in single-cell mass spectrometry. *J Am Chem Soc* 139:3920–3929. <https://doi.org/10.1021/jacs.6b12822>
29. Ong TH, Kissick DJ, Jansson ET, Comi TJ, Romanova EV, Rubakhin SS, Sweedler JV (2015) Classification of large cellular populations and discovery of rare cells using single cell matrix-assisted laser desorption/ionization time-of-flight mass spectrometry. *Anal Chem* 87(14):7036–7042. <https://doi.org/10.1021/acs.analchem.5b01557>
30. Zhang Z, Krylov S, Arriaga EA, Polakowski R, Dovichi NJ (2000) One-dimensional protein analysis of an HT29 human colon adenocarcinoma cell. *Anal Chem* 72(2):318–322
31. Hu S, Le Z, Newitt R, Aebersold R, Kraly JR, Jones M, Dovichi NJ (2003) Identification of proteins in single-cell capillary electrophoresis fingerprints based on comigration with standard proteins. *Anal Chem* 75(14):3502–3505
32. Zhu G, Sun L, Yan X, Dovichi NJ (2013) Single-shot proteomics using capillary zone electrophoresis–electrospray ionization–tandem mass spectrometry with production of more than 1 250 *Escherichia coli* peptide identifications in a 50 min separation. *Anal Chem* 85:2569–2573
33. Qu Y, Sun L, Zhang Z, Dovichi NJ (2018) Site-specific glycan heterogeneity characterization by hydrophilic interaction liquid chromatography solid-phase extraction, reversed-phase liquid chromatography fractionation, and capillary zone electrophoresis–electrospray ionization–tandem mass spectrometry. *Anal Chem* 90:1223–1233. <https://doi.org/10.1021/acs.analchem.7b03912>
34. Sibbitts J, Sellens KA, Jia S, Klasner SA, Culbertson CT (2018) Cellular analysis using microfluidics. *Anal Chem* 90(1):65–85. <https://doi.org/10.1021/acs.analchem.7b04519>
35. Armbrrecht L, Dittrich PS (2017) Recent advances in the analysis of single cells. *Anal Chem* 89(1):2–21
36. Lin L, Chen QH, Sun JS (2018) Micro/nanofluidics-enabled single-cell biochemical analysis. *TrAC-Trend Anal Chem* 99:66–74. <https://doi.org/10.1016/j.trac.2017.11.017>
37. Shear JB, Fishman HA, Allbritton NL, Garigan D, Zare RN, Scheller RH (1995) Single cells as biosensors for chemical separations. *Science* 267(5194):74–77. <https://doi.org/10.1126/science.7809609>
38. Huang B, Wu H, Bhaya D, Grossman A, Granier S, Kobilka BK, Zare RN (2007) Counting low-copy number proteins in a single cell. *Science* 315(5808):81–84. <https://doi.org/10.1126/science.1133992>
39. Zare RN, Kim S (2010) Microfluidic platforms for single-cell analysis. *Annu Rev Biomed Eng* 12:187–201. <https://doi.org/10.1146/annurev-bioeng-070909-105238>
40. Wheeler AR, Thronset WR, Whelan RJ, Leach AM, Zare RN, Liao YH, Farrell K, Manger ID, Daridon A (2003) Microfluidic device for single-cell analysis. *Anal Chem* 75(14):3581–3586
41. Mellors JS, Jorabchi K, Smith LM, Ramsey JM (2010) Integrated microfluidic device for automated single cell analysis using electrophoretic separation and electrospray ionization mass spectrometry. *Anal Chem* 82(3):967–973. <https://doi.org/10.1021/ac902218y>
42. McClain MA, Culbertson CT, Jacobson SC, Allbritton NL, Sims CE, Ramsey JM (2003) Microfluidic devices for the high-throughput chemical analysis of cells. *Anal Chem* 75(21):5646–5655. <https://doi.org/10.1021/ac0346510>
43. Broyles BS, Jacobson SC, Ramsey JM (2003) Sample filtration, concentration, and separation integrated on microfluidic devices. *Anal Chem* 75(11):2761–2767

44. Liu C, Liu J, Gao D, Ding M, Lin J-M (2010) Fabrication of microwell arrays based on two-dimensional ordered polystyrene microspheres for high-throughput single-cell analysis. *Anal Chem* 82(22):9418–9424
45. Chen Q, Wu J, Zhang Y, Lin Z, Lin J-M (2012) Targeted isolation and analysis of single tumor cells with aptamer-encoded microwell array on microfluidic device. *Lab Chip* 12(24): 5180–5185
46. Liu J, Gao D, Mao S, Lin J-M (2012) A microfluidic photolithography for controlled encapsulation of single cells inside hydrogel microstructures. *Sci China Chem* 55(4):494–501
47. Shields CW IV, Reyes CD, López GP (2015) Microfluidic cell sorting: a review of the advances in the separation of cells from debulking to rare cell isolation. *Lab Chip* 15(5): 1230–1249
48. Thompson AM, Paguirigan AL, Kreutz JE, Radich JP, Chiu DT (2014) Microfluidics for single-cell genetic analysis. *Lab Chip* 14(17):3135–3142. <https://doi.org/10.1039/c4lc00175c>
49. Sajeesh P, Sen AK (2014) Particle separation and sorting in microfluidic devices: a review. *Microfluid Nanofluid* 17(1):1–52. <https://doi.org/10.1007/s10404-013-1291-9>
50. Chen Y, Li P, Huang PH, Xie Y, Mai JD, Wang L, Nguyen NT, Huang TJ (2014) Rare cell isolation and analysis in microfluidics. *Lab Chip* 14(4):626–645. <https://doi.org/10.1039/c3lc90136j>
51. Autebert J, Coudert B, Bidard FC, Pierga JY, Descroix S, Malaquin L, Viovy JL (2012) Microfluidic: an innovative tool for efficient cell sorting. *Methods* 57(3):297–307. <https://doi.org/10.1016/j.ymeth.2012.07.002>
52. Mehrishi JN, Bauer J (2002) Electrophoresis of cells and the biological relevance of surface charge. *Electrophoresis* 23(13):1984–1994. [https://doi.org/10.1002/1522-2683\(200207\)23:13%3c1984:AID-ELPS1984%3e3.0.CO;2-U](https://doi.org/10.1002/1522-2683(200207)23:13%3c1984:AID-ELPS1984%3e3.0.CO;2-U)
53. Voldman J (2006) Electrical forces for microscale cell manipulation. *Annu Rev Biomed Eng* 8:425–454. <https://doi.org/10.1146/annurev.bioeng.8.061505.095739>
54. Shim S, Stemke-Hale K, Noshari J, Becker FF, Gascoyne PRC (2013) Dielectrophoresis has broad applicability to marker-free isolation of tumor cells from blood by microfluidic systems. *Biomicrofluidics* 7(1):011808. <https://doi.org/10.1063/1.4774307>
55. Burguillos MA, Magnusson C, Nordin M, Lenshof A, Augustsson P, Hansson MJ, Elmer E, Lilja H, Brundin P, Laurell T, Deierborg T (2013) Microchannel acoustophoresis does not impact survival or function of microglia, leukocytes or tumor cells. *PLoS ONE* 8(5):e64233. <https://doi.org/10.1371/journal.pone.0064233>
56. Skowronek V, Rambach RW, Schmid L, Haase K, Franke T (2013) Particle deflection in a poly(dimethylsiloxane) microchannel using a propagating surface acoustic wave: size and frequency dependence. *Anal Chem* 85(20):9955–9959. <https://doi.org/10.1021/ac402607p>
57. Yeo LY, Friend JR (2014) Surface acoustic wave microfluidics. *Annu Rev Fluid Mech* 46:379–406. <https://doi.org/10.1146/annurev-fluid-010313-141418>
58. Ding X, Li P, Lin SC, Stratton ZS, Nama N, Guo F, Slotcavage D, Mao X, Shi J, Costanzo F, Huang TJ (2013) Surface acoustic wave microfluidics. *Lab Chip* 13(18):3626–3649. <https://doi.org/10.1039/c3lc50361e>
59. Ashkin A (1970) Acceleration and trapping of particles by radiation pressure. *Phys Rev Lett* 24(4):156. <https://doi.org/10.1103/PhysRevLett.24.156>
60. Ashkin A, Dziedzic JM, Bjorkholm JE, Chu S (1986) Observation of a single-beam gradient force optical trap for dielectric particles. *Opt Lett* 11(5):288
61. Jonas A, Zemanek P (2008) Light at work: the use of optical forces for particle manipulation, sorting, and analysis. *Electrophoresis* 29(24):4813–4851. <https://doi.org/10.1002/elps.200800484>
62. Moffitt JR, Chemla YR, Smith SB, Bustamante C (2008) Recent advances in optical tweezers. *Annu Rev Biochem* 77:205–228. <https://doi.org/10.1146/annurev.biochem.77.043007.090225>

63. Plouffe BD, Murthy SK, Lewis LH (2015) Fundamentals and application of magnetic particles in cell isolation and enrichment: a review. *Rep Prog Phys* 78(1):016601. <https://doi.org/10.1088/0034-4885/78/1/016601>
64. Hejazian M, Li W, Nguyen NT (2015) Lab on a chip for continuous-flow magnetic cell separation. *Lab Chip* 15(4):959–970. <https://doi.org/10.1039/c4lc01422g>
65. Zborowski M, Chalmers JJ (2011) Rare cell separation and analysis by magnetic sorting. *Anal Chem* 83(21):8050–8056. <https://doi.org/10.1021/ac200550d>
66. Inglis DW, Davis JA, Austin RH, Sturm JC (2006) Critical particle size for fractionation by deterministic lateral displacement. *Lab Chip* 6(5):655–658. <https://doi.org/10.1039/b515371a>
67. McGrath J, Jimenez M, Bridle H (2014) Deterministic lateral displacement for particle separation: a review. *Lab Chip* 14(21):4139–4158. <https://doi.org/10.1039/c4lc00939h>
68. Di Carlo D (2009) Inertial microfluidics. *Lab Chip* 9(21):3038–3046. <https://doi.org/10.1039/b912547g>
69. Martel JM, Toner M (2014) Inertial focusing in microfluidics. *Annu Rev Biomed Eng* 16:371–396. <https://doi.org/10.1146/annurev-bioeng-121813-120704>
70. Geislinger TM, Franke T (2014) Hydrodynamic lift of vesicles and red blood cells in flow—from Fåhræus & Lindqvist to microfluidic cell sorting. *Adv Colloid Interfac* 208:161–176
71. Huang Q, Mao S, Khan M, Zhou Z, Lin J-M (2018) Dean flow assisted-cell ordering system for lipid profiling in single-cells using mass spectrometry. *Chem Commun* 54:2595–2598
72. Nilsson J, Evander M, Hammarstrom B, Laurell T (2009) Review of cell and particle trapping in microfluidic systems. *Anal Chim Acta* 649(2):141–157. <https://doi.org/10.1016/j.aca.2009.07.017>
73. Unger MA, Chou HP, Thorsen T, Scherer A, Quake SR (2000) Monolithic microfabricated valves and pumps by multilayer soft lithography. *Science* 288(5463):113–116
74. Thorsen T, Maerkl SJ, Quake SR (2002) Microfluidic large-scale integration. *Science* 298(5593):580–584. <https://doi.org/10.1126/science.1076996>
75. Kim S-H, Lee GH, Park JY (2013) Microwell fabrication methods and applications for cellular studies. *Biomed Eng Lett* 3(3):131–137
76. Lindström S, Andersson-Svahn A (2011) Miniaturization of biological assays—overview on microwell devices for single-cell analyses. *BBA-Gen Subjects* 1810(3):308–316
77. Lutz BR, Chen J, Schwartz DT (2006) Hydrodynamic tweezers: 1. Noncontact trapping of single cells using steady streaming microeddies. *Anal Chem* 78(15):5429–5435. <https://doi.org/10.1021/ac060555y>
78. Karimi A, Yazdi S, Ardekani AM (2013) Hydrodynamic mechanisms of cell and particle trapping in microfluidics. *Biomicrofluidics* 7(2):21501. <https://doi.org/10.1063/1.4799787>
79. Utada AS, Lorenceau E, Link DR, Kaplan PD, Stone HA, Weitz DA (2005) Monodisperse double emulsions generated from a microcapillary device. *Science* 308(5721):537–541. <https://doi.org/10.1126/science.1109164>
80. Tran TM, Lan F, Thompson CS, Abate AR (2013) From tubes to drops: droplet-based microfluidics for ultrahigh-throughput biology. *J Phys D Appl Phys* 46(11):114004. <https://doi.org/10.1088/0022-3727/46/11/114004>
81. Guo MT, Rotem A, Heyman JA, Weitz DA (2012) Droplet microfluidics for high-throughput biological assays. *Lab Chip* 12(12):2146–2155. <https://doi.org/10.1039/c2lc21147e>
82. Brown RB, Audet J (2008) Current techniques for single-cell lysis. *J R Soc Interface* 5 Suppl 2(Suppl 2):S131–138. <https://doi.org/10.1098/rsif.2008.0009.focus>
83. Nan L, Jiang Z, Wei X (2014) Emerging microfluidic devices for cell lysis: a review. *Lab Chip* 14(6):1060–1073. <https://doi.org/10.1039/c3lc51133b>
84. Kotlowski R, Martin A, Ablordey A, Chemlal K, Fonteyne PA, Portaels F (2004) One-tube cell lysis and DNA extraction procedure for PCR-based detection of *Mycobacterium ulcerans* in aquatic insects, molluscs and fish. *J Med Microbiol* 53(Pt 9):927–933. <https://doi.org/10.1099/jmm.0.45593-0>
85. Marcus JS, Anderson WF, Quake SR (2006) Microfluidic single-cell mRNA isolation and analysis. *Anal Chem* 78(9):3084–3089. <https://doi.org/10.1021/ac0519460>

86. Cichova M, Proksova M, Tothova L, Santha H, Mayer V (2012) On-line cell lysis of bacteria and its spores using a microfluidic biochip. *Cent Eur J Biol* 7(2):230–240. <https://doi.org/10.2478/s11535-012-0005-8>
87. Martin-Laurent F, Philippot L, Hallet S, Chaussod R, Germon JC, Soulas G, Catroux G (2001) DNA extraction from soils: old bias for new microbial diversity analysis methods. *Appl Environ Microbiol* 67(5):2354–2359. <https://doi.org/10.1128/AEM.67.5.2354-2359.2001>
88. Sad S, Dudani R, Gurmani K, Russell M, van Faassen H, Finlay B, Krishnan L (2008) Pathogen proliferation governs the magnitude but compromises the function of CD8 T cells. *J Immunol* 180(9):5853–5861
89. Doebler RW, Erwin B, Hickerson A, Irvine B, Woyski D, Nadim A, Sterling JD (2009) Continuous-flow, rapid lysis devices for biodefense nucleic acid diagnostic systems. *Jala* 14(3):119–125. <https://doi.org/10.1016/j.jala.2009.02.010>
90. Weaver JC (2000) Electroporation of cells and tissues. *IEEE T Plasma Sci* 28(1):24–33. <https://doi.org/10.1109/27.842820>
91. Weaver JC (2003) Electroporation of biological membranes from multicellular to nano scales. *IEEE T Dielect El In* 10(5):754–768. <https://doi.org/10.1109/Tdei.2003.1237325>
92. Tsong TY (1991) Electroporation of cell membranes. *Biophys J* 60(2):297–306. [https://doi.org/10.1016/S0006-3495\(91\)82054-9](https://doi.org/10.1016/S0006-3495(91)82054-9)
93. Hjouj M, Last D, Guez D, Daniels D, Sharabi S, Lavee J, Rubinsky B, Mardor Y (2012) MRI study on reversible and irreversible electroporation induced blood brain barrier disruption. *PLoS ONE* 7(8):e42817. <https://doi.org/10.1371/journal.pone.0042817>
94. Fox MB, Esveld DC, Valero A, Lutge R, Mastwijk HC, Bartels PV, van den Berg A, Boom RM (2006) Electroporation of cells in microfluidic devices: a review. *Anal Bioanal Chem* 385(3):474–485. <https://doi.org/10.1007/s00216-006-0327-3>
95. Wang S, Lee LJ (2013) Micro-/nanofluidics based cell electroporation. *Biomicrofluidics* 7(1):11301. <https://doi.org/10.1063/1.4774071>
96. Vogel A, Busch S, Jungnickel K, Birngruber R (1994) Mechanisms of intraocular photodisruption with picosecond and nanosecond laser pulses. *Lasers Surg Med* 15(1):32–43
97. Shaw S, Jin Y, Schiffers W, Emmony D (1996) The interaction of a single laser-generated cavity in water with a solid surface. *J Acoust Soc Am* 99(5):2811–2824
98. Vogel A, Noack J, Nahen K, Theisen D, Busch S, Parlitz U, Hammer DX, Noojin GD, Rockwell BA, Birngruber R (1999) Energy balance of optical breakdown in water at nanosecond to femtosecond time scales. *Appl Phys B-Lasers O* 68(2):271–280. <https://doi.org/10.1007/s003400050617>
99. Sims CE, Meredith GD, Krasieva TB, Berns MW, Tromberg BJ, Allbritton NL (1998) Laser-micropipet combination for single-cell analysis. *Anal Chem* 70(21):4570–4577
100. Dhawan MD, Wise F, Baeumner AJ (2002) Development of a laser-induced cell lysis system. *Anal Bioanal Chem* 374(3):421–426. <https://doi.org/10.1007/s00216-002-1489-2>
101. Quinto-Su PA, Lai HH, Yoon HH, Sims CE, Allbritton NL, Venugopalan V (2008) Examination of laser microbeam cell lysis in a PDMS microfluidic channel using time-resolved imaging. *Lab Chip* 8(3):408–414. <https://doi.org/10.1039/b715708h>
102. Cordero N, West J, Berney H (2003) Thermal modelling of Ohmic heating microreactors. *Microelectron J* 34(12):1137–1142. [https://doi.org/10.1016/S0026-2692\(03\)00204-0](https://doi.org/10.1016/S0026-2692(03)00204-0)
103. Fu R, Xu B, Li D (2006) Study of the temperature field in microchannels of a PDMS chip with embedded local heater using temperature-dependent fluorescent dye. *Int J Therm Sci* 45(9):841–847. <https://doi.org/10.1016/j.ijthermalsci.2005.11.009>
104. Waters LC, Jacobson SC, Kroutchinina N, Khandurina J, Foote RS, Ramsey JM (1998) Microchip device for cell lysis, multiplex PCR amplification, and electrophoretic sizing. *Anal Chem* 70(1):158–162
105. Zhu K, Jin H, Ma Y, Ren Z, Xiao C, He Z, Zhang F, Zhu Q, Wang B (2005) A continuous thermal lysis procedure for the large-scale preparation of plasmid DNA. *J Biotechnol* 118(3):257–264. <https://doi.org/10.1016/j.jbiotec.2005.05.003>

106. Junttila MR, de Sauvage FJ (2013) Influence of tumour micro-environment heterogeneity on therapeutic response. *Nature* 501(7467):346–354. <https://doi.org/10.1038/nature12626>
107. Junker JP, Noel ES, Guryev V, Peterson KA, Shah G, Huisken J, McMahon AP, Berezikov E, Bakkers J, van Oudenaarden A (2014) Genome-wide RNA Tomography in the zebrafish embryo. *Cell* 159(3):662–675. <https://doi.org/10.1016/j.cell.2014.09.038>
108. Chen KH, Boettiger AN, Moffitt JR, Wang S, Zhuang X (2015) RNA imaging. Spatially resolved, highly multiplexed RNA profiling in single cells. *Science* 348(6233):aaa6090. <https://doi.org/10.1126/science.aaa6090>

Chapter 2

Microfluidic Technology for Single-Cell Capture and Isolation



Jing Wu and Jin-Ming Lin

Abstract Compared to conventional biological assays that statistically analyze the average response from a large population of cells, single-cell assay can tell the differences between individual cells allowing more precise understanding of single-cell behavior. The challenge of studying single cells is requiring hundreds or thousands of isolated single cells. Numerous microfluidic-based techniques have been developed and are successfully utilized to capture single cells. In this chapter, we summarize technologies integrated onto microfluidic chips for single-cell capture and isolation. According to the principle used, these techniques can be categorized into physical and biochemical approaches. At last, the challenges and future directions about these microfluidic techniques have been remarked.

Keywords Single-cell · Capture and isolation · Physical microfluidic techniques · Biochemical microfluidic approaches

2.1 Introduction

Analysis at the single-cell level has been raised particular interests due to cell populations can be very heterogeneous. Studying the heterogeneity can reveal how cells function, transform and react to different stimuli and how these different behaviors relate to genetic and epigenetic changes [1–4]. Capture and isolation of single cells are prerequisites for understanding these cellular variations. However, efficient single-cell capture and isolation are complex tasks for any given cell population. Therefore, a large variety of technologies for single-cell capture and isolation have been studied [5]. Conventional methods for cell capture and isolation cannot

J. Wu

School of Science, China University of Geosciences (Beijing), Beijing 100083, China
e-mail: wujing@cugb.edu.cn

J.-M. Lin (✉)

Department of Chemistry, Tsinghua University, Beijing 100084, China
e-mail: jmlin@mail.tsinghua.edu.cn

© Springer Nature Singapore Pte Ltd. 2019

J.-M. Lin (ed.), *Microfluidics for Single-Cell Analysis*,

Integrated Analytical Systems, https://doi.org/10.1007/978-981-32-9729-6_2

easily manipulate single cells in standard petri dishes because of the cell sizes. In this regard, microfluidic technologies emerge as potentially powerful tools for precise control and efficient capture of target single cells from cell mixtures [6–9].

Microfluidic techniques show great promises in single-cell capture and analysis because of their inherent advantages [10–14]. (1) Miniaturization of microfluidic systems makes them possible to handle the cell transfer, capture, sorting, and analysis in a very small volume. (2) Integration of microfluidic systems combines multi-step operations and shortens the assay time. (3) Three-dimensional (3D) substrates of microchannels enhance interactions between cell surface and the local topographic substrate leading to enhanced cell capture efficiencies. (4) Biocompatibility of microfluidic systems reconstitutes the native microenvironments and presents cells in a more physiologically relevant context to keep their normal behaviors and functions. Various microscale physical traps and numerous microfluidic chips with different underlying cell isolation principles are increasingly emerging to isolate and investigate single cells [15–17].

In this chapter, we review the recent emergence of microfluidic technologies applied in single-cell capture and isolation for biomedical applications. Focus is put on the principles and advances accounting for these technologies. This chapter is divided into three sections. At first, we highlight a variety of microfluidic techniques which employ physical means to capture individual cells in the high-throughput model. Physical principle-based microscale traps contain optical tweezers, dielectrophoresis (DEP), acoustic wave and magnetic traps. Secondly, microfluidic approaches based on interactions between affinity ligands and cell surface markers have been discussed. Emphasis is put on antibody- and aptamer-based approaches. In the last section, we summarize the key advantages of these techniques and remark the challenging and future directions about the development of these approaches.

2.2 Physical Microfluidic Techniques

2.2.1 *Optical Traps*

Due to the ubiquity, non-contact and contamination-free of optical instruments in laboratories, optical traps are commonly utilized to capture and isolate single cells in microsystems. We described a photolithography approach to encapsulate single cells by generating arrayed hydrogel microstructures inside microchannels. Poly (ethylene glycol) diacrylate precursor was photopolymerized using a fluorescence microscope to generate microstructures with controlled morphology and position [18, 19]. Optical tweezers are the chief optical traps which are integrated onto microfluidic systems to trap single cells with high precision and possibility [20–22]. Optical tweezers are a single-beam optical gradient trap and manipulate cells by optical forces toward the focus point of a laser beam. The laser beam focused on a particle or cell can form a 3D optical potential well which induces optical pressure

to capture the particle or cell. The intensity and shape of spatial light distributions can be rapidly switched, so the trapped cells can be repositioned in all dimensions through moving the beam and changing focus [16, 23].

Optical tweezers were tried to be implemented on a digital microfluidic platform to accurately manipulate single magnetic beads which were used to mimic single cells and seeded in a microwell array (Fig. 2.1a). Under the optimal conditions, magnetic beads were trapped, retrieved, transported, and repositioned to a desired microwell by the optical tweezers. The optical tweezers-combined platform was presented as a powerful dynamic microwell array system for single-molecule and single-cell researches [24]. Laser tweezers Raman spectroscopy (LTRS) was proved to be a powerful tool for the label-free detection and discrimination of individual cancer cells. Microfluidic flow chamber was introduced to avoid the problem of manual trapping of cells and allow single cells to be optically trapped and analyzed in an automated fashion using LTRS[25]. Single-wall carbon nanotube electrodes were embedded into multilayer polydimethylsiloxane (PDMS) structures to integrate optoelectronic tweezers with microfluidic chip allowing single-cell sample preparation and analysis (Fig. 2.1b). Individual cells were picked up from a population with light beams depending on their optical signatures, such as size, shape, and fluorescence [26]. Due to the complexity and expensive fabrication of optical tweezers, low-throughput is their inherent limitation for wide applications in large-scale cell sample processing. Cheng et al. [27] combined optical tweezers with a tapered microfluidic nanoparticle delivery system to deliver target nanoparticles to the laser trap region by active microfluidic flow. Compared to conventional systems, it was observed a more than tenfold increase in throughput opening the door to high-throughput analysis of nanoparticles and single cells. Although the integration of optical tweezers with microfluidic devices exhibits great promise in single-cell capture and analysis, objective lens always is required. Furthermore, it is challenging to trap non-transparent or optically insensitive target for optical tweezers. Chen et al. [28] firstly reported thermal tweezers which were fabricated with a photon-free

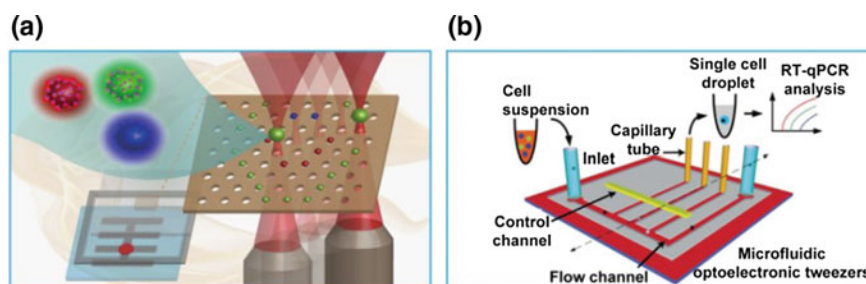


Fig. 2.1 Optical tweezers integrated on microfluidic devices. **a** Optical tweezers were implemented on a digital microfluidic platform for accurate manipulation of single magnetic beads and cells (Reprinted with permission from Ref. [24]. Copyright 2016 American Chemical Society.). **b** Schematic of the optoelectronic tweezers integrated microfluidic platform (Reprinted with permission from Ref. [26]. Copyright The Royal Society of Chemistry 2013.)

trapping technique to avoid the above problems. The thermal-gradient-induced thermophoresis was demonstrated to successfully trap polystyrene spheres and live cells. As a noninvasive and non-destructive cell manipulation method, optical tweezers are advantageous in handling small number of single cells since properly chosen forces are strong enough. Throughput enhancement and construction simplification are the two directions for future development of optical tweezers.

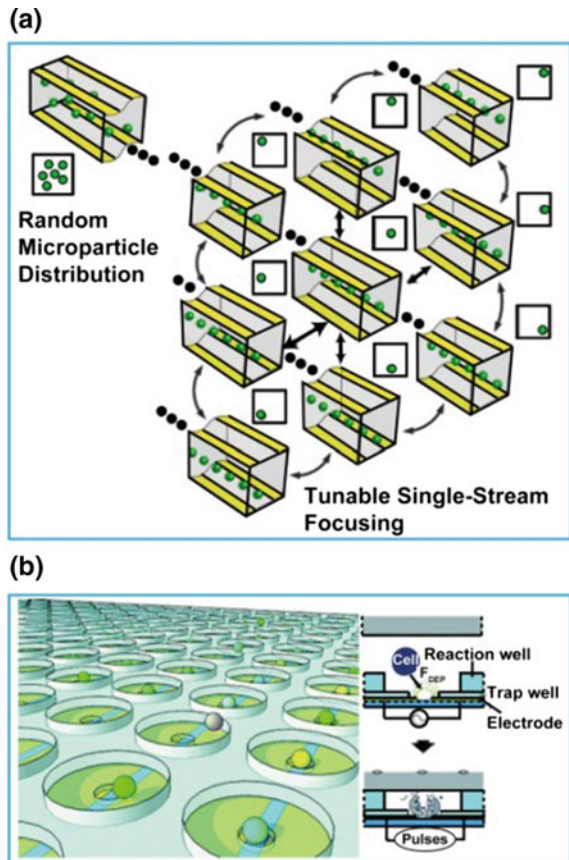
2.2.2 DEP

DEP has been widely used in manipulating and separating single cells in microsystems because of its merits of easy-operation, label-free, high-efficiency, and low-damage [29, 30]. Most cells have various dielectric characteristics, such as polarizability and conductivity, in external electric fields due to different cellular compositions and physical properties. These properties can be utilized to isolate cells by DEP which occurs when a polarizable particle or cell is placed in the non-uniform electric fields.

Both positive and negative DEP force can be used to control cells to be travelled to the designated location. Cheng et al. [31] generated positive DEP (pDEP) on a planar chip by applying an alternating current signal on a novel two-pair interdigitated array electrode (TPIDA). More than 4800 single cells were trapped and paired by the pDEP within only several minutes on a 1×1.5 cm area. The single cell-cell pairing efficiency was improved up to 74.2% by TPIDA which decreased the induced electric field during consecutive trapping of two cell types. pDEP was combined with a solenoid-valve-suction-based switch on a Raman-activated cell sorting microfluidic system for single-cell trap and release. Single cells were trapped, ordered, and positioned individually to the detection point for Raman measurement through exerting a periodical pDEP field [32]. Negative DEP (nDEP) was demonstrated to attract and repulse B-cells from each a bipolar electrode cathode and anode. The impact of faradaic ion enrichment and depletion on electric field gradients was exploited to shape and extend DEP force. This technology addressed a need for effective and inexpensive single-cell manipulation in microfluidic devices [33]. Quadrupole-electrode units were patterned onto microfluidic chips to trap and position individual living cells based on nDEP. Different types of cells were effectively distinguished as well as single-cell impedance was successfully measured in real time [34, 35]. Chiou et al. [36] fabricated a 3D tunnel DEP device with two pieces of glass substrates sandwiching a thin and open PDMS channel (Fig. 2.2a). Electrodes were laid out to provide DEP forces perpendicular to the hydrodynamic flow in the channel. A long DEP interaction zone was generated by the electrodes spanned up to several centimeters in length across the entire channel. As a result, microparticles and cells had sufficient time to migrate to the focal stream in high-speed flows. Kim et al. [37] fabricated an advanced electroactive double-well array (EdWA) which was consisted of cell-sized trap wells and high aspect ratio reaction wells (Fig. 2.2b). Trap wells were designed for

deterministic single-cell trapping using DEP and reaction wells were used to confine cell lysates extracted by lysing trapped single cells via electroporation. On-chip highly efficient single-cell arraying was successfully formed, and single-cell analysis was readily performed. Single-cell trapping, impedance measurement, and liquid manipulation by DEP were integrated into a parallel-plate device. A HeLa cell was trapped in microstructure by DEP and its impedance was measured in a SU-8 cavity between measurement electrodes [38]. Sonkusale et al. [39] applied alternating current (AC) DEP in microfluidic channel to deliver and extract cells as well as direct current (DC) electric fields to lyse cells. AC-DEP was even utilized to drive the assembly of live bacteria into miniaturized single-cell microarrays. Voltage and frequency of AC-DEP were optimized to obtain maximum cell capture efficiency [40]. Definitely, DEP is a convenient and outstanding single-cell separation method, and it still has some limitations needing to solve in future, such as application limited to cells with distinguishable electrical characteristics, damage of cells caused by electrodes, fluid convection induced by Joule heating.

Fig. 2.2 Single-cell capture via DEP on microfluidic chips. **a** Schematic representation of tunnel DEP for single-stream cell focusing in high-speed microfluidic flows (Reprinted with permission from Ref. [36]. Copyright 2016 Wiley-VCH Verlag GmbH & Co. KGaA, Weinheim). **b** Schematic illustration of an EdWA for on-chip single-cell trap and analysis (Reprinted with permission from Ref. [37]. Copyright The Royal Society of Chemistry 2016.)



2.2.3 Acoustic Waves

Capture of single cells by an acoustic wave at microlevel has been developed for decades and advances in preserving cell integrity, functionality, and viability [41, 42]. Acoustic waves are generated by acoustic field. Cells in fluid are pushed toward designated regions with a minimal acoustic radiation pressure when an acoustic field is present within a flow channel. According to the property of acoustic wave, surface acoustic waves (SAWs) are categorized into travelling SAWs (TSAWs) and standing SAWs (SSAWs).

The surface wave generated from a single interdigitated transducer (IDT) is TSAW which manipulates micro-objects via acoustic streaming flow and is mainly used to actuate fluids [43]. An acoustic topographical manipulation method was present to efficiently and reproducibly manipulate diverse microscale objects relying on the acoustic-induced localized microstreaming forces (Fig. 2.3a). Micro-objects were trapped and manipulated along a determined trajectory based on local topographic features. Microparticles with diverse geometries and densities,

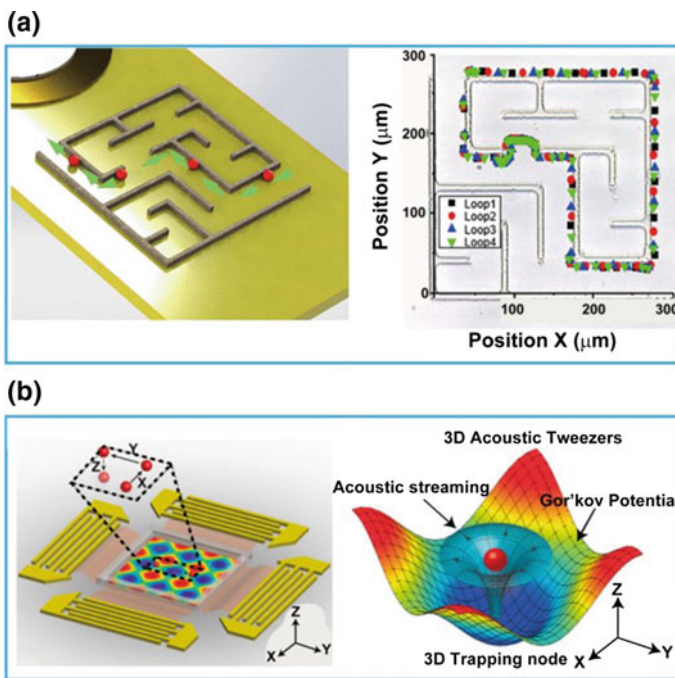


Fig. 2.3 Acoustic wave-based microfluidic devices for single-cell capture. **a** Acoustic topographical manipulation method was developed to trap micro-objects and control them along a determined trajectory relying on microstreaming forces (Reprinted with permission from Ref. [44]. Copyright 2017 American Chemical Society.). **b** Illustration of 3D acoustic tweezers and numerical simulation results mapping the acoustic field around a particle (Reprinted with permission from Ref. [49]. Copyright 2016 National Academy of Sciences.)

including live cells, could be autonomously manipulated by this method without external feedback, particle modification, or adjustment of operational parameters [44]. Commonly, TSAW-based microfluidic sorting techniques are particularly useful for small particles or cells because of the generated acoustic radiation force. In contrast, Franke et al. [45] introduced an acoustic sorting technique to sort cells or other micro-objects independent of their sizes at high rates. The acoustic sorter combined the advantages of fluorescence-activated cell and droplet sorting and showed great promises to be integrated into many available microfluidic platforms. Droplets are a powerful tool which can be used as single-cell containers [46]. TSAWs also were used to trap, incubate, and release individual selected droplets from a continuously flowing stream with a high rate [47, 48]. Through regulating the operation frequency of the TSAWs, each droplet could be individually addressed, manipulated, released, or incubated for variable times as required.

One TSAW and its reflected form which comes from a sound hard boundary or two oppositely propagating identical TSAWs come together and interfere, then, generate SSAW. SSAWs always are applied for manipulating micro-objects and microfluidic actuation. 3D acoustic tweezers were created by Huang et al. [49] to capture and manipulate microparticles and cells along three mutually orthogonal axes using SSAWs (Fig. 2.3b). Standing-wave phase shifts were used to move particles or cells in-plane, while the amplitude of acoustic vibrations was utilized to control particle or cell motion along an orthogonal plane. The 3D acoustic tweezers were successfully used to pick up, translate, and print single cells and cell assemblies to create 2D and 3D structures in a label-free, contact-free, precise, and noninvasive manner. Commonly, suspended particles or cells within microfluidic systems were controlled to migrate a distance less than half the acoustic wavelength to the nearest pressure node of SSAWs which were generated by identical frequency, counter-propagating travelling waves. Thus, a periodic pattern of particles or cells was formed. Neild et al. [50] creatively used two counter-propagating travelling waves with different frequencies to create a substantially different force field. As a result, a much longer range force field was created causing particles to be gathered together in a single trapping site. Meanwhile, the location of the single trapping site could be controlled by the relative amplitude of the two waves. Cells or particles could be exactly migrated laterally across a fluid flow to defined locations using this approach. Concentration and separation of microparticles are of the same importance as cell enrichment and isolation [51]. Sung et al. [52] designed a pumpless acoustofluidic device by positioning two parallel IDTs underneath the PDMS microchannel. Larger particles were trapped and concentrated by the virtual acoustic radiation force field generated by the IDTs while the smaller particles were allowed to pass through the acoustic filter.

Acoustic-based cell isolation approaches offer a means of capturing single cells according to their size and physical properties in a label-free, contactless, and biocompatible manner. However, the need for bulky function generator and amplifier becomes the drawback of SAW-based devices and limits their portability. Future challenges are minimizing the affiliate accessories, realizing manipulation of cells in 3D structures using 2D acoustic wave as well as keeping the intact biophysical and biochemical properties of cells.

2.2.4 Magnetic Traps

Magnetic field is used to facilitate and effectively capture and isolate single cells because almost all cells are either diamagnetic or very weakly magnetic and easy to be selectively modified. Once the cells labeled with superparamagnetic (SPM) beads are exposed to a non-uniform magnetic field, they are manipulated by the field gradient forces and migrate toward the regions with the highest magnetic flux density [53–57]. Micromagnet devices are suitable for single-cell applications because they can control SPM beads with high-resolution enabling high-efficiency separation and analysis [58]. Kim et al. [59] fabricated a universal micromagnet junction using a remote magnetic field. By carefully designing the geometry of the junctions, MCF-7 and THP-1 cells were delivered and trapped in individual apartments with high fidelity. Lee et al. [60] present converging and diverging micromagnet arrays (MMAs) to focus, sort, and separate on-chip SPM beads. Converging MMAs were used to collect the SPM beads from a large region of the chip and focus them into synchronized lines. Diverging MMAs were used to transport the SPM beads and separate them according to their sizes. The transport of SPM bead-labelled single MDA-MB-231 cells was successfully controlled by regulating the magnetization of the micromagnet, the size of the beads and the rotation of the external magnetic field. A more complex micromagnet and circuit network were designed by Lim et al. [61] A class of integrated circuits were constructed from lithographically defined, overlaid patterns of magnetic film and current lines to execute sequential and parallel, timed operations on an ensemble of single particles and cells. Magnetic patterns were used to passively control particles similar to electrical conductors, diodes, and capacitors. Current lines were used to actively switch particles between different tracks similar to gated electrical transistors. Single cells were compartmentalized in trapping station providing a mean for single-cell level sample preparation. The generation and fine-tuning of the magnetic field was very important in constructing effective single cell-based analysis of target cells. A limit range of field gradient potentially led to aggregation of cells and nanoparticles. Huang et al. [62] integrated a micromagnet into a microfluidic system to enhance localized magnetic field up to eightfold stronger than that without the micromagnets improving cell capture efficiency to over 97% (Fig. 2.4a).

Microfabricated magnetic structures also have been created resulting in some novel bioanalytical systems. Kokkinis et al. [63] reported a fully automated and computer-controlled microfluidic platform to label and separate cancer cells utilizing functionalized magnetic particles. Following magnetic separation, the magnetically labeled cells were quantified for further analysis using integrated giant magnetoresistance sensors. Chen et al. [64] separated immunomagnetically labeled cells and encapsulated them with reagents into picoliter droplets for single-cell analysis on a microfluidic chip integrated with a mobile magnetic trap array. Single-cell sorting, reagent delivery, and cell compartmentalization were successively performed on the same chip reserving cell traits as originated from its native environment and reducing contamination chance. Magnetic nanostructures modified with antibody as probes

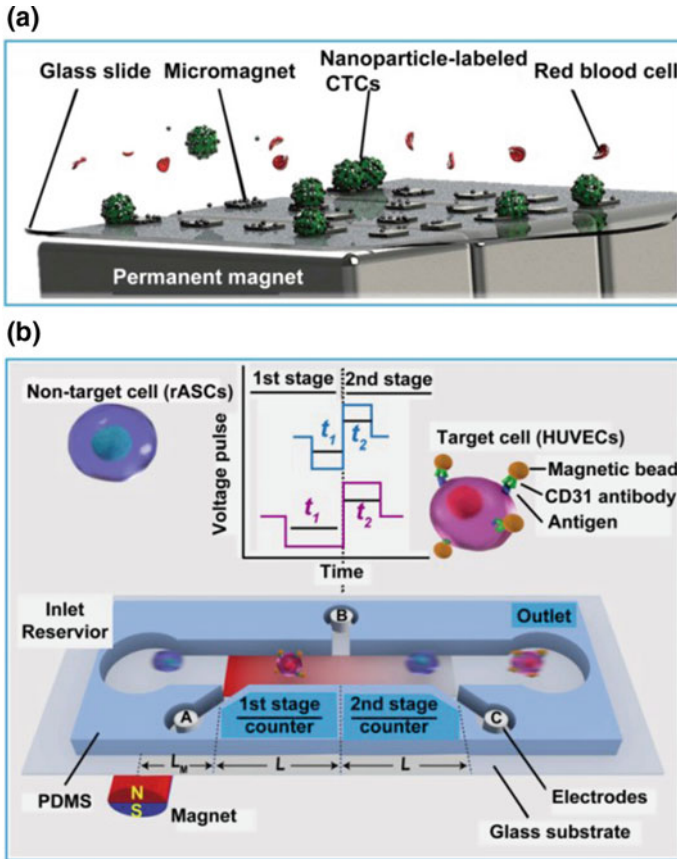


Fig. 2.4 Microfluidic magnetic traps for single-cell isolation. **a** Schematic illustration of the glass substrate patterned with micromagnets for screening of single circulating tumor cells (Reprinted with permission from Ref. [62]. Copyright 2015 Springer Nature Limited.). **b** Schematic of in situ single cell detection via microfluidic magnetic bead assay and micro Coulter counters (Reprinted with permission from Ref. [66]. Copyright 2017 Liu et al.)

were integrated onto a lateral flow immunoassay sensor to realize ultrasensitive naked-eye detection of pathogenic microorganisms at a near single-cell limit requiring no pre-enrichment or preculture steps [65]. Zhe et al. [66] present a single-cell detection device which consisted of two successive micro Coulter counters coupled with a high gradient magnetic field generated by an external magnet (Fig. 2.4b). The transit times of target and non-target cells were different, and thus, they could be identified. A target cell conjugated with magnetic beads had a longer transit time at the first counter than that at the second counter because it interacted with the magnetic field when it travelled through the two Coulter counters. In contrast, a non-target cell had nearly the same transit times through the two Coulter counters due to it had no interaction with the magnetic field.

Magnetic traps are useful in single-cell capture and suitable to be combined with other cell analysis techniques. The key for future magnetic microtrap development is to generate the magnetic flux density peaks at a spatial resolution comparable to the cell dimension and pattern the on-chip magnetic sources to produce desired magnetic flux [67].

2.2.5 *Hydrodynamic Traps*

Hydrodynamic phenomena are universal in living organisms and influence multiple cellular properties and processes. With the advent of microfluidic technologies and accumulation knowledge of fluid mechanics at the micrometer-length scale, microfluidic hydrodynamics emerges as a new generation of experimental tools emulating and providing control over cellular microenvironments experienced *in vivo* [68]. We developed a Dean flow-induced cell ordering platform to separate cells from a cell suspension and analyze lipids in single cells through connecting to an electrospray ionization mass spectrometer [69]. Microfluidic hydrodynamic cell separation methods use specific microstructures and valves in microfluidic channels to control the fluid flow and isolate single cells based on their size differences. This method presents high retrieval ability and throughput without using external apparatus.

Commonly, the cell separation methods based on hydrophoresis are simple but rely on complicated microstructures. Di Carlo et al. [70] reported the first hydrodynamic trapping device based on U-shaped trapping structures for high-throughput single-cell studies. Takeuchi et al. [71] developed a cell-trapping device to pattern single cells in well-controlled order and morphology. The device is comprised of a parylene sheet which was used for assembling cells and a microcomb which was utilized for controlling the cell-trapping area. Cooper-White et al. [72] incorporated a U-shaped hydrodynamic trap into the downstream wall of each microwell to trap single cells in a high-throughput manner and at high trapping efficiency. We simply fabricated microwell arrays for high-throughput single-cell capture and analysis by molding a monolayer of ordered PS microspheres. PS microspheres were self-assembled on a glass slide and heated to partially melt mainly from the bottom at 240 °C. The partially melted PS arrays were used as a master to microwell arrays [73]. PDMS microwell arrays were utilized by us to capture single cells with defined cell density and intercellular space. By combing with microchannels for quantum dot (QD) solution diffusion, cell cycle-dependent QD cytotoxicity and cellular uptake were observed on this microfluidic platform [74].

Circulating tumor cells (CTCs) as a strong biomarker are very rare and require precise separation and detection for effective clinical applications. We developed a particle sorter by overlapping two pieces of porous membranes. The particle sorter was capable of separating PS microbeads with different sizes as well as different components of whole blood and showed promise in CTC separation [75]. A flow-restricted microfluidic trap array reported by Lee et al. was capable of

capturing single CTCs. The extent of flow restriction was correlated with the device geometry and optimized to achieve 97% capture efficiency with a single-cell capture rate of 99% [76]. Benavente-Babace et al. [77] selectively trapped and treated single cells via co-flow within a microfluidic platform. The versatile combination of coexisting laminar flow manipulation and hydrodynamic single-cell trapping offered a cost-effective solution for studying single cells. Laminar flow was utilized by us to give in situ partial treatment on single cells. A stable distribution of microenvironments was generated around a single adherent cell realizing manipulation of partial region of the single cell [78]. We also used laminar flow as fluid cell knife to precisely cut off a single cell from its remaining portion. Temporal wound repair was successfully observed [79]. Cylindrical-shaped micropillar array was fabricated in a microfluidic device to act as a sieve for breaking cell clusters into single cells and isolate them into individual micro-hydrogels. The combination of hydrodynamic forces and a flow-focusing technique improved the probability of encapsulation of a single cell into each hydrogel with a broad range of cell concentrations [80]. Lee et al. [81] present an interfacial hydrodynamic technique to encapsulate single cells. Cells were initially trapped in micro-vortices and later released one-to-one into the droplets controlling by the width of the outer streamline that separated the vortex from the flow through the streaming passage adjacent to the aqueous-oil interface. Brouzes et al. [82] conducted true single-cell encapsulation based on the sequential capture and original encapsulation of single cells into a series of hydrodynamic traps. As shown in Fig. 2.5a, each trap consisted of two flow paths. An incoming cell progressed through the unoccupied trapping pathway until it blocked the entrance of the trapping channel. The cell plugged that flow path and further flow was diverted through the bypass channel reconfiguring the local flow topology. The same cell-plugging principle was harnessed to encapsulate single cells. The injected oil was diverted toward the bypass channel and thus surrounded the chamber containing a single cell. Droplet sequentially generated at all occupied traps resulting in true single-cell encapsulation.

Hydrodynamic traps always are combined with other microfluidic techniques to be developed for on-chip single-cell capture and manipulation. Microfluidic valving techniques are one kind of technologies frequently combined with hydrodynamic traps. Seshia et al. [83] developed a multilayer device composed of hydrodynamic trapping and microfluidic valving techniques for manipulating and imaging of single cells and particles. The flow layer in the device was designed to capture single particles or cells with trapping channels and the control layer was developed to selectively control the trap and release processes with valve channels. The trapping efficiency of single particles was greater than 95%. Single particles and cells are allowed to be trapped, released, and manipulated by simply controlling corresponding valves. Wang et al. [84] combined pneumatic microvalve arrays (P μ VAs) and hydrodynamic single-cell trapping sites in a single microfluidic device to generate single-cell arrays (Fig. 2.5b). P μ VAs were designed to guide multiple types of cells being trapped in the corresponding single-cell trapping sites located in the fluidic channel. A multiplex single-cell array with three different types of cells was successfully realized. Electrical impedance spectroscopy also was combined with

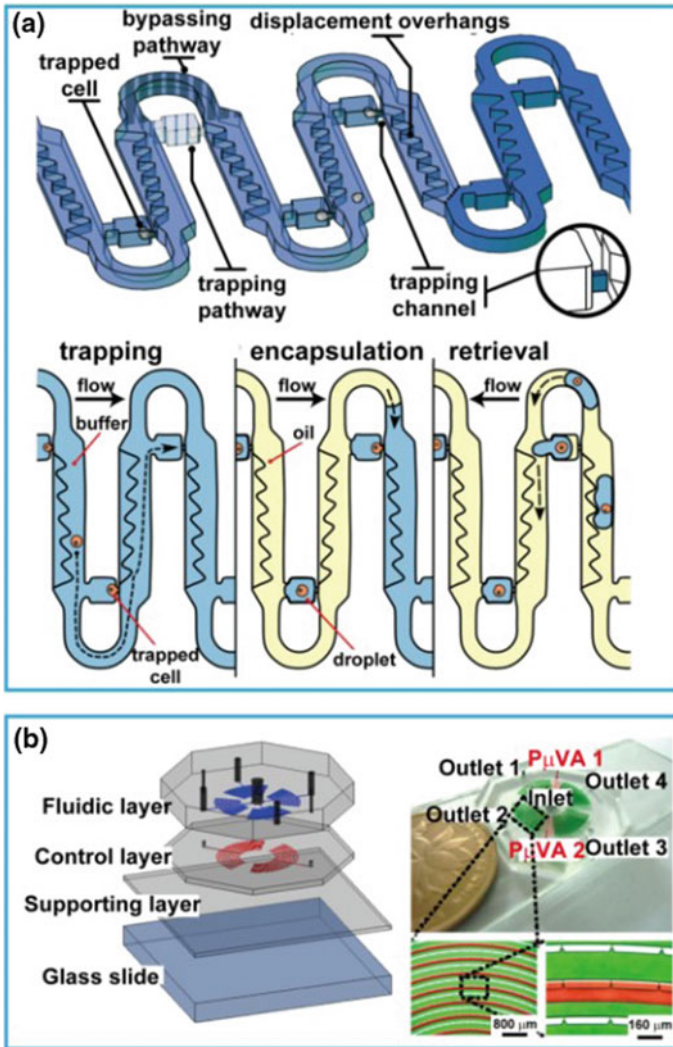


Fig. 2.5 Microfluidic hydrodynamic approaches for single cell capture and isolation. **a** Schematic representation of the microfluidic circuit and work flow for true single-cell encapsulation (Reprinted with permission from Ref. [82]. Copyright The Royal Society of Chemistry 2017.). **b** P μ VAs-combined hydrodynamic single-cell trapping sites in a single microfluidic device (Reprinted with permission from Ref. [84]. Copyright 2016 published by Elsevier B.V.)

hydrodynamic trapping to efficiently trap single cells as well as provide sensitive and label-free electrical impedance measurements of individual cells. The composite device enabled it to simultaneously analyze physical state and heterogeneity of a cell population. A hybrid microfluidic system that combined hydrodynamic trapping and acoustic switching also was demonstrated to organize an array of single cells at high

density [85]. A microfluidic trifurcation was formed by balancing the hydrodynamic resistances of three parallel channel segments in order to capture single cells in a high-density array. Then, the cells were transferred into adjacent larger compartments by an active acoustic transfer for single-cell measurements.

Microfluidic systems driven by pure hydrodynamic forces show great promises for applying in single-cell capture and isolation. Size or shape differences of the separated cells are the prerequisite for the technique to be applied. Future efforts focus on design and fabrication of the geometry of the microchannels which is critical for hydrodynamic devices.

2.3 Biochemical Microfluidic Approaches

The differences of physical properties between target cells and background cells are the prerequisite to adopt physical techniques to capture and isolate single cells. Biochemical approaches based on affinity are another way to capture and isolate cells by taking advantage of the formation of noncovalent bonds between affinity ligands and cell surface markers. These methods are particularly well suited to the conditions that target cells are physically similar to the background cells [86].

2.3.1 *Immunoaffinity*

Antibody as one kind of affinity ligand can selectively capture the target cells while others are passed through. Cell capture methods consequently constructed are called immunoaffinity-based approaches. Antibody always is modified onto microwells to efficiently capture single cells. The first microwell-based single-cell immunoassay was developed by Love et al. depending on micro-engraving method [87]. Microarrays engraved by soft lithographic method enabled a rapid and high-throughput system for identification, recovery, and clonal expansion of cells producing antigen-specific antibodies. Cytokine secretion from single cells has also been analyzed. Single cells were confined with antibody-modified sensing beads inside 20 picoliter microcompartments for monitoring cellular release of cytokine and exosome (Fig. 2.6a). ~7000 microchambers were fabricated in the roof of the microfluidic device which was micropatterned to contain cell attachment sites. The capture of cell-secreted molecules onto microbeads was followed by binding of secondary antibodies generating fluorescent signals. The fluorescent intensity indicated dynamics of single-cell secretory activity [88]. Alginate microparticles were functionalized as permeable cell culture chambers to capture single cells secreting antigen-specific antibodies and prevent the cross-talk between the neighboring encapsulated cells [89]. Photodegradable hydrogel array was micropatterned onto a reconfigurable microfluidic device to enable cell secretion analysis and cell retrieval at single-cell level (Fig. 2.6b). Fluorescence resonance

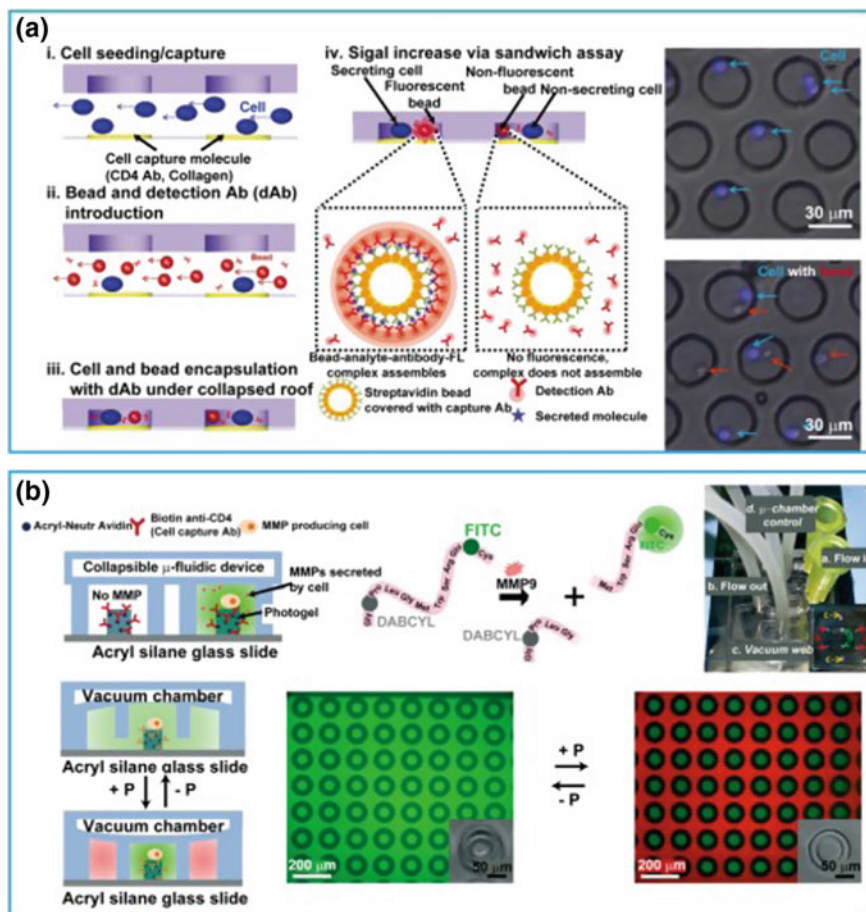


Fig. 2.6 Immunoaffinity-base approaches for single-cell capture and analysis on microfluidic devices. **a** Microcompartment arrays for isolating single cells and sensing beads modified by antibodies for monitoring cellular secretory activity (Reprinted with permission from Ref. [88]. Copyright The Royal Society of Chemistry 2016.). **b** A reconfigurable microfluidic system integrated photodegradable hydrogel microstructures for single-cell analysis and retrieval (Reprinted with permission from Ref. [90]. Copyright The Royal Society of Chemistry 2015.)

energy transfer (FRET) peptides were entrapped inside microfabricated compartments to monitor the activity of protease molecules secreted from single cells. The hydrogel islands tethering cells to the surface could be degraded by UV exposure to release specific single cells of interest [90]. Shin et al. [91] also developed a strategy to isolate and sort cells based on photodegradable hydrogel. Leukocyte-specific antibodies were printed on the photogel-covered substrates to capture specific cell and detect cytokine secretion. Single cells of interest were released through regiospecifically degrading the photogel. Huang et al. [92] developed a 3D scaffold chip with thermosensitive gelatin hydrogel coating for high-efficiency capture and

release of individual and cluster CTCs. The gelatin hydrogel was functionalized with anti-EpCAM monoclonal antibody making the 3D scaffold chip combine the specific recognition and physically obstructed effect to significantly improve cell capture efficiency. Because of the similar length scales, microfluidic approaches are suitable to isolate, analyze, and culture single cells to extend single-cell characterization from nucleic acids to proteins to final functional behavior [93, 94]. Chen et al. [95] present a constriction channel integrated microfluidic flow cytometer enabling absolute quantification of single-cell intracellular proteins. Single cells were stained with fluorescence-labeled antibodies and forced to squeeze through the constriction channel to quantify the fluorescence intensities. Solutions with fluorescence-labeled antibodies were flushed into the constriction channel to obtain calibration curves. Absolute quantification of intracellular proteins was realized by combining raw fluorescence data and calibration curves. Deng et al. [96] developed a microfluidic system conjugated with photocleavable ssDNA-encoded antibody for streamlining isolation, purification, and single-cell secretomic profiling of CTCs from whole blood. CTCs in patient blood were found to exhibit highly heterogeneous secretion profile of interleukin-8 (IL-8) and VEGF. Using the specific antigen-antibody reaction, this kind of biochemical approach for single-cell capture results in very high-accuracy enrichment. The big challenge is that the biomarker expression levels of single cells are not certain so it desirable to develop more comprehensive and efficient immunoaffinity approaches to capture single cells.

2.3.2 *Aptamer-Based Approaches*

Aptamers are short single-stranded sequences of nucleic acids which can specifically bind with target cells through folding into unique secondary and tertiary conformations [97–99]. Aptamer-based microfluidic affinity cell separation methods are consequently developed and show some attractive advantages: (1) Aptamers present higher stability that withstanding high temperature and extreme pH. (2) Surface immobilization of aptamers is more efficient because of their nanometer sizes so aptamer-based separation methods can be used to capture target cells under flowing conditions. (3) The operation process is more simple and adaptable for following single-cell analysis [100–102].

We integrated cell-recognizable aptamer-encoded microwells onto a microfluidic platform to isolate single tumor cells. The specifically designed microwells enable strong 3D local topographic interactions between target cell surface and biomolecules realizing satisfied single-cell occupancy and unique bioselectivity [103]. Cui et al. [104] designed three kinds of spectrally orthogonal surface-enhanced Raman spectroscopy (SERS) aptamer nanovectors combined with size-based microfluidic cell isolation to provide individual cells with composite spectral signatures in accordance with surface protein expression. A revised classic least square algorithm was employed to obtain the 3D phenotypic information at single-cell resolution to statistically demultiplex the complex SERS signature and profile the cellular

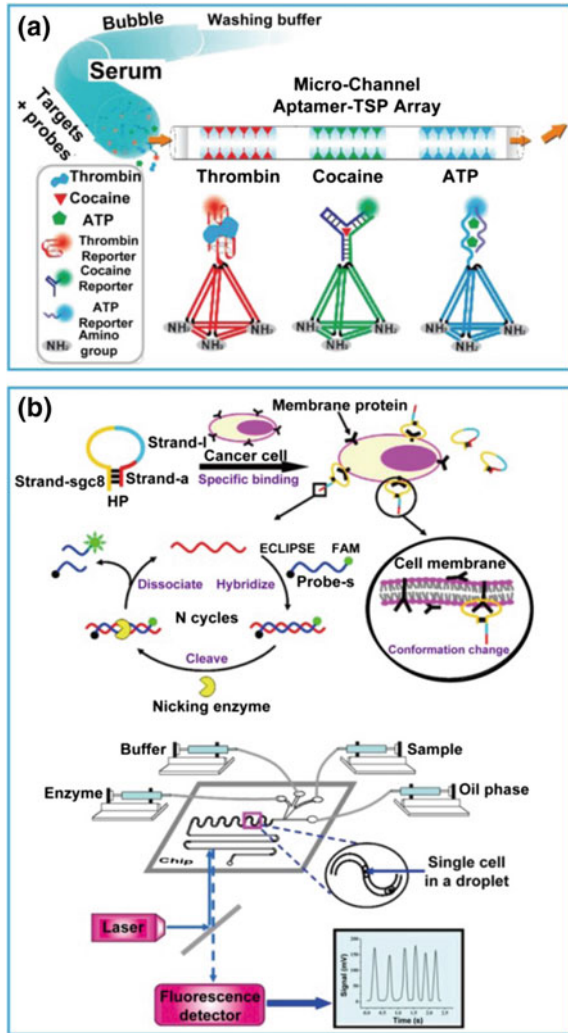
proteomic phenotype. Figdor et al. [105] developed a cell membrane-anchored fluorescent aptamer sensor and combined it with a droplet-microfluidic platform to probe the cytokine production of single cells. The type II interferon ($\text{IFN}\gamma$) aptamer was anchored to cell membrane and its two ends were labeled with a ROX fluorophore and a TAO quencher, respectively. At the initiation stage, ROX and TAO were kept in close proximity due to the formation of the hairpin structure resulting in fluorescent quench. Upon binding with $\text{IFN}\gamma$, the aptamer probe switched into a specific tertiary structure separating the fluorophore from the quencher and leading to fluorescent restoration. Pei et al. [106] immobilized DNA aptamers onto the inner surfaces of a glass capillary to develop a rapid DNA nanostructure scaffold-supported aptamer pull-down (DNAPull) assay in a nano- or picoliter droplet for applications in single-cell analysis (Fig. 2.7a). DNA aptamers were employed to ensure highly selective recognition of target molecules. Automatic sample delivery and convective transport with pressure-driven fluid flow were introduced to improve the rate of the DNAPull assay. Tang et al. [107] detected membrane protein on single living cells by aptamer and nicking enzyme-assisted fluorescence signal amplification in microfluidic droplets (Fig. 2.7b). Membrane protein-triggered conformation alteration of hairpin (HP) probe could improve the detection accuracy with the elimination of several washing and separation steps. The highly monodisperse droplet functioned as an independent microreactor for the aptamer and nicking enzyme-assisted fluorescence signal amplification providing a high-throughput platform for the detection of a single cell. Strano et al. [108] conjugated an aptamer-anchor polynucleotide sequence to near-infrared emissive single-walled carbon nanotubes to fabricate nanosensor arrays. Individual proteins from microorganisms immobilized in a microfluidic chamber were measured with ultralow detection limits and in real time. The successful detection of a unique protein product resulting from T7 bacteriophage infection of *Escherichia coli* illustrated that nanosensor arrays can enable real-time, single-cell analysis of a broad range of protein products from various cell types.

Aptamers, referred as “chemical antibodies”, have been developed to be powerful tools for cellular applications. However, aptamers are not surrogates for antibodies. Specificity is the particular advantage of aptamers also becomes their shortage. Various aptamers need to be generated or multiplexed aptamers have to be used to deal with different cell samples or target analytes. Stability is another concern for aptamers which are easily degraded by nuclease. As a result, aptamers are needed to be modified or incorporated with non-natural bases [99].

Besides antibody and aptamer, other biochemical interactions also were explored to capture single cells. We reported a live single-cell extractor (LSCE) to extract single adhered cells to understand cell heterogeneity and the connections of various single-cell behaviors (Fig. 2.8). Trypsin cell-extracting solution was injected by the tip of LSCE to digest the cell-adhesion molecules connecting the adhered cell and the extracellular matrix. The digested single cell was aspirated for the following analysis [109]. Further, the LSCE was utilized to reveal the cell-matrix adhesion

Fig. 2.7 Aptamer-based approaches for single-cell capture and analysis on microfluidic devices.

a DNaPull assay under convective flux in a glass capillary for analyzing the contents of droplets with nano- or picoliter volumes and single-cell samples (Reprinted with permission from Ref. [106]. Copyright 2017 American Chemical Society.). **b** Schematic representation of the aptamer and nicking enzyme-assisted signal amplification assay for membrane protein on single living cells combined with microfluidic droplet system (Reprinted with permission from Ref. [107]. Copyright 2014 American Chemical Society.)



strength at single-cell resolution and evaluate the influences of different biomaterials on cell adhesion [110]. Adhesion strength of single CTCs on a base layer of endothelial cells (ECs) also was clarified by the LSCE. Moreover, the drug influence on the adhesion strength of single CTCs on ECs was uncovered implying drug screening for tumor therapy [111].

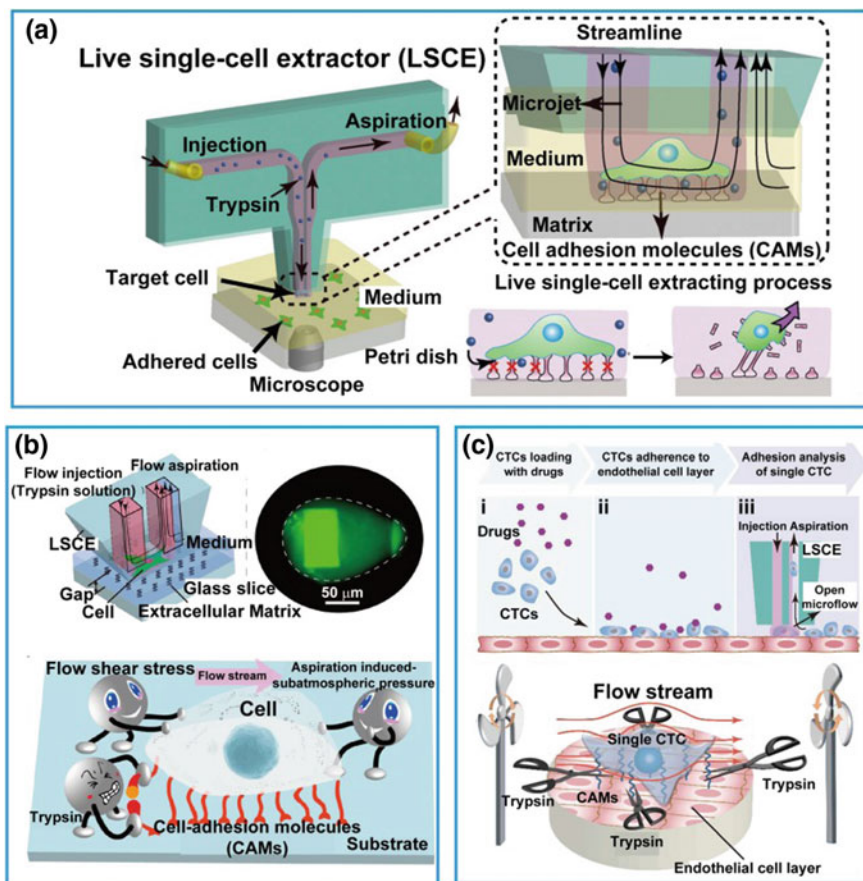


Fig. 2.8 LSCE applied in single-cell analysis. **a** Schematic illustration of LSCE (Reprinted with permission from Ref. [109]. Copyright 2018 Wiley-VCH Verlag GmbH & Co. KGaA, Weinheim.). **b** LSCE was applied in measuring cell-matrix adhesion at single-cell resolution to reveal the functions of biomaterials for adherent cell culture (Reprinted with permission from Ref. [110]. Copyright 2018 American Chemical Society.). **c** LSCE was applied in analyzing adhesion strength of single CTCs on an EC layer (Reprinted with permission from Ref. [111]. Copyright 2018 The Royal Society of Chemistry.)

2.4 Conclusions and Remarks

Cellular heterogeneity calls for analysis on single-cell level which requires capture and isolation of single cells at first. As reviewed above, a rich library of technologies is available for precise single-cell capture. All the technologies in this chapter show their own innovative advances and specific challenges.

Physical principle-based approaches capture and isolate single cells based on their physical properties and usually do not need to label cells. Optical tweezers are

universal in laboratories and capture single cells with high precision depending on the refractive index, size, or shape of the cells. The external detector complicates the microsystem and the one-beam-one-trap nature limits the throughput. High-throughput and simple fabrication are the two aims for future development of optical tweezers. DEP manipulates and separates single cells by utilizing their dielectric characteristics in the non-uniform electric fields. Joule-heating effect and damage of cells caused by microelectrodes are two defects needing to be reduced or avoided. SAWs push cells toward the designed regions with acoustic radiation pressure generated by an acoustic field preserving cell integrity, functionality and viability. However, bulky function generator and amplifier are necessary affiliate accessories for SAW-based microfluidic techniques. Future development direction is minimizing or eliminating these accessories. Single cells are facily and effectively captured by magnetic traps because they are easily to be labeled with magnetic beads. Fabrication of magnetic materials or structures compatible with microfluidic chips is future challenging. Hydrodynamic traps capture single cells according to their size or shape differences relying on complicated and specifically designed microstructures. As a result, future efforts will give on designing the geometry of the microstructures or integrating more microfluidic modules on one chip. Biochemical approaches are another way to capture single cells based on the interactions between affinity ligands and cell surface markers. Therefore, it is highly desirable to identify more biomarkers to develop more accurate capture.

High integration is one of the remarkable features of microfluidics. Consequently, the future trend is integrating multiple of these approaches to perform complex single-cell capture and isolation tasks as well as the downstream analysis on one platform.

References

1. Wu J, Chen Q, Lin J (2017) Microfluidic technologies in cell isolation and analysis for biomedical applications. *Analyst* 142(3):421–441. <https://doi.org/10.1039/c6an01939k>
2. Joensson HN, Andersson Svahn H (2012) Droplet microfluidics—a tool for single-cell analysis. *Angew Chem, Int Edit* 51(49):12176–12192. <https://doi.org/10.1002/anie.201200460>
3. Eyer K, Kuhn P, Hanke C, Dittrich PS (2012) A microchamber array for single cell isolation and analysis of intracellular biomolecules. *Lab Chip* 12(4):765–772. <https://doi.org/10.1039/c2lc20876h>
4. Lo S, Yao D (2015) Get to understand more from single-cells: current studies of microfluidic-based techniques for single-cell analysis. *Int J Mol Sci* 16(8):16763–16777. <https://doi.org/10.3390/ijms160816763>
5. Hosc S, Murthy SK, Koppes AN (2016) Microfluidic sample preparation for single cell analysis. *Anal Chem* 88(1):354–380. <https://doi.org/10.1021/acs.analchem.5b04077>
6. Schoeman RM, Kemna EWM, Wolbers F, van den Berg A (2014) High-throughput deterministic single-cell encapsulation and droplet pairing, fusion, and shrinkage in a single microfluidic device. *Electrophoresis* 35(2–3):385–392. <https://doi.org/10.1002/elps.201300179>

7. Lin L, Chen Q, Sun J (2018) Micro/nanofluidics-enabled single-cell biochemical analysis. *TrAC. Trends Anal Chem* 99:66–74. <https://doi.org/10.1016/j.trac.2017.11.017>
8. Cheng S, Xie M, Xu J, Wang J, Lv S, Guo S, Shu Y, Wang M, Dong W, Huang W (2016) High-efficiency capture of individual and cluster of circulating tumor cells by a microchip embedded with three-dimensional poly(dimethylsiloxane) scaffold. *Anal Chem* 88 (13):6773–6780. <https://doi.org/10.1021/acs.analchem.6b01130>
9. Wyatt Shields C IV, Reyes CD, Lopez GP (2015) Microfluidic cell sorting: a review of the advances in the separation of cells from debulking to rare cell isolation. *Lab Chip* 15 (5):1230–1249. <https://doi.org/10.1039/c4lc01246a>
10. Zhu X, Chu J, Wang Y (2017) Advances in microfluidics applied to single cell operation. *Biotechnol J* 13(2):1700416. <https://doi.org/10.1002/biot.201700416>
11. Khan M, Mao S, Li W, Lin J (2018) Microfluidic devices in the fast-growing domain of single-cell analysis. *Chem Eur J* 24(58):15398–15420. <https://doi.org/10.1002/chem.201800305>
12. Fan Y, Dong D, Li Q, Si H, Pei H, Li L, Tang B (2018) Fluorescent analysis of bioactive molecules in single cells based on microfluidic chips. *Lab Chip* 18(8):1151–1173. <https://doi.org/10.1039/c7lc01333g>
13. Reece A, Xia B, Jiang Z, Noren B, McBride R, Oakey J (2016) Microfluidic techniques for high throughput single cell analysis. *Curr Opin Biotech* 40:90–96. <https://doi.org/10.1016/j.copbio.2016.02.015>
14. Avesar J, Arye TB, Levenberg S (2014) Frontier microfluidic techniques for short and long-term single cell analysis. *Lab Chip* 14(13):2161–2167. <https://doi.org/10.1039/c4lc00013g>
15. Murphy TW, Zhang Q, Naler LB, Ma S, Lu C (2018) Recent advances in the use of microfluidic technologies for single cell analysis. *Analyst* 143(1):60–80. <https://doi.org/10.1039/c7an01346a>
16. Huang L, Bian S, Cheng Y, Shi G, Liu P, Ye X, Wang W (2017) Microfluidics cell sample preparation for analysis: Advances in efficient cell enrichment and precise single cell capture. *Biomicrofluidics* 11(1):11501. <https://doi.org/10.1063/1.4975666>
17. Collins DJ, Neild A, DeMello A, Liu A, Ai Y (2015) The Poisson distribution and beyond: methods for microfluidic droplet production and single cell encapsulation. *Lab Chip* 15 (17):3439–3459. <https://doi.org/10.1039/c5lc00614g>
18. Liu J, Gao D, Li H, Lin J (2009) Controlled photopolymerization of hydrogel microstructures inside microchannels for bioassays. *Lab Chip* 9(9):1301–1305. <https://doi.org/10.1039/b819219g>
19. Liu J, Gao D, Mao S, Lin J (2012) A microfluidic photolithography for controlled encapsulation of single cells inside hydrogel microstructures. *Sci China Chem* 55(4):494–501. <https://doi.org/10.1007/s11426-012-4538-5>
20. Lei T, Poon AW (2013) Silicon-on-insulator multimode-interference waveguide-based arrayed optical tweezers (SMART) for two-dimensional microparticle trapping and manipulation. *Opt Express* 21(2):1520–1530. <https://doi.org/10.1364/oe.21.001520>
21. Burger R, Kurzbuch D, Gorkin R, Kijanka G, Glynn M, McDonagh C, Ducreé J (2015) An integrated centrifugo-opto-microfluidic platform for arraying, analysis, identification and manipulation of individual cells. *Lab Chip* 15(2):378–381. <https://doi.org/10.1039/c4lc01002g>
22. Liberale C, Cojoc G, Bragheri F, Minzioni P, Perozziello G, La Rocca R, Ferrara L, Rajamanickam V, Di Fabrizio E, Cristiani I (2013) Integrated microfluidic device for single-cell trapping and spectroscopy. *Sci Rep* 3:1258. <https://doi.org/10.1038/srep01258>
23. Li X, Cheah CC, Hu S, Sun D (2013) Dynamic trapping and manipulation of biological cells with optical tweezers. *Automatica* 49(6):1614–1625. <https://doi.org/10.1016/j.automatica.2013.02.067>
24. Decrop D, Brans T, Gijsenbergh P, Lu J, Spasic D, Kokalj T, Beunis F, Goos P, Puers R, Lammertyn J (2016) Optical manipulation of single magnetic beads in a microwell array on

- a digital microfluidic chip. *Anal Chem* 88(17):8596–8603. <https://doi.org/10.1021/acs.analchem.6b01734>
25. Casabella S, Scully P, Goddard N, Gardner P (2016) Automated analysis of single cells using laser Tweezers Raman Spectroscopy. *Analyst* 141(2):689–696. <https://doi.org/10.1039/c5an01851j>
 26. Huang K, Wu Y, Lee J, Chiou P (2013) Microfluidic integrated optoelectronic tweezers for single-cell preparation and analysis. *Lab Chip* 13(18):3721–3727. <https://doi.org/10.1039/c3lc50607j>
 27. Kotnala A, Zheng Y, Fu J, Cheng W (2017) Microfluidic-based high-throughput optical trapping of nanoparticles. *Lab Chip* 17(12):2125–2134. <https://doi.org/10.1039/c7lc00286f>
 28. Chen J, Cong H, Loo F, Kang Z, Tang M, Zhang H, Wu S, Kong S, Ho H (2016) Thermal gradient induced tweezers for the manipulation of particles and cells. *Sci Rep* 6:35814. <https://doi.org/10.1038/srep35814>
 29. Li M, Anand RK (2018) Cellular dielectrophoresis coupled with single-cell analysis. *Anal Bioanal Chem* 410(10):2499–2515. <https://doi.org/10.1007/s00216-018-0896-y>
 30. Menachery A, Kumawat N, Qasaimeh M (2017) Label-free microfluidic stem cell isolation technologies. *TrAC. Trends Anal Chem* 89:1–12. <https://doi.org/10.1016/j.trac.2017.01.008>
 31. Wu C, Chen R, Liu Y, Yu Z, Jiang Y, Cheng X (2017) A planar dielectrophoresis-based chip for high-throughput cell pairing. *Lab Chip* 17(23):4008–4014. <https://doi.org/10.1039/c7lc01082f>
 32. Zhang P, Ren L, Zhang X, Shan Y, Wang Y, Ji Y, Yin H, Huang WE, Xu J, Ma B (2015) Raman-activated cell sorting based on dielectrophoretic single-cell trap and release. *Anal Chem* 87(4):2282–2289. <https://doi.org/10.1021/ac503974e>
 33. Anand RK, Johnson ES, Chiu DT (2015) Negative dielectrophoretic capture and repulsion of single cells at a bipolar electrode: the impact of faradaic ion enrichment and depletion. *J Am Chem Soc* 137(2):776–783. <https://doi.org/10.1021/ja5102689>
 34. Guo X, Zhu R, Zong X (2015) A microchip integrating cell array positioning with in situ single-cell impedance measurement. *Analyst* 140(19):6571–6578. <https://doi.org/10.1039/c5an01193k>
 35. Guo X, Zhu R (2015) Controllably moving individual living cell in an array by modulating signal phase difference based on dielectrophoresis. *Biosens Bioelectron* 68:529–535. <https://doi.org/10.1016/j.bios.2015.01.052>
 36. Kung Y, Huang K, Chong W, Chiou P (2016) Tunnel dielectrophoresis for tunable, single-stream cell focusing in physiological buffers in high-speed microfluidic flows. *Small* 12(32):4343–4348. <https://doi.org/10.1002/sml.201600996>
 37. Kim SH, Fujii T (2016) Efficient analysis of a small number of cancer cells at the single-cell level using an electroactive double-well array. *Lab Chip* 16(13):2440–2449. <https://doi.org/10.1039/c6lc00241b>
 38. Chen N, Chen C, Chen M, Jang L, Wang M (2014) Single-cell trapping and impedance measurement utilizing dielectrophoresis in a parallel-plate microfluidic device. *Sens Actuators B: Chem* 190:570–577. <https://doi.org/10.1016/j.snb.2013.08.104>
 39. Ameri SK, Singh PK, Dokmeci MR, Khademhosseini A, Xu Q, Sonkusale SR (2014) All electronic approach for high-throughput cell trapping and lysis with electrical impedance monitoring. *Biosens Bioelectron* 54:462–467. <https://doi.org/10.1016/j.bios.2013.11.031>
 40. Goel M, Verma A, Gupta S (2018) Electric-field driven assembly of live bacterial cell microarrays for rapid phenotypic assessment and cell viability testing. *Biosens Bioelectron* 111:159–165. <https://doi.org/10.1016/j.bios.2018.04.005>
 41. Nguyen EP, Lee L, Rezk AR, Sabri YM, Bhargava SK, Yeo LY (2018) Hybrid surface and bulk resonant acoustics for concurrent actuation and sensing on a single microfluidic device. *Anal Chem* 90(8):5335–5342. <https://doi.org/10.1021/acs.analchem.8b00466>
 42. Bachman H, Huang P, Zhao S, Yang S, Zhang P, Fu H, Huang TJ (2018) Acoustofluidic devices controlled by cell phones. *Lab Chip* 18(3):433–441. <https://doi.org/10.1039/c7lc01222e>

43. Barani A, Paktinat H, Janmaleki M, Mohammadi A, Mosaddegh P, Fadaei-Tehrani A, Sanati-Nezhad A (2016) Microfluidic integrated acoustic waving for manipulation of cells and molecules. *Biosens Bioelectron* 85:714–725. <https://doi.org/10.1016/j.bios.2016.05.059>
44. Lu X, Soto F, Li J, Li T, Liang Y, Wang J (2017) Topographical manipulation of microparticles and cells with acoustic microstreaming. *ACS Appl Mater Inter* 9(44):38870–38876. <https://doi.org/10.1021/acsami.7b15237>
45. Schmid L, Weitz DA, Franke T (2014) Sorting drops and cells with acoustics: acoustic microfluidic fluorescence-activated cell sorter. *Lab Chip* 14(19):3710–3718. <https://doi.org/10.1039/c4lc00588k>
46. Teh S, Lin R, Hung L, Lee AP (2008) Droplet microfluidics. *Lab Chip* 8(2):198–220. <https://doi.org/10.1039/b715524g>
47. Rambach RW, Biswas P, Yadav A, Garstecki P, Franke T (2018) Fast selective trapping and release of picoliter droplets in a 3D microfluidic PDMS multi-trap system with bubbles. *Analyst* 143(4):843–849. <https://doi.org/10.1039/c7an01100h>
48. Rambach RW, Linder K, Heymann M, Franke T (2017) Droplet trapping and fast acoustic release in a multi-height device with steady-state flow. *Lab Chip* 17(20):3422–3430. <https://doi.org/10.1039/c7lc00378a>
49. Guo F, Mao Z, Chen Y, Xie Z, Lata JP, Li P, Ren L, Liu J, Yang J, Dao M, Suresh S, Huang TJ (2016) Three-dimensional manipulation of single cells using surface acoustic waves. *Proc Natl Acad Sci U S A* 113(6):1522. <https://doi.org/10.1073/pnas.1524813113>
50. Ng JW, Devendran C, Neild A (2017) Acoustic tweezing of particles using decaying opposing travelling surface acoustic waves (DOTSAW). *Lab Chip* 17(20):3489–3497. <https://doi.org/10.1039/c7lc00862g>
51. Kishor R, Ma Z, Sreejith S, Seah YP, Wang H, Ai Y, Wang Z, Lim T, Zheng Y (2017) Real time size-dependent particle segregation and quantitative detection in a surface acoustic wave-photoacoustic integrated microfluidic system. *Sens and Actuators B-Chem* 252:568–576. <https://doi.org/10.1016/j.snb.2017.06.006>
52. Ahmed H, Destgeer G, Park J, Jung JH, Ahmad R, Park K, Sung HJ (2017) A pumpless acoustofluidic platform for size-selective concentration and separation of microparticles. *Anal Chem* 89(24):13575–13581. <https://doi.org/10.1021/acs.analchem.7b04014>
53. Alon N, Havdala T, Skaat H, Baranes K, Marcus M, Levy I, Margel S, Sharoni A, Shefi O (2015) Magnetic micro-device for manipulating PC12 cell migration and organization. *Lab Chip* 15(9):2030–2036. <https://doi.org/10.1039/c5lc00035a>
54. Cao Q, Han X, Li L (2014) Configurations and control of magnetic fields for manipulating magnetic particles in microfluidic applications: magnet systems and manipulation mechanisms. *Lab Chip* 14(15):2762–2777. <https://doi.org/10.1039/c4lc00367e>
55. Hejazian M, Li W, Nguyen N (2015) Lab on a chip for continuous-flow magnetic cell separation. *Lab Chip* 15(4):959–970. <https://doi.org/10.1039/c4lc01422g>
56. Zhang Y, Nguyen N (2017) Magnetic digital microfluidics—a review. *Lab Chip* 17(6):994–1008. <https://doi.org/10.1039/c7lc00025a>
57. Jamshaid T, Neto ETT, Eissa MM, Zine N, Kunita MH, El-Salhi AE, Elaissari A (2016) Magnetic particles: from preparation to lab-on-a-chip, biosensors, microsystems and microfluidics applications. *TrAC. Trends Anal Chem* 79:344–362. <https://doi.org/10.1016/j.trac.2015.10.022>
58. Rampini S, Li P, Lee GU (2016) Micromagnet arrays enable precise manipulation of individual biological analyte–superparamagnetic bead complexes for separation and sensing. *Lab Chip* 16(19):3645–3663. <https://doi.org/10.1039/c6lc00707d>
59. Hu X, Lim B, Torati SR, Ding J, Novosad V, Im M, Reddy V, Kim K, Jung E, Shawl AI, Kim E, Kim C (2018) Autonomous magnetic microrobots by navigating gates for multiple biomolecules delivery. *Small* 14(25):1800504. <https://doi.org/10.1002/smll.201800504>
60. Rampini S, Kilinc D, Li P, Monteil C, Gandhi D, Lee GU (2015) Micromagnet arrays for on-chip focusing, switching, and separation of superparamagnetic beads and single cells. *Lab Chip* 15(16):3370–3379. <https://doi.org/10.1039/c5lc00581g>

61. Lim B, Reddy V, Hu X, Kim K, Jadhav M, Abedini-Nassab R, Noh Y, Lim YT, Yellen BB, Kim C (2014) Magnetophoretic circuits for digital control of single particles and cells. *Nat Commun* 5:3846. <https://doi.org/10.1038/ncomms4846>
62. Huang Y, Chen P, Wu C, Hoshino K, Sokolov K, Lane N, Liu H, Huebschman M, Frenkel E, Zhang JXJ (2015) Screening and molecular analysis of single circulating tumor cells using micromagnet array. *Sci Rep* 5:16047. <https://doi.org/10.1038/srep16047>
63. Kokkinis G, Cardoso S, Keplinger F, Giouroudi I (2017) Microfluidic platform with integrated GMR sensors for quantification of cancer cells. *Sens Actuators B-Chem* 241:438–445. <https://doi.org/10.1016/j.snb.2016.09.189>
64. Chen A, Byvank T, Chang W, Bharde A, Vieira G, Miller BL, Chalmers JJ, Bashir R, Sooryakumar R (2013) On-chip magnetic separation and encapsulation of cells in droplets. *Lab Chip* 13(6):1172–1181. <https://doi.org/10.1039/c2lc41201b>
65. Ren W, Cho I, Zhou Z, Irudayaraj J (2016) Ultrasensitive detection of microbial cells using magnetic focus enhanced lateral flow sensors. *Chem Commun* 52(27):4930–4933. <https://doi.org/10.1039/c5cc10240e>
66. Liu F, Pawan KC, Zhang G, Zhe J (2017) In situ single cell detection via microfluidic magnetic bead assay. *PLoS ONE* 12(2):172697. <https://doi.org/10.1371/journal.pone.0172697>
67. Liu W, Dechev N, Foulds IG, Burke R, Parameswaran A, Park EJ (2009) A novel permalloy based magnetic single cell micro array. *Lab Chip* 9(16):2381–2390. <https://doi.org/10.1039/b821044f>
68. Huber D, Oskooei A, Casadevall I, Solvas X, DeMello A, Kaigala GV (2018) Hydrodynamics in cell studies. *Chem Rev* 118(4):2042–2079. <https://doi.org/10.1021/acs.chemrev.7b00317>
69. Huang Q, Mao S, Khan M, Zhou L, Lin J (2018) Dean flow assisted cell ordering system for lipid profiling in single-cells using mass spectrometry. *Chem Commun* 54(21):2595–2598. <https://doi.org/10.1039/c7cc09608a>
70. Carlo DD, Wu LY, Lee LP (2006) Dynamic single cell culture array. *Lab Chip* 6(11):1445–1449. <https://doi.org/10.1039/b605937f>
71. Kamiya K, Abe Y, Inoue K, Osaki T, Kawano R, Miki N, Takeuchi S (2018) Well-controlled cell-trapping systems for investigating heterogeneous cell–cell interactions. *Adv Healthc Mater* 7(6):1701208. <https://doi.org/10.1002/adhm.201701208>
72. Chen H, Sun J, Wolvetang E, Cooper-White J (2015) High-throughput, deterministic single cell trapping and long-term clonal cell culture in microfluidic devices. *Lab Chip* 15(4):1072–1083. <https://doi.org/10.1039/c4lc01176g>
73. Liu C, Liu J, Gao D, Ding M, Lin J (2010) Fabrication of microwell arrays based on two-dimensional ordered polystyrene microspheres for high-throughput single-cell analysis. *Anal Chem* 82(22):9418–9424. <https://doi.org/10.1021/ac102094r>
74. Wu J, Li H, Chen Q, Lin X, Liu W, Lin J (2014) Statistical single-cell analysis of cell cycle-dependent quantum dot cytotoxicity and cellular uptake using a microfluidic system. *RSC Adv* 4(47):24929–24934. <https://doi.org/10.1039/c4ra01665c>
75. Wei H, Chueh B, Wu H, Hall EW, Li C, Schirhagl R, Lin J, Zare RN (2011) Particle sorting using a porous membrane in a microfluidic device. *Lab Chip* 11(2):238–245. <https://doi.org/10.1039/c0lc00121j>
76. Yoon Y, Lee J, Yoo K, Sul O, Lee S, Lee S (2018) Deterministic capture of individual circulating tumor cells using a flow-restricted microfluidic trap array. *Micromachines* 9(3):106. <https://doi.org/10.3390/mi9030106>
77. Benavente-Babace A, Gallego-Pérez D, Hansford DJ, Arana S, Pérez-Lorenzo E, Mujika M (2014) Single-cell trapping and selective treatment via co-flow within a microfluidic platform. *Biosens Bioelectron* 61:298–305. <https://doi.org/10.1016/j.bios.2014.05.036>
78. Zhang Q, Mao S, Khan M, Feng S, Zhang W, Li W, Lin J (2019) In situ partial treatment of single cells by laminar flow in the “open space”. *Anal Chem* 91(2):1644–1650. <https://doi.org/10.1021/acs.analchem.8b05313>

79. Mao S, Zhang Q, Liu W, Huang Q, Khan M, Zhang W, Lin C, Uchiyama K, Lin J (2019) Chemical operations on a living single cell by open microfluidics for wound repair studies and organelle transport analysis. *Chem Sci* 10(7):2081–2087. <https://doi.org/10.1039/c8sc05104f>
80. Park KJ, Lee KG, Seok S, Choi BG, Lee M, Park TJ, Park JY, Kim DH, Lee SJ (2014) Micropillar arrays enabling single microbial cell encapsulation in hydrogels. *Lab Chip* 14(11):1873–1879. <https://doi.org/10.1039/c4lc00070f>
81. Kamalakshakurup G, Lee AP (2017) High-efficiency single cell encapsulation and size selective capture of cells in picoliter droplets based on hydrodynamic micro-vortices. *Lab Chip* 17(24):4324–4333. <https://doi.org/10.1039/c7lc00972k>
82. Sauzade M, Brouzes E (2017) Deterministic trapping, encapsulation and retrieval of single-cells. *Lab Chip* 17(13):2186–2192. <https://doi.org/10.1039/c7lc00283a>
83. Zhou Y, Basu S, Wohlfahrt KJ, Lee SF, Klenerman D, Laue ED, Seshia AA (2016) A microfluidic platform for trapping, releasing and super-resolution imaging of single cells. *Sens Actuators B-Chem* 232:680–691. <https://doi.org/10.1016/j.snb.2016.03.131>
84. Zhao L, Ma C, Shen S, Tian C, Xu J, Tu Q, Li T, Wang Y, Wang J (2016) Pneumatic microfluidics-based multiplex single-cell array. *Biosens Bioelectron* 78:423–430. <https://doi.org/10.1016/j.bios.2015.09.055>
85. Ohiri KA, Kelly ST, Motschman JD, Lin KH, Wood KC, Yellen BB (2018) An acoustofluidic trap and transfer approach for organizing a high density single cell array. *Lab Chip* 18(14):2124–2133. <https://doi.org/10.1039/c8lc00196k>
86. Gao Y, Li W, Pappas D (2013) Recent advances in microfluidic cell separations. *Analyst* 138(17):4714–4721. <https://doi.org/10.1039/c3an00315a>
87. Love JC, Ronan JL, Grotenbreg GM, van der Veen AG, Ploegh HL (2006) A microengraving method for rapid selection of single cells producing antigen-specific antibodies. *Nat Biotechnol* 24:703. <https://doi.org/10.1038/nbt1210>
88. Son KJ, Rahimian A, Shin D, Siltanen C, Patel T, Revzin A (2016) Microfluidic compartments with sensing microbeads for dynamic monitoring of cytokine and exosome release from single cells. *Analyst* 141(2):679–688. <https://doi.org/10.1039/c5an01648g>
89. Akbari S, Pirbodaghi T (2014) A droplet-based heterogeneous immunoassay for screening single cells secreting antigen-specific antibodies. *Lab Chip* 14(17):3275–3280. <https://doi.org/10.1039/c4lc00082j>
90. Son KJ, Shin D, Kwa T, You J, Gao Y, Revzin A (2015) A microsystem integrating photodegradable hydrogel microstructures and reconfigurable microfluidics for single-cell analysis and retrieval. *Lab Chip* 15(3):637–641. <https://doi.org/10.1039/c4lc00884g>
91. Shin D, You J, Rahimian A, Vu T, Siltanen C, Ehsanipour A, Stybayeva G, Sutcliffe J, Revzin A (2014) Photodegradable hydrogels for capture, detection, and release of live cells. *Angew Chem Inter Edit* 53(31):8221–8224. <https://doi.org/10.1002/anie.201404323>
92. Cheng S, Xie M, Chen Y, Xiong J, Liu Y, Chen Z, Guo S, Shu Y, Wang M, Yuan B, Dong W, Huang W (2017) Three-Dimensional scaffold chip with thermosensitive coating for capture and reversible release of individual and cluster of circulating tumor cells. *Anal Chem* 89(15):7924–7932. <https://doi.org/10.1021/acs.analchem.7b00905>
93. Kulkarni RP, Che J, Dhar M, Di Carlo D (2014) Research highlights: microfluidic single-cell analysis from nucleic acids to proteins to functions. *Lab Chip* 14(19):3663–3667. <https://doi.org/10.1039/c4lc90079k>
94. Lu Y, Yang L, Wei W, Shi Q (2017) Microchip-based single-cell functional proteomics for biomedical applications. *Lab Chip* 17(7):1250–1263. <https://doi.org/10.1039/c7lc00037e>
95. Li X, Fan B, Cao S, Chen D, Zhao X, Men D, Yue W, Wang J, Chen J (2017) A microfluidic flow cytometer enabling absolute quantification of single-cell intracellular proteins. *Lab Chip* 17(18):3129–3137. <https://doi.org/10.1039/c7lc00546f>
96. Deng Y, Zhang Y, Sun S, Wang Z, Wang M, Yu B, Czajkowsky DM, Liu B, Li Y, Wei W, Shi Q (2014) An integrated microfluidic chip system for single-cell secretion profiling of rare circulating tumor cells. *Sci Rep* 4:7499. <https://doi.org/10.1038/srep07499>

97. Iliuk AB, Hu L, Tao WA (2011) Aptamer in bioanalytical applications. *Anal Chem* 83(12):4440–4452. <https://doi.org/10.1021/ac201057w>
98. Tomas Rozenblum G, Gisela Lopez V, Daniel Vitullo A, Radrizzani M (2016) Aptamers: current challenges and future prospects. *Expert Opin Drug Dis* 11(2):127–135. <https://doi.org/10.1517/17460441.2016.1126244>
99. Xiong X, Lv Y, Chen T, Zhang X, Wang K, Tan W (2014) Nucleic acid aptamers for living cell analysis. *Annu Rev Anal Chem* 7(1):405–426. <https://doi.org/10.1146/annurev-anchem-071213-015944>
100. Yuce M, Ullah N, Budak H (2015) Trends in aptamer selection methods and applications. *Analyst* 140(16):5379–5399. <https://doi.org/10.1039/c5an00954e>
101. Qian W, Zhang Y, Chen W (2015) Capturing cancer: emerging microfluidic technologies for the capture and characterization of circulating tumor cells. *Small* 11(32):3850–3872. <https://doi.org/10.1002/sml.201403658>
102. Lin X, Sun X, Luo S, Liu B, Yang C (2016) Development of DNA-based signal amplification and microfluidic technology for protein assay: a review. *TrAC. Trends Anal Chem* 80:132–148. <https://doi.org/10.1016/j.trac.2016.02.020>
103. Chen Q, Wu J, Zhang Y, Lin Z, Lin J (2012) Targeted isolation and analysis of single tumor cells with aptamer-encoded microwell array on microfluidic device. *Lab Chip* 12(24):5180–5185. <https://doi.org/10.1039/c2lc40858a>
104. Zhang Y, Wang Z, Wu L, Zong S, Yun B, Cui Y (2018) Combining multiplex SERS nanovectors and multivariate analysis for in situ profiling of circulating tumor cell phenotype using a microfluidic chip. *Small* 14(20):1704433. <https://doi.org/10.1002/sml.201704433>
105. Qiu L, Wimmers F, Weiden J, Heus HA, Tel J, Figdor CG (2017) A membrane-anchored aptamer sensor for probing IFN γ secretion by single cells. *Chem Commun* 53(57):8066–8069. <https://doi.org/10.1039/c7cc03576d>
106. Qu X, Zhang H, Chen H, Aldalbahi A, Li L, Tian Y, Weitz DA, Pei H (2017) Convection-Driven Pull-Down assays in nanoliter droplets using scaffolded aptamers. *Anal Chem* 89(6):3468–3473. <https://doi.org/10.1021/acs.analchem.6b04475>
107. Li L, Wang Q, Feng J, Tong L, Tang B (2014) Highly sensitive and homogeneous detection of membrane protein on a single living cell by aptamer and nicking enzyme assisted signal amplification based on microfluidic droplets. *Anal Chem* 86(10):5101–5107. <https://doi.org/10.1021/ac500881p>
108. Landry MP, Ando H, Chen AY, Cao J, Kottadiel VI, Chio L, Yang D, Dong J, Lu TK, Strano MS (2017) Single-molecule detection of protein efflux from microorganisms using fluorescent single-walled carbon nanotube sensor arrays. *Nat Nanotechnol* 12:368. <https://doi.org/10.1038/nnano.2016.284>
109. Mao S, Zhang W, Huang Q, Khan M, Li H, Uchiyama K, Lin J (2018) In situ scatheless cell detachment reveals correlation between adhesion strength and viability at single-cell resolution. *Angew Chem Int Edit* 57(1):236–240. <https://doi.org/10.1002/anie.201710273>
110. Mao S, Zhang Q, Li H, Huang Q, Khan M, Uchiyama K, Lin J (2018) Measurement of cell–matrix adhesion at single-cell resolution for revealing the functions of biomaterials for adherent cell culture. *Anal Chem* 90(15):9637–9643. <https://doi.org/10.1021/acs.analchem.8b02653>
111. Mao S, Zhang Q, Li H, Zhang W, Huang Q, Khan M, Lin J (2018) Adhesion analysis of single circulating tumor cells on a base layer of endothelial cells using open microfluidics. *Chem Sci* 9(39):7694–7699. <https://doi.org/10.1039/c8sc03027h>

Chapter 3

Single-Cell Culture and Analysis on Microfluidics



Weiwei Li and Jin-Ming Lin

Abstract Heterogeneity of cell populations is a major obstacle for understanding complex biological processes. In order to have a more comprehensive quantitative comprehending of cellular processes, it is necessary to quantify the distribution of behavior in a population of individual cells. Analysis of single-cell behaviors requires efficient single-cell capture, controllable single-cell culture performance as well as reliable analysis techniques. The microfluidic system provides advanced technology for single-cell culture and observation. This chapter gives a brief account of single-cell capture by microfluidic methods, long-term single-cell culture on both two-dimensional models and three-dimensional microfluidic systems, as well as single-cell growth and differentiation in a microfluidic environment. Furthermore, the advanced methods used for characterizing on-chip single-cell culture were also discussed.

Keywords Single cell · Capture · Culture · Growth and differentiation · Analysis

3.1 Introduction

Single-cell analysis holds much promise to better understand cell behaviors and cell metabolism [1, 2]. Individual isogenic cells are not identical even in the same culture environment [3, 4] known as heterogeneity. Heterogeneity among cell populations is a major obstacle to understand complex biological processes. The averaged results from the sample of large cell populations are insufficient when considering individual cell behaviors and usually obscure the variable response of individual cells. These problems are highlighted in the research of normal and malignant stem and progenitor cell populations, because of the lack of cell purification methods [5] and the inherent stochastic nature of cells' self-renewing and differentiation [6, 7]. Cell-to-cell interactions grown in a monolayer cell culture

W. Li · J.-M. Lin (✉)

Department of Chemistry, Tsinghua University, Beijing 100084, People's Republic of China
e-mail: jmlin@mail.tsinghua.edu.cn

microenvironment are considered as one of the vital factors which influence large distributions in behavior. In this case, both contact and diffusible elements seem to be working. Therefore, single-cell analysis is increasingly being employed to a number of different biomedical fields, such as genetic analysis [8], cancer progression [9, 10], developmental biology [11], and fundamental biological studies on rare stem cells, or cancer cells [12].

The accompanying need with single-cell analysis is cell culture method to interrogate phenotypes through a culture of the rare amount of cells or single cells [13–17]. Single-cell culture is based on multiple generations from single-cell starting points. However, it is technically difficult to establish the single-cell culture platform. Technical difficulties are mainly reflected in (1) precise manipulation of cells and minimal loss of samples; (2) contact with non-biological surfaces and minimum shear stress or other damage stresses; (3) sustainable growth of target cell number and total cell number (need enough culture space, replaceable medium, etc.). In order to solve these difficulties, the development of cell culture platform requires the inherent advantages of microfluidics. Microfluidic platforms have recently been widely applied to realize cell-based assays, for example, manipulation of single cells [18], automated media perfusion [19, 20], providing cellular microenvironment and external stimuli to study cellular responses [21–24], and establishment of long-term cell culture systems.

In general, single-cell analysis requires (1) a large number of captured individual cells in order to obtain statistical significance of single-cell properties, (2) long-term clonal cell culture originated from a start of a single cell, (3) continuous observation of multiple generations of cells on their growth, differentiation, phenotype, metabolism, and other aspects. Single-cell culture is a crucial step in single-cell level analysis followed by single-cell isolation. In this chapter, we mainly present the advances, limitations, and outlooks in microfluidics based on the exploration of single-cell culture, categorized as two-dimensional (2D) and three-dimensional (3D) devices for the cultivation of a variety of cells, and analysis at single-cell level. We first introduce single-cell capture including conventional methods and microfluidic methods, and then we shift to single-cell culture based on microfluidics. In the last section, we focus on the advanced analysis techniques for single-cell culture.

3.2 Single-Cell Capture

Single-cell capture is the first step for single-cell analysis. Conventional methods for single-cell capture include micromanipulation, laser capture microdissection (LCM), and fluorescence activated cell sorting (FACS) (Fig. 3.1). Micromanipulation usually achieves through manual identification and selection with a microscope, which has the advantages of being low cost and easy-to-implement and the disadvantages of being laborious and low throughput [25]. LCM utilizes laser to cut and collect individual cells from tissues also under a microscope

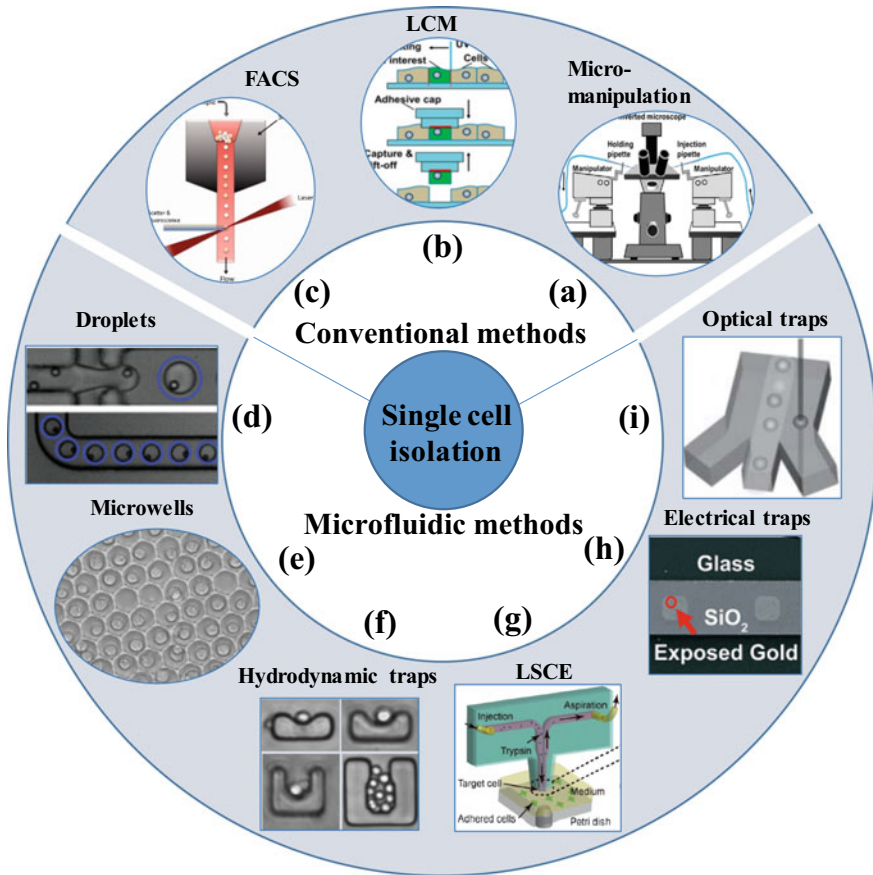


Fig. 3.1 Conventional and microfluidic methods for single-cell capture. Conventional methods includes: **a** Micromanipulation, figure was adapted from Ref. [33]; **b** Laser capture microdissection (LCM), figure was adapted from Ref. [33]; **c** Fluorescence-activated cell sorting (FACS), figure was adapted from Ref. [37]. Microfluidic methods includes: **d** Droplets, figure was adapted from Ref. [59]; **e** Microwell, figure was adapted from Ref. [63]; **f** Hydrodynamic trap, figure was adapted from Ref. [70]; **g** Live single-cell extractor (LSCE), figure was adapted from Ref. [75]; **h** Electrical traps, figure was adapted from Ref. [79]; **i** Optical traps, figure was adapted from ref. [87]

[26, 27]. LCM usually requires fixed tissue or cells and high laboratory skills. FACS is a high-throughput single cell sorting system, which could collect single cell into tubes or microwells for further experiments; while FACS is generally lack of visual inspection of the cells. Conventional micromanipulation, FACS, and LCM, could be referred to previous reviews [28–31], and here are only briefly described.

Modern approaches are based on microfluidic systems for single-cell capture and analysis, including droplet, microwell, hydrodynamic traps, live single-cell

extractor (LSCE), electrical traps, optical traps (Fig. 3.1). Microfluidic devices have more advantages than conventional approaches in single-cell capture. Microfluidic systems offer a closed platform for integrating downstream experiments, which reduce the risk of sample contamination. Miniaturized compartments for single cell reduce the experimental cost and enrich biomolecules with low concentration [32]. Moreover, most microfluidic systems could be automated to save labor, which means easy to achieve high throughput. In this part, we focus on the microfluidic design of single-cell capture for further downstream culture or analysis.

3.2.1 Conventional Methods

3.2.1.1 Micromanipulation

Micromanipulation relies on the manual selection technique typically through a micropipette combined with a microscope [33]. As shown in Fig. 3.1a, target single-cell identification is via microscope visual inspection. The micropipette moves in close proximity and picks a specific suspended cell in a petri dish or well plate. This process is usually performed manually. Micromanipulation can obtain specific cells accurately, but cannot achieve high throughput. Except single-cell capture, the micromanipulation is widely applied in the bacterial analysis [34], reproductive medicine, and forensics.

3.2.1.2 Laser Capture Microdissection

Laser capture microdissection (LCM) is a mature technique to capture single cells or tissue compartments typically from fixed tissue or cells samples [33]. As shown in Fig. 3.1b, the working process of LCM consists of laser cutting procedure and extraction of dissected tissue. Target cell or compartment is observed via a microscope and marked to be cutoff. The focused laser cuts the selected section, and then the operator extracts the dissected tissue. A particular advantage of LCM is that the access to cells in situ is beneficial for the spatial information of single cells [35, 36]. Typical samples are cryo-fixed, fixed in formalin, or embedded in paraffin, which causes cell death. Some modern LCM systems allow the extraction of living cell or tissue for downstream cell culture or analysis, such as Leica LMD7000 with live cell cutting (LCC). However, if the target cells are not precisely cut, they may be contaminated by adjacent cells. LCM allows very limited throughput.

3.2.1.3 Fluorescence-Activated Cell Sorting

Fluorescence-activated cell sorting (FACS) is a high-throughput and automatic method for cell sorting, and large amount of cells can be sorted in a very short time

[37]. FACS uses laser excitation and provides various analytical choices (Fig. 3.1c). Cell characteristics such as relative size and granularity can be obtained as forward scattering (FSC) and side scattering (SSC), respectively. In addition, cells' functional properties can be measured by fluorescence staining. The samples for FACS cover almost every cell type from blood, bone marrow, tumor, plants, protoplasts, yeast, bacteria, and viruses. Thus, FACS has a diverse spectrum of applications, such as quantification of soluble molecules and subpopulations [38], cancer diagnostics, microbial analysis [39], cell cycle analysis, hematopoietic stem cells, DNA content analysis, and apoptosis. FACS has been recognized as a worldwide standard for cell population analysis and sorting. However, the drawback to this approach is that the morphological information is limited to cell size and complexity. In addition, the open environment of FACS system increases the risk of introducing pollution.

3.2.2 *Microfluidic Methods*

3.2.2.1 **Droplets**

Droplet-based microfluidics use oil to keep aqueous droplets separated. The droplet like a separate microreactor encapsulates single cells, thus single cells can be collected [40, 41]. Droplet systems for single-cell capture typically generate droplets from a statistically dilute suspension of cells [42]. Single-cell capture via droplets is a feasible and high-throughput method. This method provided a platform for various biological assays on the single-cell level, such as single-cell culture [43, 44], single-cell counting [45], antibody detection [46], drug screening [47], RNA sequencing (RNA-seq) [48, 49], PCR [50, 51], whole genome amplification [52, 53], enzyme screening [54, 55].

Droplet-based single-cell isolation is usually consistent with Poisson distribution, which means that more than half of the droplets are cell-free [56]. Stochastic cell loading is the inherent variability of droplet contents. For single-cell analysis, it is important to improve the droplet encapsulation efficiency of a single cell, while reduce empty droplets and droplets encapsulating multiple cells. Much effort had been made to improve the efficiency of single-cell encapsulation, such as optimizing channel designs [57, 58]. Improving the efficiency of single-cell loading is another method to maximize the number of droplets containing a single cell. Edd et al. proposed a method to controllably load single cells into drops by utilizing inertial sorting to generate two trains of single cells in the loading channel (Fig. 3.1d) [59]. This method caused self-organization of cells, which conquered the intrinsic limitations arose from Poisson distribution, and ensuring that almost every drop contains a single cell. Kemna et al. introduced Dean forces by long helical microchannels and the final cell encapsulation efficiency of $\sim 80\%$ because cells were ordered in the channel before being encapsulated into droplets [60]. Droplet-based microfluidics has becoming a popular technology with extensive

applications, such as biotechnology [61], chemical analysis [62]. Droplet-based high-throughput single-cell biology is promising, but not yet realized.

3.2.2.2 Microwells

Microwell-based single-cell capture generally relies on sized well or modified surface, and cells are separated by the physical boundaries of multi-well. With the microwell array, cells that are attracted to the microwells can be preserved, and other cells outside the microwells would be washed away. Microwells provide a simple method enabling high-throughput single-cell analysis. The prominent advantages of microwells are that the microdevice is simple to operate and easy to achieve the capture of plenty cells. However, the disadvantage is that single-cell capture may occur only in part of the microwell array, and there may be a microwell with multiple cells or without any cells. Adjusting the size and shape of the microwell and optimizing the concentration of the cell suspension are the common solutions to improve the efficiency of single-cell capture.

Microfabrication technology allows the simple preparing of parallel microwells and enables high-throughput single-cell analysis. Liu et al. molded self-assembled polystyrene microspheres in poly (dimethylsiloxane) (PDMS) to produce microwell arrays for single-cell collection (Fig. 3.1e) [63]. For improving the efficiency of single-cell capture, Huang et al. constructed a truncated cone-shaped microwell array, which realized $\sim 90\%$ single-cell occupancy within a few seconds [64]. Surface modification achieved cell collecting without complicated fabrication of cell-sized microwells [65–67]. The combination of surface modification and specific size of microwells could improve the efficiency of cell occupancy. Specific aptamer and protein micropattern could also be modified in the microwell for capturing single cells from a mixture [68].

3.2.2.3 Hydrodynamic Traps

Hydrodynamic trap is a very common method for single-cell capture. The working principle of hydrodynamic trap system is that physical barriers or hydrodynamic tweezers stop the cell and remove it from the flow of cell suspension. In order to trap single cell, physical barriers are designed microscale structures, and hydrodynamic tweezers are specific and complex fluid flow profiles [69]. The advantages of using this method are that it does not require complex experimental steps and operations and could handle a large number of cells in a short time.

U-shaped traps as a popular physical barrier have been widely applied to obtain single cell. One of the typical single-cell U-shaped traps was demonstrated by Di Carlo et al. to collect single cells in large arrays (Fig. 3.1f) [70]. They used this U-shaped traps to determine single-cell enzyme kinetics for three different cell line (HeLa, 293T, Jurkat). Pattern flow channels have been introduced into the U-shaped traps structure, which allowed the fluid to fill the channel and provide a

suitable environment for cell culture [71]. Another type of hydrodynamic trap system is hydrodynamic tweezers. Lutz et al. used four vortices fabricated from cyclic oscillations of the sound waves around a cylinder to trap single cell in the vortex center [72]. In addition, hydrodynamic tweezers also have been used to trap particles [73, 74].

3.2.2.4 Live Single-Cell Extractor

Live single-cell extractor (LSCE) is a newly developing tool for collecting single adhered cell in a tissue culture. LSCE consists of injection part and aspiration part (Fig. 3.1g) [75]. The target cell is digested by the trypsin injected around the cell and then is extracted by aspiration part for further culture or analysis. A prominent advantage of LSCE is to extract live single-cell in situ without damage. Thus, it holds the spatial information of live single cells to their specific positions in the tissue. This method is usually combined with a microscope, which allows for the selecting of the target cell. LSCE takes only a few seconds to extract a single cell each time, without complicated operation. This method will provide a valuable novel tool for studying biology on the single-cell level.

The concept of LSCE was proposed by Mao et al. for revealing the correlation between adhesion strength and viability at single-cell resolution [75]. They used LSCE to extract adhered U87-MG cells (U87) and human hepatoma (HepG2) cells cultured in a culture dish. The microscopy recorded the information of individual cells' morphology and stained metabolites. The relationship among cell adhesion strength, cell morphologies as well as intracellular metabolites were explored, which revealed cell heterogeneity. Deepened on LSCE, Mao et al. clarified the cell-matrix adhesion strength on the single-cell level and revealed the effects of biomaterials on cell-matrix adhesion and heterogeneity of cell-matrix adhesion for adherent cell culture [76]. Moreover, LSCE also clarified the drug effects on the adhesion strength of individual circulating tumor cells (CTCs) on endothelial cells (ECs), which has broad prospects in drug screening for cancer therapy [77].

3.2.2.5 Electrical Traps

The cell membranes generally exhibit negative electronegativity at neutral pH, so the suspended cells are attracted toward the positive electrode. Cells have different charge, sizes, and masses, resulting different electric field force of cells; therefore, different cells can be distinguished. This is the working principle of electrophoresis (EP) [78]. However, the specificity of different cells in electrophoretic migration is not efficient. Electrical traps for single-cell capture generally include electric field-directed adhesion and dielectrophoresis (DEP). The method of electric field-directed adhesion needs cell surface modification. Toriello et al. demonstrate a microfluidic cell capture system comprised of interdigitated gold electrodes covered

in an oxide layer within the PDMS channel (Fig. 3.1h) [79]. The cell surface was modified with thiol functional groups by endogenous RGD receptors. The exposed gold pads bonded the single cell with modified thiol functional group through applying a driving electric potential. However, DEP could electrically capture cells without cell surface modification. DEP uses alternating current and generates a non-uniform electric field. DEP has been widely used for cell trap and further cell analysis. For example, Das et al. coated DEP electrodes on the microscope slide, which could collect different kinds of cells on the slide [80]. Thomas et al. designed concentric ring negative DEP (nDEP) for trapping single cell in the flow system [81]. In addition, DEP combined single-cell Raman spectra (SCRS) to capture single cells for downstream Raman detection [82, 83].

3.2.2.6 Optical Traps

Tightly focused laser beam acts as laser tweezers to trap single cell in aqueous solution. The laser beam could also act as an excitation source to generate a Raman spectrum of samples, known as laser tweezers Raman spectroscopy (LTRS) [84]. Laser tweezers could be integrated into microfluidic devices for transmission, identification, and simultaneous sorting of single cells [85, 86]. Adrian et al. presented the integrated optofluidic Raman-activated cell sorting (RACS) platforms for label-free cell sorting [87]. The specific single cells were identified by Raman spectroscopy and then captured and removed from cell suspensions (Fig. 3.1i). This method achieved automated sampling and high-throughput cell sorting. Another type of optical traps is optoelectronic tweezer, a combination of laser tweezers and DEP, which has been applied to manipulate and select single cells [88, 89].

3.3 Single-Cell Culture on Microfluidics

Many creative microfluidic platforms have been proposed for single-cell culture. Except for allowing the collecting of single cells, microfluidic platforms for single-cell culture require sufficient space for cell division and growth, timely nutritional supplementation, and appropriate microenvironment with minimal shear stress or other damage stress. In addition, access to cells of interest should be considered for subsequent study. Here, we classified microfluidic platforms by two dichotomous characteristics: two-dimensional (2D) and three-dimensional (3D). The methods and applications of single-cell culture carried out on these platforms have been described, with multiple types of cells including stem cells, tumor cells, immune cells, and so on.

3.3.1 Two-Dimensional Single-Cell Culture on Microfluidics

2D single-cell culture platforms based on microfluidics divided into two categories: closed and open microfluidics. Closed systems typically integrate hydrodynamic trapping structures and physical barriers into the platforms, which are isolated from the external physical stimulation. In contrast, open microfluidic systems, such as traditional microplate, microwells, and micropatterned surfaces, expose cells to the external physical, which allows direct access to single cells. Closed and open microfluidics with diverse designs have their own merits and demerits.

3.3.1.1 Closed Microfluidic Systems

Closed systems typically rely on hydrodynamic trapping structures and physical barriers. For example, Carlo et al. designed U-shaped hydrodynamic trapping structures on the bottom of the flow channel to trap single cells and cultured the cell in the original position for 24 h (Fig. 3.2) [90]. One of the important advantages of this single-cell culture array is controllable cell–cell interaction by both contact and diffusible elements.

To improve the single-cell capture efficiency, Kobel et al. optimized trap geometries with U-shaped hydrodynamic regions on the edge/wall of a microchannel (Fig. 3.3a) [91]. The single-cell capture efficiency of this device was nearly 100%. And this device allowed a long-term culture of individual non-adherent T-cell lymphoma cell in high throughput without a significant decrease in cell viability. Except U-shaped hydrodynamic trapping structures as efficient trap geometries, Lin et al. [92] fabricated sieve-like traps on adhesive protein micropatterns to capture single cells and cultured the trapped Hela cells on the micropatterns (Fig. 3.3b). The sieve-like trap positioning device was

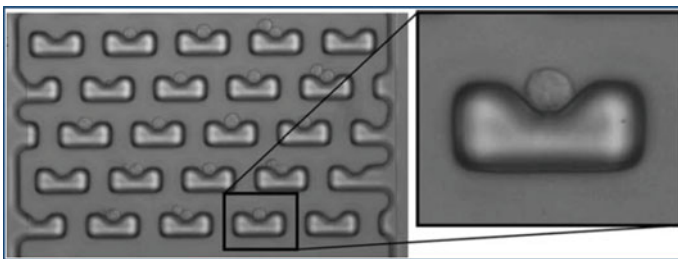


Fig. 3.2 Two-dimensional closed microfluidic systems, U-shaped hydrodynamic trapping structures, for single-cell culture. In most cases, cells rest at the identical potential minimum of the trap, while in some cases two cells are trapped in an identical manner among traps. A magnification shows the details of the trapped cell. Trapping is a gentle process, and no cell deformation is observed for routinely applied pressures. Figure was adapted from Ref. [90]

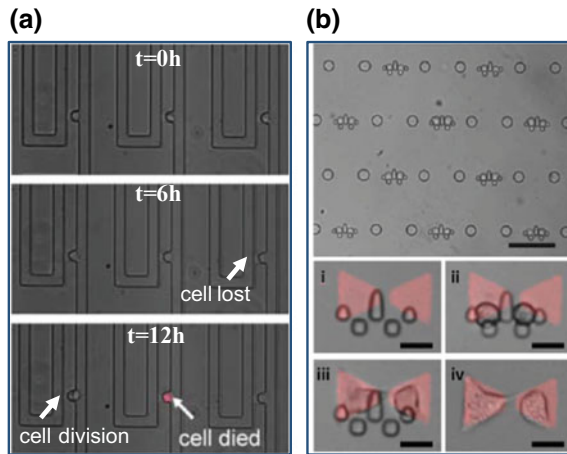
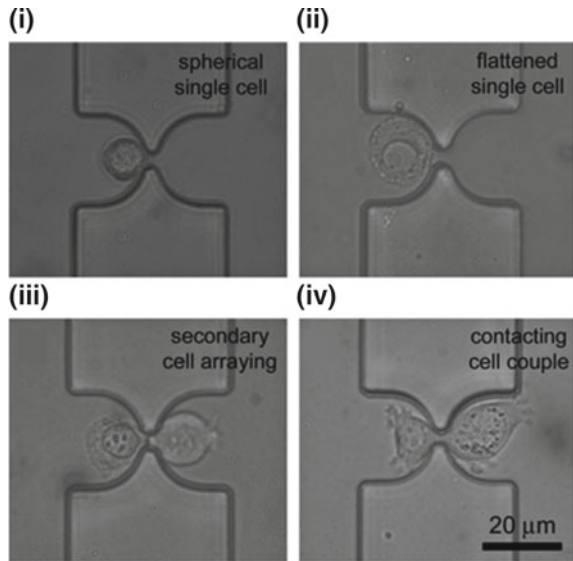


Fig. 3.3 Optimized two-dimensional closed microfluidic systems for single-cell culture. **a** Fates of non-adherent EG7 cells in a microfluidic single-cell trap. Series of typical images from a time-lapse experiment in a 2 mm device at a flow rate of 100 nl/min show a stably trapped cell and one that was lost after 6 h (bright-field image, left panel). Cell death was detected using propidium iodide (PI) added to the medium. Figure was adapted from Ref. [91]. **b** Demonstration of pairwise positioning of cells. (i) Traps were aligned to micropatterns. (ii) Single cells trapped on top of the micropatterns. (iii) Cells were allowed to spread and adhere to the micropattern. (iv) Microchannel peel-off leaving behind cells adhered to the micropattern. Scale bars of i–iv depict 50 μ m. Figure was adapted from Ref. [92]

detachable, allowing easy access to individual cells of interest for subsequent manipulations. Moreover, the micropattern with multiple protein pattern clusters could adhere different cell populations, which provided a promising opportunity for studying cell–ECM interactions and cell–cell interactions.

To investigate single cell–cell contact, Frimat et al. reported a highly parallel microfluidic method combined differential fluidic resistance trapping with cellular valving (Fig. 3.4) [93]. They applied differential fluidic resistance to sequential single-cell arraying. Continuous single-cell arrangement of the second cell type relied on the reversal of the fluid. The trapped single-cell pairs could contact with each other through the aperture. This microfluidic system is promising to study homotypic/heterotypic co-culture at the level of a pair of single cells. In addition, the long-term microfluidic culture of mammalian cells was considered difficult for reduced growth rates and deviations from normal phenotypes [94]. Lecault et al. exploited a high-throughput microfluidic system with automated medium exchange to investigate hematopoietic stem cell (HSC) proliferation control at the single-cell level [95]. Closed systems have the advantages of protecting samples from contamination and solvent (e.g., medium) evaporation. However, the disadvantages are the limited accessibility to samples of interest and increased costs from the integrated components (e.g., pumps, tubes).

Fig. 3.4 Cellular valving approach for single-cell co-culture. Figure was adapted from Ref. [93]



3.3.1.2 Open Microfluidic Systems

Microwell chips as a kind of common open microfluidic systems have been useful in single-cell culture and analysis [96]. It is easy to achieve large-scale single-cell capture and culture and get the information of single-cell metabolism. A large number of optimization methods for efficient single-cell capture were proposed [97, 98]. Cell suspensions are normally introduced manually into the microwells, and cells are randomly positioned in the wells. Cells outside the well are then washed away. Single non-adherent cells and adherent cell both could be collected by microwell chips, such as single epithelial cells [99], hematopoietic stem and progenitor cells [100], blood cells, and lymphocyte. It is more difficult to fabricate microfluidic devices for the investigation of non-adherent cells, because of restricting non-adherent cells to a known position in the microdevice. Cell seeding efficiency is the most important parameter to evaluate microwell chips. The number of wells containing cells and the number of wells containing single cells, corresponding to well occupancy and single-cell occupancy respectively, in addition, the shape, size, the number of the microwells and material are all parameters should be taken into consideration. Square, hexagonal, and round shapes are common for microwells. Larger wells provide enough space for long-term culture, while smaller wells are propitious to the collection of single cells and instant analysis (hours and days). The number of the microwells (density of wells) need considers two aspects, harboring many cells and communicating with other cells to keep normal functions (without those conditions, cells may subsequently change their normal functions, e.g., diminished viability). Various materials have been used for the fabrication of microwell chips, such as etching/drilling silicon and glass [101], polymer PDMS [102]. The surface of silicon and glass with favorable mechanical properties could

be grinded and polished chemically to be suitable for cell adhesion. Besides the mechanical properties, the optical properties should be taken into consideration. Transparent materials have good satisfactory performance, which facilitates acquiring cell images, such as flat glass surfaces and conventional microscopic slips. Polymer PDMS is another material commonly applied for well-based single-cell chips with the advantages of easy fabrication, facilitated sealing onto other materials, good light transmittance, and biologically inert property. Open microwell chips allowed cell manipulation and handling.

Revzin et al. fabricated microwells composed of PEG hydrogel walls and square glass attachment pads and modified the glass pads with T-cell specific anti-CD5 to capture T-lymphocytes with the single-cell occupancy of $\sim 95\%$ (Fig. 3.5a) [103]. They used laser capture microdissection (LCM) for the retrieval of individual cells from the microwell array, which was prepared for downstream experiments (e.g., genomic or proteomic analysis). Tokimitsu et al. picked the single antigen-specific B-cells from cell-sized microwells by using micromanipulation [104]. Microwell chips should be designed for further cell study with the possibility to retrieve samples of interest. Since most of the existing analysis techniques for cell retrieval are suitable for open microfluidic systems, thus it can be integrated with most microwell chips. Although most microwells are roofless, the wells can be sealed by the addition of a roof (e.g., a glass slide) to capture the cell in the wells from the

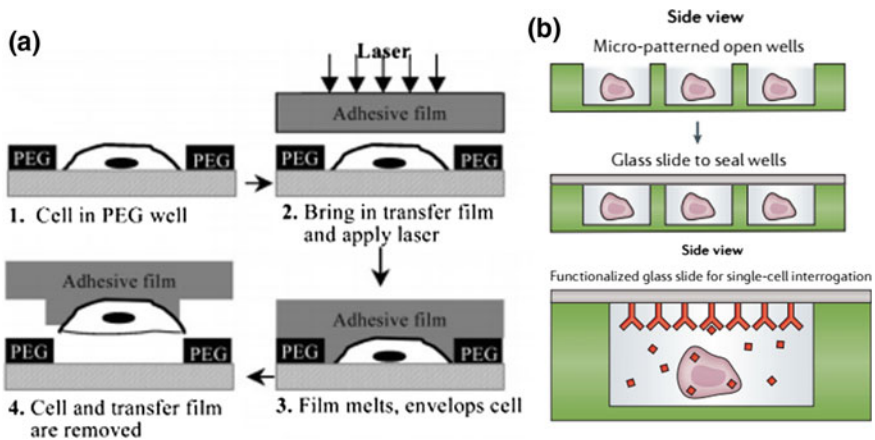


Fig. 3.5 Two-dimensional open microfluidic systems of microwell type for single-cell culture. **a** Retrieval of individual leukocytes from the cell array using LCM system. Step 1: Cells of interest are identified using light microscopy. Step 2: LCM cap containing a transfer film is brought into contact with the cell array after which focused laser beam is pulsed. Step 3: Transfer film melts and fuses with cells lying underneath. When the LCM cap is removed, cells remain preferentially attached to the transfer film. The cap is placed into an Eppendorf tube containing DNA, mRNA, or protein preparation buffers. Figure was adapted from Ref. [103]. **b** Nanowells confine cells by gravity and can subsequently be sealed with a membrane or glass slide to obtain single cells and their components. These cells or components can then be picked out of the wells for further processing or characterized in-well. Figure was adapted from Ref. [105]

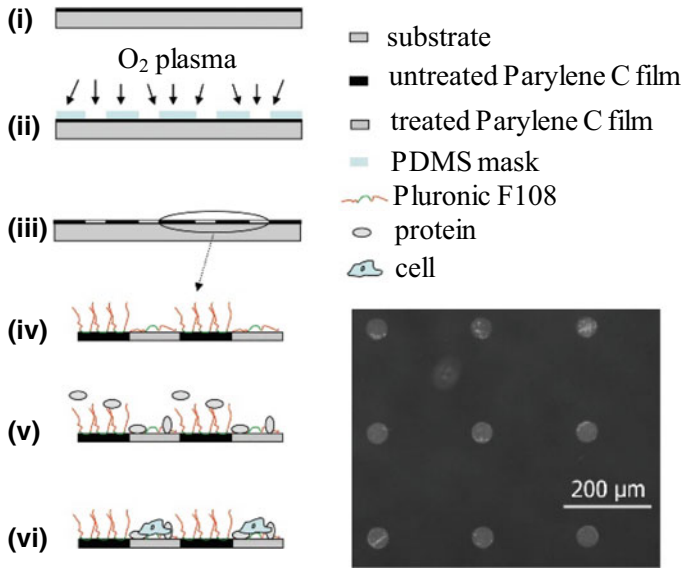


Fig. 3.6 Two-dimensional open microfluidic systems of chemically micropatterned surfaces for single-cell culture. Combination of plasma-assisted surface chemical modification, soft lithography, and protein-induced surface activation to accomplish surface patterning for single-cell culture. Figure was adapted from Ref. [108]

external environment (Fig. 3.5b) [105]. The roof could be modified as a functionalized seal to pick the cells or the components out of the wells for further analysis, for example, the analysis of the secreted cytokines or antibodies [106].

Single-cell culture is required to confine single cells to a specific location on the substrate. Chemically micropatterned surface with cytophilic and cytophobic regions (promoting and suppressing cell growth) is another strategy existing for controlling the position of single cells. Micropatterned surfaces for single-cell culture have been helpful in studying the effects of cell morphology and microenvironment on movement, migration, proliferation, and differentiation of cells [107]. Similar to the most microwell-based assay, the micropatterned surface is also a kind of open microfluidic systems. Various methods have been used to pattern cytophilic and cytophobic chemicals on the substrate for single-cell culture and analysis. Cheng et al. combined plasma-assisted surface chemical modification, soft lithography, and protein-induced surface activation to accomplish surface patterning for single-cell culture (Fig. 3.6) [108]. A polydimethylsiloxane membrane mask was put on the polystyrene film. The patterning was formed by oxygen plasma treatment which could produce hydrophilic areas. Then, the patterned film was incubated with either Pluronic F108 solution or a mixture of Pluronic F108 solution and fibronectin. Protein loading enhanced selective cell attachment on patterned dishes. Long-term (>2 weeks) single-cell culture experiments showed the influence of surface patterning on both cell and nucleus shape and also confirmed

the stability of the produced single-cell molds in serum medium. Ye et al. proposed an alternative approach based on micromolding in capillaries (MIMIC) to achieve chemical surface patterning for single-cell culture [109]: the PDMS micropattern with grid pattern was placed on the cytophilic substrate; cytophobic chemicals filled the microchannels under capillary action; discrete cell adhesion regions surrounded by cytophobic chemicals; removed the PDMS mold and seeded cells in the cytophilic pattern. The micropatterned surface for single-cell culture could be used to investigate the physiological activity of specific cells and employed for further analysis (e.g., drug screening).

3.3.2 Three-Dimensional Single-Cell Culture on Microfluidics

Traditional 2D single-cell culture models generally suspend cells freely in culture medium or randomly allowed cells adhere onto the support surface. Although 2D models have advantages of low cost, reproducibility, accessibility, and easy operation, they are insufficient to recapitulate physiological systems. The poor physiological correlation of 2D models may cause misunderstandings of the cell proliferation, differentiation, cytotoxicity, and metabolism, leading to inaccurate prediction of *in vivo* behaviors. In addition, most two-dimensional models are faced with some common limitations, such as nutrient depletion, toxin accumulation, influence of the complicated fluid shear, and random cellular migration. Thus, three-dimensional (3D) single-cell culture microfluidic platform mimics the real 3D microenvironment *in vivo* to reflect cell function and the geometry of tissues. Large amount of microfluidic devices featuring long-term 3D single-cell culture has sprung up. Microgel provides a promising strategy for single-cell 3D culture. Microgel allows long-term single-cell analysis, including heterogeneity of cellular proliferation, differentiation, and drug cytotoxicity. With the advantages of repeatability, flexibility, and highly controllable supporting microenvironment, cells could be independently packaged, cultured, monitored, or manipulated in the microgel. The structures of microgel for single-cell 3D culture are generally divided into three types: hydrogel droplets, microgel column, and microgel arrays.

In order to produce homogeneous hydrogel droplets for encapsulation of single cell, Utech et al. proposed a novel method to form alginate microgels in a highly controlled manner [110]. They added acetic acid into the continuous oil phase to dissociate Ca^{2+} -EDTA into Ca^{2+} , thus releasing Ca^{2+} to react with alginate chains (Fig. 3.7i). They used RGD-functionalized alginate to encapsulate single mesenchymal stem cells, as RGD provided integrin binding sites for cell attachment. The results showed that 25% of the droplets generated carrying single cells, while the majority of drops (70%) remained an empty and very small number of drops in contained more than one cell (Fig. 3.7ii). Improving the single-cell encapsulation efficiency has always been one of the challenges of microgel droplet technology.

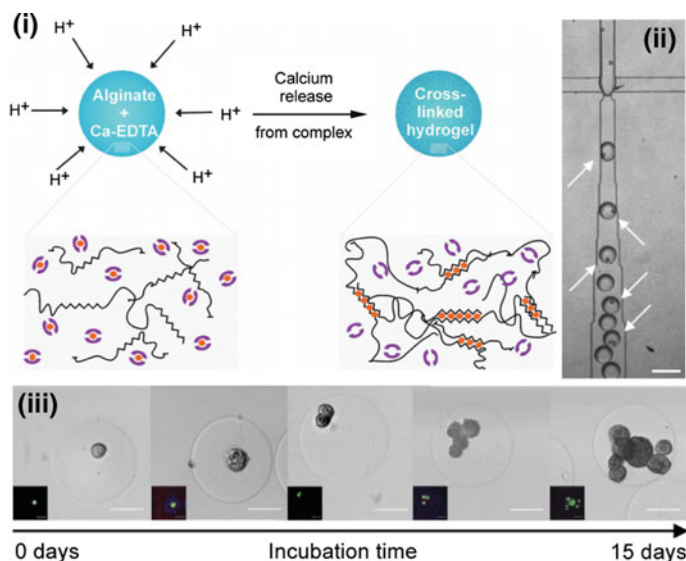


Fig. 3.7 Three-dimensional single-cell culture on microfluidics. Microfluidic generation of homogeneously cross-linked alginate microparticles by on-demand release of calcium ions from a water-soluble calcium–EDTA complex. (i) Schematic illustration of the cross-linking process. Upon addition of acid to the continuous phase, the calcium–EDTA complex dissolves, calcium ions are released, and cross-linking of alginate is induced. (ii) Cells are encapsulated using a 50 μm flow-focusing device (scale bar: 100 μm). Single-cell-containing droplets are indicated by white arrows. (iii) Representative images of cell-containing alginate gels directly after encapsulation and after being cultured for 3, 6, 12, and 15 days, respectively. The cells grow and proliferate inside the generated microenvironments while maintaining their spherical morphology. The encapsulated cells are stained using a calcein assay and analyzed via a confocal laser scanning microscope to determine the cell viability (inlets). All scale bars are 25 μm . Figure was adapted from Ref. [110]

The encapsulated cells in the droplets kept high viability for 2 weeks. The cells proliferate inside the microstructure and maintained spherical morphology (Fig. 3.7iii). Similarly, Dolega et al. presented a method for 3D single-cell culture based on a flow-focusing microfluidic system that encapsulates epithelial cells in matrigel beads to analyze clonal acinar development [111]. They cultured single prostatic and breast cells in each individual bead, and the cells proliferated and differentiated into a single acinus per bead. Compared to conventional protocols of bulky 3D culture, this method generated more uniform acini population and recorded acinar development from the very first division to the final stage. Moreover, it provided easy recovery of 3D structures for further analysis, such as the combination with large particle FACS, fundamental genomics.

Hydrogel microcolumn inside microchannels is also one of the microgel types for single-cell culture. Liu et al. developed an photopolymerization approach for controlled encapsulation of single cells in poly(ethylene glycol) diacrylate (PEG-DA) precursor [112]. As shown in Fig. 3.8, cells were suspended in PEG-DA

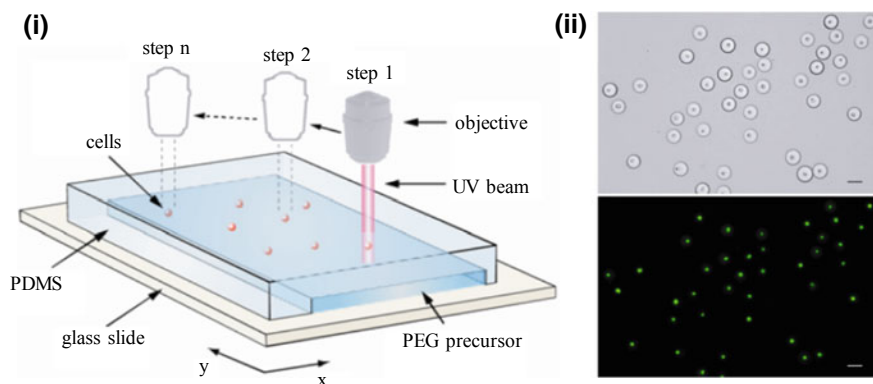


Fig. 3.8 Controlled encapsulation of single cells inside hydrogel microstructures. **i** Schematic setup of the controlled encapsulation of single cells. **ii** Bright field and fluorescence images of the large-scale encapsulation of single cells. Figure was adapted from Ref. [112]

precursor solution in the microchannel. A fluorescence microscope projection provided UV source to generate photopolymerization of PEG-DA precursor. The photopolymerization only occurred where the target cell suspended. Thus, the cell was chosen for encapsulation inside the hydrogel microstructures. The remaining freestanding cells in uncross-linked precursor were removed by TE buffer. Single cells encapsulated inside the microgel structure remained their viability for hours to days, which allowed long-term culture for further single-cell analysis [113].

Microgel arrays provide a feasible and high-throughput 3D mode for long-term single-cell culture. Large-scale microgel arrays carry out high-throughput single-cell analysis, and each unit of the arrays acts as an individual 3D cell culture room. Guan et al. developed a microcollagen gel array (μ CGA) for 3D single-cell culture [114]. The process of μ CGA fabrication was not complex: soaked the PDMS microwell array in the mixture of collagen solution and cell suspension; pressed the PDMS membrane with cells in-wells with another flat PDMS membrane; removed the cover layer after gelatinization; placed the fabricated μ CGA with cells encapsulated into culture medium; added fresh medium to supply nutrients for cell growth and proliferation (Fig. 3.9i). In order to analyze the cell proliferation heterogeneity under 3D culture conditions, they continuously recorded the proliferation of some random single cells for 11 days, which showed growth of five typical cell clones with different proliferation ability during the whole culture process (Fig. 3.9ii). Furthermore, they retrieved the cells of interest in μ CGA by integration with a microscale manipulation platform, as open culture conditions based on the microwell array allowed for more convenient retrieve of the target cells.

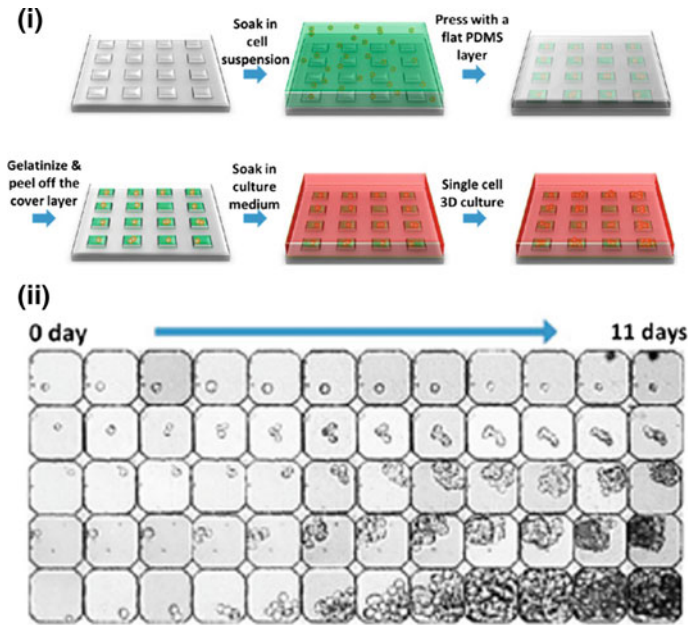


Fig. 3.9 Microcollagen gel array (μ CGA) for 3D cell culture. **i** Schematic of μ CGA fabrication process. **ii** Images of five typical single cells with significant cellular proliferation ability heterogeneity during the 11 day culture. Figure was adapted from Ref. [114]

3.4 Analysis Techniques for Single-Cell Culture

The final step for single-cell culture is to characterize and screen cell biophysical and biochemical information, such as morphology, behaviors, metabolism, and so on. A variety of technologies has been emerging for obtaining the single-cell information during a series of processes, including single-cell capture, single-cell short-term/long-term culture, single-cell lysis, and drug monitoring. Here, we covered optical, electrochemical, and mass spectrometric techniques for physical, chemical, molecular biology, and gene analysis of single cells.

3.4.1 Optical Characterization Techniques

Optical characterization is very commonly used in single-cell analysis, due to the direct visual observation of cells. Fluorescence methods play a vital role in optical characterization, providing images with high contrast and chemical-specific properties. Through fluorescence imaging, it is easy to reveal the distribution of intracellular molecules and dynamic states of biological processes, and the trace of

biomolecules. However, fluorescence imaging requires the target molecule to generate fluorescence. As to the non-luminescent molecule, fluorescent labeling or chemical modification is needed, which limits the use of fluorescence methods. Thus, label-free optical methods without the need for fluorescent labels or staining have been emerging. In addition, super-resolution microscopy allows the resolution down to 10 nm [115] and permits the observation of the submicroscopic structure of cells. It is necessary to briefly introduce recent advances in optical characterization techniques, including fluorescence techniques and label-free methods.

3.4.1.1 Fluorescence Techniques

Fluorescence resonance energy transfer (FRET) as a specialized fluorescence technique is extensively applied to biochemical reactions. The principle of FRET is that the energy transfer from an excited donor fluorophore to an acceptor molecule leading to the acceptor emitting fluorescence. FRET sensors with different excitation and emission wavelengths can be designed to analyze parameters in parallel. Ng et al. designed multi-color Förster resonance energy transfer (FRET)-based enzymatic substrates in a microfluidics platform to measure multiple specific protease activities from water-in-oil droplets encapsulating single cells [116]. They first mixed suspended cells with multiple modified FRET substrates for cell encapsulation in water-in-oil droplets (Fig. 3.10a). The secreted proteases cleaved multi-color FRET substrates to yield multiple fluorescent signals in cell-encapsulated droplets (Fig. 3.10a). They successfully used four FRET sensors with different excitation and emission wavelengths to measure different metalloproteinases of several breast cancer cell lines on the microdroplet-based platform (Fig. 3.10a). Metalloproteinases (MMPs) have been known as important biomarkers of cancer diagnosis and treatment. For example, MMP9 degrades the basement membrane of the extracellular matrix (ECM), which facilitates cancer cell invasion and metastasis [117]. Metalloproteinases were also regarded as the target in research by Son et al., who designed a micropatterned photodegradable hydrogel array integrated with reconfigurable microfluidics to enable cell-secreted metalloproteinases analysis and specific cell retrieval at the single-cell level. They also monitored the activity of protease molecules secreted from single cells through FRET peptides entrapped inside microfabricated compartments. Moreover, the gel islands could be degraded by UV exposure, which easily allowed to release specific single cells of interest.

Fluorescence in situ hybridization (FISH) relies on fluorescence labeled nucleic acid probes to localize specific sequences of DNA or RNA molecules in single cells or tissues. FISH has many advantages, such as high economy and safety without radioactive isotopes, high stability and specificity, simultaneous detection of multiple sequences through different colors displayed in the same nucleus, yet with the disadvantages of limited throughput. FISH is widely applied to identify heterogeneities in gene expression within single cells or tissues samples. For example, Perez-Toralla et al. presented a protocol for quantitative characterization of ERBB2

Analysis techniques for single cell culture

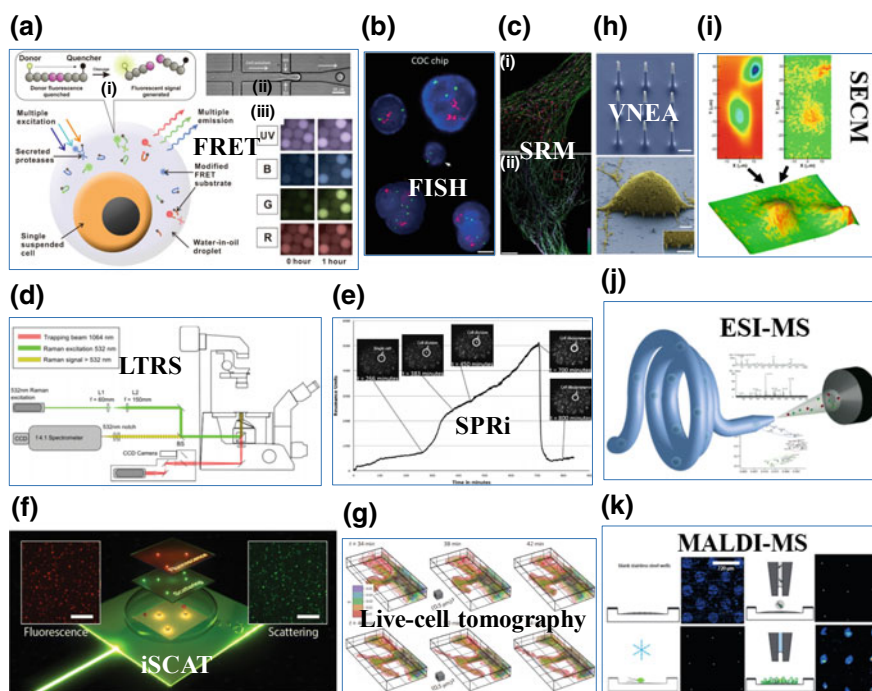


Fig. 3.10 Analysis techniques for single-cell culture. **a** Fluorescence resonance energy transfer (FRET) based enzymatic substrates and in a microfluidics platform to simultaneously measure multiple specific protease activities from water-in-oil droplets encapsulating single cells. Figure was adapted from Ref. [116]. **b** Fluorescence in situ hybridization (FISH) results for HER2 typing of cells from a pleural effusion from a breast cancer patient (sample B) on COC chip. Figure was adapted from Ref. [118]. **c** Super-resolution microscopy (SRM) imaging of fixed single cells. Figure was adapted from Ref. [119]. **d** Laser tweezers Raman spectroscopy (LTRS) setup. Figure was adapted from Ref. [120]. **e** Surface plasmon resonance imaging (SPRi) sensor showing cell division and subsequent cell removal. Figure was adapted from Ref. [121]. **f** Interferometric scattering microscopy (iSCAT). Schematic representation of the planar waveguide chip and detection of fluorescently labeled vesicles in fluorescence and scattering modes. Figure was adapted from Ref. [122]. **g** Live cell tomography. Time-lapsed refractive index change during filopodia formation of a neuronal spine. Figure was adapted from Ref. [123]. **h** SEM images of vertical nanowire electrode array (VNEA) and single cell on the VNEA pad. Figure was adapted from Ref. [125]. **i** Scanning electrochemical microscopy images (SECM) of PC12 cells. Figure was adapted from Ref. [128]. **j** Dean flow-assisted cell ordering system for lipid profiling in single cells using electrospray ionization MS (ESI-MS). Figure was adapted from Ref. [129]. **k** Matrix-assisted laser desorption/ionization MS (MALDI-MS) platform for investigations of single cells spotted into microwells on the stainless steel plate. Figure was adapted from Ref. [131]

gene by FISH based on the microfluidic chip made of cyclic olefin (Fig. 3.10b) [118]. This protocol allowed cell immobilization with minimal dead volume and performed characterization in the liquid phase. The target ERBB2 gene as a

biomarker for the monitoring of HER2+ breast cancer progression was measured quantitatively with a tenfold reduction of sample consumption and decreases the assay time by a factor of two [118].

Fluorescent super-resolution microscopy (SRM) breaks through the original optical far-field diffraction limit in principle. With the help of fluorescent molecules, it could exceed the limit of optical resolution and reach nanometer resolution. This technology is widely applied in biology, chemistry, medicine, and so on. SRM can be used to track target intracellular molecules in single-cell research. Spectacular two- and three-dimensional images of subcellular components have been obtained by SRM techniques. Although SRM could provide images with high resolution, it remains challenging to obtain multiplexed images for a large number of distinct target species. Jungmann et al. used the transient binding of short fluorescently labeled oligonucleotides (DNA-PAINT, a variation of point accumulation for imaging in nanoscale topography) for images with ultra-high resolution that achieves sub-10 nm spatial resolution *in vitro* on synthetic DNA structures [119]. They experimentally demonstrated spectacular imaging of proteins in fixed cells (Fig. 3.10c).

3.4.1.2 Label-Free Optical Methods

Laser tweezers Raman spectroscopy (LTRS) is promising in the label-free analysis of individual cells, particularly suited to the research of living cells, because it allows cells to be captured and analyzed in an aqueous environment. However, the most reported LTRS methods involved manual trapping of cells, which is time consuming. Casabella et al. proposed a LTRS with an automated microfluidic platform for single-cell Raman spectroscopy (Fig. 3.10d) [120]. They introduced simple microfluidic channel to realize an alternating flow: cells trapped by optical tweezers during low flow intervals and successfully removed once fluid flow increases. During each capture period, Raman spectroscopy was used to measure individual cells. Results showed discrimination in the Raman signals of live epithelial prostate cells and lymphocytes. This method improved the throughput and reduced the manual work of the single-cell Raman measurements.

Surface plasmon resonance imaging (SPRi) is also a popular method used for the label-free measurement of biomolecular interactions. Stojanovic et al. applied SPRi to screen and quantify antibody production from individual hybridoma cells (Fig. 3.10e) [121]. The cells from a hybridoma produced monoclonal antibodies recognizing epithelial cell adhesion molecule (EpCAM) that was preimmobilized on the SPR sensor surface. Through this method, an excreted antibody from individual cells ranged from 0.02 to 1.19 pg per cell per hour.

Interferometric scattering microscopy (iSCAT) is another optical microscopy technique without fluorescent labels. The principle of iSCAT is that light is scattered by an object leading to the change of light intensity based on interference with a reference light field. Agnarsson et al. developed evanescent light-scattering microscopy for label-free interfacial imaging [122]. The core technology of the

evanescent light-scattering microscopy is a waveguide chip consisting of a flat silica core embedded in a symmetric organic cladding with a refractive index matching that of water (Fig. 3.10f). Measurements and theoretical analysis showed that the size of single surface-bound lipid vesicles could be characterized by the light-scattering signals without employing fluorescent lipids as labels.

Live cell tomography is another new label-less super-resolution microscopy technique allowing direct imaging of unstained living biological specimens. Cotte et al. recently presented this microscopic method that 3D imaging of living cells with a resolution less than 100 nm could be obtained by phase contrast of unlabeled single cells [123]. Through this method, they realized longtime neuronal observations for synaptic remodeling in 3D (Fig. 3.10g) and direct study of bacteria (*Escherichia coli*).

3.4.2 Electrochemical Analysis

In recent years, electrochemical analysis has been applied in the field of single cells. Electrochemistry analysis can be integrated on a miniaturized platform, and microelectrodes are suitable for miniaturization of signal acquisition. Microelectrodes can be easily fabricated on various material substrates (e.g., polymers, silicon, or glass). A wide range of electrochemically active molecules could be detected by microelectrodes. Thus, microelectrodes are very useful in the quantitative measurement of neuronal communication and related neuroscience research. One of the hotspots is the fabrication of ultrasmall electrodes for measuring the neurotransmitter's release of single vesicle from living cells. Anderson et al. used carbon fiber microelectrodes to penetrate into individual cells and cell nuclei. The changes of electrode impedance with cell and nuclear penetration were measured [124]. They also monitored transmitter release from single vesicles of individual cells. However, the carbon fiber microelectrodes have to be punched into cells, which requires high experimental operation skills and is very low in throughput. In order to improve the throughput and reduce the cell damage, Robinson et al. fabricated vertical nanowire electrode array (VNEA) for parallel electrical interfacing to multiple mammalian neurons. Depending on VNEA, neuronal activity of rat cortical neurons was intracellularly recorded and stimulated. It was also possible to map multiple individual synaptic connections (Fig. 3.10h) [125]. Another common application of electrochemical methods at the single-cell level is to monitor oxidative stress. Jeffrey E. Dick recently presented a macroscopic setup for the detection of reactive oxygen species (ROS) at single cells level [126]. He monitored the consumption of a single cell's contents upon its collisions with a microelectrode under the presence of surfactants. He obtained large difference with two orders of magnitude between acute lymphoblastic lymphoma T-cells and healthy thymocytes.

Electrochemical analysis is sensitive. The introduction of the enzymatic labeling amplification step further increases the detection limit and gets faster and more

reliable signals. For example, Safaei et al. [127] used velocity valley (VV) chip to capture CTCs tagged with magnetic nanoparticles modified with the anti-EpCAM antibody. And then, they enzymatically labeled alkaline phosphatase on the cells, which catalyzed the reaction of paminophenyl phosphate to an electrochemically active reagent p-aminophenol to be measured. This method shows sensitive performance in analyzing the whole blood samples. The above methods are all based on fixed electrodes, but if the electrode is freely movable, it can be used for the two-dimensional scanning of the electrochemical properties of the underneath samples. Scanning electrochemical microscopy (SECM) is based on this principle. Koch et al. combined SECM with fast-scan cyclic voltammetry (CV) for the simultaneous measurement of impedance and amperometric current of PC12 cells [128]. Amperometric signals were converted into topographical images, because the current density depended on the distance between the tip and the cell (Fig. 3.10i). CV revealed the spatial distribution of minimum oxygen consumption. This method made it possible to achieve chemically and spatially resolved measurements along with imaging topography. However, one unavoidable disadvantage of the electrochemical method is that testing many substances simultaneously is difficult.

3.4.3 Mass Spectrometric Analysis

Mass spectrometry is a powerful tool for single-cell analysis, with the advantages of high sensitivity, simultaneous detection of multiple substances, and the ability to structure the molecules of interest. In particular, mass spectrometry can differentiate hundreds of biological molecules from the sample without labeling, thus making it attractive. However, low abundant cellular targets with any labels are still challenging in single-cell analysis through mass spectrometry. This is why most studies focus on highly abundant metabolites. Moreover, quantification by mass spectrometry generally needs internal references. Various ionization methods have been developed used for desorption/ionization of different kinds of samples in single-cell analysis field, such as electrospray/nano-electrospray ionization (ESI/Nano-ESI), laser ablation/laser desorption ionization (LA/LDI), and secondary ionization mass spectrometry (SIMS). These ionization methods provide multiple choices to ionize and analyze a wide range of substances, such as nucleotide, peptides, proteins, carbohydrates, esters, and small molecular metabolites.

3.4.3.1 Electrospray Ionization MS

Electrospray ionization MS (ESI-MS) is very suitable to investigate the samples with small volumes. In order to be supplied to ESI-MS, the single cell must be lysate. Huang et al. reported a cell ordering platform induced by Dean flow to isolate single cells from cellular suspension. The platform has been integrated with ESI-MS (Fig. 3.10j) [129]. In this method, individual cells were lysate one after

another and then analyzed ESI-MS to identify a single-cell into a subpopulation by lipid profiling. This platform made cells in suspension evenly distributed and significantly improved the efficiency of single-cell mass spectrometry. Lipid is the high abundant target to detect, and some researches more focused on other low abundant targets. For example, Gong et al. developed a probe ESI-MS spectrometry with capillary microsampling to monitor single living leave cells and analyzed the cellular stress of healthy and damaged plant leave cells [130]. The results showed the clear differences in the levels of abscisic acid as compared to other MS analysis methods. However, this method had a disadvantage that the microneedles might hamper normal cellular functions.

3.4.3.2 Matrix-Assisted Laser Desorption/Ionization MS

Matrix-assisted laser desorption/ionization MS (MALDI-MS) utilizes the power of a laser to make the sample embedded in matrix crystals desorption and ionization. This is a soft ionization technique, thus the majority of molecules maintain their original size and weight without fragment. MALDI-MS was employed in single-cell analysis over the last few years. Many efforts have been made to improve the spatial resolution and decrease the interference from the matrix material. For example, Krismer et al. screened different strains of *Chlamydomonas reinhardtii* through MALDI-MS [131]. They embedded microwells to the stainless steel plate for separating individually spotted cells. And then, they fast froze the samples and deposited the matrix to obtain the mass spectra of single cells (Fig. 3.10k). The MS results showed that the native strain with two different kinds of chlorophyll could be distinguished from the mutant strain lacking one of these chlorophyll subtypes.

3.4.3.3 Secondary Ion Mass Spectroscopy

Secondary ion mass spectrometry (SIMS) provides a tool to enable and analyze the composition of solid surfaces and thin films. The principle of SIMS is that MS investigates the release of secondary ions from the surface sputtered with an ion beam. Although SIMS has the advantages with the low detection limit and the high spatial resolution, yet samples must be placed in the ultra-high vacuum for analysis, thus inhibiting the study of living organisms. Bobrowska et al. have published a protocol of single cells preparation for the time of flight secondary ion mass spectrometry (TOF-SIMS), including the steps for pretreatment of single-cell samples (fixation, washing, dehydration) and detection by SIMS [132]. TOF-SIMS has frequently been employed for single-cell analysis. For example, it was applied to uncover differences among breast cancer cell lines, and the results showed an 18-carbon chain fatty acid only presenting in the BT-474 cell line [133]. In addition, 3D TOF-SIMS allowed for multiple MS images taken at different heights, thus creating Z-scans for samples [134].

3.5 Conclusions and Outlooks

Single-cell research is a newly established field and develops rapidly. The rapid development of this field is inseparable from the contributions of emerging microfluidic technologies. Although conventional methods for single-cell capture, in particularly FACS, are mature and used routinely, they have one or more following disadvantages: high laboratory skills, low throughput, lack of visual inspection, and the risk of introducing pollution. Emerging microfluidics for single-cell capture overcomes these shortcomings and becomes increasingly mature. However, high-throughput and efficient single-cell separation are still an important goal of microfluidics. In addition, open microfluidic techniques (e.g., microwells) provide convenience for subsequent single-cell manipulation, but also increase the risk of sample contamination; therefore, the work of microfluidic methods for single cell sorting needs continuous development. Microfluidic designers must take full account of the throughput of cell sorting, the efficiency of single-cell separation, the subsequent extraction of single cells, and sample contamination, and visual observation of cells, easy operation, and low cost are other aspects that need to be taken into account.

Single-cell culture is especially important for rare cells. Multiple generations from single-cell starting points are different from the cell populations derived randomly. Single-cell dynamic culture process provides real-time evidences for better understanding of cell behaviors and interrogation of cell phenotypes. Compared to microfluidic methods for single-cell capture, single-cell culture microfluidic platforms need bigger space for single-cell division, timely nutrition supplement for long-term cell growth, and minimum shear stress or other damage stresses. In addition, the single-cell culture platform should consider the easy acquisition of cells of interest. Similar to microfluidic single-cell capture, microfluidics provides 2D and 3D molds for single-cell culture. Although 2D models have the advantages with low cost, reproducibility, and easy operation, 3D molds simulate cell function and the geometry of tissues and organs, which is an irreplaceable advantage of 2D models. We also briefly presented advanced analytical technologies to identify heterogeneities among large cell populations, including optical characterization techniques, electrochemical analysis techniques, and mass spectrometric analysis techniques. Optical characterization techniques based on microscopy and fluorescence have the advantages of high sensitivities and spatial resolutions. Electrochemical and mass spectrometric techniques play unique roles in single-cell analysis in recent years, due to the detection of label-free biomolecules. Single-cell analysis methods are not limited to these technologies, and more novel technologies are emerging to extend our knowledge of cellular processes. However, the reliability of quantitative results is often questioned due to the limited accuracy of many analytical approaches and the lack of references. In addition, combining two or more analysis technologies can provide complementary information,

because of the complexity of cellular processes. We believe that further development of microfluidics and innovations of analytical instruments will cast light on single-cell heterogeneity and potentially promote the development of individual therapy.

References

1. Faley SL, Copland M, Wlodkovic D, Kolch W, Seale KT, Wikswa JP, Cooper JM (2009) Microfluidic single cell arrays to interrogate signalling dynamics of individual, patient-derived hematopoietic stem cells. *Lab Chip* 9(18):2659–2664. <https://doi.org/10.1039/b902083g>
2. Rao CV, Wolf DM, Arkin AP (2002) Control, exploitation and tolerance of intracellular noise. *Nature* 420(6912):231–237. <https://doi.org/10.1038/nature01258>
3. Fukano Y, Tsuyama N, Mizuno H, Date S, Takano M, Masujima T (2012) Drug metabolite heterogeneity in cultured single cells profiled by pico-trapping direct mass spectrometry. *Nanomedicine* 7(9):1365–1374. <https://doi.org/10.2217/nmm.12.34>
4. Jiang Y, Zhao H, Lin YQ, Zhu NN, Ma YR, Mao LQ (2010) Colorimetric detection of glucose in rat brain using gold nanoparticles. *Angew Chem Int Edit* 49(28):4800–4804. <https://doi.org/10.1002/anie.201001057>
5. Kent DG, Copley MR, Benz C, Wohrer S, Dykstra BJ, Ma E, Cheyne J, Zhao Y, Bowie MB, Zhao Y, Gasparetto M, Delaney A, Smith C, Marra M, Eaves CJ (2009) Prospective isolation and molecular characterization of hematopoietic stem cells with durable self-renewal potential. *Blood* 113(25):6342–6350. <https://doi.org/10.1182/blood-2008-12-192054>
6. Dykstra B, Kent D, Bowie M, McCaffrey L, Hamilton M, Lyons K, Lee SJ, Brinkman R, Eaves C (2007) Long-term propagation of distinct hematopoietic differentiation programs in vivo. *Cell Stem Cell* 1(2):218–229. <https://doi.org/10.1016/j.stem.2007.05.015>
7. Yamazaki S, Nakauchi H (2009) Insights into signaling and function of hematopoietic stem cells at the single-cell level. *Curr Opin Hematol* 16(4):255–258. <https://doi.org/10.1097/MOH.0b013e32832c6705>
8. Lasken RS, McLean JS (2014) Recent advances in genomic DNA sequencing of microbial species from single cells. *Nat Rev Genet* 15(9):577–584. <https://doi.org/10.1038/nrg3785>
9. Pardal R, Clarke MF, Morrison SJ (2003) Applying the principles of stem-cell biology to cancer. *Nat Rev Cancer* 3(12):895–902. <https://doi.org/10.1038/nrc1232>
10. Prasetyanti PR, Medema JP (2017) Intra-tumor heterogeneity from a cancer stem cell perspective. *Mol. Cancer* 16(1):41. <https://doi.org/10.1186/s12943-017-0600-4>
11. Boiani M, Scholer HR (2005) Regulatory networks in embryo-derived pluripotent stem cells. *Nat Rev Mol Cell Biol* 6(11):872–884. <https://doi.org/10.1038/nrm1744>
12. Lutolf MP, Doyonnas R, Havenstrite K, Koleckar K, Blau HM (2009) Perturbation of single hematopoietic stem cell fates in artificial niches. *Integr Biol (Camb)* 1(1):59–69. <https://doi.org/10.1039/b815718a>
13. Singhvi R, Kumar A, Lopez GP, Stephanopoulos GN, Wang DI, Whitesides GM, Ingber DE (1994) Engineering cell shape and function. *Science* 264(5159):696–698. <https://doi.org/10.1126/science.8171320>
14. Parker KK, Brock AL, Brangwynne C, Mannix RJ, Wang N, Ostuni E, Geisse NA, Adams JC, Whitesides GM, Ingber DE (2002) Directional control of lamellipodia extension by constraining cell shape and orienting cell tractional forces. *Faseb J* 16(10):1195–1204. <https://doi.org/10.1096/fj.02-0038com>
15. Chua CW, Shibata M, Lei M, Toivanen R, Barlow LJ, Bergren SK, Badani KK, Mc Kiernan JM, Benson MC, Hibshoosh H, Shen MM (2014) Single luminal epithelial

- progenitors can generate prostate organoids in culture. *Nat Cell Biol* 16(10):951–961. <https://doi.org/10.1038/ncb3047>
16. Gracz AD, Williamson IA, Roche KC, Johnston MJ, Wang F, Wang Y, Attayek PJ, Balowski J, Liu XF, Laurenza RJ, Gaynor LT, Sims CE, Galanko JA, Li L, Allbritton NL, Magness ST (2015) A high-throughput platform for stem cell niche co-cultures and downstream gene expression analysis. *Nat Cell Biol* 17(3):340–349. <https://doi.org/10.1038/ncb3104>
 17. Pushkarsky I, Tseng P, Black D, France B, Warfe L, Koziolwhite CJ, Jester WF, Trinh RK, Lin J, Scumpia PO (2018) Elastomeric sensor surfaces for high-throughput single-cell force cytometry. *Nat Biomed Eng* 2(2):124–137. <https://doi.org/10.1038/s41551-018-0193-2>
 18. Roman GT, Chen YL, Viberg P, Culbertson AH, Culbertson CT (2007) Single-cell manipulation and analysis using microfluidic devices. *Anal Bioanal Chem* 387(1):9–12. <https://doi.org/10.1007/s00216-006-0670-4>
 19. Titmarsh D, Hidalgo A, Turner J, Wolvetang E, Cooper-White J (2011) Optimization of flowrate for expansion of human embryonic stem cells in perfusion microbioreactors. *Biotechnol Bioeng* 108(12):2894–2904. <https://doi.org/10.1002/bit.23260>
 20. Kim L, Toh YC, Voldman J, Yu H (2007) A practical guide to microfluidic perfusion culture of adherent mammalian cells. *Lab Chip* 7(6):681–694. <https://doi.org/10.1039/b704602b>
 21. Wu MH, Huang SB, Lee GB (2010) Microfluidic cell culture systems for drug research. *Lab Chip* 10(8):939–956. <https://doi.org/10.1039/b921695b>
 22. Chen HY, Cornwell J, Zhang H, Lim T, Resurreccion R, Port T, Rosengarten G, Nordon RE (2013) Cardiac-like flow generator for long-term imaging of endothelial cell responses to circulatory pulsatile flow at microscale. *Lab Chip* 13(15):2999–3007. <https://doi.org/10.1039/c3lc50123j>
 23. Gao D, Liu HX, Jiang YY, Lin JM (2012) Recent developments in microfluidic devices for in vitro cell culture for cell-biology research. *Trac-Trend. Anal Chem* 35(35):150–164. <https://doi.org/10.1016/j.trac.2012.02.008>
 24. Titmarsh DM, Hudson JE, Hidalgo A, Elefanty AG, Stanley EG, Wolvetang EJ, Cooper-White JJ (2012) Microbioreactor arrays for full factorial screening of exogenous and paracrine factors in human embryonic stem cell differentiation. *PLoS ONE* 7(12):e52405. <https://doi.org/10.1371/journal.pone.0052405>
 25. Lee LM, Liu AP (2014) The application of micropipette aspiration in molecular mechanics of single cells. *J Nanotechnol Eng Med* 5(4):0408011–0408016. <https://doi.org/10.1115/1.4029936>
 26. Datta S, Malhotra L, Dickerson R, Chaffee S, Sen CK, Roy S (2015) Laser capture microdissection: big data from small samples. *Histol Histopathol* 30(11):1255–1269. <https://doi.org/10.14670/HH-11-622>
 27. Espina V, Wulfskuhle JD, Calvert VS, VanMeter A, Zhou W, Coukos G, Geho DH, Petricoin EF 3rd, Liotta LA (2006) Laser-capture microdissection. *Nat Protoc* 1(2):586–603. <https://doi.org/10.1038/nprot.2006.85>
 28. Hu P, Zhang W, Xin H, Deng G (2016) Single cell isolation and analysis. *Front Cell Dev Biol* 4:116–127. <https://doi.org/10.3389/fcell.2016.00116>
 29. Hodne K, Weltzien FA (2015) Single-cell isolation and gene analysis: pitfalls and possibilities. *Int J Mol Sci* 16(11):26832–26849. <https://doi.org/10.3390/ijms161125996>
 30. Orfao A, RuizArguelles A (1996) General concepts about cell sorting techniques. *Clin Biochem* 29(1):5–9. [https://doi.org/10.1016/0009-9120\(95\)02017-9](https://doi.org/10.1016/0009-9120(95)02017-9)
 31. Andersson H, van den Berg A (2004) Microtechnologies and nanotechnologies for single-cell analysis. *Curr Opin Biotechnol* 15(1):44–49. <https://doi.org/10.1016/j.copbio.2004.01.004>
 32. Livesey FJ (2003) Strategies for microarray analysis of limiting amounts of RNA. *Brief Funct Genomic Proteomic* 2(1):31–36. <https://doi.org/10.1093/bfgp/2.1.31>
 33. Gross A, Schoendube J, Zimmermann S, Steeb M, Zengerle R, Koltay P (2015) Technologies for single-cell isolation. *Int J Mol Sci* 16(8):16897–16919. <https://doi.org/10.3390/ijms160816897>

34. Brehmstecher BF, Johnson EA (2004) Single-Cell Microbiology: tools, technologies, and applications. *Microbiol Mol Biol R* 68(3):538–559. <https://doi.org/10.1128/mmlbr.68.3.538-559.2004>
35. Fink L, Kwapiszewska G, Wilhelm J, Bohle RM (2006) Laser-microdissection for cell type- and compartment-specific analyses on genomic and proteomic level. *Exp Toxicol Pathol* 57(6):25–29. <https://doi.org/10.1016/j.etp.2006.02.010>
36. Fink L, Bohle RM (2005) Laser microdissection and RNA analysis. *Methods Mol Biol* 293(293):167–185. <https://doi.org/10.1385/1-59259-853-6:167>
37. Adan A, Alizada G, Kiraz Y, Baran Y, Nalbant A (2017) Flow cytometry: basic principles and applications. *Crit Rev Biotechnol* 37(2):163–176. <https://doi.org/10.3109/07388551.2015.1128876>
38. Valet G (2003) Past and present concepts in flow cytometry: a European perspective. *J Biol Regul Homeost Agents* 17(3):213–222. <https://doi.org/10.1089/104303403322124828>
39. Davey HM, Kell DB (1996) Flow cytometry and cell sorting of heterogeneous microbial populations: the importance of single-cell analyses. *Microbiol Rev* 60(4):641–696. <https://doi.org/10.1006/mpat.1996.0079>
40. Joensson HN (2012) Droplet Microfluidics—A Tool for Single-Cell Analysis. *Angew Chem Int Edit* 51(49):12176–12192. <https://doi.org/10.1002/anie.201200460>
41. Guo MT, Rotem A, Heyman JA, Weitz DA (2012) Droplet microfluidics for high-throughput biological assays. *Lab Chip* 12(12):2146–2155. <https://doi.org/10.1039/c2lc21147e>
42. Kähler S, Angilã FE, Duan H, Agresti JJ, Wintner A, Schmitz C, Rowat AC, Merten CA, Pisignano D, Griffiths AD (2008) Drop-based microfluidic devices for encapsulation of single cells. *Lab Chip* 8(7):1110–1115. <https://doi.org/10.1039/b802941e>
43. Wang BL, Ghaderi A, Zhou H, Agresti J, Weitz DA, Fink GR, Stephanopoulos G (2014) Microfluidic high-throughput culturing of single cells for selection based on extracellular metabolite production or consumption. *Nat Biotechnol* 32(5):473–478. <https://doi.org/10.1038/nbt.2857>
44. Chen F, Zhan Y, Geng T, Lian H, Xu P, Lu C (2011) Chemical transfection of cells in picoliter aqueous droplets in fluorocarbon oil. *Anal Chem* 83(22):8816–8820. <https://doi.org/10.1021/ac2022794>
45. Lu H, Caen O, Vrigon J, Zonta E, El Harrak Z, Nizard P, Baret JC, Taly V (2017) High throughput single cell counting in droplet-based microfluidics. *Sci Rep* 7(1):1366. <https://doi.org/10.1038/s41598-017-01454-4>
46. Mazutis L, Gilbert J, Ung WL, Weitz DA, Griffiths AD, Heyman JA (2013) Single-cell analysis and sorting using droplet-based microfluidics. *Nat Protoc* 8(5):870–891. <https://doi.org/10.1038/nprot.2013.046>
47. Brouzes E, Medkova M, Savenelli N, Marran D, Twardowski M, Hutchison JB, Rothberg JM, Link DR, Perrimon N, Samuels ML (2009) Droplet microfluidic technology for single-cell high-throughput screening. *Proc Natl Acad Sci USA* 106(34):14195–14200. <https://doi.org/10.1073/pnas.0903542106>
48. Macosko EZ, Basu A, Satija R, Nemes J, Shekhar K, Goldman M, Tirosh I, Bialas AR, Kamitaki N, Martersteck EM, Trombetta JJ, Weitz DA, Sanes JR, Shalek AK, Regev A, McCarroll SA (2015) Highly Parallel genome-wide expression profiling of individual cells using nanoliter droplets. *Cell* 161(5):1202–1214. <https://doi.org/10.1016/j.cell.2015.05.002>
49. Klein AM, Mazutis L, Akartuna I, Tallapragada N, Veres A, Li V, Peshkin L, Weitz DA, Kirschner MW (2015) Droplet barcoding for single-cell transcriptomics applied to embryonic stem cells. *Cell* 161(5):1187–1201. <https://doi.org/10.1016/j.cell.2015.04.044>
50. Geng T, Novak R, Mathies RA (2014) Single-cell forensic short tandem repeat typing within microfluidic droplets. *Anal Chem* 86(1):703–712. <https://doi.org/10.1021/ac403137h>
51. Zhang W, Li N, Koga D, Zhang Y, Zeng H, Nakajima H, Lin JM, Uchiyama K (2018) Inkjet printing based droplet generation for integrated online digital polymerase chain reaction. *Anal Chem* 90(8):5329–5334. <https://doi.org/10.1021/acs.analchem.8b00463>

52. Fu Y, Li C, Lu S, Zhou W, Tang F, Xie XS, Huang Y (2015) Uniform and accurate single-cell sequencing based on emulsion whole-genome amplification. *Proc Natl Acad Sci USA* 112(38):11923–11928. <https://doi.org/10.1073/pnas.1513988112>
53. Leung K, Zahn H, Leaver T, Konwar KM, Hanson NW, Page AP, Lo CC, Chain PS, Hallam SJ, Hansen CL (2012) A programmable droplet-based microfluidic device applied to multiparameter analysis of single microbes and microbial communities. *Proc Natl Acad Sci USA* 109(20):7665–7670. <https://doi.org/10.1073/pnas.1106752109>
54. Sjostrom SL, Bai Y, Huang M, Liu Z, Nielsen J, Joensson HN, Andersson Svahn H (2014) High-throughput screening for industrial enzyme production hosts by droplet microfluidics. *Lab Chip* 14(4):806–813. <https://doi.org/10.1039/c3lc51202a>
55. Zinchenko A, Devenish SRA, Kintses B, Colin PY, Fischlechner M, Hollfelder F (2014) One in a million: flow cytometric sorting of singlecell-lysate assays in monodisperse picolitre double emulsion droplets for directed evolution. *Anal Chem* 86(5):2526–2533. <https://doi.org/10.1021/ac403585p>
56. Lim SW, Tran TM, Abate AR (2015) PCR-activated cell sorting for cultivation-free enrichment and sequencing of rare microbes. *PLoS ONE* 10(1):e0113549. <https://doi.org/10.1371/journal.pone.0113549>
57. Jing TY, Ramji R, Warkiani ME, Han J, Lim CT, Chen CH (2015) Jetting microfluidics with size-sorting capability for single-cell protease detection. *Biosens Bioelectron* 66:19–23. <https://doi.org/10.1016/j.bios.2014.11.001>
58. Park SY, Wu TH, Chen Y, Teitell MA, Chiou PY (2011) High-speed droplet generation on demand driven by pulse laser-induced cavitation. *Lab Chip* 11(6):1010–1012. <https://doi.org/10.1039/c0lc00555j>
59. Edd JF, Carlo DD, Humphry KJ, Köster S, Irimia D, Weitz DA, Toner M (2008) Controlled encapsulation of single cells into monodisperse picoliter drops. *Lab Chip* 8(8):1262–1264. <https://doi.org/10.1039/b805456h>
60. Kemna EWM, Schoeman RM, Wolbers F, Vermes I, Weitz DA, van den Berg A (2012) High-yield cell ordering and deterministic cell-in-droplet encapsulation using Dean flow in a curved microchannel. *Lab Chip* 12(16):2881–2887. <https://doi.org/10.1039/c2lc00013j>
61. Margulies M, Egholm M, Altman WE, Attiya S, Bader JS, Bemben LA, Berka J, Braverman MS, Chen YJ, Chen Z, Dewell SB, Du L, Fierro JM, Gomes XV, Godwin BC, He W, Helgesen S, Ho CH, Irzyk GP, Jando SC, Alenquer ML, Jarvie TP, Jirage KB, Kim JB, Knight JR, Lanza JR, Leamon JH, Lefkowitz SM, Lei M, Li J, Lohman KL, Lu H, Makhijani VB, McDade KE, McKenna MP, Myers EW, Nickerson E, Nobile JR, Plant R, Puc BP, Ronan MT, Roth GT, Sarkis GJ, Simons JF, Simpson JW, Srinivasan M, Tartaro KR, Tomasz A, Vogt KA, Volkmer GA, Wang SH, Wang Y, Weiner MP, Yu P, Begley RF, Rothberg JM (2005) Genome sequencing in microfabricated high-density picolitre reactors. *Nature* 437(7057):376–380. <https://doi.org/10.1038/nature03959>
62. Theberge AB, Courtois F, Schaerli Y, Fischlechner M, Abell C, Hollfelder F, Huck WTS (2010) Cheminform abstract: microdroplets in microfluidics: an evolving platform for discoveries in chemistry and biology. *Angew Chem Int Edit* 41(45):5846–5868. <https://doi.org/10.1002/anie.200906653>
63. Liu C, Liu J, Gao D, Ding M, Lin JM (2010) Fabrication of microwell arrays based on two-dimensional ordered polystyrene microspheres for high-throughput single-cell analysis. *Anal Chem* 82(22):9418–9424. <https://doi.org/10.1021/ac102094r>
64. Huang L, Chen Y, Chen Y, Wu H (2015) Centrifugation-assisted single-cell trapping (CAsCT) in a truncated cone-shaped microwell array (TCMA) chip for the real-time observation of cellular apoptosis. *Anal Chem* 87(24):12169–12176. <https://doi.org/10.1021/acs.analchem.5b03031>
65. Lin LI, Chao SH, Meldrum DR (2009) Practical, microfabrication-free device for single-cell isolation. *PLoS ONE* 4(8):e6710. <https://doi.org/10.1371/journal.pone.0006710>
66. Jang K, Xu Y, Tanaka Y, Sato K, Mawatari K, Konno T, Ishihara K, Kitamori T (2010) Single-cell attachment and culture method using a photochemical reaction in a closed microfluidic system. *Biomicrofluidics* 4(3):032208. <https://doi.org/10.1063/1.3494287> 1539

67. Shi X, Lin LI, Chen SY, Chao SH, Zhang W, Meldrum DR (2011) Real-time PCR of single bacterial cells on an array of adhering droplets. *Lab Chip* 11(13):2276–2281. <https://doi.org/10.1039/c1lc20207c>
68. Chen Q, Wu J, Zhang Y, Lin Z, Lin JM (2012) Targeted isolation and analysis of single tumor cells with aptamer-encoded microwell array on microfluidic device. *Lab Chip* 12(24):5180–5185. <https://doi.org/10.1039/c2lc40858a>
69. Karimi A, Yazdi S, Ardekani AM (2013) Hydrodynamic mechanisms of cell and particle trapping in microfluidics. *Biomicrofluidics* 7(2):21501. <https://doi.org/10.1063/1.4799787>
70. Carlo DD, Nima Aghdam A, Lee LP (2006) Single-cell enzyme concentrations, kinetics, and inhibition analysis using high-density hydrodynamic cell isolation arrays. *Anal Chem* 78(14):4925–4930. <https://doi.org/10.1021/ac060541s>
71. Chen H, Sun J, Wolvetang E, Cooper-White J (2015) High-throughput, deterministic single cell trapping and long-term clonal cell culture in microfluidic devices. *Lab Chip* 15(4):1072–1083. <https://doi.org/10.1039/c4lc01176g>
72. Lutz BR, Chen J, Schwartz DT (2005) Microscopic steady streaming eddies created around short cylinders in a channel: flow visualization and Stokes layer scaling. *Phys Fluids* 17(2):023601. <https://doi.org/10.1063/1.1824137> 3430
73. Lieu VH, House TA, Schwartz DT (2012) Hydrodynamic tweezers: impact of design geometry on flow and microparticle trapping. *Anal Chem* 84(4):1963–1968. <https://doi.org/10.1021/ac203002z>
74. Tanyeri M, Schroeder CM (2013) Manipulation and confinement of single particles using fluid flow. *Nano Lett* 13(6):2357–2364. <https://doi.org/10.1021/nl4008437>
75. Mao S, Zhang W, Huang Q, Khan M, Li H, Uchiyama K, Lin JM (2017) In situ scatheless cell detachment reveals connections between adhesion strength and viability at single-cell resolution. *Angew Chem Int Edit* 130(1):236–240. <https://doi.org/10.1002/ange.201710273>
76. Mao S, Zhang Q, Li H, Huang Q, Khan M, Uchiyama K, Lin J-M (2018) Measurement of cell–matrix adhesion at single-cell resolution for revealing the functions of biomaterials for adherent cell culture. *Anal Chem* 90(15):9637–9643. <https://doi.org/10.1021/acs.analchem.8b02653>
77. Mao S, Zhang Q, Li HF, Zhang WL, Huang QS, Khan M, Lin JM (2018) Adhesion analysis of single circulating tumor cells on a base layer of endothelial cells using open microfluidics. *Chem Sci* 9(39):7694–7699. <https://doi.org/10.1039/c8sc03027h>
78. Voldman J (2006) Electrical forces for microscale cell manipulation. *Annu Rev Biomed Eng* 8(8):425–454. <https://doi.org/10.1146/annurev.bioeng.8.061505.095739>
79. Toriello NM, Douglas ES, Mathies RA (2005) Microfluidic device for electric field-driven single-cell capture and activation. *Anal Chem* 77(21):6935–6941. <https://doi.org/10.1021/ac051032d>
80. Das CM, Becker F, Vernon S, Noshari J, Joyce C, Gascoyne PR (2005) Dielectrophoretic segregation of different human cell types on microscope slides. *Anal Chem* 77(9):2708–2719. <https://doi.org/10.1021/ac048196z>
81. Thomas RSW, Mitchell PD, Oreffo ROC, Morgan H (2010) Trapping single human osteoblast-like cells from a heterogeneous population using a dielectrophoretic microfluidic device. *Biomicrofluidics* 4(2):022806. <https://doi.org/10.1063/1.3406951> 11
82. Chrimes AF, Khoshmanesh K, Tang SY, Wood BR, Stoddart PR, Collins SS, Mitchell A, Kalantar-zadeh K (2013) In situ SERS probing of nano-silver coated individual yeast cells. *Biosens Bioelectron* 49(11):536–541. <https://doi.org/10.1016/j.bios.2013.05.053>
83. Zhang P, Ren L, Zhang X, Shan Y, Wang Y, Ji Y, Yin H, Huang WE, Xu J, Ma B (2015) Raman-activated cell sorting based on dielectrophoretic single-cell trap and release. *Anal Chem* 87(4):2282–2289. <https://doi.org/10.1021/ac503974e>
84. Chan JW, Esposito AP, Talley CE, Hollars CW, Lane SM, Huser T (2004) Reagentless identification of single bacterial spores in aqueous solution by confocal laser tweezers Raman spectroscopy. *Anal Chem* 76(3):599–603. <https://doi.org/10.1021/ac0350155>

85. Chen K, Qin YJ, Zheng F, Sun MH, Shi DR (2006) Diagnosis of colorectal cancer using Raman spectroscopy of laser-trapped single living epithelial cells. *Opt Lett* 31(13):2015–2017. <https://doi.org/10.1364/Ol.31.002015>
86. Singh GP, Volpe G, Creely CM, Grötsch H, Geli IM, Petrov D (2010) The lag phase and G1 phase of a single yeast cell monitored by Raman microspectroscopy. *J Raman Spectrosc* 37(8):858–864. <https://doi.org/10.1002/jrs.1520>
87. Lau AY, Lee LP, Chan JW (2008) An integrated optofluidic platform for Raman-activated cell sorting. *Lab Chip* 8(7):1116–1120. <https://doi.org/10.1039/B803598A>
88. Pei YC, Ohta AT, Wu MC (2005) Massively parallel manipulation of single cells and microparticles using optical images. *Nature* 436(7049):370–372. <https://doi.org/10.1038/nature03831>
89. Huang KW, Wu YC, Lee JA, Chiou PY (2013) Microfluidic integrated optoelectronic tweezers for single-cell preparation and analysis. *Lab Chip* 13(18):3721–3727. <https://doi.org/10.1039/c3lc50607j>
90. Di Carlo D, Wu LY, Lee LP (2006) Dynamic single cell culture array. *Lab Chip* 6(11):1445–1449. <https://doi.org/10.1039/b605937f>
91. Kobel S, Valero A, Latt J, Renaud P, Lutolf M (2010) Optimization of microfluidic single cell trapping for long-term on-chip culture. *Lab Chip* 10(7):857–863. <https://doi.org/10.1039/b918055a>
92. Lin L, Chu YS, Thiery JP, Lim CT, Rodriguez I (2013) Microfluidic cell trap array for controlled positioning of single cells on adhesive micropatterns. *Lab Chip* 13(4):714–721. <https://doi.org/10.1039/c2lc41070b>
93. Frimat JP, Becker M, Chiang YY, Marggraf U, Janasek D, Hengstler JG, Franzke J, West J (2011) A microfluidic array with cellular valving for single cell co-culture. *Lab Chip* 11(2):231–237. <https://doi.org/10.1039/c0lc00172d>
94. Korin N, Bransky A, Dinnar U, Levenberg S (2009) Periodic “flow-stop” perfusion microchannel bioreactors for mammalian and human embryonic stem cell long-term culture. *Biomed Microdevices* 11(1):87–94. <https://doi.org/10.1007/s10544-008-9212-5>
95. Lecault V, Vaninsberghe M, Sekulovic S, Knapp DJ, Wohrer S, Bowden W, Viel F, McLaughlin T, Jarandehi A, Miller M, Falconnet D, White AK, Kent DG, Copley MR, Taghipour F, Eaves CJ, Humphries RK, Piret JM, Hansen CL (2011) High-throughput analysis of single hematopoietic stem cell proliferation in microfluidic cell culture arrays. *Nat Methods* 8(7):581–586. <https://doi.org/10.1038/nmeth.1614>
96. Lindstrom S, Andersson-Svahn H (2011) Miniaturization of biological assays—overview on microwell devices for single-cell analyses. *Biochim Biophys Acta* 1810(3):308–316. <https://doi.org/10.1016/j.bbagen.2010.04.009>
97. Taylor LC, Walt DR (2000) Application of high-density optical microwell arrays in a live-cell biosensing system. *Anal Biochem* 278(2):132–142. <https://doi.org/10.1006/abio.1999.4440>
98. Wood DK, Weingeist DM, Bhatia SN, Engelward BP (2010) Single cell trapping and DNA damage analysis using microwell arrays. *Proc Natl Acad Sci U S A* 107(22):10008–10013. <https://doi.org/10.1073/pnas.1004056107>
99. Dusseiller MR, Schlaepfer D, Koch M, Kroschewski R, Textor M (2005) An inverted microcontact printing method on topographically structured polystyrene chips for arrayed micro-3-D culturing of single cells. *Biomaterials* 26(29):5917–5925. <https://doi.org/10.1016/j.biomaterials.2005.02.032>
100. Kurth I, Franke K, Pompe T, Bornhauser M, Werner C (2009) Hematopoietic stem and progenitor cells in adhesive microcavities. *Integr Biol* 1(5–6):427–434. <https://doi.org/10.1039/b903711j>
101. Deutsch M, Deutsch A, Shirihai O, Hurevich I, Afrimzon E, Shafran Y, Zurgil N (2006) A novel miniature cell retainer for correlative high-content analysis of individual untethered non-adherent cells. *Lab Chip* 6(8):995–1000. <https://doi.org/10.1039/b603961h>
102. And JRR, Folch A (2005) Large-scale single-cell trapping and imaging using microwell arrays. *Anal Chem* 77(17):5628–5634. <https://doi.org/10.1021/ac0505977>

103. Revzin A, Sekine K, Sin A, Tompkins RG, Toner M (2005) Development of a microfabricated cytometry platform for characterization and sorting of individual leukocytes. *Lab Chip* 5(1):30–37. <https://doi.org/10.1039/b405557h>
104. Tokimitsu Y, Kishi H, Kondo S, Honda R, Tajiri K, Motoki K, Ozawa T, Kadowaki S, Obata T, Fujiki S (2010) Single lymphocyte analysis with a microwell array chip. *Cytom Part A* 71A(12):1003–1010. <https://doi.org/10.1002/cyto.a.20478>
105. Prakadan SM, Shalek AK, Weitz DA (2017) Scaling by shrinking: empowering single-cell ‘omics’ with microfluidic devices. *Nat Rev Genet* 18(6):345–361. <https://doi.org/10.1038/nrg.2017.15>
106. Love JC, Ronan JL, Grotenbreg GM, van der Veen AG, Ploegh HL (2006) A microengraving method for rapid selection of single cells producing antigen-specific antibodies. *Nat Biotechnol* 24(6):703–707. <https://doi.org/10.1038/nbt1210>
107. Thakar RG, Cheng Q, Patel S, Chu J, Nasir M, Liepmann D, Komvopoulos K, Li S (2009) Cell-shape regulation of smooth muscle cell proliferation. *Biophys J* 96(8):3423–3432. <https://doi.org/10.1016/j.bpj.2008.11.074>
108. Cheng Q, Komvopoulos K (2010) Integration of plasma-assisted surface chemical modification, soft lithography, and protein surface activation for single-cell patterning. *Appl Phys Lett* 97(4):043705. <https://doi.org/10.1063/1.3462326>
109. Fang Y, Jin J, Chang H, Li X, Deng J, Ma Z, Yuan W (2015) Improved single-cell culture achieved using micromolding in capillaries technology coupled with poly (HEMA). *Biomicrofluidics* 9(4):044106. <https://doi.org/10.1063/1.4926807>
110. Utech S, Prodanovic R, Mao AS, Ostafe R, Mooney DJ, Weitz DA (2015) Microfluidic generation of monodisperse, structurally homogeneous alginate microgels for cell encapsulation and 3D cell culture. *Adv Healthc Mater* 4(11):1628–1633. <https://doi.org/10.1002/adhm.201500021>
111. Dolega ME, Abeille F, Picollet-D’hahan N, Gidrol X (2015) Controlled 3D culture in Matrigel microbeads to analyze clonal acinar development. *Biomaterials* 52(1):347–357. <https://doi.org/10.1016/j.biomaterials.2015.02.042>
112. Liu JJ, Gao D, Mao SF, Lin JM (2012) A microfluidic photolithography for controlled encapsulation of single cells inside hydrogel microstructures. *Sci China Chem* 55(4):494–501. <https://doi.org/10.1007/s11426-012-4538-5>
113. Liu J, Gao D, Li H-F, Lin J-M (2009) Controlled photopolymerization of hydrogel microstructures inside microchannels for bioassays. *Lab Chip* 9(9):1301–1305. <https://doi.org/10.1039/B819219G>
114. Guan Z, Jia S, Zhu Z, Zhang M, Yang CJ (2014) Facile and rapid generation of large-scale microcollagen gel array for long-term single-cell 3D culture and cell proliferation heterogeneity analysis. *Anal Chem* 86(5):2789–2797. <https://doi.org/10.1021/ac500088m>
115. Sydor AM, Czymmek KJ, Puchner EM, Mennella V (2015) Super-resolution microscopy: from single molecules to supramolecular assemblies. *Trends Cell Biol* 25(12):730–748. <https://doi.org/10.1016/j.tcb.2015.10.004>
116. Ng EX, Miller MA, Jing TY, Chen CH (2016) Single cell multiplexed assay for proteolytic activity using droplet microfluidics. *Biosens Bioelectron* 81:408–414. <https://doi.org/10.1016/j.bios.2016.03.002>
117. Lukaszewicz-Zajac M, Mroczko B, Szmitekowski M (2009) The significance of metalloproteinases and their inhibitors in gastric cancer. *Postepy Hig Med Dosw* 63(835515):258–265. <https://doi.org/10.1016/j.lfs.2009.03.019>
118. Perez-Toralla K, Mottet G, Guneri ET, Champ J, Bidard FC, Pierga JY, Kljanienco J, Draskovic I, Malaquin L, Viovy JL, Descroix S (2015) FISH in chips: turning microfluidic fluorescence in situ hybridization into a quantitative and clinically reliable molecular diagnosis tool. *Lab Chip* 15(3):811–822. <https://doi.org/10.1039/c4lc01059k>
119. Jungmann R, Avendano MS, Woehrstein JB, Dai M, Shih WM, Yin P (2014) Multiplexed 3D cellular super-resolution imaging with DNA-PAINT and exchange-PAINT. *Nat Methods* 11(3):313–318. <https://doi.org/10.1038/nmeth.2835>

120. Casabella S, Scully P, Goddard N, Gardner P (2016) Automated analysis of single cells using laser tweezers raman spectroscopy. *Analyst* 141(2):689–696. <https://doi.org/10.1039/c5an01851j>
121. Stojanovic I, van der Velden TJG, Mulder HW, Schasfoort RBM, Terstappen LWMM (2015) Quantification of antibody production of individual hybridoma cells by surface plasmon resonance imaging. *Anal Biochem* 485:112–118. <https://doi.org/10.1016/j.ab.2015.06.018>
122. Agnarsson B, Lundgren A, Gunnarsson A, Rabe M, Kunze A, Mapar M, Simonsson L, Bally M, Zhdanov VP, Hook F (2015) Evanescent light-scattering microscopy for label-free interfacial imaging: from single sub-100 nm vesicles to live cells. *ACS Nano* 9(12):11849–11862. <https://doi.org/10.1021/acs.nano.5b04168>
123. Cotte Y, Toy F, Jourdain P, Pavillon N, Boss D, Magistretti P, Marquet P, Depeursinge C (2013) Marker-free phase nanoscopy. *Nat Photonics* 7(2):113–117. <https://doi.org/10.1038/nphoton.2013.116>
124. Anderson SE, Bau HH (2015) Carbon nanoelectrodes for single-cell probing. *Nanotechnology* 26(18):185101. <https://doi.org/10.1088/0957-4484/26/18/185101>
125. Robinson JT, Jorgolli M, Shalek AK, Yoon MH, Gertner RS, Park H (2012) Vertical nanowire electrode arrays as a scalable platform for intracellular interfacing to neuronal circuits. *Nat Nanotechnol* 7(3):180–184. <https://doi.org/10.1038/NNano.2011.249>
126. Dick JE (2016) Electrochemical detection of single cancer and healthy cell collisions on a microelectrode. *Chem Commun* 52(72):10906–10909. <https://doi.org/10.1039/c6cc04515d>
127. Safaei TS, Mohamadi RM, Sargent EH, Kelley SO (2015) In situ electrochemical ELISA for specific identification of captured cancer cells. *ACS Appl Mater Inter* 7(26):14165–14169. <https://doi.org/10.1021/acsami.5b02404>
128. Koch JA, Baur MB, Woodall EL, Baur JE (2012) Alternating current scanning electrochemical microscopy with simultaneous fast-scan cyclic voltammetry. *Anal Chem* 84(21):9537–9543. <https://doi.org/10.1021/ac302402p>
129. Huang QS, Mao SF, Khan M, Zhou L, Lin JM (2018) Dean flow assisted cell ordering system for lipid profiling in single-cells using mass spectrometry. *Chem Commun* 54(21):2595–2598. <https://doi.org/10.1039/c7cc09608a>
130. Gong XY, Zhao YY, Cai SQ, Fu SJ, Yang CD, Zhang SC, Zhang XR (2014) Single cell analysis with probe ESI-mass spectrometry: detection of metabolites at cellular and subcellular levels. *Anal Chem* 86(8):3809–3816. <https://doi.org/10.1021/ac500882e>
131. Krismer J, Sobek J, Steinhoff RF, Fagerer SR, Pabst M, Zenobi R (2015) Screening of chlamydomonas reinhardtii populations with single-cell resolution by using a high-throughput microscale sample preparation for matrix-assisted laser desorption ionization mass spectrometry. *Appl Environ Microb* 81(16):5546–5551. <https://doi.org/10.1128/Aem.01201-15>
132. Bobrowska J, Pabijan J, Wiltowska-Zuber J, Jany BR, Krok F, Awsiuk K, Rysz J, Budkowski A, Lekka M (2016) Protocol of single cells preparation for time of flight secondary ion mass spectrometry. *Anal Biochem* 511:52–60. <https://doi.org/10.1016/j.ab.2016.06.011>
133. Robinson MA, Graham DJ, Morrish F, Hockenbery D, Gamble LJ (2015) Lipid analysis of eight human breast cancer cell lines with ToF-SIMS. *Biointerphases* 11(2):02A303. <https://doi.org/10.1116/1.4929633>
134. Passarelli MK, Newman CF, Marshall PS, West A, Gilmore IS, Bunch J, Alexander MR, Dollery CT (2015) Single-cell analysis: visualizing pharmaceutical and metabolite uptake in cells with label-free 3d mass spectrometry imaging. *Anal Chem* 87(13):6696–6702. <https://doi.org/10.1021/acs.analchem.5b00842>

Chapter 4

Microfluidic Technology for Single-Cell Manipulation



Weifei Zhang, Nan Li and Jin-Ming Lin

Abstract Single-cell analysis has attracted much attention in the field of biological and biomedical study owing to the heterogeneity among individual cells. This poses significant challenges to conventional bulk assays which would mask rare but important information owing to the assumption of average behavior. To avoid the interference of useless cells and obtain the single cells in the trial of genomics, proteomics, metabonomics, and single-cell behavior study, various cell manipulation techniques have been developed for single-cell research. In this chapter, we introduce the principles of droplet generation and single-cell encapsulation and review the latest achievements of cell manipulation technique by categorizing externally applied manipulation forces: microstructures, electrical, optical, magnetic, acoustic, and mechanical. This chapter will also introduce our latest work and provide important references and ideas for the development of droplet microfluidic-based single-cell manipulation.

Keyword Microfluidics · Droplet · Single-cell encapsulation · Cell manipulation · Single-cell lysis

4.1 Introduction

The cell as the fundamental unit of life has been extensively studied for expressions of genes, proteins, and metabolites [1–3]. In conventional methods for biochemical analysis, samples are usually collected from a large number of cells treated with certain stimulus in order to obtain sufficient molecules for meeting the sensitivity of the detection instrument. Thus, the results are averaged over the number of cells. However, it has been frequently found that the behaviors of individual cells are not identical even with the same type cells cultured in the same microenvironment. As a result, the bulk assays usually mask some rare but crucial information and even

W. Zhang · N. Li · J.-M. Lin (✉)
Department of Chemistry, Tsinghua University, Beijing 100084, People's Republic of China
e-mail: jmlin@mail.tsinghua.edu.cn

© Springer Nature Singapore Pte Ltd. 2019
J.-M. Lin (ed.), *Microfluidics for Single-Cell Analysis*,
Integrated Analytical Systems, https://doi.org/10.1007/978-981-32-9729-6_4

cause some misleading interpretations [4–6]. Therefore, to characterize the cell-to-cell differences and discern cellular subpopulations, single-cell analysis becomes necessary [7, 8].

To accurately describe and elucidate the heterogeneities among single cells, systems with high throughput and sensitivity are needed. These two requirements have driven the development of microfluidic system, where an aqueous flow is segmented into individual droplets within an immiscible carrier fluid (often a mineral or fluorinated oil) to encapsulate single cell [9–11]. Such systems offer several key advantages for single-cell analysis. The first is parallelization: multiple identical microreactor units can be formed in a short time, and parallel processing can easily be achieved, allowing large data sets to be acquired efficiently. The second is miniaturization: droplet reactors have small dimensions, in the range from subnanoliter to picoliter level, making it possible for the single-cell analysis. The third is compartmentalization: droplets formed in the microfluidic channels can be used as independent units for manipulation [12–14]. Owing to these advantages, recently droplet microfluidic technology has been applied to various fields of single-cell research, such as signal response, nucleic acid analysis [15–18], protein analysis [19–21], and metabolite analysis [22, 23].

In this chapter, we will introduce the recent developments and outstanding achievements of droplet microfluidic technology in single-cell manipulation. Based on the study procedure, the main content is divided into four parts: droplet generation, single-cell encapsulation, cell manipulation, and single-cell lysis. This chapter will also discuss the challenges and prospect of droplet microfluidics in single-cell analysis and provide important reference for the development of biomedical research and application.

4.2 Droplet Generation

Although the variety of methods have been developed to drive the dispersed phase into the continuous phase and form the droplets, the fluid behavior can be characterized through some crucial dimensionless numbers, which are calculated via the parameters of the fluid properties, flow conditions, and geometric features. The significant physical parameters, which determine droplet formation, can be characterized through calculation of the capillary number $Ca = \mu U / \gamma$, where μ (Pa s) and U (m s^{-1}) are the viscosity and velocity of the continuous phase, and γ (N m^{-1}) is the surface tension of the droplet interface. With the increase of Ca value, the various flow regimes are defined as the squeezing, dripping, and jetting, which are depicted in Fig. 4.1. For a more detailed discussion of these three regimes, some brilliant publications or reviews are recommended to the readers [24, 25]. In addition, there are also some other dimensionless number which are related to the droplet breakup under a high flow rate or a large-dimensional geometry. For example, Weber number (We) is used to report the relative importance of inertia with respect to interfacial tension; Bond number (Bo) reflects the relative

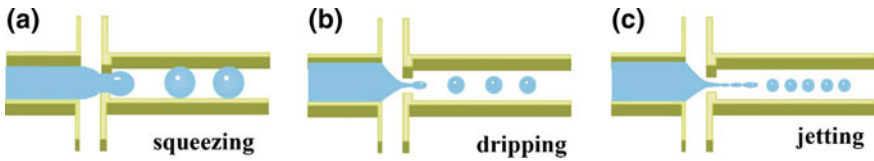


Fig. 4.1 Three regimes for droplet generation, squeezing, dripping, and jetting with an increase of capillary number

importance of gravitational forces with reference to interfacial tension; and Reynolds number (Re) indicates the relative importance of inertial forces with respect to viscous forces.

4.2.1 Droplet Generation by Passive Methods

In passive methods driven by the external pumps, two immiscible fluids (dispersed phase and continuous phase) meet at a junction, which determines interface deformation and droplet breakup, as shown in Fig. 4.2a [22]. According to the

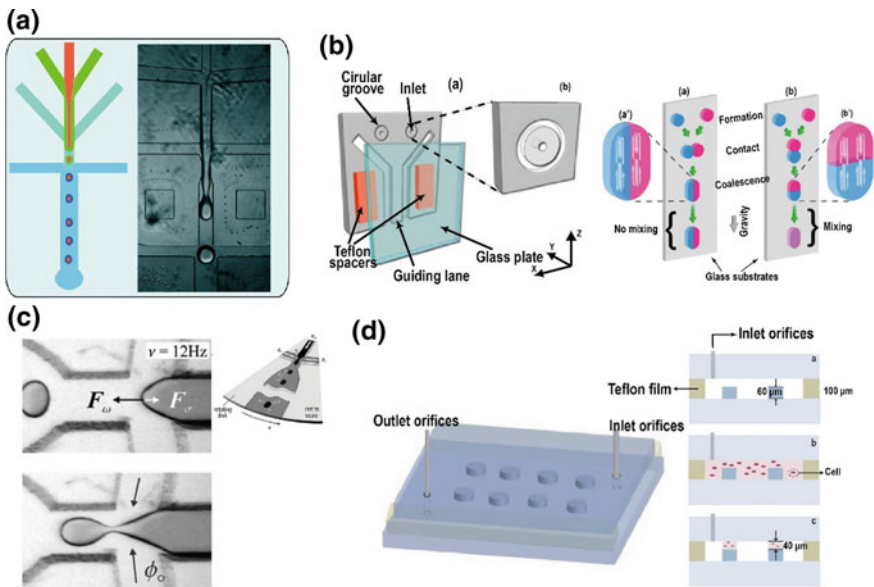


Fig. 4.2 Droplet generation by passive method. **a** Droplets can be generated by two immiscible fluids, and the droplet size can be adjusted by changing the ratio of oil and water flow rates, which were controlled through a syringe- or pressure-driven pump [22]. **b** Droplets were produced by a circular groove surrounded inlet [26]. **c** Droplets were generated by centripetal forces using a rotating microfluidic device [27]. **d** Droplets were generated through protrudent circular plot arrays based on surface tension [28]

complex geometrical design of the microchannel junction, the droplet formation can be classified into coflow, cross-flow, and flow-focusing categories. Besides, Lin's laboratory also reported an approach to generate monodispersed droplets on a microfluidic chip without using a carrier liquid, which employed a circular groove surrounded inlet for the droplet formation, as shown in Fig. 4.2b [26]. However, exert pumps are not the only way to produce pressure gradients for droplet generation. Häberle et al. have presented a method which used a rotating microfluidic device to generate the centripetal force for droplet generation in a traditional flow-focusing geometry, as shown in Fig. 4.2c [27]. Li et al. developed a microdevice with protrudent circular plot arrays for the formation of nanoliter droplets by surface tension without any additional equipment, as shown in Fig. 4.2d [28].

4.2.1.1 Coflow

In the coflow category, the two immiscible phases flow in a set of coaxial microchannels in the same direction. The dispersed fluid flows into an inner channel, and the continuous phase is introduced into an outer concentric channel as shown in Fig. 4.3a. Fischer et al. [29] were the first to report the coflow experimental setup, which consisted of a cylindrical glass capillary tube nested within a square glass tube. By ensuring that the inner dimension of the square tube was the same as the outer diameter of the cylindrical tube, a good alignment to form a coaxial geometry was achieved. Thorough experimental data provided by the authors indicated that the fluid properties and flow rates were two important factors to determine the droplet size. Increasing the continuous flow velocity reduced the droplet size owing to a higher shear stress, while increasing the dispersed flow rate resulted in an increase of droplet size, as a larger volume of dispersed fluid entered a droplet before breakup. In comparison with the velocity, the viscosity of the two phases had rather weak effects on the droplet size.

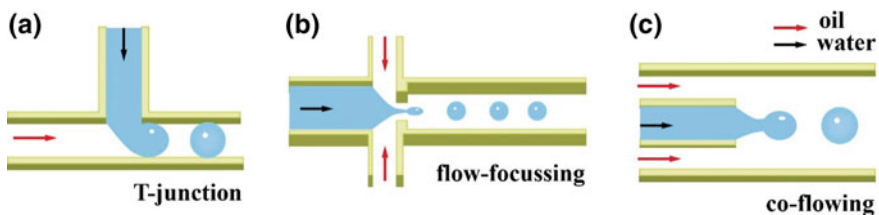


Fig. 4.3 Scheme of three geometrical designs of the microchannel junction: coflowing, cross-flowing, and flow-focusing

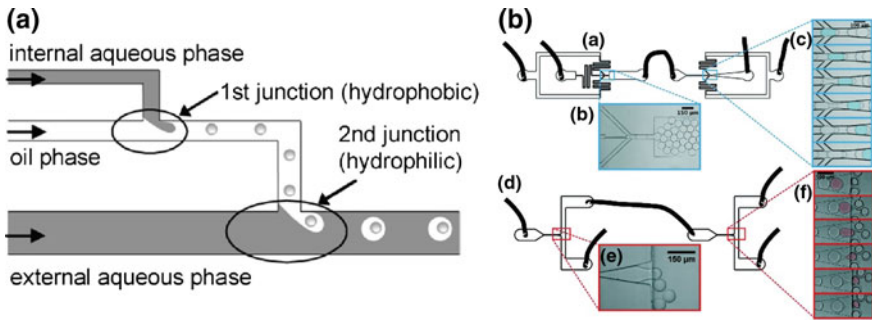


Fig. 4.4 Common methods for generating multilayered droplets. **a** A double T-junction cross structure for double emulsions [32]. **b** A double flow-focusing structure for double emulsions [35]

4.2.1.2 Cross-Flow

Cross-flow category is achieved by using angled microchannels. T-junction is a common structure, in which dispersed and continuous phases flow through orthogonal channels at a cross junction, as shown in Fig. 4.3b. Thorsen was the first to use T-junction to generate droplets [30]. In this configuration, the main channel is introduced with the continuous phase and the side channel is infused with the dispersed phase. These two immiscible phases are intersected at focused zone in a perpendicular way to generate droplets under the regulation of surface tension and shear stress. The two asymmetric forces from side channel and main channel, together with the surface tension, break the dispersed phase to independent droplets [31]. The droplet formation process can be summarized as dropping, spraying, and deformation. The droplet size and formation rate can be effectively adjusted by changing the flow velocity, channel size, and liquid viscosity. Additionally, multi-emulsions can be generated through reasonable use of multiple T-junction (Fig. 4.4a) [32]. However, it should be noted, the asymmetry force in droplet generation process will have a great influence on the cells encapsulated in droplets, and thus, T-junction had better be used in other aspects instead of cell analysis.

In addition, some other modified geometry designs are also developed for various purposes. For instance, a “K-junction” type was reported to provide an exit channel for the waste [33]. And a “V-junction” type was designed for a high degree of operational flexibility [34].

4.2.1.3 Flow-Focusing

The flow-focusing geometry is composed of three channels, one main channel and two symmetric side channels. These channels are focused on a narrow region connecting the downstream channel, and two immiscible phases flow coaxially through this narrow region, which has the function of shear-focusing and thus

contributes to uniform droplet generation, as shown in Fig. 4.3c. Currently, this method has the ability to make relatively small droplets and the droplet-generation process is closely related to the size of the narrow region. This design has an advantage that the dispersed phase in focused zone will only suffer from the driving force. Since the side channels are symmetrical, force from other directions would be counteracted, which will reduce the interference to cells and keep the droplets stable. Similarly, the size of the droplet is determined by the flow ratio of the two phases. The larger the velocity of the continuous phase is, the smaller and faster the generated droplet is. Besides the size of the focusing region, the viscosity of the liquid also influences the formation and size of droplets. Similar to the multiple T-junction, the application of multiple flow-focusing structures can also obtain multilayered droplets (Fig. 4.4b) [35].

4.2.2 Droplet Generation by Active Methods

As for active methods, the droplet generation can occur on-demand with the application of an active, short-duration external forced. According to the categories of energy sources, active method-based droplet generation can be classified into electrical, magnetic, thermal, and mechanical methods.

4.2.2.1 Electrical Method

Electrical source can be used to modulate the size of droplets. Our group reported a series of work that utilized the piezoelectric inkjet to generate drop-on-demand monodispersed droplets with the volume of picoliter level. This method was easy to control and the droplet size can be regulated by adjusting the piezoelectric actuation including driving voltage and pulse width. As an ideal generator of droplets, inkjet was coupled to various analytical instruments, such as mass spectrometry and capillary electrophoresis. Chen et al. integrated drop-on-demand inkjet cell printing and probe electrospray ionization mass spectrometry (PESI-MS) to study the single-cell lipid. The single-cell-containing droplets were generated via inkjet sampling, followed by precisely dripping onto a tungsten-made electrospray ionization needle for immediate spray under a high-voltage electric field, as shown in Fig. 4.5a [36]. Zhang et al. combined the inkjet printing system with capillary electrophoresis (CE) to investigate the separation of cells, which validated the feasibility of inkjet printing for mammalian cells to achieve the drop-on-demand and convenient sampling into capillary [37]. Further, they developed a novel and flexible online digital polymerase chain reaction (dPCR) system, which consisted of an inkjet for generating the droplets, a coiled fused-silica capillary for thermal cycling, and a laser-induced fluorescence detector (LIFD) for positive droplet counting. Upon inkjet printing, monodisperse droplets were continuously generated in the oil phase and then introduced into the capillary in the form of a stable

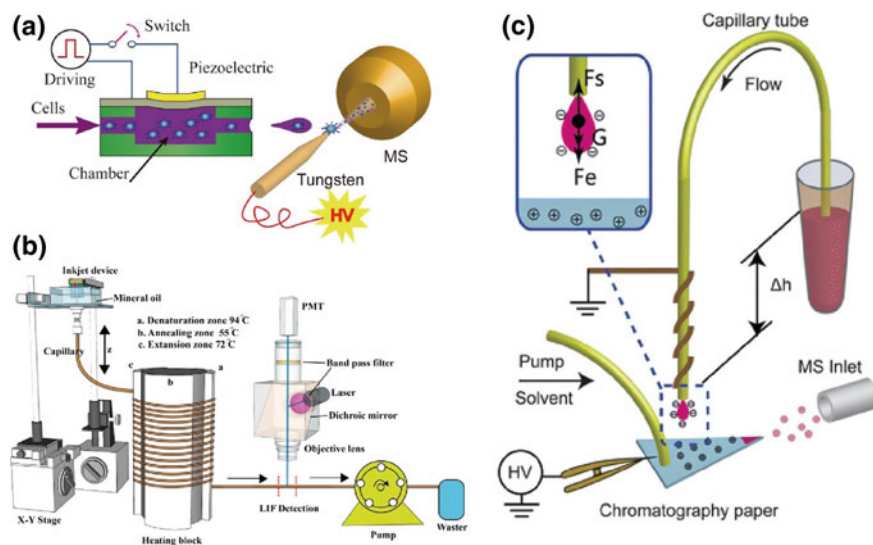


Fig. 4.5 Droplet generation by electrical methods. **a** Inkjet printing-based droplet single-cell MS analysis [36]. **b** Inkjet printing-based droplet PCR analysis [15]. **c** Droplet generation *via* gravity and electrostatic attraction for ESI-MS analysis [39]

dispersion. The droplets containing one or zero molecules of target DNA passed through the helical capillary that was attached to a cylindrical thermal cycler for PCR amplification, resulting in the generation of fluorescence for the DNA-positive droplet, as shown in Fig. 4.5b [15]. Korenaga et al. also utilized the inkjet printing technique as a sample introduction method to pattern cells onto ITO glass substrate for MALDI-MS detection, allowing the sample diameter with the range of a few hundred micrometers [38]. Apart from inkjet for the droplet formation, Liu et al. generated submicroliter droplets via gravity and electrostatic attraction and provided a proof-of-principle experiment to show the utilization of paper-based electrospray ionization mass spectrometry (ESI-MS) in the online analysis of the generated droplets, as shown in Fig. 4.5c [39]. Further, based on this mechanism and protocol of droplet formation, they established a homemade microdialysis module for ESI-MS [40]. Besides, Link et al. incorporated electrodes with a constant direct current voltage into the flow-focusing device, as shown in Fig. 4.6a, where the water flow acted as a conductor, and the oil stream served as an insulator. This led to the accumulation of charge at the droplet interface, and thus, electrical field force also played an important part in controlling the droplet size apart from the interfacial tension and viscous force [41]. The higher the voltage was, the smaller the droplet size was. Additionally, an alternating current can also be applied to generate the droplets via the electrowetting-on-dielectric (EWOD) effect, because the contact angle between the conductive liquid flow and the channel could be reduced by exerting an electrical field.

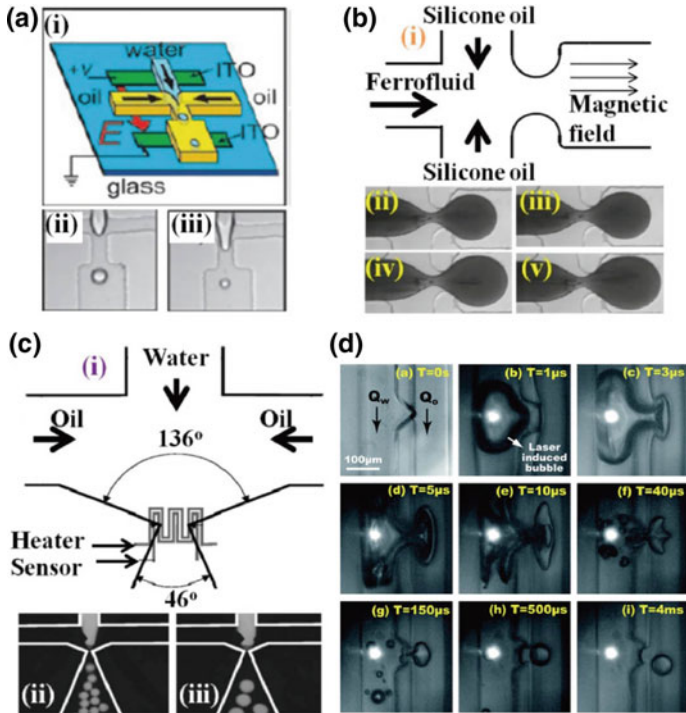


Fig. 4.6 Droplet generation by active methods. **a** Droplet generation by applying a direct current voltage [41]. **b** Droplet generation by applying a magnetic field [42]. **c** Droplet generation by thermal method [43]. **d** Droplet generation by optical method [45]

4.2.2.2 Magnetic Method

The droplet formation can also be achieved through the non-contact, magnetic control, such as ferrofluids which can be suspended in either aqueous or oily carrier liquid. Nguyen et al. reported a method to use an aqueous ferrofluid as the dispersed phase, and the magnetic force could drag the ferrofluid tip forward until the droplet formation, Fig. 4.6b [42]. A magnetic bond number, B_m , indicating the relative strength of the magnetic force to interfacial tension, is used to characterize the droplet behavior.

4.2.2.3 Thermal Method

The thermal source can be used to control the droplet generation owing to the dependency of Ca on the temperature, because the fluid properties such as viscosity and interfacial tension can vary with the temperature. The whole device or junction can be heated, and thermal resource can also be introduced through a localized laser

irradiation. A previous study has report that the droplet generation was modulated by integrating a microheater and a temperature sensor into a flow-focusing device, as shown in Fig. 4.6c [43]. The fluid viscosity and interfacial tension were normalized as the functions of the temperature, and the results suggested that the droplet size could be well controlled by the temperature.

4.2.2.4 Optical Method

Optical method has been used to generate picoliter-level droplet, even achieving to create femtoliter-volume droplets on-demand in nanofluidic channels [44]. Park et al. used a focused pulsed laser to produce a cavitating microbubble in the neighborhood of a T-junction position, generating picoliter-level monodispersed W/O droplets during a few milliseconds with a rate of up to 10 kHz (Fig. 4.6d) [45].

4.3 Single-Cell Encapsulation

Since the delivery of cells to the droplet-generation nozzle is a random process with a Poisson distribution, accurate control of the number of cells in each droplet is challenging [46]. Usually, the cell suspension is largely diluted for the requirement of single-cell encapsulation, which leads to a large number of empty droplets [47]. Consequently, a variety of methods to remove droplets containing no cells have been developed. Viovy et al. were the first to report a purely hydrodynamic approach to confine the single cells into a picoliter-level droplet prior to spontaneous self-sorting based on the sizes. A cell-triggered Rayleigh–Plateau instability in a flow-focusing structure helps the single cells to be encapsulated in the droplets. Two extra hydrodynamic mechanisms, lateral drift of deformable objects in a shear flow and sterically driven dispersion in a compressional flow, realized the self-sorting, as shown in Fig. 4.7a [48]. This method was demonstrated to have a significant improvement in single-cell encapsulation and the sorting rate could reach 70–80%. Further, Chen et al. presented a passive separation strategy, which used a droplet jetting channel generator and a deterministic lateral displacement (DLD) size-sorting channel to encapsulate single cells into aqueous droplets and separated cell-encapsulated droplets from empty droplets for subsequent assays. Due to the cell-triggered Rayleigh–Plateau instability in the process of droplet jetting, large cell-containing droplets (diameter 25 μm) and small empty droplets (diameter 14 μm) were generated. Then, size-based sorting was performed inside the DLD micropillar channel, where the critical dimension for separation is defined by geometric design [49]. Furthermore, to avoid the restrictions of cell stochastic encapsulation, one cell should be present whenever a droplet is produced. This can be achieved by regulating cells in the direction of flow with the same frequency when they enter the microfluidic nozzle. Toner et al. have reported a method that allowed cells self-organizing into two evenly spaced streams and 80% single-cell

encapsulation efficiency could be obtained when a high-density suspension of cells was forced to travel rapidly through a high aspect-ratio microchannel, as shown in Fig. 4.7b [50]. Kemna et al. used a Dean-coupled inertial ordering of cells in a simple curved continuous microchannel to achieve single-cell encapsulation in picoliter droplets with an efficiency of up to 77%, as shown in Fig. 4.7c [51]. Further, another method was developed by using a short pinched flow channel composed of contracting and expanding chambers to conduct inertial focusing along the channel center, which quantified the single-cell encapsulation efficiency >55%, as shown in Fig. 4.7d [52].

Although a variety of studies have been reported to circumvent the block of low single-cell encapsulation efficiency, yet the optimal encapsulation efficiency was less than 80%. Thus, more studies are suggested to further address this issue from the point of technical development.

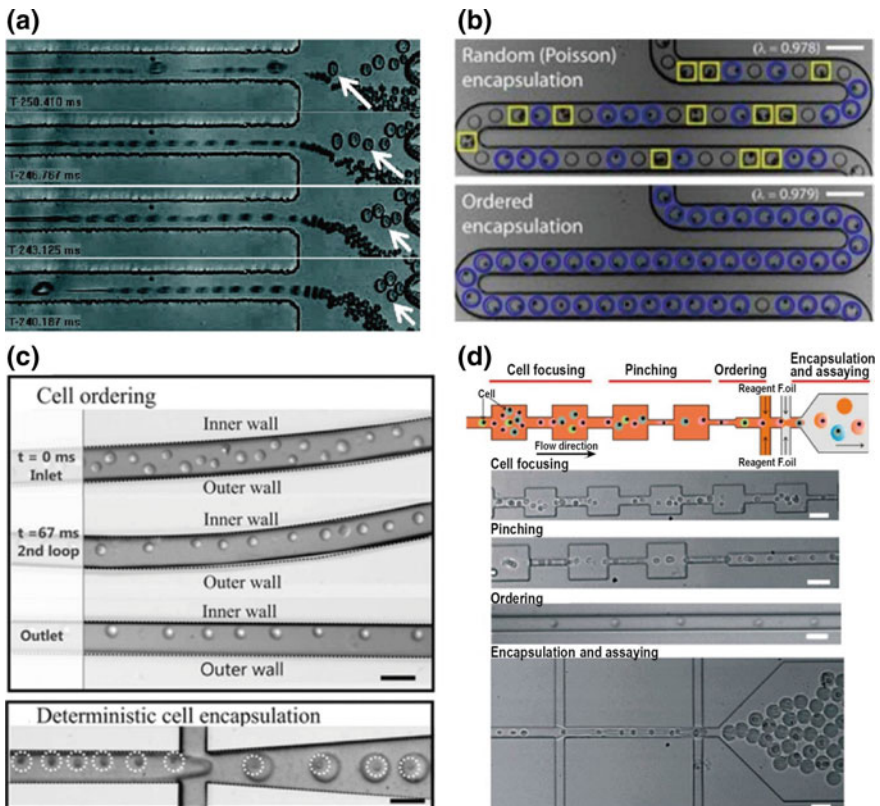


Fig. 4.7 Methods for improving the single-cell encapsulation efficiency. **a** Size-based droplet sorting after single-cell encapsulation by a hydrodynamic approach [48]. **b–d** Inertial flow-based cell spacing and single-cell encapsulation via **(b)** a high aspect-ratio straight channel [50], **c** A curved channel [51], **d** A short pinched flow channel [52]

4.4 Cell Manipulation

With the development of microfluidic chip, the cell manipulation technology coupled with microfluidic techniques becomes a promising tool for single-cell-level manipulation. To reduce the interference of useless cells and obtain the single pure target cell for the single-cell analysis, such as genetic analysis, protein analysis, and metabolism analysis, a variety of single-cell manipulation techniques have been developed. These manipulation techniques can be divided into passive and active methods [53]. Passive methods use rationally designed microfluidic structures to control cell positions, for instance, pinched flow [54] and deterministic lateral displacement [55]. Active methods use actuators to manipulate cells and are classified depending on the externally applied manipulation forces: electrical [56], optical [57], magnetic [58], acoustic [59], and mechanical. The advantages and drawbacks of each cell manipulation technique were described in this part.

4.4.1 *Microstructures Manipulation*

The precise design of microstructures including microwells, microbarriers, and microtraps can be used in biological study, such as cell capture, pairing, patterning, and subsequent cell culture [60–62]. These approaches have the advantages on high-throughput, high-efficient, and ease of operation and have been extensively used in single-cell systems. Sarioglu et al. [63] developed a Cluster-Chip that contained a series of triangular pillars, and these unique geometries were exploited to differentiate CTC clusters from single cells in blood. This strategy realized specific and label-free isolation of CTC clusters from patients with various cancer types, and then achieved the release of CTC clusters, allowing for downstream molecular and functional assays. Lecault et al. [64] developed a microfluidic platform containing thousands of nanoliter-scale chambers for longer-term mammalian cell culture. This platform enabled in situ immunostaining and recovery of viable cells, and was applied to high-throughput investigation of hematopoietic stem cell proliferation at the single-cell level.

4.4.2 *Electrical Manipulation*

Electrokinetic forces originating from the electric field have been widely applied to microfluidic cell manipulation owing to the feasibility of integrating microelectrodes in microfluidic chips [65]. Generally, electrokinetic manipulations were classified into three categories: electrophoresis [66], dielectrophoresis [67], and electroosmosis [68], and these techniques have all been realized on microfluidic chips.

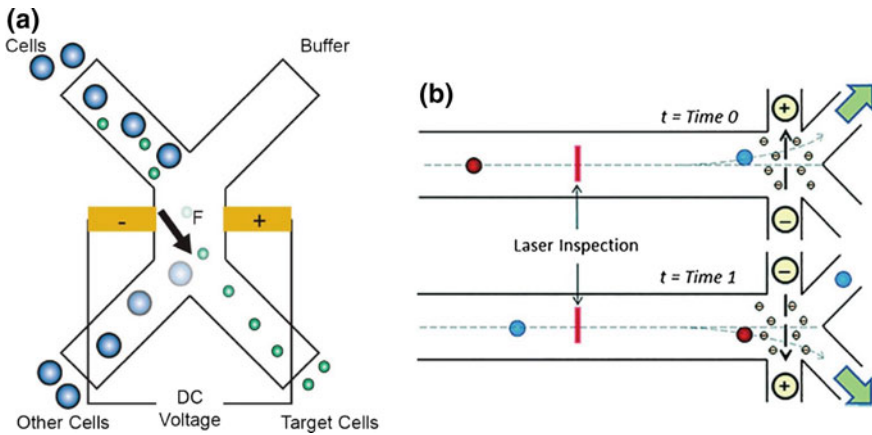


Fig. 4.8 Schematics of electrical manipulation techniques for single cells. **a** Electrophoresis manipulation. Cells with negative charge move toward the positive electrode. **b** Electroosmotic flow manipulation. Negatively charged ions moving toward the positive electrode induce secondary fluid movements for cell manipulation [70]

4.4.2.1 Electrophoresis

Generally, most cells membrane were negative at neutral pH. Thus, suspended cells with negative charge will move toward a positive electrode direction under the application of a constant electric field [69]. In a solution, the cells obtain a velocity resulted from a force balance, where the dominant forces exerting on the cell are the Coulomb and drag forces. For the separation of different cell types, it is necessary for the cells to have different charge or size [65], and this separation mode is called electrophoresis (EP) (Fig. 4.8a) [70]. Takahashi et al. [71] have developed a device which enabled two laminar flow streams to converge at the center. Cells are introduced in one stream and imaged thirty times per second as they pass the convergence point. At the position where the electrodes were connected between the two streams with an applied voltage, certain specific cell was recognized depending on the phase contrast and fluorescence, and the electrophoretic force causes the cell to jump from one stream to the other. Likewise, Guo et al. [72] sorted single-cell-containing droplets into different streams through a pulsed electric field. However, it should be noted, it is not a good alternative to use electrophoresis to separate the heterogeneous cell suspensions, because the specificity of electrophoretic migration is not obvious between cells [65, 73].

4.4.2.2 Dielectrophoresis

In comparison with electrophoresis, dielectrophoresis is a more popular method for cell manipulation owing to the higher specificity in dielectric properties among

various cell types. There are also some other advantages, such as harmless to the cell, pre-treatment free, high precision and easy to manipulate an individual cell. And this term “dielectrophoresis” was first presented by Pohl in 1951, who used small plastic particles suspended in insulating dielectric liquids to perform significant early experiments and found that the particles could move in response to the application of a non-uniform alternating current or direct current electric field [74]. Currently, dielectrophoresis has been developed in single-cell manipulation field by acting a non-uniform electric field upon a neutral object. The magnitude of DEP force is determined by the size, shape, electrical property of the single cell, and the electric field gradient. For a spherical cell, it could be assumed that the electric field (E) does not change significantly over the cell surface. As a result, the time-averaged dielectrophoresis force ($\langle F_{\text{DEP}} \rangle$) could be calculated according to the following equation.

$$\langle F_{\text{DEP}} \rangle = 2\pi r^3 \varepsilon_m \text{Re}[f_{\text{CM}}(\omega)] \nabla |E|^2$$

Here, r was the radius of cells, ε_m was the permittivity of the culture medium, and $\nabla |E|^2$ described the intensity of the electric field at each point, regardless of the direction. And an important term, real part of Clausius–Mossotti (CM) factor ($\text{Re}[f_{\text{CM}}(\omega)]$) determined the direction of the dielectrophoresis force and controlled the direction of cell motion, which was defined based on the dielectric properties of the cells and culture medium, and was a function of the applied frequency. The Clausius–Mossotti factor can be described as a function of the medium and the particle complex permittivities as follows:

$$f_{\text{CM}}(\omega) = \frac{\varepsilon_c^*(\omega) - \varepsilon_m^*(\omega)}{\varepsilon_c^*(\omega) + 2\varepsilon_m^*(\omega)}$$

where $\varepsilon_c^*(\omega)$ and $\varepsilon_m^*(\omega)$ represent complex permittivity of cells and culture medium, respectively. And complex permittivity is dependent on permittivity (ε), conductivity (σ), and angular frequency ($\omega = 2\pi f$) of the applied electric field, which can be described as follows:

$$\varepsilon_{c \text{ or } m}^* = \varepsilon_0 \varepsilon_{c \text{ or } m} - j \frac{\sigma_{c \text{ or } m}}{2\pi f}$$

For mammalian cells, dielectric properties can be formulated by the protoplast model. CM factor for live cells can be rewritten as the following equation:

$$f_{\text{CM}}(\omega) = - \frac{\omega^2(\tau_m \tau_c^* - \tau_c \tau_m) + j\omega(\tau_m^* - \tau_m - \tau_c^*) - 1}{\omega^2(2\tau_m \tau_c^* + \tau_c \tau_m^*) - j\omega(\tau_m^* + 2\tau_m + \tau_c^*) - 2}$$

where $\tau_c^* = c_m r / \sigma_c$ and $\tau_c = \varepsilon_c / \sigma_c$ are time constants for cells. c_m is membrane capacitance. σ_c and ε_c are conductivity and permittivity of cells, respectively. In addition, $\tau_m^* = c_m r / \sigma_m$ and $\tau_m = \varepsilon_m / \sigma_m$ are time constants for medium. σ_c and ε_c

represent conductivity and permittivity of medium, respectively. The value of f_{CM} factor is limited within -0.5 to 1 and changed with the frequency. When the value is <0 , the cells are less polarizable than the culture medium and suffered from a negative dielectrophoresis force, which drives the cell to move toward the direction of weak electric field intensity. When the value >0 , the cell will move toward the strong electric field under the manipulation of a positive dielectrophoresis force. Based on the theory of dielectrophoresis, a large number of device have been designed for single-cell manipulation including cell separation [75], trapping/capturing and release [76].

The electric field gradient can be determined by different electrode shapes. Consequently, various electrode shapes have been designed for cells or particles manipulation, such as ring electrode Fig. 4.9a and b [77], quadrupole electrode Fig. 4.9c, d [78]. Further, actuation electrodes have been integrated into microfluidic chip for the dielectrophoresis manipulation of single cell. Park used such an integrated chip to detect the trapping single cell through the impedance method, as shown in Fig. 4.10 [79]. For high-efficient single-cell trapping and analysis, an integrated microfluidic chip containing a microwell array inside was reported [80].

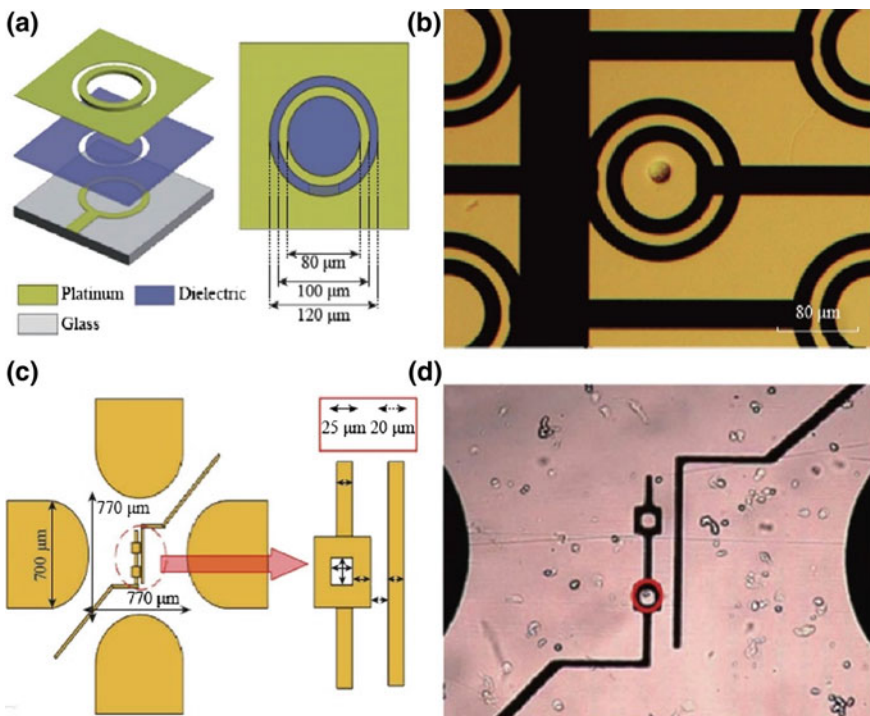


Fig. 4.9 Different electrodes applied with voltage to generate non-uniform electric field for single-cell manipulation. **a, b** Ring electrode [77]. **c, d** Quadrupole electrode [78]

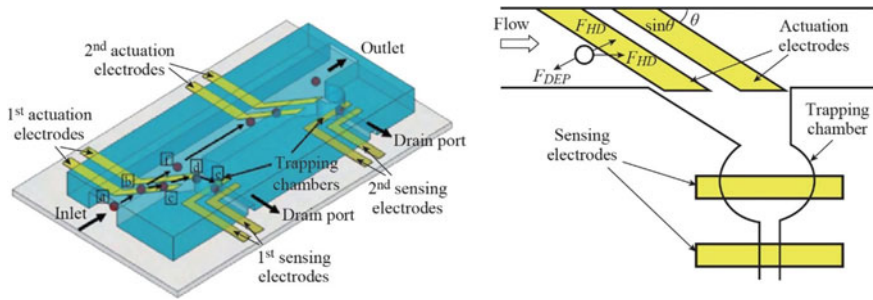


Fig. 4.10 Schematic of the microfluidic chip and illustration of the forces acted on the particle [79]

4.4.2.3 Electroosmotic Flow

Similar to preceding discussion about electrophoresis and dielectrophoresis, electroosmotic-based separation was also caused by an applied electric field. However, they have different phenomenological process. Electroosmotic flow (EOF) refers to fluid motion with the direction of inducing solvated ion transport under an electric field (Fig. 4.8b) [70]. Dittrich and Schwille have reported a sorting microchip that leveraged a pump to drive primary flow to create electroosmotic flow, and this pressure-driven method enabled a fast and stable flow rate, allowing a high-throughput cell sorting [81]. The advantage of electroosmotic flow typically lies in the precise control of volumetric flow through various channels occupying the same microfluidic device. However, to use the electroosmotic flow to manipulate the single cell, the electrodes have to be fabricated on the microfluidic chip, leading to complicated operation. What is worse, it is harmful for cells to be exposed to electric fields, resulting in a decrease of cell viability. Despite all these defects, this method has the ability to precisely control small volumes-based cell separation.

4.4.3 Optical Manipulation

A few decades ago, a focused laser was found that could propel microparticles in a liquid, and this was the origination of optical manipulation [82]. In the following, these researchers used a tightly focused laser to achieve stable trapping, forming the foundation of contemporary “optical tweezers” [83]. Optical tweezers are significant tools and have been used to manipulate single cells on microfluidic chips, which rely on a tightly focused laser beam to manipulate single cells with little damage to the cell behaviors. In an optical process, single cells are easily trapped at the focal point of laser beams, which enables the isolation of single cells with great convenience (Fig. 4.11a) [84]. Similar to the dielectrophoresis, the behavior of cells

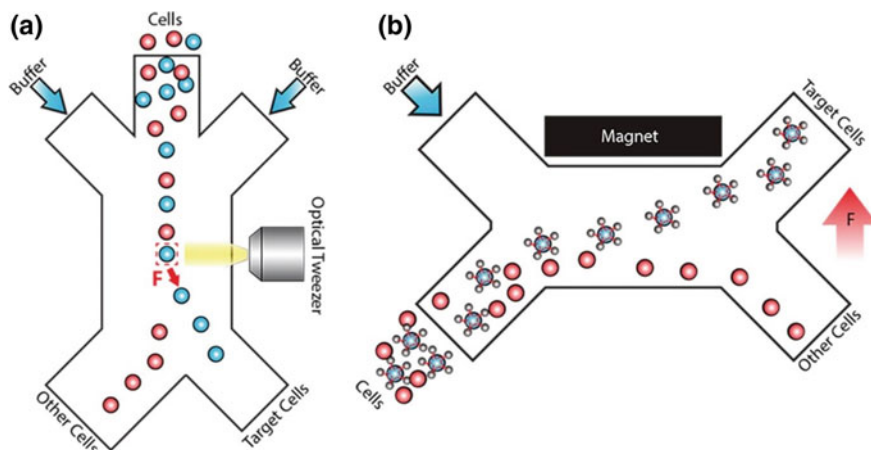


Fig. 4.11 Schematics of single-cell manipulation via optical and magnetic method. **a** The cells are repositioned toward the appropriate outlet under the manipulation of the optical tweezers. **b** The target cells labeled with magnetic beads are manipulated to move toward a distinct outlet compared to the nontarget cells [84]

is determined by their refractive index compared to the surrounding fluid. The cells will migrate toward the region of highest light intensity when the cells' refractive index is higher than that of the surrounding fluid and vice versa. More detailed descriptions can be found elsewhere [85, 86]. Osellame et al. integrated a femtosecond laser to an optofluidic device for optical trapping and stretching of single red blood cells, which provided accurate alignment between the optical and fluidic components, as shown in Fig. 4.12a [87]. Kim et al. integrated optical tweezers to microfluidic chip as a generic single-cell manipulation tool for handling small cell population sorting with high accuracy, as shown in Fig. 4.12b [88]. Kovac et al. have fabricated a microwell array on a microfluidic chip, where the mammalian cells could load. Then, target cells were selected by microscopy and were levitated from their wells into a flow field for collection by using the scattering force from a focused infrared laser, as shown in Fig. 4.12c [89].

4.4.4 Magnetic Manipulation

Magnetic manipulation methods are required to conjugate the magnetic particles to cells via a cell-specific antibody on the magnetic particle. Subsequently, these specific cells can be separated by passing the sample through a microfluidic device exerted a magnetic field or magnetized surface (Fig. 4.11b) [84]. In comparison with the electrical cell manipulation, which requires electrodes in contact with the cell suspension and may damage the cell viability owing to the electrochemical reactions at the electrode fluid interface, magnetic manipulation enables simplicity

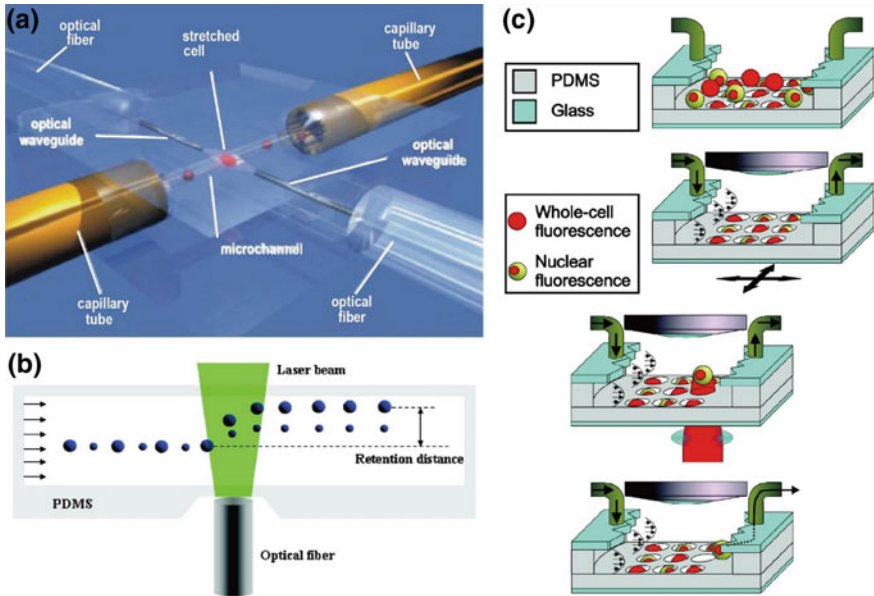


Fig. 4.12 Single-cell manipulation by optical methods. Various structures of optical manipulation devices. **a** Single cells are trapped at the focal point of laser beams [87]. **b** Sing cells are separated depending on the size of cells by optical force [88]. **c** Single cells trapped in a microwell are pushed out of the microwell by using an optical manipulation technique [89]

and capacity to separate via action at a distance is a significant advantage compared to. Wang et al. have reported that they isolated CTCs from whole blood through treating whole blood with magnetic nanoparticles that were functionalized with anti-EpCAM antibody [90]. Liu et al. developed a simple and straightforward approach, which used NIH 3T3 cells incubated in a medium containing magnetic fibers as assay samples, to fabricate magnetic nanofiber segments for cell manipulation. The result showed that cells can be conveniently manipulated with a magnet, as shown in Fig. 4.13 [91].

4.4.5 Acoustic Manipulation

Recently, acoustic manipulation has attracted much attention owing to the negligible impact on cell viability [92]. The mechanism of acoustic manipulation was that an acoustically generated pressure wave can induce cell movement, and several subdistinctions of acoustic cell manipulation was classified depending on the wave type: bulk standing waves, standing surface acoustic waves, and traveling waves.

Bulk standing waves can be created in microfluidic channels when the applied wavelength matches the spatial channel dimension. Consequently, along the wave's

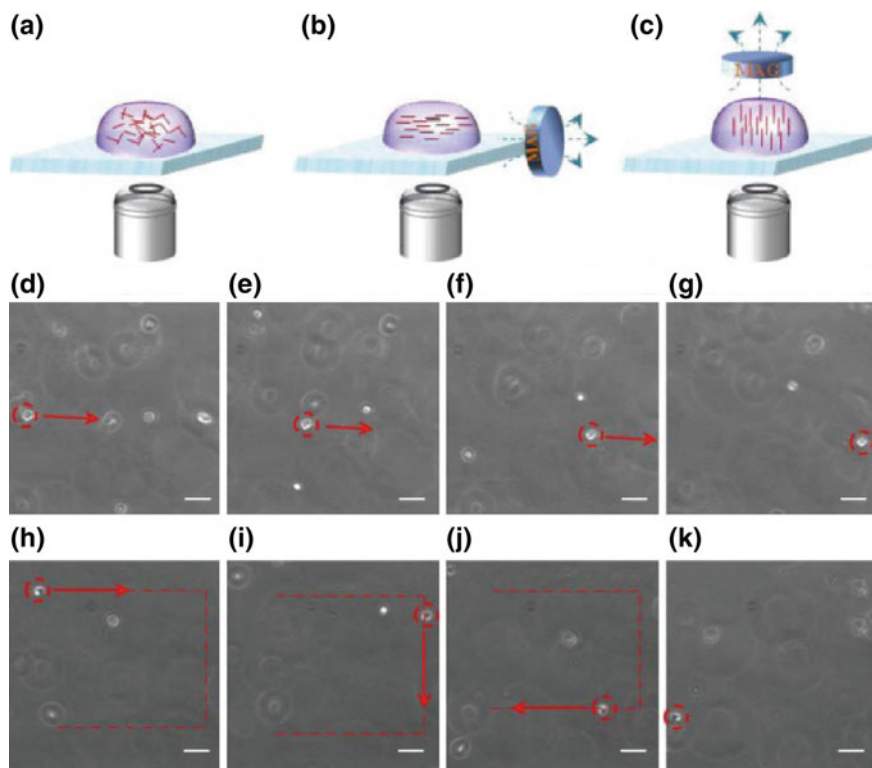


Fig. 4.13 a–c Schematic of magnetic particle doped nanofiber segments in water drops on a glass slide. d–k Showing cell movement path, controlled by an external magnetic field. The scale bar is 20 μm [91]

path, two distinct regions appear across the channel, where the first is termed a node without a pressure fluctuation and the second is termed an antinode with a fluctuating pressure alternating between a minimum and maximum, as shown in Fig. 4.14a [70]. Cells will have a response to the standing wave according to their acoustic contrast factor when they flow through the channel. And the acoustic contrast factor is determined by cell density and compressibility relative to the surrounding medium. Cells having a positive acoustic contrast factor will move toward the node, while cells with negative acoustic contrast factors will be driven to the antinodes. Thus, the single cells can be divided into different outlets. Grenvall et al. [93] integrated a two-dimensional acoustic focusing region on a microfluidic chip, where the cells could be separated to five different outlets based on the size of the cells, as shown in Fig. 4.15. This device has capacity to sort white blood cells of high purity and viability.

Standing surface acoustic waves (SSAW) are formed along the bottom of a microfluidic channel using interdigital transducers (IDTs) that are mounted on a microfluidic chip in the form of a piezoelectric substrate. The modes of acoustic

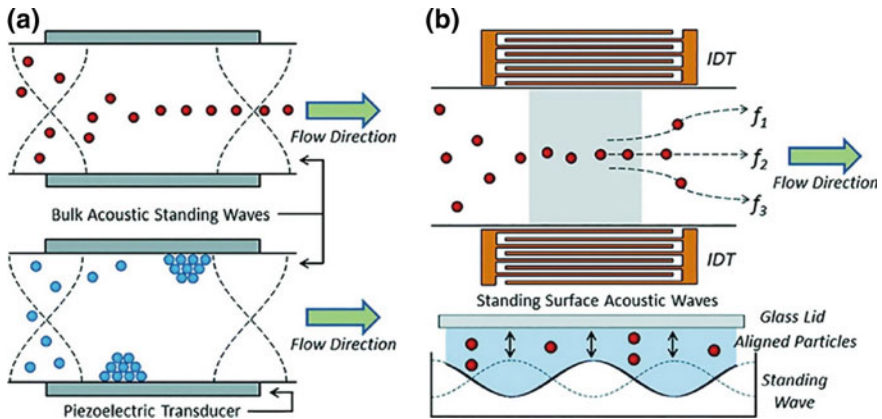


Fig. 4.14 Schematics of cell manipulation by acoustic methods. **a** Acoustic manipulation via bulk standing waves, where the cells’ acoustic contrast factor determines their migration to the node or antinode. **b** Acoustic manipulation via standing surface waves, where the acoustic waves are generated by interdigitated electrodes position cells at distinct streamlines [70]

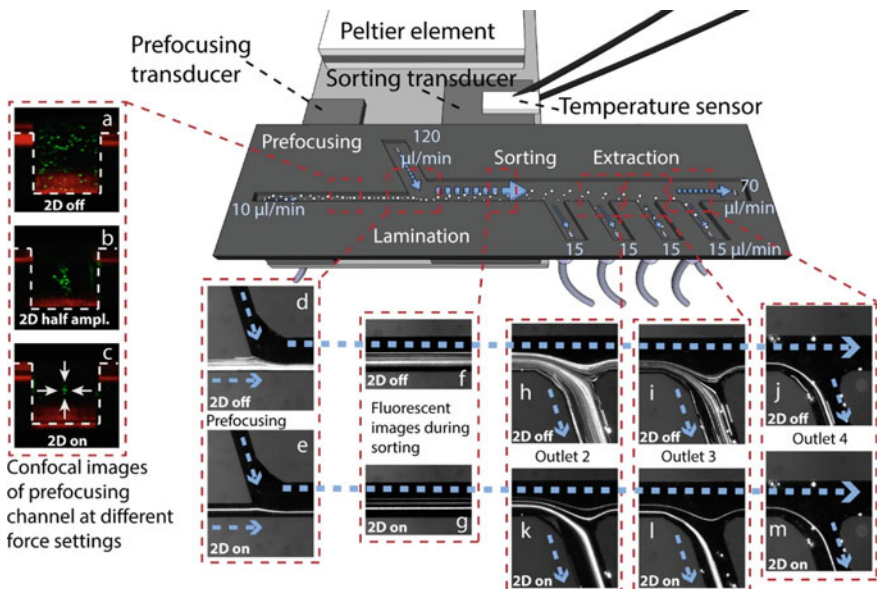


Fig. 4.15 A schematic of on-chip cell manipulation with two-dimensional acoustically focused region [93]

wave in the fluid varied from a transverse wave to a longitudinal wave, allowing the generation of a pressure node. The cells are separated into different streamlines and outlets through these acoustic waves generated by the cross-shaped electrodes, as

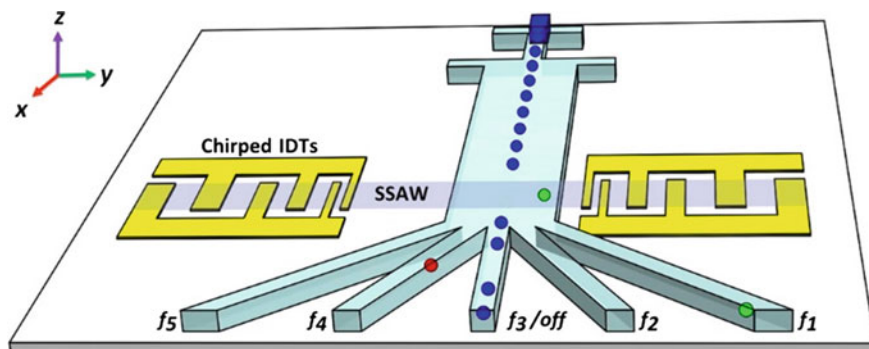


Fig. 4.16 A schematic of droplet-sorting device according to the principle of standing surface acoustic wave [94]

shown in Fig. 4.14b [70]. Since the standing surface acoustic wave has the ability to move the cells or particles into different deflection based on the different contrast factors in the fluid, it is a flexible approach for single-cell manipulation in comparison with bulk standing waves. Li et al. [94] have reported to use a standing surface acoustic waves-based chip to manipulate the W/O droplets into five different outlets, as shown in Fig. 4.16.

Although most of the acoustic-based cell manipulation is based on standing waves, traveling acoustic wave is still an alternative for single-cell manipulation. Contrary to the standing wave which usually needs to match the wavelength of the acoustic wave with the width of the microfluidic channel, the traveling wave breaks this restrict without the limitation of wavelength. Schmid et al. applied a fluorescence-induced traveling wave to sort cells into three channels and the cell sorting rate was increased by a factor of 10 in comparison with the use of a standing surface acoustic wave [95].

Similar to electrically based cell sorting, it is necessary for the acoustic method to integrate a sensor on the chip, leading to a complex manufacturing and an increased cost.

4.4.6 Mechanical Manipulation

Mechanical methods use mechanical forces, such as gravity, hydrodynamic, and suction to manipulate cells. Rettig et al. designed different microwell dimension arrays for large-scale single-cell trapping [96]. They investigated some parameters, including microwell diameter, microwell depth, and settle time, to maximize single-cell occupancy for two cell types. There are also some other structures for

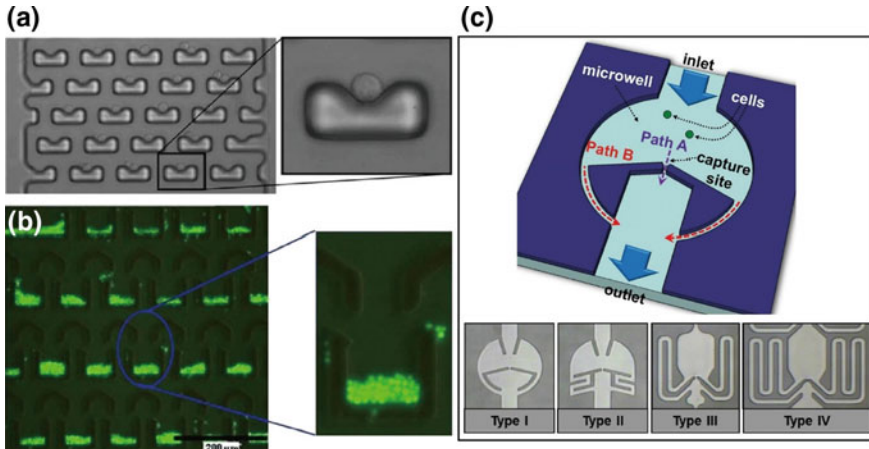


Fig. 4.17 Different shapes for cells trapping. **a** Cells capture by a U-shaped structure [97]. **b** Cells captured in U-shape with Y-shaped fluidic guide [98]. **c** Four kinds of different structure for cells capture [99]

cell manipulation base on hydrodynamic. For example, a physical U-shape hydrodynamic trapping structures array has been developed for single-cell trapping and culture, as shown in Fig. 4.17a [97]. Chen et al. designed another structure for cells capture, where the first layer consists of spacers to create a small gap between the upper layer and glass and the second layer is a U-shaped compartment with sharp corners at the fore-end. And a Y-shaped fluidic guide structures are designed on the top of each U-shaped capture structures, shown in Fig. 4.17b [98]. Furthermore, there was another highly efficient single-cell capture device using hydrodynamic guiding structures, and four types of cell capture module were designed and tested for optimal structure. The results showed that the capturing efficient of this single-cell capture chip was more than 80% and the structures for single-cell trapping were shown in Fig. 4.17c [99].

Despite the continuous improvement of the structures, however, those designs only can be used for one or several kinds of cells owing to its manipulation principle based on both geometric size of cells and capture structures. Thus, the method leveraged suction for cell manipulation was presented. A micromanipulation method for single prokaryotic cells extracting was proposed, shown in Fig. 4.18 [100]. Similarly, another design depending on the method of suction was presented by Anis and coauthors. They integrated a picoliter pump into a robotic manipulation system, where this picoliter pump could automatically select and transfer single target cells onto analysis locations. Using this method, they successfully accomplished single-cell manipulation with Barrett's esophagus cells [101].

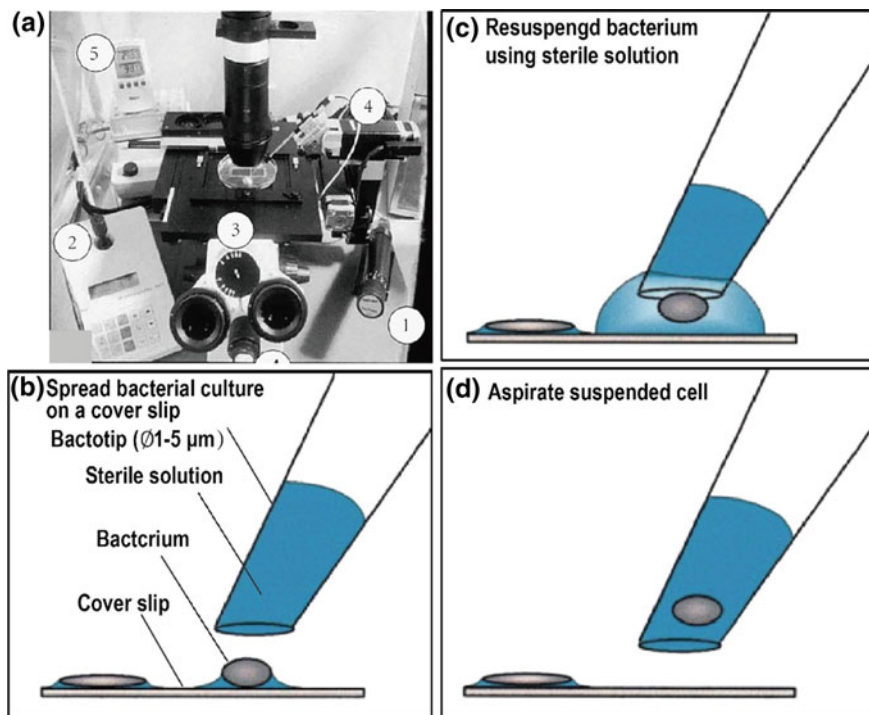


Fig. 4.18 Workstation and schematics of procedure for isolating the single bacterial cell. **a** Aspirate the spread cells through a Bactotip. **b** Spread bacterial culture on a cover slip. **c** Suspend bacterium using sterile solution. **d** Aspirate suspended cell [100]

4.5 Single-Cell Lysis on Microfluidics

Once a target single cell is captured, the biomolecules in the cells are required to be extracted for the following assay. To extract the molecule inside the cells, the cell plasma membrane has to be disrupted. Conventional strategies for membrane disruption can be classified into two aspects, non-detergent and detergent-based. Non-detergent-based methods include mechanical agitation, liquid homogenization, temperature cycling, and sonication. However, these methods are suitable for many cells in suspension or larger tissue samples rather than single-cell analysis. Detergent-based cell lysis is much milder and quicker approach in comparison with mechanical, sonication, and freeze–thaw cell lysis, and can be scaled down for single cells. Detergents play a role in disrupting interactions between lipids and proteins, and can be characterized depending on the nature of their hydrophobic tail and hydrophilic head. For the selection of detergent, general rules are useful; nonionic or zwitterionic detergents are less denaturing compared with ionic detergents, and therefore, they are used when the native protein structure or function need to be maintained. To maintain the native structure and expression of the

biomolecules, a frequent goal of cell lysis is to minimize their alteration as much as possible. That is to say, the lysis approach must be both gentle and rapid. For single-cell analysis, some commonly used methods, such as sonication, freeze–thaw, and detergent may exist their disadvantages: excessive heat generation, long protocols, and arduous implementation. However, the development of microfluidic technology has enabled new cell lysis approaches, specifically suited for single cells.

4.5.1 Mechanical Lysis

Mechanical force induced by shear, compression, collision with sharp features, and so on has been used to puncture the cell membranes. Kim et al. [102] fabricated a microfluidic chip with spatio-specific and reversible channel for the mechanical strain application and release, and this design was successfully applied to single-cell lysis. In this performance, channels were created via applied strain and a single cell was placed in the newly formed channel, subsequently, the strain was released and the channel was collapsed, the single cell was lysed via compression. However, it is a pity that this method required manual handling to put the single cells into the channels. Hoefemann et al. [103] proposed a single-cell lysis method using a continuous microfluidic flow, which can lyse the single cell in less than 20 ms with 100% efficiency. When the cells passed through an integrated heater, they were compressed against the channel ceiling owing to the generated bubbles, as shown in Fig. 4.19a. However, it should be noted that a following single-cell assay was not performed in this report. Consequently, we should consider some factors, such as lysate diffusion and compartmentalization before we used this method for the single-cell molecular analysis.

4.5.2 Thermal Lysis

Thermal lysis can be a good alternative when some additional reagent such as enzymatic or detergent may contaminate the intracellular biomolecules. However, as some biomolecules are heat-sensitive, careful consideration and precise control of the temperature is required. Consequently, it is rare for protein analysis to use thermal cell lysis. Instead, this method is frequently used for parallel, on-chip PCR analysis that requires additional temperature cycling. Gong et al. loaded a large number of single cells into on-chip wells and conducted cell lysis by heating the chip to 50 °C for 40 min, followed by DNA amplification through temperature cycle [104]. Besides, the lysis time is also another critical limitation for thermal lysis. Considering that the occurrence of thermal lysis generally needs a timescale of minutes, thus this technique is not suitable for monitoring intracellular signaling events which occur within seconds [105]. This reason explains that thermal lysis is

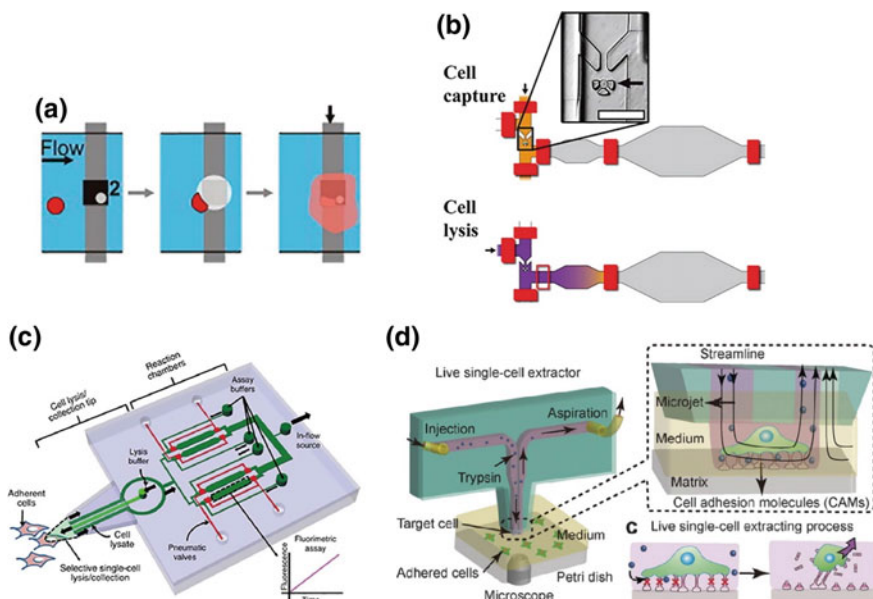


Fig. 4.19 Schematics of methods for single-cell lysis. **a** Single-cell lysis by mechanical methods. Single cells are lysed when passed through the bubble generated above the heater [103]. **b** Single-cell lysis by chemical methods. Lysis buffer is mixed with the single cell trapped in the chamber [106]. **c** A microfluidic device for single-cell lysis in adherent cell culture. The device tip is positioned at the single cell and a hydrodynamically focused lysis buffer selectively lyses the target cell [117]. **d** A microfluidic chip for live single-cell extraction, which can be used to study the single-cell detachment process

most frequently used for gene expression with the occurrence of several hours. In addition, thermal lysis has also been applied to some droplet microfluidic platforms for continuous single-cell PCR research.

4.5.3 Chemical Lysis

Chemical lysis has become a popular technique for single-cell lysis owing to its long history of application to bulk cellular analysis. The instruction of reagents can be regarded as a guide for selecting the appropriate lysing protocol for single cell. Many factors can determine the lysing speed, including the kind of detergent or enzyme being utilized, the concentration, and the contact efficiency. Ionic detergents such as sodium dodecyl sulfate have a fast lysis rate in comparison with nonionic detergents such as Triton X-100. However, the proteins will be denatured under the condition of ionic detergents. Generally speaking, the maximal contact efficiency is desirable for faster cell lysis, while it is challenged to perform this in

microfluidic systems, because molecular transport and mixing are dominated by diffusion in such a device where microscale flows typically occur in the viscous flow regime. Shi et al. [106] have reported a method that they used cell lysis buffer, which was brought into contact with cells strictly via diffusion, to lyse single cells isolated in microfluidic chambers. 20 min lysis buffer diffusion was allowed, and another 20 min was used for incubation. As mentioned above, the lysis time limits the study for faster occurring intracellular events. To overcome this obstacle, some additional installations, such as peristaltic pumps, syringe pumps, actuating valves (Fig. 4.19b), or manual pipet injections are applied to sequentially move reagents across cells for a thorough mixture [107–111]. Additionally, chemical lysis can be used for continuous single-cell analysis by simultaneously performing cell compartmentalization and lysis. DeKosky et al. [112] used a flow-focusing nozzle to encapsulate single lymphocytes in lithium dodecyl sulfate-containing droplets, and the lysis efficiency was reported to reach 100%. A large number of research about RNA sequencing [113, 114], PCR [113, 115], and single-cell enzyme activity [116] have been reported by using the droplets for single-cell compartmentalization and chemical lysis.

Despite the great progress of single-cell lysis, most of them require cells to be in suspension for the manipulation, making it difficult to correlate single-cell data with their native context such as intact tissue or adherent cultures. Some previous reports have suggested that cell surface receptor activation or protein modification would change upon removing from native context and these changes are challenged to be measured [105]. To circumvent this limitation, Sarkar et al. [117] presented a strategy that can selectively lyse a single cell and capture lysate in adherent status with a minimal dilution. In this microfluidic chip, an outflow of lysis buffer was produced at a device tip, and the lysis buffer is hydrodynamically confined to a small scale by a balanced surrounding inflow of lysis buffer, as shown in Fig. 4.19c. Similarly, Lin's laboratory [3] presented a live single-cell extractor (LSCE) for the study of adhered single cells on a cell culture dish based on laminar flow (Fig. 4.19d). The tip of the LSCE fabricated with PDMS was immersed perpendicularly into a Petri dish, where the adhered single cells were extracted in automated mode. A stable microjet of laminar flow occurred underneath the tip of the LSCE when the ratio of aspiration to injection was sufficiently high, allowing the extraction of adhered cells. Despite the low throughput and manual position, this method is unique in its ability to analyze single-cell protein activity in adherent cell culture.

4.5.4 *Electrical Lysis*

The bilayer of cell membrane suffers from reorientation and thermal phase transitions and new pores can be formed upon exposure to an electric field [118]. The formation of the pore is reversible when the electric field is mild (0.2–1 V) and the exposure time is short, which is termed electroporation and is frequently applied to

deliver therapeutic and genetic materials into cells [119]. On the contrary, the formation of the pore is permanent with strong electric fields or prolonged exposure, leading to an unbalanced osmotic pressure between the cytosol and the surrounding media, followed by the swell and rupture of the cells. Additionally, a high electric field can also cause rapid cell rupture [120]. Electrical cell lysis is preferred because it can be tuned for rapid cell lysis without denaturing target biomolecules. Another advantage is that the cell membrane or organelle membrane can be selectively ruptured owing to the difference between their membrane potential [121]. Young et al. designed a microfluidic device for electroosmotic flow positioning and electrical lysis of a single lymphoma cell with a success rate of 80%. And it takes approximately 60 s on average from cell injection to cell lysis [122]. Kim et al. loaded 95% 3600 wells with single cells by integrating microwell compartmentalization, DEP immobilization, and electrical cell lysis all on one chip. Under the condition of pressure-driven flow, reagent exchange was done rapidly in 30 s without perturbing the cell positioning [80]. The lysates can be confined by physically closing the wells through pressing a PDMS membrane on top of the wells. Subsequently, 100% of trapped cells were simultaneously lysed under a series of 30 V electrical pulses. Contrary to the thermal lysis or chemical lysis, electrical methods offer rapid cell lysis without the damage of an assay's target biomolecule and avoid potential target contamination. Nevertheless, electrical lysis is not free limitation because electrical lysis requires integration of electrodes and respective control systems on a microfluidic chip, causing a block to clinical application.

4.6 Conclusions and Perspective

Since the technological advances in amplification, sequencing, and microfluidics, the single-cell analysis becomes particularly exciting, and the single-cell research is believed to have a profound influence in cancer diagnosis, immunology, and stem cell research. Up to now, a number of single-cell manipulation techniques have been reported, especially for the droplet-based microfluidic. There is no doubt that innovative manipulation techniques have made great contributions to the field of single-cell analysis and will continue to play an important role. However, despite the great progress in single-cell manipulation, most of them still require further parameter optimization for standardization and commercialization. Moreover, the manipulation techniques should also fulfill some purposes, such as obtaining the target cell with high purity, high efficient, high throughput, low injury, and high precision. Besides, many studies ignored the influence from the cells' native tissue, leading to the cell's behavior change. To analyze the exact preclinical samples for current clinical trials, single-cell manipulation techniques need to be further developed for handling the cell in native context.

References

1. Zhang L, Vertes A (2018) Single-cell mass spectrometry approaches to explore cellular heterogeneity. *Angew Chem Int Ed* 57(17):4466–4477. <https://doi.org/10.1002/anie.201709719>
2. Altschuler SJ, Wu LF (2010) Cellular heterogeneity: do differences make a difference? *Cell* 141(4):559–563. <https://doi.org/10.1016/j.cell.2010.04.033>
3. Mao S, Zhang W, Huang Q, Khan M, Li H, Uchiyama K, Lin JM (2018) In situ scatheless cell detachment reveals correlation between adhesion strength and viability at single-cell resolution. *Angew Chem Int Ed* 57(1):236–240. <https://doi.org/10.1002/anie.201710273>
4. Zhu Z, Yang CJ (2016) Hydrogel droplet microfluidics for high-throughput single molecule/cell analysis. *Acc Chem Res* 50(1):22–31. <https://doi.org/10.1021/acs.accounts.6b00370>
5. Buettner F, Natarajan KN, Casale FP, Proserpio V, Scialdone A, Theis FJ, Teichmann SA, Marioni JC, Stegle O (2015) Computational analysis of cell-to-cell heterogeneity in single-cell RNA-sequencing data reveals hidden subpopulations of cells. *Nat Biotechnol* 33(2):155–160. <https://doi.org/10.1038/nbt.3102>
6. Qin Y, Wu L, Schneider T, Yen GS, Wang J, Xu S, Li M, Paguirigan AL, Smith JL, Radich JP (2018) A self-digitization dielectrophoretic (SD-DEP) chip for high-efficiency single-cell capture, on-demand compartmentalization, and downstream nucleic acid analysis. *Angew Chem Int Ed* 130(35):11548–11553. <https://doi.org/10.1002/anie.201807314>
7. Fritzsche FS, Dusny C, Frick O, Schmid A (2012) Single-cell analysis in biotechnology, systems biology, and biocatalysis. *Annu Rev Chem Biomol Eng* 3:129–155. <https://doi.org/10.1146/annurev-chembioeng-062011-081056>
8. Huang Q, Mao S, Khan M, Zhou L, Lin J-M (2018) Dean flow assisted cell ordering system for lipid profiling in single-cells using mass spectrometry. *Chem Commun* 54(21):2595–2598. <https://doi.org/10.1039/c7cc09608a>
9. Lan F, Demaree B, Ahmed N, Abate AR (2017) Single-cell genome sequencing at ultra-high-throughput with microfluidic droplet barcoding. *Nat Biotechnol* 35(7):640. <https://doi.org/10.1038/nbt.3880>
10. Terekhov SS, Smirnov IV, Stepanova AV, Bobik TV, Mokrushina YA, Ponomarenko NA, Belogurov AA, Rubtsova MP, Kartseva OV, Gomzikova MO, Moskovtsev AA (2017) Microfluidic droplet platform for ultrahigh-throughput single-cell screening of biodiversity. *Proc Natl Acad Sci USA* 114(10):201621226. <https://doi.org/10.1073/pnas.1621226114>
11. Wood DK, Weingeist DM, Bhatia SN, Engelward BP (2010) Single cell trapping and DNA damage analysis using microwell arrays. *Proc Natl Acad Sci USA* 107(22):10008–10013. <https://doi.org/10.1073/pnas.1004056107>
12. Cole RH, Tang S-Y, Siltanen CA, Shahi P, Zhang JQ, Poust S, Gartner ZJ, Abate AR (2017) Printed droplet microfluidics for on demand dispensing of picoliter droplets and cells. *Proc Natl Acad Sci USA* 114(33):8728–8733. <https://doi.org/10.1073/pnas.1704020114>
13. Joensson HN, Andersson Svahn H (2012) Droplet microfluidics—a tool for single-cell analysis. *Angew Chem Int Ed* 51(49):12176–12192. <https://doi.org/10.1002/anie.201200460>
14. Shang L, Cheng Y, Zhao Y (2017) Emerging droplet microfluidics. *Chem Rev* 117(12):7964–8040. <https://doi.org/10.1021/acs.chemrev.6b00848>
15. Zhang W, Li N, Koga D, Zhang Y, Zeng H, Nakajima H, Lin J-M, Uchiyama K (2018) Inkjet printing based droplet generation for integrated online digital polymerase chain reaction. *Anal Chem* 90(8):5329–5334. <https://doi.org/10.1021/acs.analchem.8b00463>
16. Yusof A, Keegan H, Spillane CD, Sheils OM, Martin CM, O’Leary JJ, Zengerle R, Koltay P (2011) Inkjet-like printing of single-cells. *Lab Chip* 11(14):2447–2454. <https://doi.org/10.1039/c1lc20176j>
17. Zhong Q, Bhattacharya S, Kotsopoulos S, Olson J, Taly V, Griffiths AD, Link DR, Larson JW (2011) Multiplex digital PCR: breaking the one target per color barrier of quantitative PCR. *Lab Chip* 11(13):2167–2174. <https://doi.org/10.1039/c1lc20126c>

18. Pekin D, Skhiri Y, Baret JC, Le CD, Mazutis L, Salem CB, Millot F, El HA, Hutchison JB, Larson JW (2011) Quantitative and sensitive detection of rare mutations using droplet-based microfluidics. *Lab Chip* 11(13):2156–2166. <https://doi.org/10.1039/c1lc20128j>
19. Konry T, Dominguezvillar M, Baecherallan C, Hafler DA, Yarmush ML (2011) Droplet-based microfluidic platforms for single T cell secretion analysis of IL-10 cytokine. *Biosens Bioelectron* 26(5):2707–2710. <https://doi.org/10.1016/j.bios.2010.09.006>
20. Konry T, Golberg A, Yarmush M (2013) Live single cell functional phenotyping in droplet nano-liter reactors. *Sci Rep* 3(11):3179. <https://doi.org/10.1038/srep03179>
21. Solvas XCI, Niu X, Leeper K, Cho S, Chang SI, Edel JB, Demello AJ (2011) Fluorescence detection methods for microfluidic droplet platforms. *J Vis Exp* 58:3437. <https://doi.org/10.3791/3437>
22. Chen Q, Utech S, Chen D, Prodanovic R, Lin J-M, Weitz DA (2016) Controlled assembly of heterotypic cells in a core–shell scaffold: organ in a droplet. *Lab Chip* 16(8):1346–1349. <https://doi.org/10.1039/C6LC00231E>
23. Chen Q, Dong C, Jing W, Lin JM (2016) Flexible control of cellular encapsulation, permeability, and release in a droplet-templated bifunctional copolymer scaffold. *Biomicrofluidics* 10(6):064115. <https://doi.org/10.1063/1.4972107>
24. Christopher GF, Anna SL (2007) Microfluidic methods for generating continuous droplet streams. *J Phys D Appl Phys* 40(19):R319–R336(318). <https://doi.org/10.1088/0022-3727/40/19/r01>
25. de Menech M, Garstecki P, Jousse F, Stone HA (2008) Transition from squeezing to dripping in a microfluidic T-shaped junction. *J Fluid Mech* 595(595):141–161. <https://doi.org/10.1017/S002211200700910X>
26. Liu J, Lin J-M, Knopp D (2008) Using a circular groove surrounded inlet to generate monodisperse droplets inside a microfluidic chip in a gravity-driven manner. *J Micromech Microeng* 18(9):095014. <https://doi.org/10.1088/0960-1317/18/9/095014>
27. Haeberle S, Zengerle R, Ducrée J (2007) Centrifugal generation and manipulation of droplet emulsions. *Microfluid Nanofluid* 3(1):65–75. <https://doi.org/10.1007/s10404-006-0106-7>
28. Li H-F, Pang Y-F, Liu J-J, Lin J-M (2011) Suspending nanoliter droplet arrays for cell capture and copper ion stimulation. *Sens Actuators B: Chem* 155(1):415–421. <https://doi.org/10.1016/j.snb.2010.12.023>
29. Cramer C, Fischer P, Windhab EJ (2004) Drop formation in a co-flowing ambient fluid. *Chem Eng Sci* 59(15):3045–3058. <https://doi.org/10.1016/j.ces.2004.04.006>
30. Thorsen T, Roberts RW, Arnold FH, Quake SR (2001) Dynamic pattern formation in a vesicle-generating microfluidic device. *Phys Rev Lett* 86(18):4163–4166. <https://doi.org/10.1103/physrevlett.86.4163>
31. Basova EY, Foret F (2014) Droplet microfluidics in (bio)chemical analysis. *Analyst* 140(1):22–38. <https://doi.org/10.1039/c4an01209g>
32. Okushima S, Nisisako T, Torii T, Higuchi T (2004) Controlled production of monodisperse double emulsions by two-step droplet breakup in microfluidic devices. *Langmuir* 20(23):9905–9908. <https://doi.org/10.1021/la0480336>
33. Lin R, Fisher JS, Simon MG, Lee AP (2012) Novel on-demand droplet generation for selective fluid sample extraction. *Biomicrofluidics* 6(2):024103. <https://doi.org/10.1063/1.3699972>
34. Ding Y, i Solvas XC (2015) “V-junction”: a novel structure for high-speed generation of bespoke droplet flows. *Analyst* 140(2):414–421. <https://doi.org/10.1039/c4an01730g>
35. Eggersdorfer M, Zheng W, Nawar S, Mercandetti C, Ofner A, Leibacher I, Koehler S, Weitz D (2017) Tandem emulsification for high-throughput production of double emulsions. *Lab Chip* 17(5):936–942. <https://doi.org/10.1039/C6LC01553K>
36. Chen F, Lin L, Zhang J, He Z, Uchiyama K, Lin J-M (2016) Single-cell analysis using drop-on-demand inkjet printing and probe electrospray ionization mass spectrometry. *Anal Chem* 88(8):4354–4360. <https://doi.org/10.1021/acs.analchem.5b04749>

37. Zhang W, Li N, Zeng H, Nakajima H, Lin J-M, Uchiyama K (2017) Inkjet printing based separation of mammalian cells by capillary electrophoresis. *Anal Chem* 89(17):8674–8677. <https://doi.org/10.1021/acs.analchem.7b02624>
38. Korenaga A, Chen F, Li H, Uchiyama K, Lin J-M (2017) Inkjet automated single cells and matrices printing system for matrix-assisted laser desorption/ionization mass spectrometry. *Talanta* 162:474–478. <https://doi.org/10.1016/j.talanta.2016.10.055>
39. Liu W, Mao S, Wu J, Lin J-M (2013) Development and applications of paper-based electrospray ionization-mass spectrometry for monitoring of sequentially generated droplets. *Analyst* 138(7):2163–2170. <https://doi.org/10.1039/C3AN36404F>
40. Liu W, Wang N, Lin X, Ma Y, Lin J-M (2014) Interfacing microsampling droplets and mass spectrometry by paper spray ionization for online chemical monitoring of cell culture. *Anal Chem* 86(14):7128–7134. <https://doi.org/10.1021/ac501678q>
41. Link DR, Grasland-Mongrain E, Duri A, Sarrazin F, Cheng Z, Cristobal G, Marquez M, Weitz DA (2006) Electric control of droplets in microfluidic devices. *Angew Chem Int Ed* 45(16):2556–2560. <https://doi.org/10.1002/anie.200503540>
42. Liu J, Tan S-H, Yap YF, Ng MY, Nguyen N-T (2011) Numerical and experimental investigations of the formation process of ferrofluid droplets. *Microfluid Nanofluid* 11(2):177–187. <https://doi.org/10.1007/s10404-011-0784-7>
43. Nguyen NT, Ting TH, Yap YF, Wong TN, Chai CK, Ong WL, Zhou J, Tan SH, Yobas L (2007) Thermally mediated droplet formation in microchannels. *Appl Phys Lett* 91(8):s10404
44. Xiong S, Chin LK, Ando K, Tandiono T, Liu AQ, Ohl CD (2015) Droplet generation via a single bubble transformation in a nanofluidic channel. *Lab Chip* 15(6):1451–1457. <https://doi.org/10.1039/c4lc01184h>
45. Park SY, Wu TH, Chen Y, Teitell MA, Chiou PY (2011) High-speed droplet generation on demand driven by pulse laser-induced cavitation. *Lab Chip* 11(6):1010–1012. <https://doi.org/10.1039/c0lc00555j>
46. Huebner A, Srisa-Art M, Holt D, Abell C, Hollfelder F, Demello AJ, Edel JB (2007) Quantitative detection of protein expression in single cells using droplet microfluidics. *Chem Commun* 28(12):1218–1220. <https://doi.org/10.1039/b618570c>
47. Collins DJ, Neild A, Demello A, Liu AQ, Ai Y (2015) The Poisson distribution and beyond: methods for microfluidic droplet production and single cell encapsulation. *Lab Chip* 15(17):3439–3459. <https://doi.org/10.1039/c5lc00614g>
48. Chabert M, Vivoy JL (2008) Microfluidic high-throughput encapsulation and hydrodynamic self-sorting of single cells. *Proc Natl Acad Sci USA* 105(9):3191–3196. <https://doi.org/10.1073/pnas.0708321105>
49. Jing T, Ramji R, Warkiani ME, Han J, Lim CT, Chen CH (2015) Jetting microfluidics with size-sorting capability for single-cell protease detection. *Biosens Bioelectron* 66:19–23. <https://doi.org/10.1016/j.bios.2014.11.001>
50. Edd JF, Di Carlo D, Humphry KJ, Köster S, Irimia D, Weitz DA, Toner M (2008) Controlled encapsulation of single-cells into monodisperse picolitre drops. *Lab Chip* 8(8):1262–1264. <https://doi.org/10.1039/b805456h>
51. Kemna EW, Schoeman RM, Wolbers F, Vermes I, Weitz DA, Van Den Berg A (2012) High-yield cell ordering and deterministic cell-in-droplet encapsulation using Dean flow in a curved microchannel. *Lab Chip* 12(16):2881–2887. <https://doi.org/10.1039/c2lc00013j>
52. Ramji R, Wang M, Bhagat AAS, Weng DTS, Thakor NV, Lim CT, Chen CH (2014) Single cell kinase signaling assay using pinched flow coupled droplet microfluidics. *Biomicrofluidics* 8(3):47–53. <https://doi.org/10.1063/1.4878635>
53. Novo P, Dell’Aica M, Janasek D, Zahedi RP (2016) High spatial and temporal resolution cell manipulation techniques in microchannels. *Analyst* 141(6):1888–1905. <https://doi.org/10.1039/C6AN00027D>
54. Dudani JS, Gossett DR, Tse HT, Di CD (2013) Pinched-flow hydrodynamic stretching of single-cells. *Lab Chip* 13(18):3728–3734. <https://doi.org/10.1039/c3lc50649e>

55. Mcgrath J, Jimenez M, Bridle H (2014) Deterministic lateral displacement for particle separation: a review. *Lab Chip* 14(21):4139–4158. <https://doi.org/10.1039/C4LC00939H>
56. Cheng Q, Huang H, Chen L, Li X, Ge Z, Chen T, Yang Z, Sun L (2014) Dielectrophoresis for bioparticle manipulation. *Int J Mol Sci* 15(10):18281. <https://doi.org/10.3390/ijms151018281>
57. Zhang H, Liu KK (2008) Optical tweezers for single cells. *J R Soc Interface* 5(24):671–690. <https://doi.org/10.1098/rsif.2008.0052>
58. Lim B, Reddy V, Hu XH, Kim KW, Jadhav M, Abedini-Nassab R, Noh YW, Yong TL, Yellen BB, Kim CG (2014) Magnetophoretic circuits for digital control of single particles and cells. *Nat Commun* 5:3846. <https://doi.org/10.1038/ncomms4846>
59. Ahmed D, Ozcelik A, Bojanala N, Nama N, Upadhyay A, Chen Y, Hannarose W, Huang TJ (2016) Rotational manipulation of single cells and organisms using acoustic waves. *Nat Commun* 7:11085. <https://doi.org/10.1038/ncomms11085>
60. Yarmush ML, King KR (2009) Living-cell microarrays. *Annu Rev Biomed Eng* 11(1):235. <https://doi.org/10.1146/annurev.bioeng.10.061807.160502>
61. Jonczyk R, Kurth T, Lavrentieva A, Walter JG, Scheper T, Stahl F (2016) Living cell microarrays: an overview of concepts. *Microarrays* 5(2):11. <https://doi.org/10.3390/microarrays5020011>
62. Lin L, Chu YS, Thiery JP, Lim CT, Rodriguez I (2013) Microfluidic cell trap array for controlled positioning of single cells on adhesive micropatterns. *Lab Chip* 13(4):714. <https://doi.org/10.1039/c2lc41070b>
63. Sarioglu AF, Aceto N, Kojic N, Donaldson MC, Zeinali M, Hamza B, Engstrom A, Zhu H, Sundaresan TK, Miyamoto DT (2015) A microfluidic device for label-free, physical capture of circulating tumor cell clusters. *Nat Methods* 12(7):685–691. <https://doi.org/10.1038/nmeth.3404>
64. Lecault V, Vaninsberghe M, Sekulovic S, Knapp DJHF, Wohrer S, Bowden W, Viel F, Mclaughlin T, Jarandehi A, Miller M (2011) High-throughput analysis of single hematopoietic stem cell proliferation in microfluidic cell culture arrays. *Nat Methods* 8(7):581. <https://doi.org/10.1038/nmeth.1614>
65. Voldman J (2006) Electrical forces for microscale cell manipulation. *Annu Rev Biomed Eng* 8(8):425–454. <https://doi.org/10.1146/annurev.bioeng.8.061505.095739>
66. Yasukawa T, Nagamine K, Horiguchi Y, Shiku H, Koide M, Itayama T, Shiraishi F, Matsue T (2008) Electrophoretic cell manipulation and electrochemical gene-function analysis based on a yeast two-hybrid system in a microfluidic device. *Anal Chem* 80(10):3722–3727. <https://doi.org/10.1021/ac800143t>
67. Park K, Suk HJ, Akin D, Bashir R (2009) Dielectrophoresis-based cell manipulation using electrodes on a reusable printed circuit board. *Lab Chip* 9(15):2224–2229. <https://doi.org/10.1039/b904328d>
68. Glawdel T, Ren CL (2009) Electro-osmotic flow control for living cell analysis in microfluidic PDMS chips. *Mech Res Commun* 36(1):75–81. <https://doi.org/10.1016/j.mechrescom.2008.06.015>
69. Mehrishi JN, Bauer J (2015) Electrophoresis of cells and the biological relevance of surface charge. *Electrophoresis* 23(13):1984–1994. [https://doi.org/10.1002/1522-2683\(200207\)23:13%3c1984:AID-ELPS1984%3e3.0.CO;2-U](https://doi.org/10.1002/1522-2683(200207)23:13%3c1984:AID-ELPS1984%3e3.0.CO;2-U)
70. Wyatt Shields Iv C, Reyes CD, López GP (2015) Microfluidic cell sorting: a review of the advances in the separation of cells from debulking to rare cell isolation. *Lab Chip* 15(5):1230–1249. <https://doi.org/10.1039/C4LC01246A>
71. Takahashi K, Hattori A, Suzuki I, Ichiki T, Yasuda K (2004) Non-destructive on-chip cell sorting system with real-time microscopic image processing. *J Nanobiotechnol* 2(1):5. <https://doi.org/10.1186/1477-3155-2-5>
72. Guo F, Ji XH, Liu K, He RX, Zhao LB, Guo ZX, Liu W, Guo SS, Zhao XZ (2010) Droplet electric separator microfluidic device for cell sorting. *Appl Phys Lett* 96(19):1392. <https://doi.org/10.1063/1.3360812>

73. Plouffe BD, Murthy SK, Lewis LH (2015) Fundamentals and application of magnetic particles in cell isolation and enrichment: a review. *Rep Prog Phys* 78(1):016601. <https://doi.org/10.1088/0034-4885/78/1/016601>
74. Pohl HA (1951) The motion and precipitation of suspensoids in divergent electric fields. *J Appl Phys* 22(7):869–871. <https://doi.org/10.1063/1.1700065>
75. Gascoyne PR, Vykoukal J (2015) Particle separation by dielectrophoresis. *Electrophoresis* 23(13):1973–1983. [https://doi.org/10.1002/1522-2683\(200207\)23:13%3c1973::AID-ELPS1973%3e3.0.CO;2-1](https://doi.org/10.1002/1522-2683(200207)23:13%3c1973::AID-ELPS1973%3e3.0.CO;2-1)
76. Chuang CH, Wu YT (2012) Dielectrophoretic chip with multilayer electrodes and micro-cavity array for trapping and programmably releasing single cells. *Biomed Microdevices* 14(2):271–278. <https://doi.org/10.1007/s10544-011-9603-x>
77. Thomas RS, Morgan H, Green NG (2009) Negative DEP traps for single cell immobilisation. *Lab Chip* 9(11):1534–1540. <https://doi.org/10.1039/B819267G>
78. Jang L-S, Huang P-H, Lan K-C (2009) Single-cell trapping utilizing negative dielectrophoretic quadrupole and microwell electrodes. *Biosens Bioelectron* 24(12):3637–3644. <https://doi.org/10.1016/j.bios.2009.05.027>
79. Park H, Kim D, Yun KS (2010) Single-cell manipulation on microfluidic chip by dielectrophoretic actuation and impedance detection. *Sens Actuators B-Chem* 150(1):167–173. <https://doi.org/10.1016/j.snb.2010.07.020>
80. Kim SH, Yamamoto T, Fourmy D, Fujii T (2011) Electroactive microwell arrays for highly efficient single-cell trapping and analysis. *Small* 7(22):3239–3247. <https://doi.org/10.1002/smll.201101028>
81. Dittrich PS, Schwille P (2003) An integrated microfluidic system for reaction, high-sensitivity detection, and sorting of fluorescent cells and particles. *Anal Chem* 75(21):5767–5774. <https://doi.org/10.1021/ac034568c>
82. Ashkin A (1970) Acceleration and trapping of particles by radiation pressure. *Phys Rev Lett* 24(4):156. <https://doi.org/10.1103/physrevlett.24.156>
83. Ashkin A, Dziedzic JM, Bjorkholm J, Chu S (1986) Observation of a single-beam gradient force optical trap for dielectric particles. *Opt Lett* 11(5):288–290. <https://doi.org/10.1364/OL.11.000288>
84. Hoscic S, Murthy SK, Koppes AN (2016) Microfluidic sample preparation for single cell analysis. *Anal Chem* 88(1):354–380. <https://doi.org/10.1021/acs.analchem.5b04077>
85. Jonáš A, Zemanek P (2008) Light at work: the use of optical forces for particle manipulation, sorting, and analysis. *Electrophoresis* 29(24):4813–4851. <https://doi.org/10.1002/elps.200800484>
86. Moffitt JR, Chemla YR, Smith SB, Bustamante C (2008) Recent advances in optical tweezers. *Annu Rev Biochem* 77:205–228. <https://doi.org/10.1146/annurev.biochem.77.043007.090225>
87. Bellini N, Vishnubhatla KC, Bragheri F, Ferrara L, Minzioni P, Ramponi R, Cristiani I, Osellame R (2010) Femtosecond laser fabricated monolithic chip for optical trapping and stretching of single cells. *Opt Express* 18(5):4679–4688. <https://doi.org/10.1364/OE.18.004679>
88. Kim SB, Yoon SY, Sung HJ, Kim SS (2008) Cross-type optical particle separation in a microchannel. *Anal Chem* 80(7):2628–2630. <https://doi.org/10.1021/ac8000918>
89. Kovac J, Voldman J (2007) Intuitive, image-based cell sorting using optofluidic cell sorting. *Anal Chem* 79(24):9321–9330. <https://doi.org/10.1021/ac071366y>
90. Wang C, Ye M, Cheng L, Li R, Zhu W, Shi Z, Fan C, He J, Liu J, Liu Z (2015) Simultaneous isolation and detection of circulating tumor cells with a microfluidic silicon-nanowire-array integrated with magnetic upconversion nanoprobe. *Biomaterials* 54:55–62. <https://doi.org/10.1016/j.biomaterials.2015.03.004>
91. Liu J, Shi J, Jiang L, Zhang F, Wang L, Yamamoto S, Takano M, Chang M, Zhang H, Chen Y (2012) Segmented magnetic nanofibers for single cell manipulation. *Appl Surf Sci* 258(19):7530–7535. <https://doi.org/10.1016/j.apsusc.2012.04.077>

92. Burguillos MA, Magnusson C, Nordin M, Lenshof A, Augustsson P, Hansson MJ, Elmer E, Lilja H, Brundin P, Laurell T (2013) Microchannel acoustophoresis does not impact survival or function of microglia, leukocytes or tumor cells. *PLoS One* 8(5):e64233. <https://doi.org/10.1371/journal.pone.0064233>
93. Grenvall C, Magnusson C, Lilja H, Laurell T (2015) Concurrent isolation of lymphocytes and granulocytes using prefocused free flow acoustophoresis. *Anal Chem* 87(11):5596. <https://doi.org/10.1021/acs.analchem.5b00370>
94. Li S, Ding X, Guo F, Chen Y, Lapsley MI, Lin SCS, Wang L, Mccoy JP, Cameron CE, Huang TJ (2013) An on-chip, multichannel droplet sorter using standing surface acoustic waves. *Anal Chem* 85(11):5468–5474. <https://doi.org/10.1021/ac400548d>
95. Schmid L, Weitz DA, Franke T (2014) Sorting drops and cells with acoustics: acoustic microfluidic fluorescence-activated cell sorter. *Lab Chip* 14(19):3710–3718. <https://doi.org/10.1039/c4lc00588k>
96. And JRR, Folch A (2005) Large-scale single-cell trapping and imaging using microwell arrays. *Anal Chem* 77(17):5628–5634. <https://doi.org/10.1021/ac0505977>
97. Carlo DD, Wu LY, Lee LP (2006) Dynamic single cell culture array. *Lab Chip* 6(11):1445–1449. <https://doi.org/10.1039/b605937f>
98. Chen J, Chen D, Yuan T, Chen X, Zhu J, Morschhauser A, Nestler J, Otto T, Gessner T (2014) Microfluidic chips for cells capture using 3-D hydrodynamic structure array. *Microsyst Technol* 20(3):485–491. <https://doi.org/10.1007/s00542-013-1933-6>
99. Chung J, Kim YJ, Yoon E (2011) Highly-efficient single-cell capture in microfluidic array chips using differential hydrodynamic guiding structures. *Appl Phys Lett* 98(12):123701. <https://doi.org/10.1063/1.3565236>
100. Fröhlich J, König H (2000) New techniques for isolation of single prokaryotic cells 1. *FEMS Microbiol Rev* 24(5):567–572. <https://doi.org/10.1111/j.1574-6976.2000.tb00558.x>
101. Anis Y, Houkal J, Holl M, Johnson R, Meldrum D (2011) Diaphragm pico-liter pump for single-cell manipulation. *Biomed Microdevices* 13(4):651–659. <https://doi.org/10.1007/s10544-011-9535-5>
102. Kim BC, Moraes C, Huang J, Matsuoka T, Thouless MD, Takayama S (2015) Fracture-based fabrication of normally closed, adjustable, and fully reversible microscale fluidic channels. *Small* 10(19):4020–4029. <https://doi.org/10.1002/smll.201400147>
103. Hoefemann H, Wadle S, Bakhtina N, Kondrashov V, Wangler N, Zengerle R (2012) Sorting and lysis of single cells by BubbleJet technology. *Sens Actuators B-Chem* 168(12):442–445. <https://doi.org/10.1016/j.snb.2012.04.005>
104. Gong Y, Ogunniyi AO, Love JC (2010) Massively parallel detection of gene expression in single cells using subnanolitre wells. *Lab Chip* 10(18):2334–2337. <https://doi.org/10.1039/c004847j>
105. Liu ET, Lauffenburger DA (2009) *Systems biomedicine: concepts and perspectives*. Academic Press, Salt Lake
106. Shi Q, Qin L, Wei W, Geng F, Fan R, Shin YS, Guo D, Hood L, Mischel PS, Heath JR (2012) Single-cell proteomic chip for profiling intracellular signaling pathways in single tumor cells. *Proc Natl Acad Sci USA* 109(2):419–424. <https://doi.org/10.1073/pnas.1110865109>
107. White AK, Heyries KA, Doolin C, Vaninsbergh M, Hansen CL (2013) High-throughput microfluidic single-cell digital polymerase chain reaction. *Anal Chem* 85(15):7182–7190. <https://doi.org/10.1021/ac400896j>
108. Treutlein B, Brownfield DG, Wu AR, Neff NF, Mantalas GL, Espinoza FH, Desai TJ, Krasnow MA, Quake SR (2014) Reconstructing lineage hierarchies of the distal lung epithelium using single-cell RNA-seq. *Nature* 509(7500):371–375. <https://doi.org/10.1038/nature13173>
109. Streets AM, Zhang X, Cao C, Pang Y, Wu X, Xiong L, Yang L, Fu Y, Zhao L, Tang F (2014) Microfluidic single-cell whole-transcriptome sequencing. *Proc Natl Acad Sci USA* 111(19):7048. <https://doi.org/10.1073/pnas.1402030111>

110. Fan HC, Wang J, Potanina A, Quake SR (2011) Whole-genome molecular haplotyping of single cells. *Nat Biotechnol* 29(1):51–57. <https://doi.org/10.1038/nbt.1739>
111. Sun H, Olsen T, Zhu J, Tao J, Ponnaiya B, Amundson SA, Brenner DJ, Lin Q (2014) A Bead-based microfluidic approach to integrated single-cell gene expression analysis by quantitative RT-PCR. *RSC Adv* 5(7):4886–4893. <https://doi.org/10.1039/C4RA13356K>
112. DeKosky BJ, Kojima T, Rodin A, Charab W, Ippolito GC, Ellington AD, Georgiou G (2015) In-depth determination and analysis of the human paired heavy-and light-chain antibody repertoire. *Nat Med* 21(1):86. https://doi.org/10.1007/978-3-319-58518-5_3
113. Macosko E, Basu A, Satija R, Nemes J, Shekhar K, Goldman M, Tirosh I, Bialas A, Kamitaki N, Martersteck E (2015) Highly parallel genome-wide expression profiling of individual cells using nanoliter droplets. *Cell* 161(5):1202–1214. <https://doi.org/10.1016/j.cell.2015.05.002>
114. Klein Allon M, Mazutis L, Akartuna I, Tallapragada N, Veres A, Li V, Peshkin L, Weitz David A, Kirschner Marc W (2015) Droplet barcoding for single-cell transcriptomics applied to embryonic stem cells. *Cell* 161(5):1187–1201. <https://doi.org/10.1016/j.cell.2015.04.044>
115. Rival A, Jary D, Delattre C, Fouillet Y, Castellan G, Belleminecomte A, Gidrol X (2014) An EWOD-based microfluidic chip for single-cell isolation, mRNA purification and subsequent multiplex qPCR. *Lab Chip* 14(19):3739–3749. <https://doi.org/10.1039/C4LC00592A>
116. Zinchenko A, Devenish SR, Kintsos B, Colin PY, Fischlechner M, Hollfelder F (2014) One in a million: flow cytometric sorting of single cell-lysate assays in monodisperse picolitre double emulsion droplets for directed evolution. *Anal Chem* 86(5):2526–2533. <https://doi.org/10.1021/ac403585p>
117. Sarkar A, Kolitz S, Lauffenburger DA, Han J (2014) Microfluidic probe for single-cell lysis and analysis in adherent tissue culture. *Nat Commun* 5(5):3421. <https://doi.org/10.1038/ncomms4421>
118. Tsong TY (1991) Electroporation of cell membranes. *Biophys J* 60(2):297–306. <https://doi.org/10.3109/07388559609147426>
119. Sersa G, Miklavcic D, Cemazar M, Rudolf Z, Pucihar G, Snoj M (2008) Electrochemotherapy in treatment of tumours. *Eur J Surg Oncol* 34(2):232–240. <https://doi.org/10.1016/j.ejso.2007.05.016>
120. Lee SW, Tai YC (1999) A micro cell lysis device. *Sens Actuator A-Phys* 73(1–2):74–79. [https://doi.org/10.1016/S0924-4247\(98\)00257-X](https://doi.org/10.1016/S0924-4247(98)00257-X)
121. Lu H, Schmidt MA, Jensen KF (2004) A microfluidic electroporation device for cell lysis. *Lab Chip* 5(1):23–29. <https://doi.org/10.1039/B406205A>
122. Chao-Wang Y, Jia-Ling H, Chyung A (2012) Development of an integrated chip for automatic tracking and positioning manipulation for single cell lysis. *Sensors* 12(3):2400–2413. <https://doi.org/10.3390/s120302400>

Chapter 5

Droplet-Based Microfluidics for Single-Cell Encapsulation and Analysis



Qiushui Chen and Jin-Ming Lin

Abstract Droplet microfluidic techniques have been rapidly developed as a powerful tool to perform high-throughput and low-cost analysis of single cells. Microscale droplets can be easily produced by a microfluidic manipulation to encapsulate and manipulate single cells for precise analysis. This offers a new approach to measure genetic and functional heterogeneity of cell division, growth, metabolism, and apoptosis. Functional characteristics of cellular molecules, such as DNA, RNA, and proteins, can be realized at a single-cell level. In this chapter, we will present a general introduction to single-cell analysis involving droplet-based microfluidic techniques. We will highlight the current state of droplet-based microfluidic single-cell analysis for deep insights understanding the biological process at the single-cell level.

Keywords Single-cell analysis · Droplet microfluidics · High throughput · Screening

5.1 Introduction

The emerging technology of single-cell analysis brings great opportunities for physics, biologists, and chemists to gain insights into cell biology [1–3]. Through directly observing and measuring dynamic cellular processes at a single-cell level, people can study time-resolved changes in cells, which is not impossible without advanced single-cell techniques [4–6]. In the past two decades, microfabrication techniques have been developed to perform miniaturized analytical tools for cell researches [7–10]. The concept of “cells on chips” has been proposed to precise control of cells for culture, separation, sorting, and analysis [11–15]. Microfluidic device enables to integrate several individual analytical operations in a microfluidic channel for single-cell study [8, 16, 17].

Q. Chen · J.-M. Lin (✉)

Department of Chemistry, Tsinghua University, Beijing 100084, People’s Republic of China
e-mail: jmlin@mail.tsinghua.edu.cn

In particular, droplet microfluidics has been developed as a powerful tool to achieve single-cell encapsulation and analysis [18]. Microscale-sized droplets can be generated by introducing two immiscible fluids in a microfluidic channel. For example, an aqueous microdroplet (1 pL–10 nL) can be produced by introducing an immiscible oil in a microfluidic device [19]. This technique has become a useful tool for single-cell analysis with small sample consumption and high throughputs [20]. The use of biological compatible surfactant and hydrogels is able to prepare highly stable droplets for on-chip cell encapsulation, off-chip cell culture, and fast cell screening in a microfluidic chip [21]. Typically, droplet is generated quickly and manipulated digitally, enabling a high-throughput (up to 5000 per second) screening. These droplets offer physically and chemically isolated environment to avoid cross-contamination among single cells, opening the opportunity for droplet-based manipulation of cells, such as single-cell encapsulation, single-cell culture, and single-cell analysis. In this regard, droplet-microfluidic technique enables to design a whole workflow for cell screening.

Nowadays, droplet microfluidics has been increasingly emerged as an important tool for single-cell analysis, because of their unique merits of high-throughput analysis, low reagent consumption, dynamic reagent control, biological compatibility, and high sensitivity [22, 23]. Single-cell encapsulation in a microscale droplet can be cultured and further analyzed by performing polymerase chain reaction (PCR), sorting and detection for studies of gene and protein expression at a single-cell level [24–26]. This microfluidic platform employs droplets as spatially separate compartmentalization to facilitate single-cell studies. In addition, high-throughput droplet microfluidics can be rapidly manipulated and analyzed at a rate of over 1000 droplets per second [27]. In this chapter, we describe the aspects of droplet-based microfluidic technology for high-throughput and sensitive single-cell analysis. We will introduce the basic concept and classical technique to generate droplets in a microfluidic device. We will discuss the unique advantages of the droplet-microfluidic approach. Next, we will describe representative examples of applications that are challenging to perform with conventional high-throughput screening methods and are facilitated by droplet-microfluidic techniques.

5.2 Droplet-Microfluidic Device

Droplet-generation microfluidic devices are excellent tools for generating highly reproducible micro-sized droplets [28]. Typically, two different microfluidic systems are mainly used for production of monodisperse droplets, including glass-capillary microfluidics and glass-polydimethylsiloxane (PDMS) microfluidic device (Fig. 5.1) [29, 30]. For cell encapsulation, the most popular device is PDMS-based microfluidic device, which is commonly fabricated by soft lithography [31, 32]. Notably, PDMS is a type of soft material allowing for permeability to O₂ and CO₂, because its porous structure allows gas bubbles diffusing to the channels [33]. The biological compatibility and light transparency of PDMS devices are important for

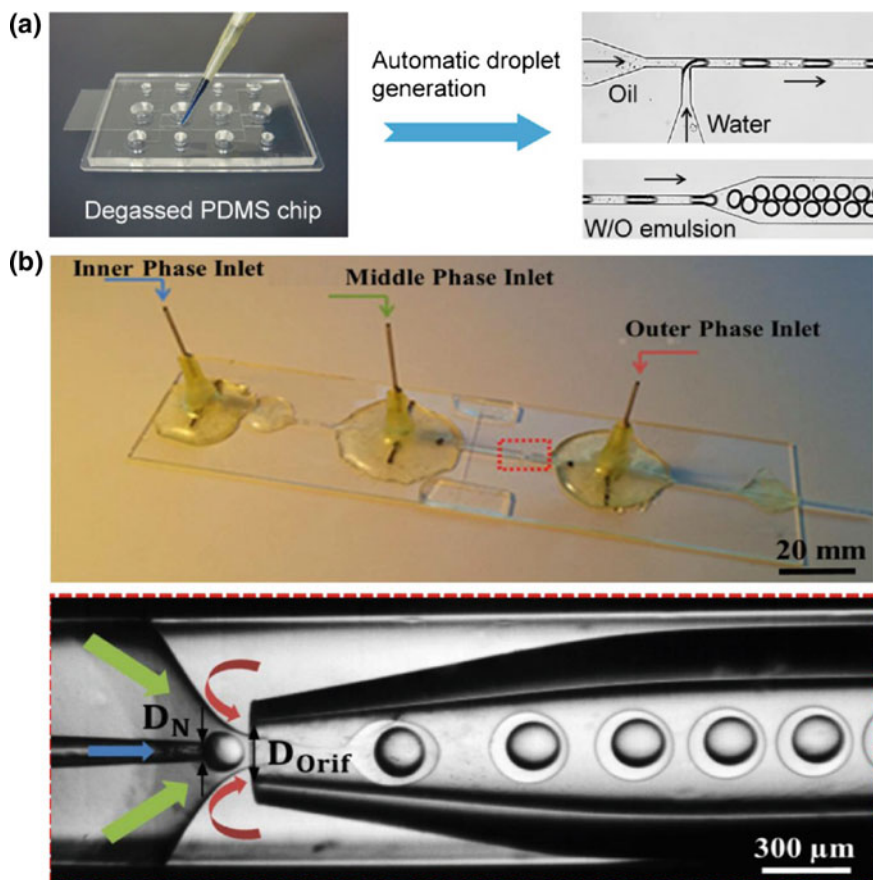


Fig. 5.1 Two typical types of microfluidic devices for droplet generation. **a** PDMS/glass microfluidic device for production of monodisperse microdroplets. Left, photographic images. Right, microscopic images of droplet generation. Reproduced with permission from Ref. [29]. Copyright 2015 American Chemical Society. **b** Three-phase glass-capillary device for double-emulsion generation. Microscopic image of droplet generation is from the region marked by red-dashed line. The directions of inner, middle, and outer fluids are, respectively, indicated by blue, green, and red arrows. Reproduced with permission from Ref. [30]. Copyright 2015 Elsevier

real-time observation of cell operation and culture on a microfluidic chip. However, the PDMS is inherently hydrophobic, and surface treatment to microchannels can be employed to achieve required wetting properties for generation of stable liquid emulsion. For instance, glass-PDMS devices treated with Aquapel flushing are generally applied to generate aqueous-in-oil droplets [34]. Another consideration for the use of PDMS device for cell-based droplet generation is that soft lithography technique is able to precisely design small microchannels for single-cell encapsulation. In this respect, it easily controls the cell encapsulation in each droplet using microfluidic techniques.

5.3 Microfluidics Droplet Generation

Microfluidic technique is a powerful tool to produce highly monodisperse droplets with a narrow distribution of emulsion sizes [35]. One typical technique to generate monodisperse droplets is breaking an aqueous phase in a co-flowing continuous phase containing a stabilizing surfactant in a capillary device (Fig. 5.2) [36]. Another classical approach for producing monodisperse droplets is to use T-junction microfluidic device through injecting water into a continuous oil phase. Typically, generation of droplets in a microfluidic device commonly requires two immiscible solution phases that are continuous phase and dispersed phase. Control of the size of droplets is generally achieved by designing the geometry of microchannels and adjusting the flow rate of continuous phase/dispersed phase. The droplets are generated by competing stresses, and the surfactant is able to stabilize the emulsions in the continuous phase.

Generally, there are three typical methods used for microfluidic droplet generation, including cross-flowing droplet formation in a T-junction, flow-focusing droplet formation, and co-flowing droplet formation (Fig. 5.3) [37]. Cross-flowing technique is a popular method to generate droplets by running continuous and aqueous phases at an angle to each other in a microfluidic device. T-shaped or Y-shaped junctions are two classical geometries designed in microchannels for droplet generation, where the dispersed phase is intersected in the continuous phase. The size and generation rate of droplets depend on the flow rate and its ratio of the two phases, as well as the capillary number. Commonly, the capillary number is determined by the viscosity and superficial velocity of the continuous phase and their interfacial tension. Flow-focusing technique is a general method used to generate monodisperse droplets by flowing dispersed phase to the continuous phase at an angle [38]. In a typical procedure, the dispersed phase suffers from a constraint

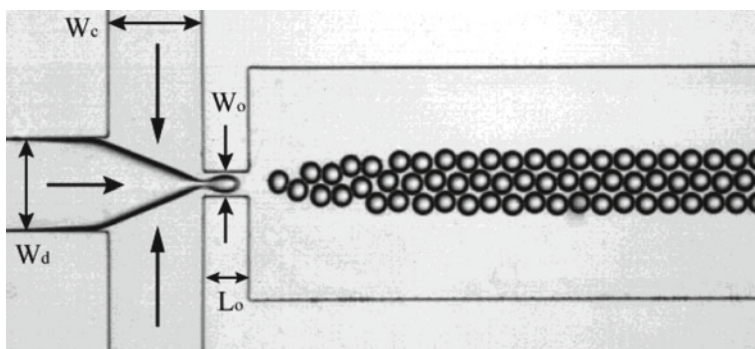


Fig. 5.2 Microfluidic droplet generation by a typical flow-focusing device. Both widths of the inlets of continuous phase (W_c) and dispersed phase (W_d) are 200 μm . The width of the orifice (W_o) is 50 μm . The length of the orifice (L_o) is 100 μm . Reproduced with permission from Ref. [36]

in the microchannel to create droplets due to symmetric shearing. Typically, the device is usually designed with a narrowing constraint channel and followed with a channel of equal or greater width. This method is able to precisely control the size and generation rate of droplets with stable operation. Co-flowing technique is a strategy to produce droplets by enclosing the dispersed phase inside a continuous phase channel. Typically, this method is operated by a glass-capillary microfluidic device.

Different from the conventional two-phase methods described above, several strategies for droplet generation have also been developed based on gravity microfluidic and piezoelectric ink-jet printing. For example, Zhang et al. demonstrated a microfluidic approach to produce monodisperse droplets through a gravity-driven manner (Fig. 5.4) [39]. Using this design, droplets can be produced by cutting a microfluidic continuous flow at a circular groove surrounded nozzle. Notably, this technique avoided using a second immiscible solution and surfactant, thus exhibiting unique advantages for biochemical analysis. However, this technique is difficult to achieve precise control over the sizes of droplets and also has a limitation at throughputs [40]. Alternatively, Liu et al. developed a surface-tension-based technique for microfluidic droplet formation using a capillary tube [41]. Sub-microliter droplets were produced on the basis of gravity and electrostatic attraction via a capillary tube while applied with a high voltage. To achieve the high-throughput generation of size-controllable droplets, a piezoelectric ink-jet printing method was developed [42]. Taking the advantages of using the ink-printing technique, the droplets can be produced on-demand through combined with the micromotor X-Y platform. Droplets with volumes of picoliters to nanoliters can be controlled by the driving voltage and pulse width of the ink-jet system. The droplet generation can also be well controlled to enable high-throughput operation by adjusting the frequency of the applied pulse.

Apart from the above-mentioned droplet formation approaches, we also introduce several other techniques to produce droplets. For example, water-oil-water double emulsion can be generated by typical glass-capillary microfluidic devices. In addition, the droplets can also be produced by water-in-water phases with an oil phase. The droplets can be actively produced by coupling with an electric, magnetic, and centrifugal methods. These methods allow generating droplets with

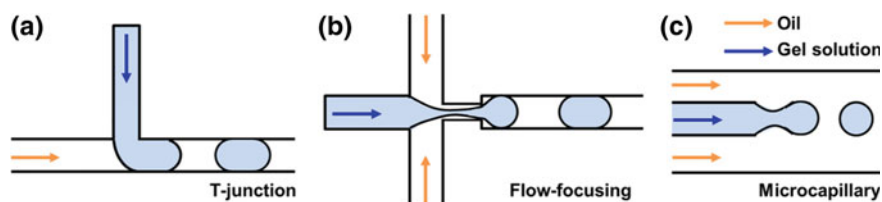


Fig. 5.3 Three typical types of typical microfluidic geometries commonly used for droplet generation: **a** T-junction device, **b** flow-focusing device, and **c** microcapillary device. Reproduced with permission from Ref. [37]. Copyright 2015 Royal Society of Chemistry

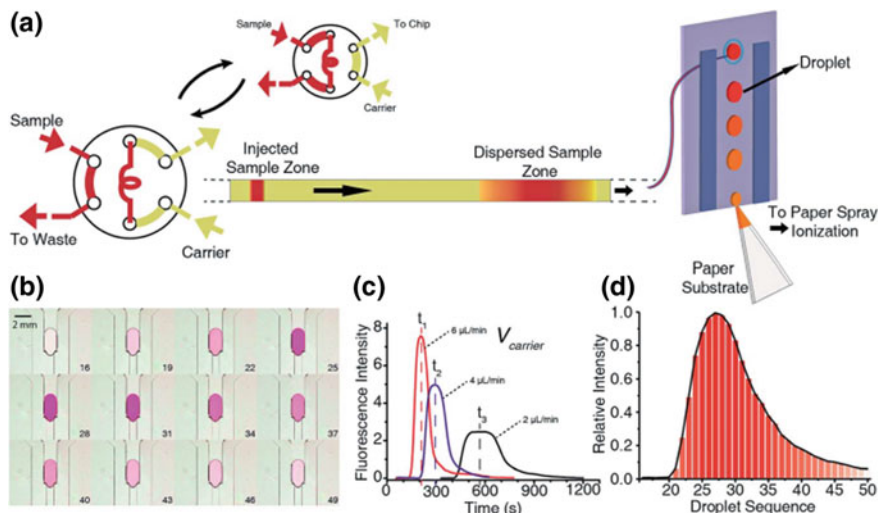


Fig. 5.4 Injection analysis-based generation of droplets in a gravity-driven microfluidic chip. **a** Generation of concentration gradient droplets using a flow tube. **b** Images for droplets with a concentration gradient of rhodamine B-methanol solution. **c**, **d** Time-dependent fluorescent intensity of rhodamine B in droplets. Reproduced with permission from Ref. [39]. Copyright 2014 Royal Society of Chemistry

precise control over their volume, but with a lower generation rate. The advantages of “on-demand” droplet formation are very suitable for single-cell encapsulation and subsequent analysis.

5.4 Single-Cell Encapsulation in Droplets

Cells from human patient samples and cultured cell lines can be encapsulated in each droplet at high throughput for culture and analysis using droplet-microfluidic technique [43]. In particular, single-cell-laden droplets enable to effectively serve as a separated counterpart for the study of individual cells (Fig. 5.5) [44, 45]. The recent development of droplet-based single-cell technique is able to provide many unprecedented advantages, including manipulation, culture, and analysis of single cells within isolated microenvironments [46]. The strategy for single-cell encapsulation commonly involves two steps, including the dispersion of cells in water or hydrogel precursor solution and generation of droplets or hydrogel particles via in situ cross-linking [47]. For single-cell encapsulation, cells are delivered to droplet nozzles at random, where cell occupancy in a population of droplets is generally Poisson-distributed [37]. Existing techniques are not able to yield a high occupancy of single-cell encapsulation in droplets and high polymer-to-cell ratio. Each droplet will be not occupied by cells or contains more than one cell. Cell

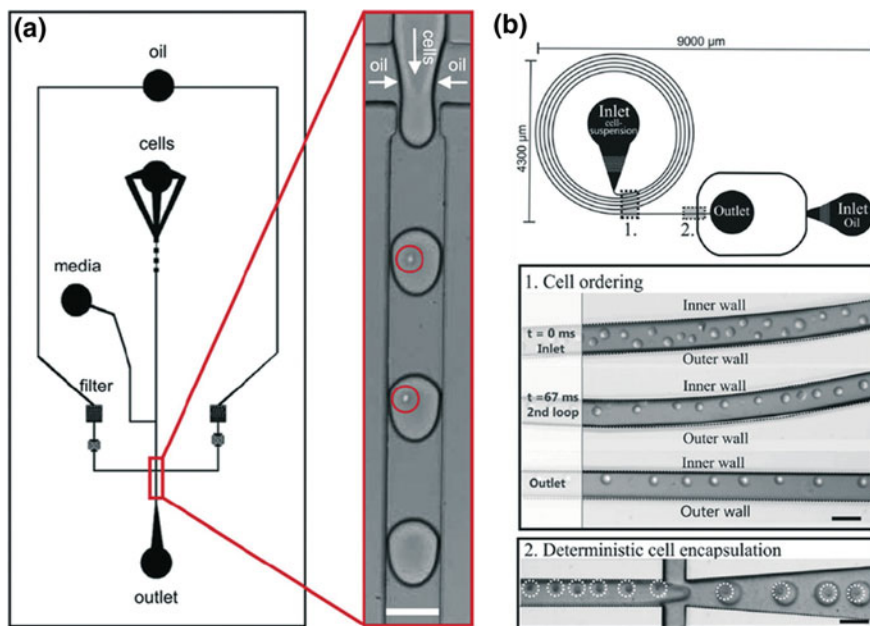


Fig. 5.5 Performance of single-cell encapsulation using droplet microfluidics. **a** Schematic of droplet-microfluidic device for single-cell encapsulation and microscopic image of single cells encapsulated in droplets. The encapsulated cells were labeled by red circles. Reproduced with permission from Ref. [44]. Copyright 2008 Elsevier. **b** Schematic of droplet-microfluidic device for deterministic cell encapsulation. The encapsulated cells were labeled by white dotted circles. Reproduced with permission from Ref. [45]. Copyright 2012 Royal Society of Chemistry

concentration can be adjusted to control the Poisson distribution, which has been developed for high-throughput encapsulation of cells. Although the Poisson-distributed cell occupancy is a technical challenge in droplet microfluidics, the generated droplets without cells can be easily differentiated by a dielectrophoretic sorting technique through detecting their fluorescence or others. Several hydrodynamic techniques were developed to separate single-cell-contained droplets with no cells contained droplets based on size or fluorescent labeling.

Achieving a large population of cell-containing droplets with high single-cell occupancy is important for high-efficiency cell analysis and the studies on cell–cell interactions. The Poisson distribution of cell occupancy is the main problem. Recently, recent work has addressed this issue by developing a microfluidic-based method to encapsulate single cells with high occupancy [48]. This microfluidic-based method for single-cell encapsulation is able to achieve the proportion of cell-containing droplets by a factor of ten, with encapsulation efficiencies over 90%. The strategy provides unique advancements to achieve high-efficiency single-cell encapsulation, a one-step method to significantly increase the proportion of

cell-containing microgels. The approach offers an opportunity for applications in cell encapsulation, cell culture, cell analysis, and cell delivery at a single-cell level [49].

5.5 Hydrogel for Cell Encapsulation in Droplets

The technology of cell encapsulation in droplets has been widely used for high-throughput cell-based assays. Generally, the droplets are composed of cells and water solution. However, to maintain long-term cell culture or cell culture media exchange, natural and synthetic biomaterial polymer, especially biocompatible hydrogel, has been widely used to prepare droplets [50, 51]. At first, cells are dispersed in the hydrogel precursors, and then, these cell-containing hydrogel precursors were emulsified by a second oil phase containing a biocompatible surfactant. Next, the generated hydrogel droplets can be cross-linked to form cell-containing microgels by various methods, including light-induced polymerization, temperature change-induced solidification, and cation chelator-based gelation. In particular, the morphology and functions of hydrogel materials are highly relevant to their properties and polymerization method. Polysaccharide-based natural hydrogels (alginate, agarose, and chitosan) and protein hydrogel (collagen, gelatin, and fibrin) are usually polymerized by a physiological condition (Fig. 5.6) [52]. For instance, agarose can be gelled by controlling its temperature (15–30 °C) [53], and alginate precursors can form hydrogels by introducing alkaline earth ions (Ca^{2+} , Ba^{2+} , or Sr^{2+}) [54]. Collagen is able to form a hydrogel by controlling the temperature at neutral pH condition [55]. Thus, the mild and biocompatible condition for microgel formation is suitable for microscale tissue engineering, cell culture, and cell analysis.

Despite existing unique advantage of excellent biocompatibility, natural hydrogels are not easy to be chemically modified with specific properties [56]. In contrast, synthetic polymer is an excellent alternative to fabricate cell-containing microgels, such as poly(acrylamide), poly(ethylene glycol), poly(acrylic acid), and poly(vinyl alcohol). These polymer hydrogels can be modified with some desired functional groups, such as degradable linkages, peptides, and oligonucleotides. For example, poly(ethylene glycol) (PEG) can be covalently conjugated with cell-adherent peptides, such as RGD [57]. The RDG-PEG co-polymers can be fabricated to microgels for cell studied. In a typical procedure, aqueous monomer precursors are mixed with linker units and initiators and then polymerized under a specific condition, for example UV-Vis light exposure. Compared to natural hydrogels, a unique advantage of these synthetic polymers is their good mechanical property. This feature makes them suitable to serve as biological scaffolds for tissue engineering.

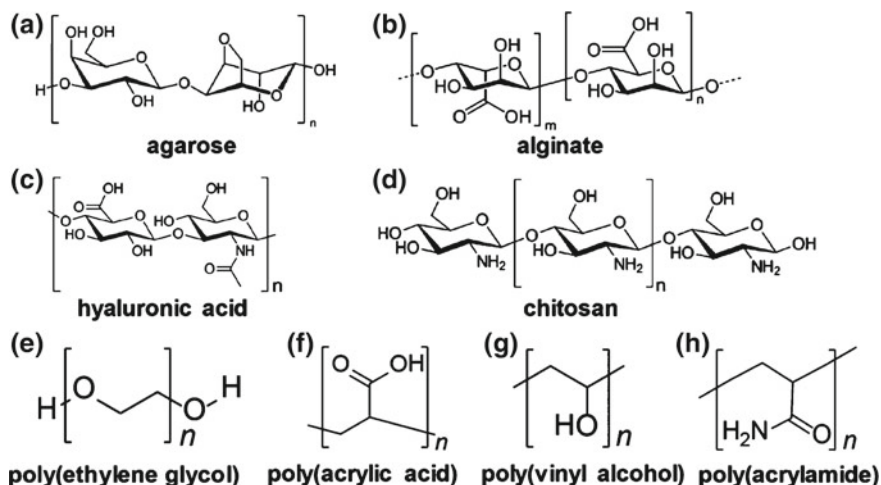


Fig. 5.6 Molecular structures of natural hydrogels and synthetic polymer hydrogels. **a–h** Agarose, alginate, hyaluronic acid, chitosan, poly(ethylene glycol) (PEG), poly(acrylic acid) (PAA), poly(vinyl alcohol) (PVA), and poly(acrylamide) (PAA). Reproduced with permission from Ref. [52]. Copyright 2017 American Chemical Society

5.6 Cell Culture in Droplets

The technology of microfluidic cell encapsulation in droplets offers a powerful tool for the studies of single cells, since the droplets can be used as a well-defined, controllable isolated compartment for single-cell encapsulation, culture, manipulation, and analysis (Fig. 5.7) [58]. The picoliter compartment of the droplets has a similar size with cells for microscale operation. For single-cell culture, hydrogel droplets not only provide an isolated compartment for cell encapsulation, but also allow for exchange of nutrients, gas, and metabolites with outer cell culture medium. Droplet microgels have been widely used to realize long-term cell culture with high cell viability, such as mammalian cells, bacteria, yeast, and even stem cells [44, 59–62]. For instance, Clausell-Tormos et al. demonstrated that single cells (Jurkat and HEK293T cell line) could remain with high viability of more than 80% for 3 days [44]. Cell proliferation at single-cell level has also been observed in alginate microgels [58].

Since the hydrogels allow for molecule exchange from outer solution, fluorescence-based cell live/dead assays can be performed to measure the viability of encapsulated cells inside the microgels. Brouzes et al. demonstrated that human U937 cells have a viability of 80% after 4-day culture [61]. The 15% of cell death is likely to be attributed to shear stress or surfactants during cell encapsulation into droplets. It is noted that fluorinated oils are found to benefit for long-term cell culture because of its ability to efficiently transport oxygen and carbon dioxide, as well as its very low solubility in water phase. Another issue is that the proliferation

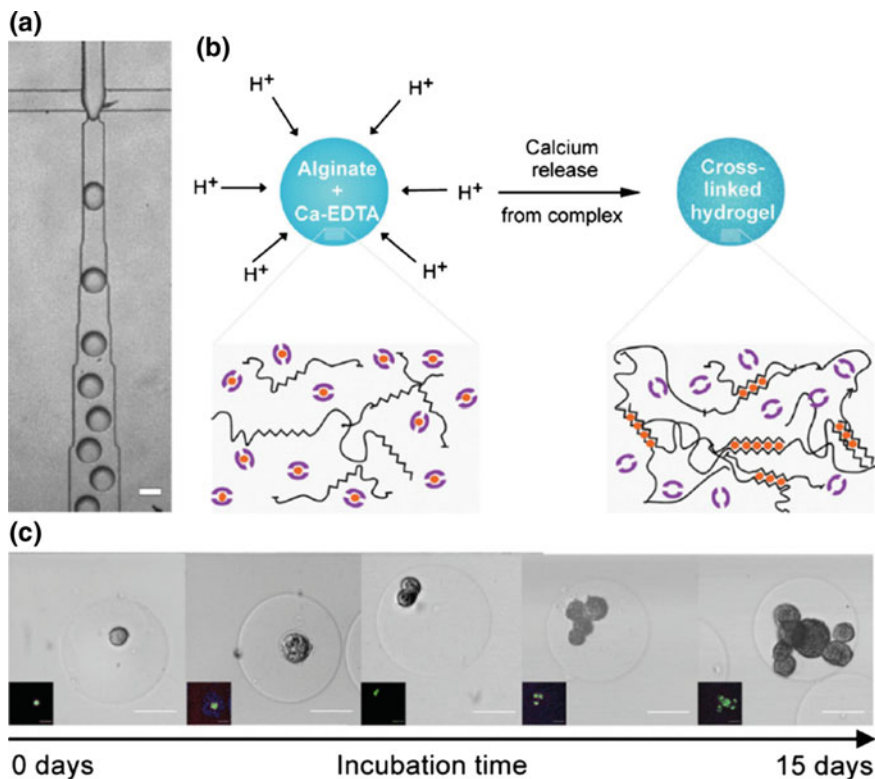


Fig. 5.7 **a** Microscopic image of fabrication of alginate hydrogel droplets using a microfluidic flow-focusing device (scale bar 50 μm). **b** Schematic of cross-linking process of alginate microgel. Acetic acid was added to the continuous phase and calcium-EDTA complex was dissolved into hydrogel precursor solution. The alginate was cross-linked when calcium ions were released by the entering acid. **c** Microscopic images of single-cell-containing alginate microgels. The single cells were encapsulated and then continuously cultured for 3, 6, 12, and 15 days, respectively. The cells were stained by Calcein AM dyes and imaged under confocal microscope to indicate cell viability. All scale bars are 25 μm . Reproduced with permission from Ref. [58]. Copyright 2015 Wiley-VCH

of the encapsulated cells was found to be slow, perhaps due to the lack of cell-to-cell interaction and realistic 3D cell microenvironment. It is still challenged to mimic normal cell microenvironment for mammalian cell proliferation in droplets.

5.7 Droplet Microfluidics for Single-Cell Analysis

Droplet-microfluidic technology is a powerful tool for precise encapsulation of single cells and high-throughput analysis within monodisperse microdroplets [63]. For cell analysis in a single droplet, this technique is able to manipulate them for mixing, splitting, and sorting for assay purpose [64–66]. Notably, droplets are able to be stable for a long time, and cells encapsulated in hydrogel droplets can be cultured for surviving for a week. In this regard, droplet microfluidics can offer an excellent platform for high-efficiency single-cell analysis. To achieve single-cell analysis, droplet-microfluidic platform can couple with various analytical approaches, including fluorescence, mass spectrometry, electrochemistry, and surface-enhanced Raman scattering [67–70]. Importantly, droplet-microfluidic technique offers unique advantages of high-through analysis and reduced biological reagent and avoided cross-contamination. These features make droplet microfluidics as a powerful platform for heterogeneity analysis of single cells, such as cell proliferation, protein secretion, DNA sequencing, enzyme kinetics, and stem cell differentiation.

5.8 Single-Cell Nucleic Acid Sequencing

Droplet-microfluidic technique has been used to perform rapid, low-cost, and high-throughput single-cell nucleic acid sequencing [2]. Advanced technology for nucleic acid sequencing is fundamentally important for cell research, disease diagnosis, and clinical therapy [71]. To ensure the sensitivity of DNA sequencing, polymerase chain reaction (PCR) has been used as a robust amplification tool coupling with droplet microfluidics, which is known as digital droplet PCR [34, 72, 73]. In this technique, samples are diluted into millions of droplets (Fig. 5.8) [74–76]. PCR amplification is run in each droplet, and target DNA can be sensitively detected by a droplet sorting-based counting technique. Because of the strong capability of rapid sorting from millions of droplets, this technique enables for detection of the gene mutation for cancer diagnosis and prognosis. It allows rapid screening and counting and quantification of mutants from a few copies among many wild types. Pekin et al. reported the use of digital droplet PCR technique to achieve accurate detection of mutation genes from a large population of samples [77]. In a typical procedure, target DNA samples were diluted and encapsulated into microscale droplets, which contained fluorescently labeled reverse primers, PCR primer-immobilized microbeads, DNA polymerase, and deoxyribonucleotide triphosphate. After the PCR reaction is completed, the droplets can be sorted and detected by flow cytometer. Benefiting from the advantages of single-cell PCR, this approach exists a high sensitivity for mutation detection at a single-cell level.

Nevertheless, the performance of single-cell DNA sequencing is still very challenged due to closed droplet compartment, because single-cell droplets need

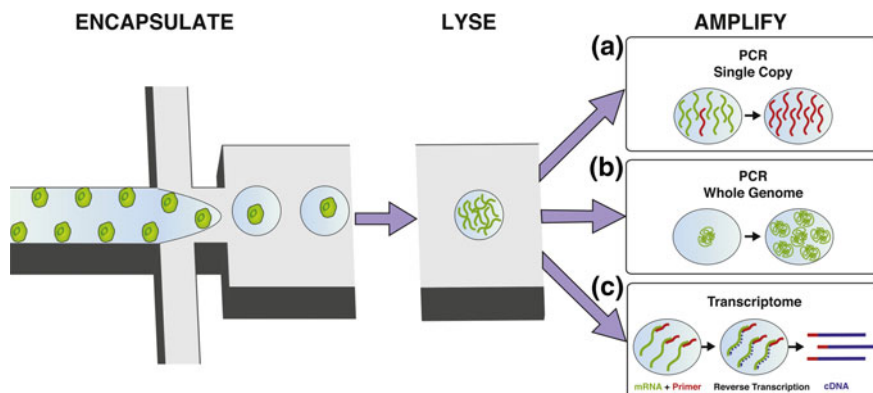


Fig. 5.8 Schematic illustration of single-cell encapsulation using droplet-microfluidic technique for gene analysis. **a** Single-copy PCR amplification in a droplet. Reproduced with permission from Ref. [74]. Copyright 2008 American Chemical Society. **b** Whole genome PCR amplification in a droplet. Reproduced with permission from Ref. [75]. Copyright 2015 Wiley-VCH. **c** Barcoding for single-cell transcriptomics in a droplet. Reproduced with permission from Ref. [76]. Copyright 2015 Elsevier

complex processes, including cell lysis, DNA extraction, and PCT reaction [78]. To address this issue, hydrogel-based droplets have been developed as an ideal platform for efficient cell lysis and DNA extraction, as well as used for PCR amplification due to the penetration of small molecules (Fig. 5.9) [79]. Novak et al. reported an agarose-based droplet-microfluidic technique to screen mutation at a single-cell level [30]. In a typical procedure, single cancer cells were encapsulated in each agarose hydrogel-based droplet containing primer-immobilized microbeads. After agarose gelation, the single-cell microgel particles were extracted from the oil phase to the aqueous phase, and the cells were lysed to release DNA. The DNA-contained microgels can be washed for a further PCR. Finally, flow cytometry was employed to achieve a high-throughput analysis. Meanwhile, reverse-transcription PCR (RT-PCR) technique was also coupled with droplet microfluidics for single-cell DNA sequencing. Yang et al. developed an RT-PCR-based agarose droplet-microfluidic technique for detection of mRNA expression in cancer cells [31]. Therefore, droplet microfluidics offers many advantages (low cost, high throughput, rapid analysis, high sensitivity, and so on) for applications in the detection of single cells in complex biological samples.

5.9 Single-Cell Protein Detection

Detection of cancer cell-specific protein expression is an important pathway for early diagnosis [80]. Droplet microfluidics is an advanced technique that is particularly suitably used for high-throughput analysis of protein secretion from single

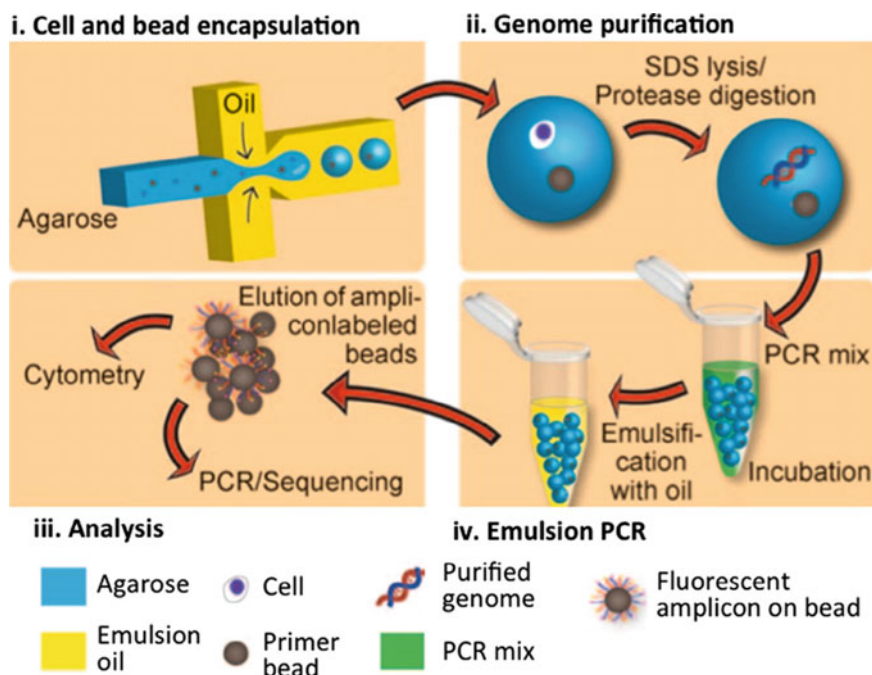


Fig. 5.9 Illustration of digital PCR combined with droplet microfluidics for single-cell analysis. Agarose hydrogel droplet was used for cell encapsulation and PCR reactor. Reproduced with permission from Ref. [79]. Copyright 2011 Wiley-VCH

cells through rapid sorting and detection of each droplet [61, 81, 82]. Unlike amplification techniques used in single-cell DNA sequencing, there is a challenge for this technique used in protein detection at a single-cell level—the low sensitivity of flow cytometry and low concentration of protein expression in single cells. Here we introduce recent development for single-cell protein analysis based on droplet microfluidics

In many types of cancer cells, cell-surface proteins are usually serving as a type of specific biomarkers for cancer diagnosis and therapy. Detection of overexpressed proteins in cancer cell surface can provide direct evidence for cancer diagnosis, prognosis, and therapy guidance. For example, EpCAM proteins are generally expressed in breast cancer cells. In order to detect low-abundance cell-surface proteins, an enzymatic amplification strategy has been developed to enhance the sensitivity of flow cytometry when coupled with droplet-microfluidic system [83]. In this typical procedure, cell-surface protein biomarkers were labeled with biotinylated antibodies and then coupling with streptavidin-conjugated galactosidase. When incubating with the fluorogenic substrate in droplets, the enzyme-labeled cell in each droplet can be easily detected by a photomultiplier tube. It should be noted that the enzymatic reaction is critical to achieving

fluorescence signal amplification for sensitive analysis. Apart from the enzymatic reaction-based signal amplification, rolling circle amplification (RCA) was also coupled with droplet microfluidics to enhance detection sensitivity [84]. In a typical procedure, the surface of biomarker protein-expressed cancer cells was labeled with biotinylated antibodies, binding with DNA primers for RCA reaction. Combining with the RCA tool and fluorescence labeling, biomarker proteins on the cancer cell surface can be easily detected from the single cells using droplet microfluidics.

Detection of biomarker proteins secreted from tumor cells is also widely employed for cancer diagnosis in clinical [85]. Compared with conventional immunoassays that detect protein biomarkers from a large population of cell samples, protein biomarker analysis from single cells can provide a precise and systematic result for cancer-specific biomarkers expressed from tumor cells (Fig. 5.10) [66]. In particular, droplet-microfluidic technique offers unique advantages to monitor the small population of circulating tumor cells [86]. In addition, droplet microfluidics has been developed to detect cell heterogeneity of cytokine secretion from cancer cells. In this technique, single cancer cells were encapsulated into agarose hydrogel droplets containing specific antibodies-functionalized microbeads [87]. The cytokines were secreted from cancer cells and confined into the hydrogel droplets, and then captured by antibody-functionalized microbeads. After the microbeads were labeled with fluorescence dyes, the droplets were detected by

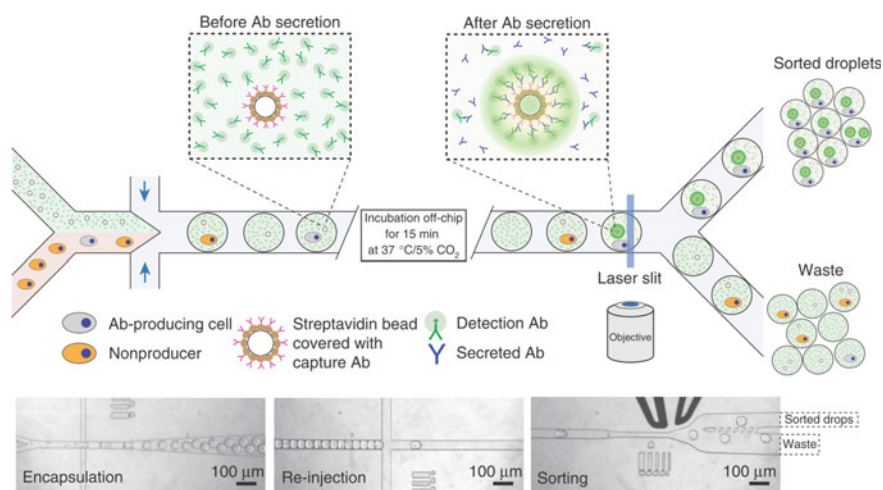


Fig. 5.10 Schematic of droplet-based microfluidics for single-cell analysis and sorting. Two different types of cells were mixed together and introduced into a microchannel together with microbeads. The antibodies secreted from cells were specifically captured by the microbeads and labeled by fluorescence dyes. The single-cell droplets were re-injected into a second microfluidic device, and then droplets containing green fluorescence were sorted by a fluorescence-activated droplet sorter. The bottom three images showed encapsulation of cells and beads in a droplet (left), re-injection of droplets (middle), and microfluidic droplet sorting (right). Reproduced with permission from Ref. [66]. Copyright 2012 Nature Publishing Group

flow cytometry for single-cell analysis. Recently, droplet-microfluidic technique has been developed to study the stimulation, functions, and intracellular cell signaling of live single cells. For example, Konry et al. reported the development of droplet microfluidics to detect cell surface and secreted proteins from single cells [84]. In this study, lipopolysaccharide stimulation of single cells in each droplet was directly analyzed by bead-based immunoassay and fluorophore-antibody staining. In a next-step work, droplet microfluidics was further used to investigate intracellular signaling between two different types of single cells. Therefore, the single-cell protein analysis using droplet microfluidics will offer new opportunities for cancer diagnosis and biological researched in the future [88].

5.10 Droplet Mass Spectrometry for Single-Cell Analysis

Droplet-microfluidic technique has been emerged as an excellent tool to couple with mass spectrometry for rapid and high-throughput analysis of single cells, because mass spectrometry is able to achieve a qualitative and quantitative detection of cell components in each droplet [89]. The unique advantages of mass spectrometry can identify and measure the molecular structure of cells directly without specific labeling. Zhang et al. developed a method of paper spray mass spectrometry to monitor the chemical reaction in each micro-sized droplet [39]. Upon the capillary wicking effect, the droplets were transferred to the tip of the paper substrate, and a process of paper spray ionization under a high voltage was applied to ionize the molecules for mass spectrometry analysis. In a further development, the droplet mass spectrometry was implemented by gravity and electrostatic attraction using a capillary tube, which was demonstrated to be more controllable. The volume of each droplet was controlled in a range from 0.7 to 2.4 μL and with a time interval of 15–60 s. Online mass spectrometry analysis of droplets was realized via paper electrospray ionization. As a set of proof-of-concept experiments, direct analysis of molecules in apples demonstrated the potential application of this approach in real-sample analysis [41]. In a parallel study, this technique was established for online monitoring of cell culture using paper spray ionization-based droplet mass spectrometry (Fig. 5.11) [90]. In a typical procedure, the droplets were generated by electrostatic interaction with precise control over a time duration. As a result, the as-developed droplet mass spectrometry was successfully performed for online monitoring of the effect of hormones on hepatic cells and glucose metabolism in cell culture solution.

The piezoelectric ink-jet printing offers a new tool to implement droplet mass spectrometry for single-cell analysis. Taking the advantages of controllable operation for droplet generation, drop-on-demand ink-jet printing can be coupled with electrospray ionization mass spectrometry to achieve lipid profiling of single cells (Fig. 5.12) [42]. Typically, the single-cell-contained droplets were produced through ink-jet sampling of a cell suspension, and then precisely dripped onto a

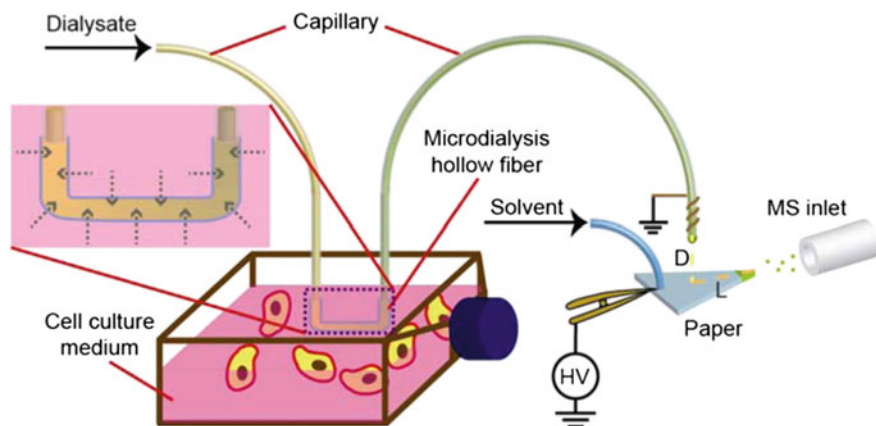


Fig. 5.11 Design of paper spray ionization-based droplet mass spectrometry for online monitoring of cell culture. Reproduced with permission from Ref. [90]. Copyright 2014 American Chemical Society

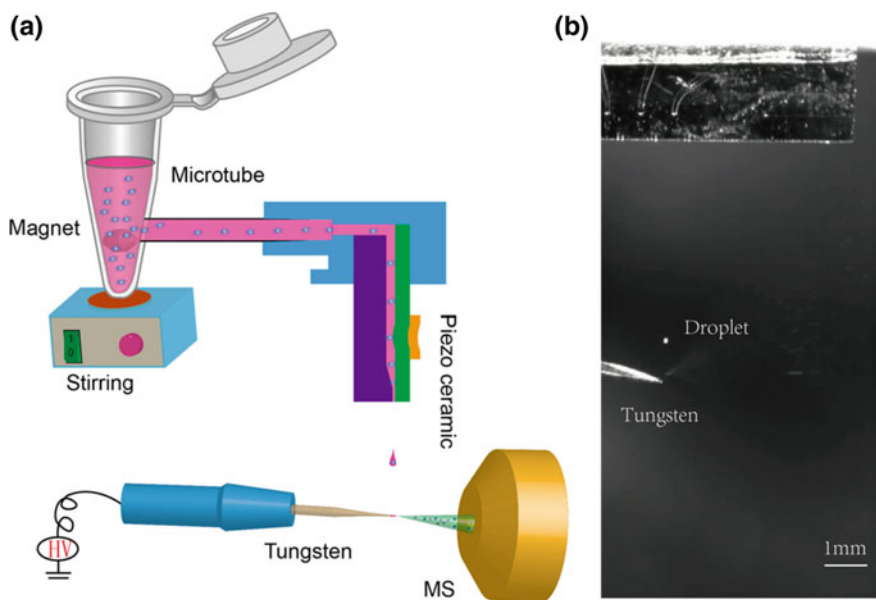


Fig. 5.12 Illustration of the experimental setup of piezoelectric ink-jet printing-based droplet mass spectrometry. **a** Cells were ink-jet-printed onto the tungsten tip for mass spectrometry analysis. **b** Photographic image of ink-jet printing cell-containing droplets and the process of electrospray ionization under a high voltage. Reproduced with permission from Ref. [42]. Copyright 2016 American Chemical Society

needle for electrospray ionization under a high-voltage electric field, which enables for achieving lipid fingerprints of single cells by mass spectrometry. It is worth to mention that the technique of ink-jet printing-based droplet formation can be applied to achieve an online digital polymerase chain reaction [91] and thus is potential for single-cell sequencing analysis. To improve the efficiency of single-cell mass spectrometry, a microfluidic technique of Dean flow-assisted cell ordering was connected with electrospray ionization mass spectrometry for lipid detection in a single-cell level [92]. If gas phase is used to generate cell-contained droplets, this platform could provide a facile method for high-efficiency droplet mass spectrometry and for direct analysis of lipids in single cells.

5.11 Conclusion and Outlook

Droplet microfluidics has been rapidly developed as one of the most compelling tools for single-cell analysis based on providing isolating compartments with the same size scale as cells. Considering that the droplet microfluidics offers the ability to encapsulate single cells in a small volume of droplets and sorting a large population of cells, this technique provides several unique advantages for single-cell analysis, including low cost, high throughputs, rapid sorting, and precise detection. In this regard, droplet microfluidics holds great potential for the investigation of cell heterogeneities, elucidating cell complexity at single-cell levels. Compared to conventional assays that are not able to isolate and detect low-abundance molecules in a mixed population, droplet microfluidics is more effective to realize more precise analysis for single cells. By combining signal amplification strategies like PCR, RCA, and enzyme reactions, droplet-microfluidic techniques are able to achieve single-cell analysis with high sensitivity, high speed, and high throughputs. With the fast development in the past years, droplet microfluidics for single-cell encapsulation and analysis has become a very compelling tool for the studies of fundamental cell biology and disease diagnosis, especially for screening a large population of disease cells for precision medicine. For example, droplet microfluidics has been widely developed for CTC detection and single-cell analysis of nucleic acid and proteins. Droplet-based microfluidics is thus promising and used as next-generation sequencing technology.

Despite the progress made during the past years, the performance of droplet microfluidics for single-cell analysis still needs to be further improved, such as detection sensitivity, single-cell efficiency, systematic integration capability, automation, and particularly their complex operation. For applications of droplet microfluidics in biological assays, digital droplet analysis still lacks sensitivity for low-abundant biomarkers from single cells. In addition, the portability of this system needs to be improved for future development, such as inexpensive point-of-care applications. As a result of these limitations, electrochemical detection-based microelectrodes and optofluidic signal-based optical fiber could be excellent to perform droplet detection for portable diagnostic devices. On a separate

note, because recent studies of single-cell encapsulation and analysis with droplet microfluidics turn to long culture periods and clinical applications, there is of great demand to develop a strategy for unperturbed droplet microenvironment for cells residing. Nonetheless, the technical advances of droplet microfluidics for single-cell analysis show great potential to make an additional scientific impact and support scientific progress in fundamental researches of cells.

References

1. Maxmen A (2011) Single-cell analysis: Imaging is everything. *Nature* 480(7375):139–141. <https://doi.org/10.1038/nj7375-139a>
2. Reece A, Xia B, Jiang Z, Noren B, McBride R, Oakey J (2016) Microfluidic techniques for high throughput single cell analysis. *Curr Opin Biotechnol* 40:90–96. <https://doi.org/10.1016/j.copbio.2016.02.015>
3. Wu J, Li H, Chen Q, Lin X, Liu W, Lin JM (2014) Statistical single-cell analysis of cell cycle-dependent quantum dot cytotoxicity and cellular uptake using a microfluidic system. *RSC Adv* 4:24929–24934. <https://doi.org/10.1039/C4RA01665C>
4. Khan M, Mao S, Li W, Lin JM (2018) Microfluidic devices in the fast-growing domain of single-cell analysis. *Chem Eur J* 24(58):15398–15420. <https://doi.org/10.1002/chem.201800305>
5. Zhang Q, Mao S, Khan M, Feng S, Zhang W, Li W et al (2018) In situ partial treatment of single cells by laminar flow in the “open space”. *Anal Chem* 91:1644–1650. <https://doi.org/10.1021/acs.analchem.8b05313>
6. Mao S, Zhang Q, Liu W, Huang Q, Khan M, Zhang W et al (2019) Chemical operations on a living single cell by open microfluidics for wound repair studies and organelle transport analysis. *Chem Sci* 10:2081–2087. <https://doi.org/10.1039/C8SC05104F>
7. Chen Q, He Z, Liu W, Lin X, Wu J, Li H et al (2015) Engineering cell-compatible paper chips for cell culturing, drug screening, and mass spectrometric sensing. *Adv Healthc Mater* 4(15):2291–2296. <https://doi.org/10.1002/adhm.20150038>
8. Chen Q, Lin JM (2018) Microfluidic cell isolation and recognition for biomedical applications. In: *Cell analysis on microfluidics*. Springer, pp 95–118. https://doi.org/10.1007/978-981-10-5394-8_3
9. Chen Q, Wu J, Zhang Y, Lin JM (2012) Qualitative and quantitative analysis of tumor cell metabolism via stable isotope labeling assisted microfluidic chip electrospray ionization mass spectrometry. *Anal Chem* 84(3):1695–1701. <https://doi.org/10.1021/ac300003k>
10. Chen Q, Wu J, Zhuang Q, Lin X, Zhang J, Lin JM (2013) Microfluidic isolation of highly pure embryonic stem cells using feeder-separated co-culture system. *Sci Rep* 3:2433. <https://doi.org/10.1038/srep02433>
11. El-Ali J, Sorger PK, Jensen KF (2006) Cells on chips. *Nature* 442:403–411. <https://doi.org/10.1038/nature05063>
12. Yu L, Ng SR, Xu Y, Dong H, Wang YJ, Li CM (2013) Advances of lab-on-a-chip in isolation, detection and post-processing of circulating tumour cells. *Lab Chip* 13:3163–3182. <https://doi.org/10.1039/C3LC00052D>
13. Wheeler AR, Thronset WR, Whelan RJ, Leach AM, Zare RN, Liao YH et al (2013) Microfluidic device for single-cell analysis. *Anal Chem* 75:3581–3586. <https://doi.org/10.1021/ac0340758>
14. Sackmann EK, Fulton AL, Beebe DJ (2014) The present and future role of microfluidics in biomedical research. *Nature* 507:181–189. <https://doi.org/10.1038/nature13118>

15. Wu J, Chen Q, Lin JM (2016) Biochemical analysis on microfluidic chips. *Trends Anal Chem* 80:213–231. <https://doi.org/10.1016/j.trac.2016.03.013>
16. Chen Q, Wu J, Zhang Y, Lin Z, Lin JM (2012) Targeted isolation and analysis of single tumor cells with aptamer-encoded microwell array on microfluidic device. *Lab Chip* 12:5180–5185. <https://doi.org/10.1039/C2LC40858A>
17. Mao S, Zhang W, Huang Q, Khan M, Li H, Uchiyama K et al (2018) In situ scatheless cell detachment reveals correlation between adhesion strength and viability at single-cell resolution. *Angew Chem Int Ed* 57:236–240. <https://doi.org/10.1002/anie.201710273>
18. Teh SY, Lin R, Hung LH, Lee AP (2008) Droplet microfluidics. *Lab Chip* 8:198–220. <https://doi.org/10.1039/B715524G>
19. Casadevall i Solvas X, deMello A (2011) Droplet microfluidics: recent developments and future applications. *Chem Commun* 47:1936–1942. <https://doi.org/10.1039/c0cc02474k>
20. Shang L, Cheng Y, Zhao Y (2017) Emerging droplet microfluidics. *Chem Rev* 117:7964–8040. <https://doi.org/10.1021/acs.chemrev.6b00848>
21. Baret JC (2012) Surfactants in droplet-based microfluidics. *Lab Chip* 12:422–433. <https://doi.org/10.1039/C1LC20582J>
22. Yin H, Marshall D (2012) Microfluidics for single cell analysis. *Curr Opin Biotechnol* 23:110–119. <https://doi.org/10.1016/j.copbio.2011.11.002>
23. Huebner A, Srisa-Art M, Holt D, Abell C, Hollfelder F, deMello AJ et al (2007) Quantitative detection of protein expression in single cells using droplet microfluidics. *Chem Commun* 1218–1220. <https://doi.org/10.1039/b618570c>
24. Zhu Z, Zhang W, Leng X, Zhang M, Guan Z, Lu J et al (2012) Highly sensitive and quantitative detection of rare pathogens through agarose droplet microfluidic emulsion PCR at the single-cell level. *Lab Chip* 12:3907–3913. <https://doi.org/10.1039/C2LC40461C>
25. Leng X, Zhang W, Wang C, Cui L, Yang CJ (2010) Agarose droplet microfluidics for highly parallel and efficient single molecule emulsion PCR. *Lab Chip* 10:2841–2843. <https://doi.org/10.1039/C0LC00145G>
26. Zeng Y, Novak R, Shuga J, Smith MT, Mathies RA (2010) High-performance single cell genetic analysis using microfluidic emulsion generator arrays. *Anal Chem* 82:3183–3190. <https://doi.org/10.1021/ac902683t>
27. Chen Q, Chen D, Wu J, Lin JM (2016) Flexible control of cellular encapsulation, permeability, and release in a droplet-templated bifunctional copolymer scaffold. *Biomicrofluidics* 10:064115. <https://doi.org/10.1063/1.4972107>
28. Wang N, Mao S, Liu W, Wu J, Li H, Lin JM (2014) Online monodisperse droplets based liquid–liquid extraction on a continuously flowing system by using microfluidic devices. *RSC Adv* 4:11919–11926. <https://doi.org/10.1039/C4RA00984C>
29. Tanaka H, Yamamoto S, Nakamura A, Nakashoji Y, Okura N, Nakamoto N et al (2015) Hands-off preparation of monodisperse emulsion droplets using a poly(dimethylsiloxane) microfluidic chip for droplet digital PCR. *Anal Chem* 87:4134–4143. <https://doi.org/10.1021/ac503169h>
30. Nabavi SA, Vladislavljević GT, Gu S, Ekanem EE (2015) Double emulsion production in glass capillary microfluidic device: parametric investigation of droplet generation behaviour. *Chem Eng Sci* 130:183–196. <https://doi.org/10.1016/j.ces.2015.03.004>
31. Chen Q, Utech S, Chen D, Prodanovic R, Lin JM, Weitz DA (2016) Controlled assembly of heterotypic cells in a core-shell scaffold: organ in a droplet. *Lab Chip* 16:1346–1349. <https://doi.org/10.1039/C6LC00231E>
32. Xia Y, Whitesides GM (1998) Soft Lithography. *Angew Chem Int Ed* 37:550–575. [https://doi.org/10.1002/\(SICI\)1521-3773\(19980316\)37:5%3c550::AID-ANIE550%3e3.0.CO;2-G](https://doi.org/10.1002/(SICI)1521-3773(19980316)37:5%3c550::AID-ANIE550%3e3.0.CO;2-G)
33. Toepke MW, Beebe DJ (2006) PDMS absorption of small molecules and consequences in microfluidic applications. *Lab Chip* 6:1484–1486. <https://doi.org/10.1039/B612140C>
34. Beer NR, Wheeler EK, Lee-Houghton L, Watkins N, Nasarabadi S, Hebert N et al (2008) On-chip single-copy real-time reverse-transcription PCR in isolated picoliter droplets. *Anal Chem* 80:1854–1858. <https://doi.org/10.1021/ac800048k>

35. Joensson HN, Andersson Svahn H (2012) Droplet microfluidics—a tool for single-cell analysis. *Angew Chem Int Ed* 51:12176–12192. <https://doi.org/10.1002/anie.201200460>
36. Gu H, Duits MH, Mugele F (2011) Droplets formation and merging in two-phase flow microfluidics. *Int J Mol Sci* 12:2572–2597. <https://doi.org/10.3390/ijms12042572>
37. Collins DJ, Neild A, deMello A, Liu AQ, Ai Y (2015) The Poisson distribution and beyond: methods for microfluidic droplet production and single cell encapsulation. *Lab Chip* 15:3439–3459. <https://doi.org/10.1039/C5LC00614G>
38. Chen D, Amstad E, Zhao C-X, Cai L, Fan J, Chen Q et al (2017) Biocompatible amphiphilic hydrogel-solid dimer particles as colloidal surfactants. *ACS Nano* 11:11978–11985. <https://doi.org/10.1021/acsnano.7b03110>
39. Zhang Y, Li H, Ma Y, Lin JM (2014) Paper spray mass spectrometry-based method for analysis of droplets in a gravity-driven microfluidic chip. *Analyst* 139:1023–1029. <https://doi.org/10.1039/C3AN01769A>
40. Liu J, Lin JM, Knopp D (2008) Using a circular groove surrounded inlet to generate monodisperse droplets inside a microfluidic chip in a gravity-driven manner. *J Micromech Microeng* 18:095014. <https://doi.org/10.1088/0960-1317/18/9/095014>
41. Liu W, Mao S, Wu J, Lin JM (2013) Development and applications of paper-based electrospray ionization-mass spectrometry for monitoring of sequentially generated droplets. *Analyst* 138:2163–2170. <https://doi.org/10.1039/C3AN36404F>
42. Chen F, Lin L, Zhang J, He Z, Uchiyama K, Lin JM (2016) Single-cell analysis using drop-on-demand inkjet printing and probe electrospray ionization mass spectrometry. *Anal Chem* 88:4354–4360. <https://doi.org/10.1021/acs.analchem.5b04749>
43. Shembekar N, Chaipan C, Utharala R, Merten CA (2016) Droplet-based microfluidics in drug discovery, transcriptomics and high-throughput molecular genetics. *Lab Chip* 16:1314–1331. <https://doi.org/10.1039/C6LC00249H>
44. Clausell-Tormos J, Lieber D, Baret J-C, El-Harrak A, Miller OJ, Frenz L et al (2008) Droplet-based microfluidic platforms for the encapsulation and screening of mammalian cells and multicellular organisms. *Chem Biol* 15:427–437. <https://doi.org/10.1016/j.chembiol.2008.04.004>
45. Kemna EW, Schoeman RM, Wolbers F, Vermes I, Weitz DA, Van Den Berg A (2012) High-yield cell ordering and deterministic cell-in-droplet encapsulation using Dean flow in a curved microchannel. *Lab Chip* 12:2881–2887. <https://doi.org/10.1039/C2LC00013J>
46. Li W, Zhang L, Ge X, Xu B, Zhang W, Qu L et al (2018) Microfluidic fabrication of microparticles for biomedical applications. *Chem Soc Rev* 47:5646–5683. <https://doi.org/10.1039/C7CS00263G>
47. Lima AC, Sher P, Mano JF (2012) Production methodologies of polymeric and hydrogel particles for drug delivery applications. *Expert Opin Drug Deliv* 9:231–248. <https://doi.org/10.1517/17425247.2012.652614>
48. Mao AS, Shin J-W, Utech S, Wang H, Uzun O, Li W et al (2017) Deterministic encapsulation of single cells in thin tunable microgels for niche modelling and therapeutic delivery. *Nat Mater* 16:236–243. <https://doi.org/10.1038/nmat4781>
49. Kamperman T, Karperien M, Le Gac S, Leijten J (2018) Single-cell microgels: technology, challenges, and applications. *Trends Biotechnol* 2018(36):850–865. <https://doi.org/10.1016/j.tibtech.2018.03.001>
50. Tumarkin E, Kumacheva E (2009) Microfluidic generation of microgels from synthetic and natural polymers. *Chem Soc Rev* 38:2161–2168. <https://doi.org/10.1039/B809915B>
51. Wan J (2012) Microfluidic-based synthesis of hydrogel particles for cell microencapsulation and cell-based drug delivery. *Polymers* 4:1084–1108. <https://doi.org/10.3390/polym4021084>
52. Zhu Z, Yang CJ (2016) Hydrogel droplet microfluidics for high-throughput single molecule/cell analysis. *Acc Chem Res* 50:22–31. <https://doi.org/10.1021/acs.accounts.6b00370>
53. Rinaudo M (2008) Main properties and current applications of some polysaccharides as biomaterials. *Polym Int* 57:397–430. <https://doi.org/10.1002/pi.2378>
54. Lee KY, Mooney DJ (2012) Alginate: properties and biomedical applications. *Prog Polym Sci* 37:106–126. <https://doi.org/10.1016/j.progpolymsci.2011.06.003>

55. Williams BR, Gelman RA, Poppke DC, Piez KA (1978) Collagen fibril formation. Optimal in vitro conditions and preliminary kinetic results. *J Biol Chem* 253:6578–6585
56. Wu J, Xie L, Lin WZY, Chen Q (2017) Biomimetic nanofibrous scaffolds for neural tissue engineering and drug development. *Drug Discov Today* 22:1375–1384. <https://doi.org/10.1016/j.drudis.2017.03.007>
57. Hern DL, Hubbell JA (1998) Incorporation of adhesion peptides into nonadhesive hydrogels useful for tissue resurfacing. *J Biomed Mater Res* 39:266–276. [https://doi.org/10.1002/\(SICI\)1097-4636\(199802\)39:2%3c266:AID-JBM14%3e3.0.CO;2-B](https://doi.org/10.1002/(SICI)1097-4636(199802)39:2%3c266:AID-JBM14%3e3.0.CO;2-B)
58. Utech S, Prodanovic R, Mao AS, Ostafe R, Mooney DJ, Weitz DA (2015) Microfluidic generation of monodisperse, structurally homogeneous alginate microgels for cell encapsulation and 3D cell culture. *Adv Healthc Mater* 4:1628–1633. <https://doi.org/10.1002/adhm.201500021>
59. Huebner A, Srisa-Art M, Holt D, Abell C, Hollfelder F, Edel J (2007) Quantitative detection of protein expression in single cells using droplet microfluidics. *Chem Commun* 1218–1220. <https://doi.org/10.1039/b618570c>
60. Martin K, Henkel T, Baier V, Grodrian A, Schön T, Roth M et al (2003) Generation of larger numbers of separated microbial populations by cultivation in segmented-flow microdevices. *Lab Chip* 3:202–207. <https://doi.org/10.1039/B301258C>
61. Brouzes E, Medkova M, Savenelli N, Marran D, Twardowski M, Hutchison JB et al (2009) Droplet microfluidic technology for single-cell high-throughput screening. *Proc Natl Acad Sci USA* 106:14195–14200. <https://doi.org/10.1073/pnas.0903542106>
62. Holtze C, Rowat A, Agresti J, Hutchison J, Angile F, Schmitz C et al (2008) Biocompatible surfactants for water-in-fluorocarbon emulsions. *Lab Chip* 8:1632–1639. <https://doi.org/10.1039/B806706F>
63. Li H-F, Pang Y-F, Liu J-J, Lin J-M (2011) Suspending nanoliter droplet arrays for cell capture and copper ion stimulation. *Sens Actuators B Chem* 155:415–421. <https://doi.org/10.1016/j.snb.2010.12.023>
64. Song H, Bringer MR, Tice JD, Gerdtz CJ, Ismagilov RF (2003) Experimental test of scaling of mixing by chaotic advection in droplets moving through microfluidic channels. *Appl Phys Lett* 83:4664–4666. <https://doi.org/10.1063/1.1630378>
65. Link D, Anna SL, Weitz D, Stone H (2004) Geometrically mediated breakup of drops in microfluidic devices. *Phys Rev Lett* 92:054503. <https://doi.org/10.1103/physrevlett.92.054503>
66. Mazutis L, Gilbert J, Ung WL, Weitz DA, Griffiths AD, Heyman JA (2013) Single-cell analysis and sorting using droplet-based microfluidics. *Nat Protoc* 8:870–891. <https://doi.org/10.1038/nprot.2013.046>
67. Liu W, Chen Q, Lin X, Lin J-M (2015) Online multi-channel microfluidic chip-mass spectrometry and its application for quantifying noncovalent protein–protein interactions. *Analyst* 140:1551–1554. <https://doi.org/10.1039/C4AN02370F>
68. Rackus DG, Shamsi MH, Wheeler AR (2015) Electrochemistry, biosensors and microfluidics: a convergence of fields. *Chem Soc Rev* 44:5320–5340. <https://doi.org/10.1039/C4CS00369A>
69. Han Z, Li W, Huang Y, Zheng B (2009) Measuring rapid enzymatic kinetics by electrochemical method in droplet-based microfluidic devices with pneumatic valves. *Anal Chem* 81:5840–5845. <https://doi.org/10.1021/ac900811y>
70. Cecchini MP, Hong J, Lim C, Choo J, Albrecht T, deMello AJ et al (2011) Ultrafast surface enhanced resonance Raman scattering detection in droplet-based microfluidic systems. *Anal Chem* 83:3076–30781. <https://doi.org/10.1021/ac103329b>
71. Kang D-K, Ali MM, Zhang K, Pone EJ, Zhao W (2014) Droplet microfluidics for single-molecule and single-cell analysis in cancer research, diagnosis and therapy. *Trends Anal Chem* 58:145–153. <https://doi.org/10.1016/j.trac.2014.03.006>
72. Kiss MM, Ortoleva-Donnelly L, Beer NR, Warner J, Bailey CG, Colston BW et al (2008) High-throughput quantitative polymerase chain reaction in picoliter droplets. *Anal Chem* 80:8975–8981. <https://doi.org/10.1021/ac801276c>

73. Schaerli Y, Wootton RC, Robinson T, Stein V, Dunsby C, Neil MA et al (2008) Continuous-flow polymerase chain reaction of single-copy DNA in microfluidic micro-droplets. *Anal Chem* 81:302–306. <https://doi.org/10.1021/ac802038c>
74. Kumaresan P, Yang CJ, Cronier SA, Blazej RG, Mathies RA (2008) High-throughput single copy DNA amplification and cell analysis in engineered nanoliter droplets. *Anal Chem* 80:3522–3529. <https://doi.org/10.1021/ac800327d>
75. Han HS, Cantalupo PG, Rotem A, Cockrell SK, Carbonnaux M, Pipas JM et al (2015) Whole-genome sequencing of a single viral species from a highly heterogeneous sample. *Angew Chem Int Ed* 54:13985–13988. <https://doi.org/10.1002/anie.201507047>
76. Klein AM, Mazutis L, Akartuna I, Tallapragada N, Veres A, Li V et al (2015) Droplet barcoding for single-cell transcriptomics applied to embryonic stem cells. *Cell* 161:1187–1201. <https://doi.org/10.1016/j.cell.2015.04.044>
77. Pekin D, Skhiri Y, Baret J-C, Le Corre D, Mazutis L, Salem CB et al (2011) Quantitative and sensitive detection of rare mutations using droplet-based microfluidics. *Lab Chip* 11:2156–2166. <https://doi.org/10.1039/C1LC20128J>
78. Chao T-C, Ros A (2008) Microfluidic single-cell analysis of intracellular compounds. *J R Soc Interface* 5:139–150. <https://doi.org/10.1098/rsif.2008.0233.focus>
79. Novak R, Zeng Y, Shuga J, Venugopalan G, Fletcher DA, Smith MT et al (2011) Single-cell multiplex gene detection and sequencing with microfluidically generated agarose emulsions. *Angew Chem Int Ed* 50:390–395. <https://doi.org/10.1002/anie.201006089>
80. Reiter RE, Gu Z, Watabe T, Thomas G, Szigeti K, Davis E et al (1998) Prostate stem cell antigen: a cell surface marker overexpressed in prostate cancer. *Proc Natl Acad Sci USA* 95:1735–1740. <https://doi.org/10.1073/pnas.95.4.1735>
81. Shahi P, Kim SC, Haliburton JR, Gartner ZJ, Abate AR (2017) Abseq: ultrahigh-throughput single cell protein profiling with droplet microfluidic barcoding. *Sci Rep* 7:44447. <https://doi.org/10.1038/srep44447>
82. Fallah-Araghi A, Baret J-C, Ryckelynck M, Griffiths AD (2012) A completely in vitro ultrahigh-throughput droplet-based microfluidic screening system for protein engineering and directed evolution. *Lab Chip* 12:882–891. <https://doi.org/10.1039/C2LC21035E>
83. Joensson HN, Samuels ML, Brouzes ER, Medkova M, Uhlén M, Link DR et al (2009) Detection and analysis of low-abundance cell-surface biomarkers using enzymatic amplification in microfluidic droplets. *Angew Chem* 121:2556–2559. <https://doi.org/10.1002/anie.200804326>
84. Konry T, Smolina I, Yarmush JM, Irimia D, Yarmush ML (2011) Ultrasensitive detection of low-abundance surface-marker protein using isothermal rolling circle amplification in a microfluidic nanoliter platform. *Small* 7:395–400. <https://doi.org/10.1002/sml.201001620>
85. Giljohann DA, Mirkin CA (2009) Drivers of bdiagnostic development. *Nature* 462:461–464. <https://doi.org/10.1038/nature08605>
86. Del Ben F, Turetta M, Celetti G, Piruska A, Bulfoni M, Cesselli D et al (2016) A Method for detecting circulating tumor cells based on the measurement of single-cell metabolism in droplet-based microfluidics. *Angew Chem* 128:8723–8726. <https://doi.org/10.1002/anie.201602328>
87. Chokkalingam V, Tel J, Wimmers F, Liu X, Semenov S, Thiele J et al (2013) Probing cellular heterogeneity in cytokine-secreting immune cells using droplet-based microfluidics. *Lab Chip* 13:4740–4744. <https://doi.org/10.1039/C3LC50945A>
88. Shim J-u, Ranasinghe RT, Smith CA, Ibrahim SM, Hollfelder F, Huck WT et al (2013) Ultrarapid generation of femtoliter microfluidic droplets for single-molecule-counting immunoassays. *ACS Nano* 7:5955–5964. <https://doi.org/10.1021/nn401661d>
89. Luo C, Ma Y, Li H, Chen F, Uchiyama K, Lin JM (2013) Generation of picoliter droplets of liquid for electrospray ionization with piezoelectric inkjet. *J Mass Spectrom* 48:321–328. <https://doi.org/10.1002/jms.3159>
90. Liu W, Wang N, Lin X, Ma Y, Lin JM (2014) Interfacing microsampling droplets and mass spectrometry by paper spray ionization for online chemical monitoring of cell culture. *Anal Chem* 86:7128–7134. <https://doi.org/10.1021/ac501678q>

91. Zhang W, Li N, Koga D, Zhang Y, Zeng H, Nakajima H et al (2018) Inkjet printing based droplet generation for integrated online digital polymerase chain reaction. *Anal Chem* 90:5329–5334. <https://doi.org/10.1021/acs.analchem.8b00463>
92. Huang Q, Mao S, Khan M, Zhou L, Lin JM (2018) Dean flow assisted cell ordering system for lipid profiling in single-cells using mass spectrometry. *Chem Commun* 54:2595–2598. <https://doi.org/10.1039/C7CC09608A>

Chapter 6

Microfluidics for Single-Cell Genomics



Mashooq Khan and Jin-Ming Lin

Abstract Genomics is the systematic study of entire deoxyribonucleic acid (DNA) sequencing of an organism or virus. A single-cell DNA sequencing explores the heterogeneity among a cellular population of a biological sample and also predicts the growth and function of a living entity. However, efficient extraction of chromosomes from a single living cell requires sophisticated methods for sample preparation. Microfluidic devices offer several improvements including, effective heat transfer (enhanced the multiplication of DNA) and small volume (enabled the accurate quantification of DNA molecules) within the lysate of a single cell. However, at present, only one step such as single-cell isolation, cell lysis, or chromosome isolation from an individual cell and its amplification can be performed on-chip. Besides, microfluidics relies on external techniques for analysis of DNA. Therefore, the integration of multi-microfluidic systems is required for automated genome investigation. This chapter describes the advancement, limitations, and future prospects of microfluidic/nanofluidic for single-cell analysis.

Keywords Genomics · Single-cell · Microfluidic · DNA · Cellular heterogeneity · Cellular population

6.1 Introduction

The deoxyribonucleic acid (DNA) encodes proteins is the heritable program, which led to the development of a research field, genetics and genomics. Genomics is the systematic study of DNA, referring to elucidate the entire complement of heredity information of an organism or virus. Organisms are a bodily outcome of their genome; therefore, genomics is a significant tool to explore their growth and function. The human genome project (HGP) was launched to identify all of the approximate forty thousand genes (a distinct sequence of DNA or RNA) and

M. Khan · J.-M. Lin (✉)

Department of Chemistry, Tsinghua University, Beijing 100084, People's Republic of China
e-mail: jmlin@mail.tsinghua.edu.cn

© Springer Nature Singapore Pte Ltd. 2019
J.-M. Lin (ed.), *Microfluidics for Single-Cell Analysis*,
Integrated Analytical Systems, https://doi.org/10.1007/978-981-32-9729-6_6

determine the primary structure of 3 billion base pairs, which was a pivotal moment in life sciences [1]. Like any other great discoveries, the completion of HGP raises more questions and spurred research in previously unknown areas. Therefore, the demand for DNA sequencing increased in both academic research and clinical research. The HGP also stimulated a healthy race among the researchers, for the development of high-throughput and cost-effective sequencing strategies. Organisms are phenotypically diverse. The order of genes on a DNA carries many folds of genetic information. Therefore, after completion of the HGP, the cancer genome atlas (CGA) project was initiated to link certain genetic alteration to a specific disease. This explored an astonishing discrepancy in a similar disease of different individuals. A deep understanding of the genetic information on diseases leads to the identification of heterogeneity in cell populations within individuals. Intra-sample heterogeneity can be valuable information to note the disease progression and treatment within individuals. The study of this variation can lead us to comprehend the part of the intercellular difference in evaluation and therapy of diseases and implications for personalized drugs [2].

The genomic heterogeneity holds a significant role among populations in general and a single-cell population in particular. Finding the variation among individual cells of a population reveals its behaviors and heterogeneity. Contrary to conventional genome sequencing, which considers the mean of characteristics, the single-cell study allows the recognition of critical alteration from one cell to another of the seemingly identical cells. Single-cell genome sequencing requires several steps from tissue dissociation to DNA analysis (Fig. 6.1), and each step is a puzzle to solve. For example, a small tumor tissue contains millions of cells and each individual cell has a minute amount of genetic material making it defying to identify the variation among single cells [3]. Therefore, an ultra-efficient method is required for sample preparation and analysis of the tiny amount of genetic materials in a single cell. The resolution and precision of the analysis techniques have been improved over a few decades, which open the gate to investigate the initial ultra-low concentration materials. In this context, the comparative hybridization arrays could characterize the chromosomal variation through RNA sequencing from a tiny amount of the starting RNA of a sample. The high-resolution techniques have enabled us to recognize the occurrence of previously undetectable low-frequency traits. However, the requirement for microgram or nanogram amount of the sample, where the available starting material (DNA) is in picogram, hindered our ability to explore the cellular biochemistry. In addition, the effective isolation and processing of a sample material without contamination and sample loss sets another hurdle for analyses at a single-cell resolution. In this contribution, the microfluidic system offers a high-throughput platform to achieve single-cell analysis. Our group published a number of reviews and articles focused on microfluidic devices for single-cell sample preparation and recommended for further reading [4–6].

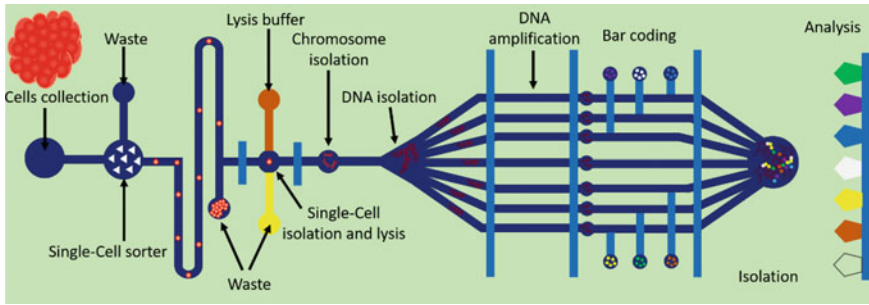


Fig. 6.1 Schematic of the microfluidic model for single-cell genomics

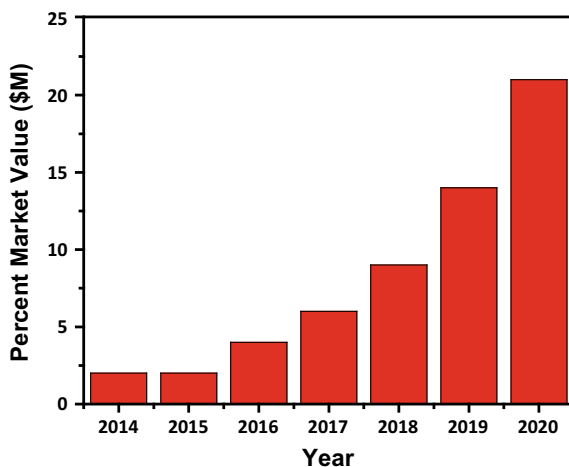
6.2 Microfluidics for Single-Cell Genomics

Gel matrices, electrophoresis, flow sorting, optical tweezers, and microfluidic-based methods have been utilized to obtain and process DNA from numerous single cells. For a method to address the limitations and to be profitably used for the analysis of single-cell genomics must be able to,

- Isolate and manipulate DNA materials in minute quantity with high precision.
- Have high resolution for effective amplification of a single molecule.
- Carry out measurement with high accuracy, because a single-cell measurement can be performed only one time.
- Generate statistically meaningful high-throughput data.
- Avoid external or in-system contamination.
- Perform automated human-interference-free processing.

The invention of microfluidics launched a new platform for point-of-care diagnostics and offered a striking way out for many hurdles in biological and chemical analyses. Microfluidics offered the transportability, automated processing, design flexibility, effective heat transfer, and high surface area per unit volume. This also enabled the assimilation of several liquid processes including sampling, sequential loading, pumping, and washing [7]. Microfluidics has shown overwhelming performance in areas other than genetic research [8] and could fit precisely to the size of an individual cell, because of the offered designed flexibility within the range of ten to hundreds of micrometer [9]. This reduced the dilution of lysate, which is a notable problem due to a tiny amount of the starting material in a single cell. Furthermore, microfluidic dimension allows a custom-made simple experimental setup for a particular analytical problem [10]. The proficient heat transfers reduced the time required for DNA amplification, and the small volume enabled precise quantification of genetic material at single-cell/single-molecule level. In comparison with conventional methods, microfluidics enhanced the compatibility of the cells and minimized the labor work [11–14]. Microfluidic devices also reduced the hazard of ex- and in-system contamination. For effective

Fig. 6.2 Market value per year of microfluidic sample preparation for single-cell genomics. *Courtesy* Web information of Yole development



quantification, the microfluidic interface is easy to couple with sensitive detection techniques, such as mass spectrometry, electrochemical detector, laser-induced fluorescence [15, 16], and others. Mass spectrometry in integration with microfluidic has been frequently practiced for single-cell analysis, because of high mass accuracy and sensitivity [17–20]. In this context, Roussel and Clerc authored a report that multiple microfluidic players researching microfluidic sample preparation techniques. They also described that microfluidic-based devices’ market is prepared to expand abruptly above \$100 M in 2020. Among them, the market growth of microfluidic devices for single-cell genomics will be a raised from 2% in 2014 to 21% in 2020 (Fig. 6.2). In this perspective, we will review the course and latitude of the microfluidic platform for single-cell genomics and address the future perspective where further improvement is needed.

6.3 Experimental Design of Single-Cell Genomics

Single-cell DNA sequencing helps us to understand the complex biological composition and function of an individual and also reveals the genetic disorder to explore a particular disease. However, to carry out genome-wide haplotyping, each single-cell genomic technique requires the isolation and processing of cells from complex body tissue. Besides, technical hurdles arise from the complex data output [21]. Therefore, to perform efficient single-cell DNA sequencing, a systematic route has to be followed as described in Sects. 6.3.1–6.3.3.

6.3.1 *Single-Cell Isolation for Genome Sequencing*

The first step is to obtain a healthy single cell from a targeted biological sample. The microfluidic platform could perform high-throughput sorting of single cells into individual partitions. The cells under investigation can be microscopically monitored and processed. As mentioned earlier the microfluidic platform minimized the dilution of sub-cellular components, which is significant for the analysis of molecules of minute concentration in a single cell [22]. Furthermore, the large surface area per unit volume ensures a uniform heat transfer and temperature control, which is critical for the multiplication of genetic materials. For example, Fluidigm C1 array (a commercial microfluidic device for single-cell isolation) [23], microwells, di-electrophoresis, droplets, valve, Brownian motion, and hydrodynamic have been utilized for high-throughput single-cell isolation and was reviewed previously in detail [4].

6.3.2 *Whole-Genome Amplification (WGA)*

Each cell of an organism divides multiple times in her life span. During the cell division, less likely but error can arise in DNA replication resulting in somatic mutations. The mutation can originate fatal diseases. Besides, the abnormalities in chromosome have been largely observed during the growth of mammalian germline [21]. DNA sequencing can give information about all kinds of somatic and germline alterations, such as deletion, insertion, substitution, structural rearrangement, and copy number variations. Moreover, single-nucleotide polymorphism-based quantification of paternal and maternal allele frequencies can give information about genetic inheritance. However, due to a tiny amount of genetic material (~ 10 picogram) in an individual cell, whole-genome amplification (WGA) is required for performing DNA sequencing [24]. Until now, on-chip polymerase chain reaction (PCR), multiple displacement amplification (MDA), a combination of PCR and MDA, and multiple annealing and looping-based amplification cycles (MALBAC) have been utilized to carry out a single-cell WGA.

6.3.2.1 *Microfluidic-Based PCR*

The PCR can generate several millions of copies of a single DNA molecule in few cycles. Typically, a single cycle of PCR has three steps: denaturation, annealing, and extension. In denaturation, the temperature of about 95 °C is applied to unzip a double-stranded DNA into two single strands of DNA (ssDNA). In annealing, the ssDNA is subjected to short single strands of complementary DNA (primer) at ~ 56 °C in the presence of polymerase enzyme. In extension, the temperature is raised to 72 °C to achieve high activity of the polymerase. From free nucleotides, in

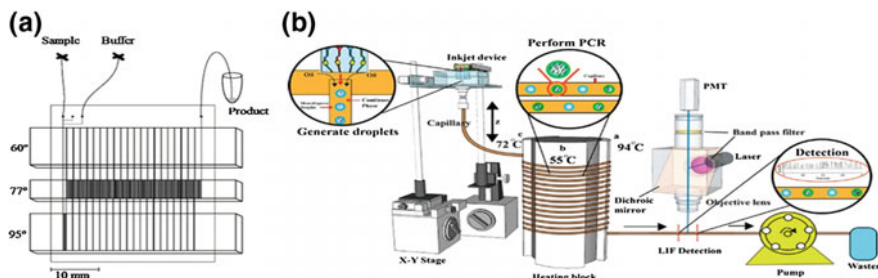


Fig. 6.3 **a** Microfluidic and **b** inject droplet models of PCR. Reprinted with permission from Ref. [25]. Copyright 1998 Science Publishing and [26] Copyright 2018 American Chemical Society, respectively

solution, the active polymerase synthesizes a second complementary ssDNA, and thus, a copy of the initial DNA is formed. By repeating the cycles, an exponential increase in DNA copies are obtained. As the heating and cooling cycles are involving in PCR, miniaturization of the system could largely reduce the analysis time. Therefore, among the research community, microfluidic-based PCR devices gain considerable attention, due to rapid and uniform heat transfer [25]. In this system, a sample of $\sim 10 \mu\text{L}$ containing DNA has flowed through a coiled microchannel. The sample passed through the loops of the channel in three temperature regions for several cycles within tens of seconds (Fig. 6.3a). Our group also developed a droplet-based digital PCR (dPCR) platform [26]. In this system, the droplets were generated through an ink-jet. The droplets contained DNA and PCR liquid was passed through a channel of fused silica. The channel was coiled around a thermal cycler of 36 cycles of different temperature zones. A laser-induced fluorescence detector (LIFD) was focused at the downstream of the capillary to count droplets contained DNA (positive counting) and without DNA (negative counting) (Fig. 6.3b). As previously reviewed in detail [27], numerous microfluidic-based PCR platforms for multiplication of nucleic acid have been developed and recommended for further reading.

6.3.2.2 Microfluidic-Based MDA

The understanding of genomic heterogeneity requires the sequencing of genomic materials from large numbers of single cells. The WGA usually cope with challenges of contamination, multiplication bias, and poor monitoring. To overcome these limitations, the MDA technique for single-cell WGA was applied. Figure 6.4 shows the droplet-based MDA [28]. Firstly, a cell or nucleus was introduced into droplets deposited on a substrate. Then, to each droplet, the lysis buffer was added. Subsequently, each droplet was covered with oil and incubated at 65°C for 10 min on a heating plate. Afterward, the oil was washed out from the droplets. REPLI-g-Single-Cell-Master-Mix supplemented with 0.1% of Tween 20 surfactant

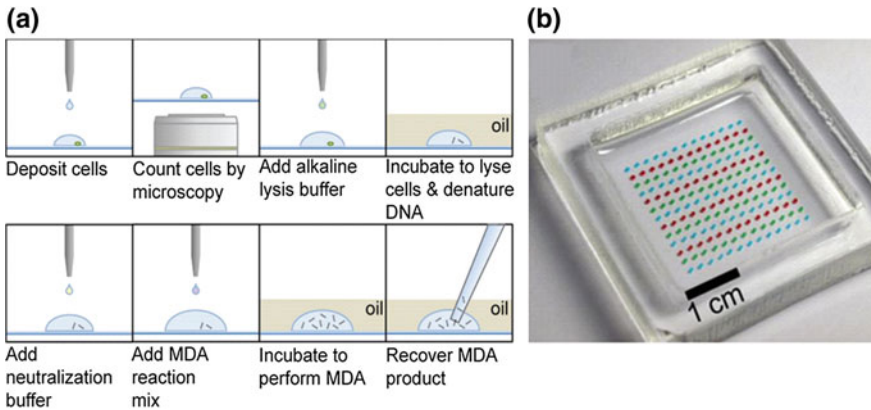


Fig. 6.4 Microdroplet model for multiple displacement amplification. Reprinted with permission from Ref. [28]. Copyright 2016 the Proceeding of the National Academy of Sciences

and 5% glycerol was added to each droplet and was again covered with oil. The reaction was incubated at 30 °C for a specified time, followed by the termination of amplification at 65 °C for 15 min. The oil was then removed and an inert dye was added to visualize each reaction, which facilitated manual extraction. The array was re-covered with oil, and the droplets were pipetted out in a 96-well plate-containing EDTA buffer to assess the yield.

The introduction of MDA largely minimized the predisposition in amplification, contamination, generation of non-desirable product, and costs [29]. However, due to the processing of a small number of single cells and manual selection through microscopy, it was hard to achieve the utmost robustness, performance, and scalability. However, the MDA suffers from a non-desirable multiplication of genetic materials when a sub-nanogram of starting DNA was used.

6.3.2.3 Microfluidic-Based MALBAC

Typically, the WGA product contaminates from exogenous and pre-existed DNA. Microfluidic-based PCR [30, 31] and MDA [32] intrinsically reduced these contaminations. In order to further improve the WGA, a microfluidic-based MALBAC device was designed [33]. This performed WGA from eight single cells introduced in eight parallel channels (each channel held a single cell) (Fig. 6.5). The collected cells were lysed within the channel, and the obtained genetic material was subjected to a two-step process: pre-amplification and PCR amplification. The WGA can be achieved in 4 h. The MALBAC efficiently reduced the contamination and cost, due to high reproducibility and accurate identification of copy number variations. Besides, it required minimum of single-cell handling skills. Moreover, MALBAC offers easy scalability and integration for high-throughput product yield and analysis.

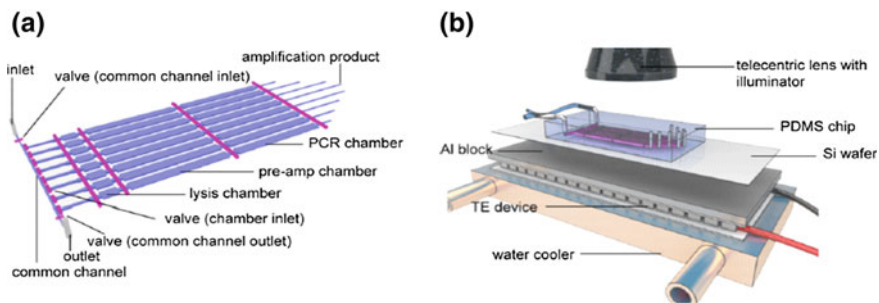


Fig. 6.5 Microfluidic device for multiple annealing and looping-based amplification cycles (MALBAC). **a** Schematic of MALBAC and **b** the MALBAC device placed on a heating cycler. Reprinted with permission from Ref. [31]. Copyright 2014 American Chemical Society

6.3.3 Microfluidic-Based Genome Sequencing and Analysis

After obtaining the WGA product for analysis, the genome sequence analysis can be performed using the following steps.

- Obtain the file for sequence reads.
- Examine the quality of reads and trim the bases of poor-quality bases.
- Trim the adaptor sequences remained at the end of reads.
- Avoid flawed mapping by neglecting the reads of too-short length.
- Remove the PCR duplicates.
- Map the reads data to a reference genome from an online database, such as the UCSC genome browser [34, 35]. This is a key step for genomic analysis.
- The reads data those map to more than a single locus should be discarded or counted with reduced uniform weight for each locus in such a way that the weights of each read add up to one.
- The product is ready for subsequent processing, which depends on the type of analysis.

The number of copies of DNA at a location in a genome is termed as DNA copy number. The normal human autosomal chromosomes copy number is two. The gains or losses of copy number are common in chromosomal abnormalities, and their study is significant for identifying and validating the cancer genes. The basic principles for determining the copy number variations (CNVs) are first to alleviate the local variability in reads coverage by segmenting the genome into bins. Then, the number of reads within each bin for GC-bias ($G = \text{guanine}$, $C = \text{cytosine}$) CNV breakpoints can be determined based on a comparison of the change in reads number between adjacent bins to a background model. For example, Venkatraman and Olshen [36] developed the circular binary segmentation algorithm to divide the genome into regions of equal copy number. To obtain the corresponding P -values, the algorithm tests for change points using a maximal t -statistic with a permutation reference distribution. The number of computations required for the maximal test

statistic is $O(N^2)$, where N is the number of markers. This makes the full permutation approach computationally prohibitive for the newer arrays that contain tens of thousands of markers and highlights the need for a faster algorithm. Similarly, numerous tools such as hidden Markov models (HMMs) have been developed to analyze CNV. The QuantiSNP, PennCNV, and GenoCN utilize HMMs with six copy number states but vary in how transition and emission probabilities are calculated. Performance of these CNV detection algorithms has been shown to be variable between both genotyping platforms and data sets [37].

The Bayesian framework can be used for SNP detection. Herein, the genotype with the highest posterior probability is emitted for each locus, if its log odds ratio exceeds a defined threshold. A comparative analysis of existing software tools for SNP calling from next-generation sequencing data was comprehensively reviewed previously and is recommended for further reading [38]. An advanced method for the detection of structural rearrangements utilizes paired-end read information by creating a bona fide list of discordantly mapped read pairs and identifies candidate rearrangements supported by more than one pair from this list [39]. Although correction of GC bias is possible [40], other confounding factors such as allelic dropout or preferential allelic amplification cannot be easily corrected for and may introduce false positives in SNP and CNV detection. Random sequencing errors represent another source of uncertainty for SNP detection. To increase confidence, repeated detection of a given anomaly in more than a single daughter of the same cell is required [41]. Finally, another confounding factor can be the cell-cycle phase since replication domains of cells in S phase can be mistaken as genuine structural aberrations. This problem can be avoided by using only nuclei in G1 or G2/M phase. Limiting the analysis to the G2/M phase comes with the additional advantage of having duplicated material after replication of the entire genome.

6.4 Microfluidic Platforms for Single-Cell Genomics

The process of how genetic material can be obtained and process from a single-cell or a cellular population has been discussed. In order to perform these operations, various designs of microfluidic platforms have been utilized. In this contribution, the commonly utilized microfluidic-based strategies for single-cell DNA sequencing are reviewed in the following sections.

6.4.1 Valves

The microfluidic valve system was the pioneering work for genome profiling of single cells. Fan and coworker [42] reported a direct deterministic phasing (DDP) approach using a microfluidic device consisting of cell sorting, chromosome release, chromosome partitioning, amplification, and product retrieval regions

(Fig. 6.6a). A single cell (in metaphase) from cell suspension was microscopically identified and trapped in the sorting region. The metaphase chromosomes were then obtained and separated in 48 partitions. The chromosomes were amplified in these compartments. The WGA product was separately collected from each segment, and the SNP measurement was performed. This design has the limitations of processing a single cell at a time and manual selection of the phase cell through microscopy. However, a simple engineering solution is required to integrate computer vision for phase cell selection and simultaneous multiple cells' processing and therefore has potential application for single-cell DNA sequencing, personal genomics, and statistical genetics. A similar microfluidic system was used to profile de novo and recombination map from 91 single sperm cells of an individual [29]. Their results were consistent with population-wide at a low resolution, while differences were observed from pedigree data at a high resolution.

There is a growing curiosity to profile the single-cell genetic signature of cancer and other diseases to identify causal and regulatory mutations. These diseases are caused by the origination of genetic mutation in a somatic cell, which creates a diverse clonal population. The proliferation of mutated cells forms a complex polyclonal network, and therefore, the genetic sequencing of these low abundant populations cannot be interrogated. Thus, useful statistical information can only be

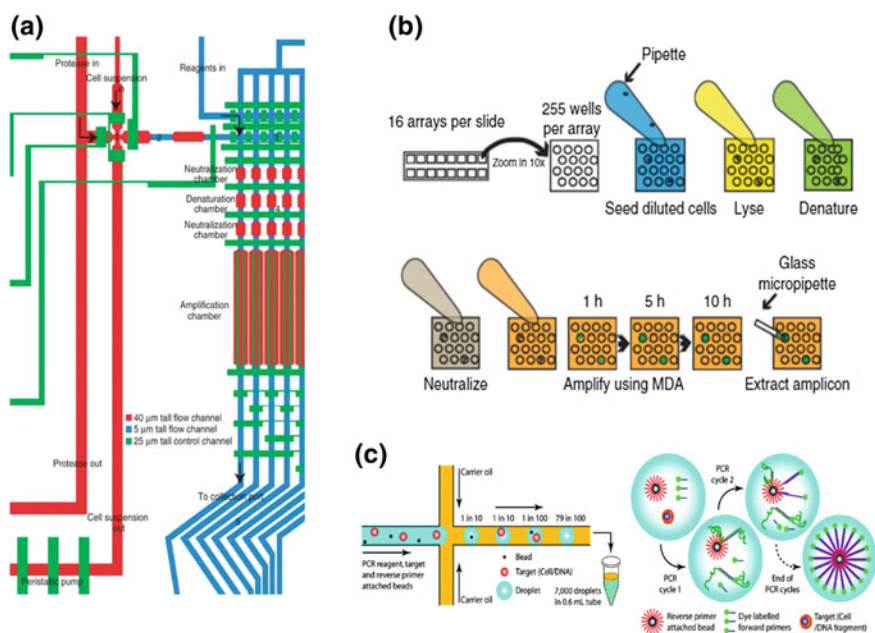


Fig. 6.6 Microfluidic platforms for single-cell genomics, **a** valve, republished with permission from Ref. [40], Copyright 2011 Nature Publishing, **b** microwells, reprinted with permission from Ref. [46], Copyright 2013 Nature Publishing, and **c** droplets, reprinted with permission from Ref. [51], Copyright 2013 American Chemical Society

obtained from the manipulation of genetic material individually from each single cell. The initial success of microfluidic valve-based single-cell genomics inspired the invention of Fluidigm C1 AutoPrep System. This system can automatically capture single cells and has the ability to simultaneously process 96 single cells. This system was utilized in a number of studies for the WGA of single tumor cells. For example, Szulwach et al. [43] used it for sequencing of GM12752 and CRL2339 cells. The cells were captured and lysed, and then MDA was performed to obtain the WGA product from 96 single cells. They obtained $\sim 150\text{--}250$ ng of genetic material from a single cell in the processing time of ~ 8 h. A large amount of DNA obtained enabled the targeted whole-exome and whole-genome sequencing (WGS) of each cell. The Fluidigm C1 platform was frequently utilized for single-cell sequencing [44, 45]. However, the fixed chip architecture of this system limited the selection of cells to a certain size window.

6.4.2 *Micro-/Nanowells*

Micro-/nanowell-based isolation of a single cell is another potential technique for the profiling of genomic material. For example, Goldstein and coworker [46] utilized ICELL8 to perform the parallel single-cell genes sequencing. The ICELL8 is a 41 mm^2 aluminum alloy-made square microchip containing about 5184 (72×72) wells. Each well contained pre-printed oligonucleotides and held 150 nL liquid. Each oligonucleotide includes an 11 base pair-specific primer oligo-(dT₃₀) for cell barcoding and a molecular identifier (UMI, 10 bp). The barcode and UMI recognize the generated complementary DNA and mRNA molecules, respectively, from each individual cell. Integrated imaging software was utilized to automatically select wells containing a single cell. They fluorescently labeled the cells with live/dead stain prior to dispensing into wells. The cells were then lysed using freeze-thaw, and complementary DNA from numerous cells were collected in a single tube. The product was then purified and amplified. They were able to discriminate different types of cells in a cellular population.

The precision medicine for each cancer patient required the accurate representation of genomic future of his/her tumor. However, the access to tumor tissue is difficult and yield as well as the purity of a biopsy sample is low. These limitations can be overcome by obtaining and amplification of DNA from circulating tumor cells (CTCs). Thus, the genomic variant determination in CTCs can provide a routine analysis of metastatic colonization. Therefore, Lohr et al. [47] obtain a single CTC from pre-peripheral in nanowells, and a cell with an epithelial cell adhesion expression was collected through a micropipette. The whole-exome and WGA sequencing were performed, which allowed the investigation of mutational patterns and lineage assignment of various CTC. Their findings showed that CTC sequencing is scalable to map the genetic material of an individual with cancer. Their finding was also critical to evaluate the genetic state of metastasis and cancer dissemination, the evolution of the tumor, and development of precision medicine.

For high-quality genome sequencing, it is necessary to obtain a relatively large amount of sequence data to avoid amplification bias. The amplification bias arises from the repetition of priming on a favorable location during the WGA. Therefore, the bias can be minimized by controlling the reaction to achieve enough amplification and reduce the iterations of repetition priming. Moreover, decreasing the reaction volume can significantly increase the concentration of the template genome, which can improve amplification uniformity. Therefore, Gole et al. [48] performed the genetic amplification of single cells in thousands of nanoliter reactors using a microwell displacement amplification system (MIDAS) (Fig. 6.6b). Each reactor was capable to carry a reaction in a volume of 12 nL (the smallest volume implemented until now). The MIDAS was coupled with a low-input library construction method, and a highly uniform coverage in the genomes of both microbial and mammalian cells was achieved.

Compared to the valve, the nanowells have higher throughput. Nanowells enabled the selection of the desired cell and controlled on-chip reaction. However, at present only a small number of cells can be used for follow-up profiling. Future work in nanowell-based genome sequencing requires automation and scalability.

6.4.3 Droplets

The monodisperse droplet of femto-liter [49] and pico-liter [50, 51] volume can be produced from two immiscible liquids in microfluidics. Each droplet can be used as a compartment to hold a single cell [52]. The droplets that contained single cells can be placed in conventional petri dishes, vials, and well plates for further processing. Mathies et al. introduced droplet to perform single-cell DNA mapping [53]. They reported a single copy genetic amplification (SSGA) technique, which yields a high-throughput multiplied DNA product from a single template copy in each droplet. The SCGA rapidly generated monodisperse 2-5 nL volume droplets in oil at the cross-junction (Fig. 6.6c). Each droplet holds PCR reagent, in which a target cell or DNA was captured. Thousands of droplets comprise PCR reagents, one cell and one primer-laden bead were collected with 1% efficiency in a reaction tube, and WGA was performed. Since then, the droplet-based genomics gone beyond performing amplification and newer studies enabled droplets platform for detection. To improve the single-cell WGA quality, Fu et al. [54] extracted genetic material from a single cell and fragmented them into many droplets instead of locating the whole genetic material in one droplet. Then, they generated MDA libraries of a single cell in droplets and were able to control amplification, which prevented the domination of a specific sequence.

Most of the droplet-based genomics suffered from challenges of efficient cell lysis, the ineffective release of chromatin DNA, significant amplification in a high concentration of unrefined lysate. Therefore, DNA genotyping of eukaryotic cells has not been demonstrated in droplets microfluidic. To explore the genetic diversity of a tumor population, Pellegrino et al. [55] used a microfluidic approach to label

the WGA product from thousands of individually encapsulated cells in droplets. The label enables to identify and collect the genetic material of cells from sequencing data of the next generation. Acute myeloid leukemia (AML) cells were sequenced from two patients, and up to sixty-two disease-related loci from more than sixteen thousand cells were genotyped. This approach was able to selectively recognize cells concealing mutation from pathogen and unveiled a complicated clonal evolution of AML cancer, which was not noticeable through bulk sequencing. They anticipated that their method could ease the routine investigation of AML heterogeneity, which could lead to better recognition and cure of tumor.

The existing methods to generate DNA sequences utilizing DNA oligonucleotides assembly are expensive and laborious. Therefore, demands for custom DNA manufacture raised for application in synthetic biology. Khilko et al. [56] developed a gene assembly protocol through a Mondrian digital microfluidic device. They performed enzyme correction, optimized Gibson assembly, and carried out PCR in a single reaction to assemble twelve oligonucleotides into a double-stranded DNA of 339 base pair sequence, encrypting segment of hemagglutinin gene of influenza virus. The volume of the reaction was further minimized to 0.6–1.2 μL . The microfluidic assembly approaches were effective and had error frequency of ~ 4 errors/kb, with errors originated from the prototype oligonucleotide production. In comparison with conventional benchtop method, additional magnesium chloride PEG 8000 and Phusion polymerase were required for the optimization of PCR and to achieve smooth assembly multiplication as well as flawless products. The error frequency was minimized to 1.8 errors/kb, after one cycle of error correction.

6.4.4 Hydrogel Droplets

Microfluidic-based hydrogel droplet method is an ideal platform to overcome the challenges of parallel handling of considerable amounts of cells, loss of starting material, and augmentation bias. Besides, hydrogel droplets provide a rigid 3D network, which reserved the DNA from the lysed cells and allows the penetration of chemicals for amplification [57]. Novak and coworker [58] utilized agarose gel to encapsulate single cells and primer-functionalized beads. The cells in the agarose gel droplet were subjected to lysis for the extraction of genetic material. Due to the small pore size of gel droplets, the extracted DNA reserved inside. The genetic material was treated with the PCR solution, and the gel droplets were re-emulsified for an extensive parallel amplification and analysis. The approach enabled the on-chip capture and lysis of cells as well as amplification of genetic materials and offered a robust podium for single-cell genome sequencing. Bigdeli et al. [59] sprayed the cell suspension into alginate droplets for encapsulation of single cells. The encapsulated cells were then lysed inside the hydrogel droplets, and a two-step WGA was performed. The WGA product of high molecular weight was reserved inside the gel beads, which minimized the contamination. The DNA from every

single bead was extracted for further processing. The integration of MALBAC with this system could improve the quality of this approach for high and more uniform genome coverage.

Each human cell exhibits a diploid genome containing a copy of both paternal and maternal chromosomes. The origin, structure, and order of genes and their variant are significant for the understanding of human genetic variation. That the adjacent regions of a genomic variation are specific to a particular homolog is an essential requirement for categorization of the whole genetic variation. Zheng et al. [60] used microfluidic-base linked-read sequencing technology to investigate the haplotype of a germline from nanogram (ng) of the starting DNA. They allocated ~ 300 genomic equivalents or 1 ng of high molecular weight DNA across hundred thousand of gel droplets. The genetic material was barcoded inside the droplets and subjected to random priming and multiplication. The labeled DNA was extracted from the droplets, and then modified libraries were prepared. Subsequently, the libraries were subjected to standard Illumina short-read sequencing. This method minimized the chances of coincidental overlap labeling and improved overall phasing performance.

6.4.5 Emulsion

With the small amount and precious starting material demand a robust method for performing WGA. Fu and coworker [54] developed an emulsion-based WGA method, where the individual human umbilical vein endothelial cell (HUVEC) cells were lysed, and the released genetic materials was unzipped upon heating to yield ssDNA. The ssDNA was then encapsulated in aqueous picoliter volume droplets at 4 °C to avoid the start of amplification. After inhibition of the enzyme through heat and de-emulsification, the amplification uniformity was accomplished in the aqueous solution. The WGA products were used to assemble sequencing libraries. This approach reduced the multiplication bias while keeping high precision of duplication.

6.5 Summary and Future Directions

The cells of a multi-cellular organism originated from programmable division and proliferation of a single zygote. Then, these encoded cells regulate the functions and characteristics of an organism. Any mutation in the codes of single cell results in fetal diseases and dysfunction [61]. Besides, each type of cell carries distinct epigenetic features; therefore, consideration of epigenetic regulations is critical for the development of disease therapy. In the chapter, the micro-/nanofluidic-based techniques were discussed for single-cell genomics. The single-cell isolation strategies can be coupled with lysis method to extract the intact chromosomes and

then the segregation of chromosomes into separate chambers of small volume [62] for multiplication and sequencing. Single-cell genome sequencing is challenging due to the tiny amount of the starting genetic material. Therefore, whole-genome amplification (WGA) techniques such as on-chip PCR, dPCR ($d = \text{digital}$), MDA, and MALBAC was developed. These methods have the benefits of uniform heat transfer, due to a small volume of the reaction materials. Later on, the PCR was provided with an underneath thin-heating-film [63] and infrared heater [64] to replace thermoelectric devices, which reduced the number of heating cycles. The integration of microwells, valve, and droplets achieved on-chip WGA in a closed system and reduced biasness and contamination. Owing to the hurdles of parallel liquid processing and microfabrication, the largest platform of only 100 reactions chamber is available. The droplet system required a continuous supply of reagents for parallel genome processing. The WGA methods have considerably established, but these could not explore the haplotype arrangement of homologous chromosomes. Besides, only one step at a time can be performed on these devices. In addition, these systems required external methods for monitoring, quantification of genetic product, and analysis. Thus, the on-chip whole-genome human-interference-free automated sequencing will be a major puzzle to solve.

References

1. International Human Genome Sequencing C, Lander ES, Linton LM, Birren B, Nusbaum C, Zody MC, Baldwin J, Devon K, Dewar K, Doyle M, FitzHugh W, Funke R, Gage D, Harris K, Heaford A, Howland J, Kann L, Lehoczky J, LeVine R, McEwan P, McKernan K, Meldrim J, Mesirov JP, Miranda C, Morris W, Naylor J, Raymond C, Rosetti M, Santos R, Sheridan A, Sougnez C, Stange-Thomann N, Stojanovic N, Subramanian A, Wyman D, Rogers J, Sulston J, Ainscough R, Beck S, Bentley D, Burton J, Clee C, Carter N, Coulson A, Deadman R, Deloukas P, Dunham A, Dunham I, Durbin R, French L, Grafham D, Gregory S, Hubbard T, Humphray S, Hunt A, Jones M, Lloyd C, McMurray A, Matthews L, Mercer S, Milne S, Mullikin JC, Mungall A, Plumb R, Ross M, Shownkeen R, Sims S, Waterston RH, Wilson RK, Hillier LW, McPherson JD, Marra MA, Mardis ER, Fulton LA, Chinwalla AT, Pepin KH, Gish WR, Chissoe SL, Wendl MC, Delehaunty KD, Miner TL, Delehaunty A, Kramer JB, Cook LL, Fulton RS, Johnson DL, Minx PJ, Clifton SW, Hawkins T, Branscomb E, Predki P, Richardson P, Wenning S, Slezak T, Doggett N, Cheng J-F, Olsen A, Lucas S, Elkin C, Uberbacher E, Frazier M, Gibbs RA, Muzny DM, Scherer SE, Bouck JB, Sodergren EJ, Worley KC, Rives CM, Gorrell JH, Metzker ML, Naylor SL, Kucherlapati RS, Nelson DL, Weinstock GM, Sakaki Y, Fujiyama A, Hattori M, Yada T, Toyoda A, Itoh T, Kawagoe C, Watanabe H, Totoki Y, Taylor T, Weissenbach J, Heilig R, Saurin W, Artiguenave F, Brottier P, Bruls T, Pelletier E, Robert C, Wincker P, Rosenthal A, Platzer M, Nyakatura G, Taudien S, Rump A, Smith DR, Doucette-Stamm L, Rubenfield M, Weinstock K, Lee HM, Dubois J, Yang H, Yu J, Wang J, Huang G, Gu J, Hood L, Rowen L, Madan A, Qin S, Davis RW, Federspiel NA, Abola AP, Proctor MJ, Roe BA, Chen F, Pan H, Ramser J, Lehrach H, Reinhardt R, McCombie WR, de la Bastide M, Dedhia N, Blöcker H, Hornischer K, Nordsiek G, Agarwala R, Aravind L, Bailey JA, Bateman A, Batzoglou S, Birney E, Bork P, Brown DG, Burge CB, Cerutti L, Chen H-C, Church D, Clamp M, Copley RR, Doerks T, Eddy SR, Eichler EE, Furey TS, Galagan J, Gilbert JGR, Harmon C, Hayashizaki Y, Haussler D, Hermjakob H, Hokamp K, Jang W,

- Johnson LS, Jones TA, Kasif S, Kasprzyk A, Kennedy S, Kent WJ, Kitts P, Koonin EV, Korf I, Kulp D, Lancet D, Lowe TM, McLysaght A, Mikkelsen T, Moran JV, Mulder N, Pollara VJ, Ponting CP, Schuler G, Schultz J, Slater G, Smit AFA, Stupka E, Szustakowski J, Thierry-Mieg D, Thierry-Mieg J, Wagner L, Wallis J, Wheeler R, Williams A, Wolf YI, Wolfe KH, Yang S-P, Yeh R-F, Collins F, Guyer MS, Peterson J, Felsenfeld A, Wetterstrand KA, Myers RM, Schmutz J, Dickson M, Grimwood J, Cox DR, Olson MV, Kaul R, Raymond C, Shimizu N, Kawasaki K, Minoshima S, Evans GA, Athanasiou M, Schultz R, Patrinos A, Morgan MJ (2001) Initial sequencing and analysis of the human genome. *Nature* 409:860. <https://doi.org/10.1038/35057062>
- Zhang J, Späth SS, Marjani SL, Zhang W, Pan X (2018) Characterization of cancer genomic heterogeneity by next-generation sequencing advances precision medicine in cancer treatment. *Prec Clin Med* 1(1):29–48. <https://doi.org/10.1093/pcmedi/pby007>
 - Gawad C, Koh W, Quake SR (2016) Single-cell genome sequencing: current state of the science. *Nat Rev Genet* 17:175. <https://doi.org/10.1038/nrg.2015.16>
 - Khan M, Mao S, Li W, Lin JM (2018) Microfluidic devices in the fast-growing domain of single-cell analysis. *Chem Eur J* 24(58):15398–15420. <https://doi.org/10.1002/chem.201800305>
 - Huang Q, Mao S, Khan M, Zhou L, Lin JM (2018) Dean flow assisted cell ordering system for lipid profiling in single-cells using mass spectrometry. *Chem Comm* 54(21):2595–2598. <https://doi.org/10.1039/C7CC09608A>
 - Huang Q, Mao S, Khan M, Lin JM (2019) Single-cell assay on microfluidic devices. *Analyst* 144(3):808–823. <https://doi.org/10.1039/C8AN01079J>
 - Khan M, Park S-Y (2014) General liquid-crystal droplets produced by microfluidics for urea detection. *Sens Actuator B-Chem* 202:516–522. <https://doi.org/10.1016/j.snb.2014.05.115>
 - Ros A, Grief D (2008) In: Anselmetti D (ed) *Single cell analysis technologies and applications*. Wiley-VCH, pp 91–108
 - Wu J, Chen Q, Liu W, Lin J-M (2013) A simple and versatile microfluidic cell density gradient generator for quantum dot cytotoxicity assay. *Lab Chip* 13(10):1948–1954. <https://doi.org/10.1039/C3LC00041A>
 - Sung WC, Makamba H, Chen SH (2005) Chip-based microfluidic devices coupled with electrospray ionization-mass spectrometry. *Electrophoresis* 26(9):1783–1791. <https://doi.org/10.1002/elps.200410346>
 - Gijis MAM, Lacharme F, Lehmann U (2010) Microfluidic applications of magnetic particles for biological analysis and catalysis. *Chem Rev* 110(3):1518–1563. <https://doi.org/10.1021/cr9001929>
 - Jiang H, Weng X, Li D (2011) Microfluidic whole-blood immunoassays. *Microfluid Nanofluid* 10(5):941–964. <https://doi.org/10.1007/s10404-010-0718-9>
 - Jeon S, Kim US, Jeon W, Shin CB, Hong S, Choi I, Lee S, Yi J (2009) Fabrication of multicomponent protein microarrays with microfluidic devices of poly(dimethylsiloxane). *Macromol Res* 17(3):192–196. <https://doi.org/10.1007/bf03218678>
 - Choi C-H, Jung J-H, Hwang T-S, Lee C-S (2009) In situ microfluidic synthesis of monodisperse PEG microspheres. *Macromol Res* 17(3):163–167. <https://doi.org/10.1007/bf03218673>
 - He X, Chen Q, Zhang Y, Lin JM (2014) Recent advances in microchip-mass spectrometry for biological analysis. *TrAC-Trends Anal Chem* 53:84–97. <https://doi.org/10.1016/j.trac.2013.09.013>
 - Jie M, Mao S, Li H, Lin JM (2017) Multi-channel microfluidic chip-mass spectrometry platform for cell analysis. *Chin Chem Lett* 28(8):1625–1630. <https://doi.org/10.1016/j.ccl.2017.05.024>
 - Mao S, Zhang J, Li H, Lin JM (2013) Strategy for signaling molecule detection by using an integrated microfluidic device coupled with mass spectrometry to study cell-to-cell communication. *Anal Chem* 85(2):868–876. <https://doi.org/10.1021/ac303164b>
 - Lin L, Lin X, Lin L, Feng Q, Kitamori T, Lin JM, Sun J (2017) Integrated microfluidic platform with multiple functions to probe tumor–endothelial cell interaction. *Anal Chem* 89(18):10037–10044. <https://doi.org/10.1021/acs.analchem.7b02593>

19. Liu W, Lin JM (2016) Online monitoring of lactate efflux by multi-channel microfluidic chip-mass spectrometry for rapid drug evaluation. *ACS Sens* 1(4):344–347. <https://doi.org/10.1021/acssensors.5b00221>
20. Gao D, Liu H, Lin JM, Wang Y, Jiang Y (2013) Characterization of drug permeability in Caco-2 monolayers by mass spectrometry on a membrane-based microfluidic device. *Lab Chip* 13(5):978–985. <https://doi.org/10.1039/C2LC41215B>
21. Grün D, van Oudenaarden A (2015) Design and analysis of single-cell sequencing experiments. *Cell* 163(4):799–810. <https://doi.org/10.1016/j.cell.2015.10.039>
22. Livesey FJ (2003) Strategies for microarray analysis of limiting amounts of RNA. *Brief Func Genomics Proteomics* 2(1):31–36
23. Hosis S, Murthy SK, Koppes AN (2016) Microfluidic sample preparation for single cell analysis. *Anal Chem* 88(1):354–380. <https://doi.org/10.1021/acs.analchem.5b04077>
24. Cheung VG, Nelson SF (1996) Whole genome amplification using a degenerate oligonucleotide primer allows hundreds of genotypes to be performed on less than one nanogram of genomic DNA. *Proc Natl Acad Sci* 93(25):14676–14679. <https://doi.org/10.1073/pnas.93.25.14676>
25. Kopp MU, Mello AJd, Manz A (1998) Chemical amplification: continuous-flow PCR on a chip. *Science* 280:1046–1048. <https://doi.org/10.1126/science.280.5366.1046>
26. Zhang W, Li N, Koga D, Zhang Y, Zeng H, Nakajima H, Lin JM, Uchiyama K (2018) Inkjet printing based droplet generation for integrated online digital polymerase chain reaction. *Anal Chem* 90:5329–5334. <https://doi.org/10.1021/acs.analchem.8b00463>
27. Ahrberg CD, Manz A, Chung BG (2016) Polymerase chain reaction in microfluidic devices. *Lab Chip* 16(20):3866–3884. <https://doi.org/10.1039/C6LC00984K>
28. Leung K, Klaus A, Lin BK, Laks E, Biele J, Lai D, Bashashati A, Huang Y-F, Aniba R, Moksa M, Steif A, Mes-Masson A-M, Hirst M, Shah SP, Aparicio S, Hansen CL (2016) Robust high-performance nanoliter-volume single-cell multiple displacement amplification on planar substrates. *Proc Natl Acad Sci* 113(30):8484–8489. <https://doi.org/10.1073/pnas.1520964113>
29. Wang J, Fan HC, Behr B, Quake SR (2012) Genome-wide single-cell analysis of recombination activity and de novo mutation rates in human sperm. *Cell* 150(2):402–412. <https://doi.org/10.1016/j.cell.2012.06.030>
30. Marcus JS, Anderson WF, Quake SR (2006) Parallel picoliter RT-PCR assays using microfluidics. *Anal Chem* 78(3):956–958. <https://doi.org/10.1021/ac0513865>
31. White AK, VanInsberghe M, Petriv OL, Hamidi M, Sikorski D, Marra MA, Piret J, Aparicio S, Hansen CL (2011) High-throughput microfluidic single-cell RT-qPCR. *Proc Natl Acad Sci* 108(34):13999–14004. <https://doi.org/10.1073/pnas.1019446108>
32. Marcy Y, Ishoey T, Lasken RS, Stockwell TB, Walenz BP, Halpern AL, Beeson KY, Goldberg SMD, Quake SR (2007) Nanoliter reactors improve multiple displacement amplification of genomes from single cells. *PLoS Genet* 3(9):e155. <https://doi.org/10.1371/journal.pgen.0030155>
33. Yu Z, Lu S, Huang Y (2014) Microfluidic whole genome amplification device for single cell sequencing. *Anal Chem* 86(19):9386–9390. <https://doi.org/10.1021/ac5032176>
34. Meyer LR, Zweig AS, Hinrichs AS, Karolchik D, Kuhn RM, Wong M, Sloan CA, Rosenbloom KR, Roe G, Rhead B, Raney BJ, Pohl A, Malladi VS, Li CH, Lee BT, Learned K, Kirkup V, Hsu F, Heitner S, Harte RA, Haeussler M, Guruvadoo L, Goldman M, Giardine BM, Fujita PA, Dreszer TR, Diekhans M, Cline MS, Clawson H, Barber GP, Haussler D, Kent WJ (2013) The UCSC genome browser database: extensions and updates 2013. *Nucl Acids Res* 41(D1):D64–D69. <https://doi.org/10.1093/nar/gks1048>
35. Cunningham F, Amode MR, Barrell D, Beal K, Billis K, Brent S, Carvalho-Silva D, Clapham P, Coates G, Fitzgerald S, Gil L, Girón CG, Gordon L, Hourlier T, Hunt SE, Janacek SH, Johnson N, Juettemann T, Kähäri AK, Keenan S, Martin FJ, Maurel T, McLaren W, Murphy DN, Nag R, Overduin B, Parker A, Patricio M, Perry E, Pignatelli M, Riat HS, Sheppard D, Taylor K, Thormann A, Vullo A, Wilder SP, Zadissa A, Aken BL, Birney E, Harrow J, Kinsella R, Muffato M, Ruffier M, Ruffier M, Searle SMJ, Spudich G, Trevanion SJ,

- Yates A, Zerbino DR, Flicek P (2015) Ensembl 2015. *Nucl Acids Res* 43(D1):D662–D669. <https://doi.org/10.1093/nar/gku1010>
36. Venkatraman ES, Olshen AB (2007) A faster circular binary segmentation algorithm for the analysis of array CGH data. *Bioinformatics* 23(6):657–663. <https://doi.org/10.1093/bioinformatics/btl646>
 37. Seiser EL, Innocenti F (2015) Hidden markov model-based CNV detection algorithms for illumina genotyping microarrays. *Cancer inform* 13(Suppl 7):77–83. <https://doi.org/10.4137/CIN.S16345>
 38. Nielsen R, Paul JS, Albrechtsen A, Song YS (2011) Genotype and SNP calling from next-generation sequencing data. *Nat Rev Genet* 12:443. <https://doi.org/10.1038/nrg2986>
 39. Voet T, Kumar P, Van Loo P, Cooke SL, Marshall J, Lin M-L, Zamani Esteki M, Van der Aa N, Mateiu L, McBride DJ, Bignell GR, McLaren S, Teague J, Butler A, Raine K, Stebbings LA, Quail MA, D’Hooghe T, Moreau Y, Futreal PA, Stratton MR, Vermeesch JR, Campbell PJ (2013) Single-cell paired-end genome sequencing reveals structural variation per cell cycle. *Nucl Acids Res* 41(12):6119–6138. <https://doi.org/10.1093/nar/gkt345>
 40. Baslan T, Kendall J, Rodgers L, Cox H, Riggs M, Stepansky A, Troge J, Ravi K, Esposito D, Lakshmi B, Wigler M, Navin N, Hicks J (2012) Genome-wide copy number analysis of single cells. *Nat Protoc* 7:1024. <https://doi.org/10.1038/nprot.2012.039>
 41. Zong C, Lu S, Chapman AR, Xie XS (2012) Genome-wide detection of single-nucleotide and copy-number variations of a single human cell. *Science* 338(6114):1622–1626. <https://doi.org/10.1126/science.1229164>
 42. Fan HC, Wang J, Potanina A, Quake SR (2010) Whole-genome molecular haplotyping of single cells. *Nat Biotech* 29:51. <https://doi.org/10.1038/nbt.1739>
 43. Szulwach KE, Chen P, Wang X, Wang J, Weaver LS, Gonzales ML, Sun G, Unger MA, Ramakrishnan R (2015) Single-cell genetic analysis using automated microfluidics to resolve somatic mosaicism. *PLoS ONE* 10(8):e0135007–e0135007. <https://doi.org/10.1371/journal.pone.0135007>
 44. Islam S, Zeisel A, Joost S, La Manno G, Zajac P, Kasper M, Lönnerberg P, Linnarsson S (2013) Quantitative single-cell RNA-seq with unique molecular identifiers. *Nat Meth* 11:163. <https://doi.org/10.1038/nmeth.2772>
 45. Pollen AA, Nowakowski TJ, Shuga J, Wang X, Leyrat AA, Lui JH, Li N, Szpankowski L, Fowler B, Chen P, Ramalingam N, Sun G, Thu M, Norris M, Lebofsky R, Toppani D, Kemp DW II, Wong M, Clerkson B, Jones BN, Wu S, Knutsson L, Alvarado B, Wang J, Weaver LS, May AP, Jones RC, Unger MA, Kriegstein AR, West JAA (2014) Low-coverage single-cell mRNA sequencing reveals cellular heterogeneity and activated signaling pathways in developing cerebral cortex. *Nat Biotechnol* 32:1053. <https://doi.org/10.1038/nbt.2967>
 46. Goldstein LD, Chen Y-JJ, Dunne J, Mir A, Hubschle H, Guillery J, Yuan W, Zhang J, Stinson J, Jaiswal B, Pahuja KB, Mann I, Schaal T, Chan L, Anandkrishnan S, Lin C-W, Espinoza P, Husain S, Shapiro H, Swaminathan K, Wei S, Srinivasan M, Seshagiri S, Modrusan Z (2017) Massively parallel nanowell-based single-cell gene expression profiling. *BMC Genom* 18(1):519. <https://doi.org/10.1186/s12864-017-3893-1>
 47. Lohr JG, Adalsteinsson VA, Cibulskis K, Choudhury AD, Rosenberg M, Cruz-Gordillo P, Francis JM, Zhang C-Z, Shalek AK, Satija R, Trombetta JJ, Lu D, Tallapragada N, Tahirova N, Kim S, Blumenstiel B, Sougnez C, Lowe A, Wong B, Auclair D, Van Allen EM, Nakabayashi M, Lis RT, Lee G-SM, Li T, Chabot MS, Ly A, Taplin M-E, Clancy TE, Loda M, Regev A, Meyerson M, Hahn WC, Kantoff PW, Golub TR, Getz G, Boehm JS, Love JC (2014) Whole-exome sequencing of circulating tumor cells provides a window into metastatic prostate cancer. *Nat Biotechnol* 32:479. <https://doi.org/10.1038/nbt.2892>
 48. Gole J, Gore A, Richards A, Chiu Y-J, Fung H-L, Bushman D, Chiang H-I, Chun J, Lo Y-H, Zhang K (2013) Massively parallel polymerase cloning and genome sequencing of single cells using nanoliter microwells. *Nat Biotechnol* 31(12):1126–1132. <https://doi.org/10.1038/nbt.2720>
 49. He M, Edgar JS, Jeffries GD, Lorenz RM, Shelby JP, Chiu DT (2005) Selective encapsulation of single cells and subcellular organelles into picoliter- and femtoliter-volume droplets. *Anal Chem* 77(6):1539–1544. <https://doi.org/10.1021/ac0480850>

50. Lim SW, Tran TM, Abate AR (2015) PCR-activated cell sorting for cultivation-free enrichment and sequencing of rare microbes. *PLoS ONE* 10(1):e0113549. <https://doi.org/10.1371/journal.pone.0113549>
51. Kiss MM, Ortoleva-Donnelly L, Beer NR, Warner J, Bailey CG, Colston BW, Rothberg JM, Link DR, Leamon JH (2008) High-throughput quantitative polymerase chain reaction in picoliter droplets. *Anal Chem* 80(23):8975–8981
52. Utada AS, Lenceau E, Link DR, Kaplan PD, Stone HA, Weitz DA (2005) Monodisperse double emulsions generated from a microcapillary device. *Science* 308(5721):537–541. <https://doi.org/10.1126/science.1109164>
53. Kumaresan P, Yang CJ, Cronier SA, Blazej RG, Mathies RA (2008) High-throughput single copy DNA amplification and cell analysis in engineered nanoliter droplets. *Anal Chem* 80(10):3522–3529. <https://doi.org/10.1021/ac800327d>
54. Fu Y, Li C, Lu S, Zhou W, Tang F, Xie XS, Huang Y (2015) Uniform and accurate single-cell sequencing based on emulsion whole-genome amplification. *Proc Natl Acad Sci USA* 112(38):11923–11928. <https://doi.org/10.1073/pnas.1513988112>
55. Pellegrino M, Sciambi A, Treusch S, Durruthy-Durruthy R, Gokhale K, Jacob J, Chen TX, Geis JA, Oldham W, Matthews J, Kantarjian H, Futreal PA, Patel K, Jones KW, Takahashi K, Eastburn DJ (2018) High-throughput single-cell DNA sequencing of acute myeloid leukemia tumors with droplet microfluidics. *Genome Res* 28(9):1345–1352. <https://doi.org/10.1101/gr.232272.117>
56. Khilko Y, Weyman PD, Glass JI, Adams MD, McNeil MA, Griffin PB (2018) DNA assembly with error correction on a droplet digital microfluidics platform. *BMC Biotechnol* 18(1):37. <https://doi.org/10.1186/s12896-018-0439-9>
57. Zhu Z, Yang CJ (2017) Hydrogel droplet microfluidics for high-throughput single molecule/cell analysis. *Acc Chem Res* 50(1):22–31. <https://doi.org/10.1021/acs.accounts.6b00370>
58. Novak R, Zeng Y, Shuga J, Venugopalan G, Fletcher DA, Smith MT, Mathies RA (2011) Single-cell multiplex gene detection and sequencing with microfluidically generated agarose emulsions. *Angew Chem Intl Ed* 50(2):390–395. <https://doi.org/10.1002/anie.201006089>
59. Bigdeli S, Dettloff RO, Frank CW, Davis RW, Crosby LD (2015) A simple method for encapsulating single cells in alginate microspheres allows for direct PCR and whole genome amplification. *PLoS ONE* 10(2):e0117738. <https://doi.org/10.1371/journal.pone.0117738>
60. Zheng GXY, Lau BT, Schnall-Levin M, Jarosz M, Bell JM, Hindson CM, Kyriazopoulou-Panagiotopoulou S, Masquelier DA, Merrill L, Terry JM, Mudivarti PA, Wyatt PW, Bharadwaj R, Makarewicz AJ, Li Y, Belgrader P, Price AD, Lowe AJ, Marks P, Vurens GM, Hardenbol P, Montesclaros L, Luo M, Greenfield L, Wong A, Birch DE, Short SW, Bjornson KP, Patel P, Hopmans ES, Wood C, Kaur S, Lockwood GK, Stafford D, Delaney JP, Wu I, Ordonez HS, Grimes SM, Greer S, Lee JY, Belhocine K, Giorda KM, Heaton WH, McDermott GP, Bent ZW, Meschi F, Kondov NO, Wilson R, Bernate JA, Gauby S, Kindwall A, Bermejo C, Fehr AN, Chan A, Saxonov S, Ness KD, Hindson BJ, Ji HP (2016) Haplotyping germline and cancer genomes with high-throughput linked-read sequencing. *Nat Biotechnol* 34:303. <https://doi.org/10.1038/nbt.3432>
61. Macaulay IC, Ponting CP, Voet T (2017) Single-cell multiomics: multiple measurements from single cells. *Trends Genet* 33(2):155–168. <https://doi.org/10.1016/j.tig.2016.12.003>
62. Aguilar CA, Craighead HG (2013) Micro- and nanoscale devices for the investigation of epigenetics and chromatin dynamics. *Nat Nanotechnol* 8(10):709–718. <https://doi.org/10.1038/nnano.2013.195>
63. Lagally ET, Medintz I, Mathies RA (2001) Single-molecule DNA amplification and analysis in an integrated microfluidic device. *Anal Chem* 73(3):565–570. <https://doi.org/10.1021/ac001026b>
64. Le Roux D, Root BE, Reedy CR, Hickey JA, Scott ON, Bienvenue JM, Landers JP, Chassagne L, de Mazancourt P (2014) DNA analysis using an integrated microchip for multiplex PCR amplification and electrophoresis for reference samples. *Anal Chem* 86(16):8192–8199. <https://doi.org/10.1021/ac501666b>

Chapter 7

Microfluidics-Mass Spectrometry Combination Systems for Single-Cell Analysis



Dan Gao, Chao Song and Jin-Ming Lin

Abstract Due to the existence of heterogeneities in individual cells, analysis of intercellular contents at the single-cell level has become an important direction in modern bioanalytical chemistry. The advances in miniaturized analytical systems and emerging microfluidic tools bring a new opportunity for single-cell analysis. Microfluidic systems have abilities to *the* single cell and *reagents* manipulation with minimal dilution, automatic and parallel sample preparation, and compatible with different detection techniques, which made them powerful tools for single-cell analysis. Mass spectrometry (MS) is one of the most popular analytical methods for the detection of unknown chemicals because of its unique advantages, such as label-free detection, high sensitivity, high chemical specificity, and board detection range. Recently, the coupling of microfluidics to MS for single-cell analysis has attracted substantial *interests and developments*. Nowadays, different types of ionization methods including electrospray ionization (ESI), laser desorption ionization (LDI), secondary ionization (SI), and inductively coupled plasma (ICP) have been coupled to a mass spectrometer. Owing to these ionization methods, a board range of chemicals can be detected by MS, such as proteins, metabolites, lipids, peptides, glycomics, elements, and so on. Recent progress in the fields of technologies and applications in the microfluidics-MS combination systems for single-cell analysis is described. Several analytical procedures integrated on the microfluidics such as single-cell manipulation and sample pretreatment before introduction into the mass spectrometer are reviewed. The future research opportunities by focusing on key performances of throughput, multiparametric target detection, and highly automated analysis are also discussed.

Keywords Single-cell analysis · Microfluidics · Mass spectrometry · Single-cell manipulation · Mass spectrometry interface

D. Gao · C. Song · J.-M. Lin (✉)

Department of Chemistry, Tsinghua University, Beijing 100084, People's Republic of China
e-mail: jmlin@mail.tsinghua.edu.cn

D. Gao · C. Song

State Key Laboratory of Chemical Oncogenomics, Graduate School at Shenzhen,
Tsinghua University, Shenzhen 518055, People's Republic of China

© Springer Nature Singapore Pte Ltd. 2019

J.-M. Lin (ed.), *Microfluidics for Single-Cell Analysis*,

Integrated Analytical Systems, https://doi.org/10.1007/978-981-32-9729-6_7

7.1 Introduction

Single-cell analysis is a rapidly developing research field in recent years. Numerous researches have demonstrated that cells derived from a mother cell or from the same type of cell exhibit heterogeneity even if under the same physiological conditions or external stimuli [1, 2]. Moreover, single-cell analysis is regarded as a key step to help us comprehensively understand the cellular and subcellular endogenous substances like protein, metabolites, and nucleic acids for cell proteomics, metabolomics, genomics, and transcriptomics studies [3]. Therefore, it attracts researchers from various research fields. With respect to doctors and pharmacists, cell heterogeneity may have an impact in the understanding of diseases such as cancer, the mechanism of emerged drug-resistant cells, and the function of the immune system. With regard to biologists, cell heterogeneity may reveal insights into the fundamental biological and physiological behaviors including the size, growth rate, and morphology [4]. For analytical chemists, they are committed to develop new analytical methods to overcome the limits in single-cell analysis. Compared with conventional bulk cell assays, single-cell analysis suffers from several challenges. The biggest challenges arise from small size and volume of a cell, small concentrations of cellular components, and cellular ingredients with a wide range of concentration levels [5]. These complex and dynamic intercellular processes put forward higher requirements to scientists to develop higher sensitive, higher selective, and higher spatial-resolved methods for single-cell analysis. Earlier methods for single-cell analysis are mainly based on flow cytometry or laser scanning cytometry by rapidly screening fluorescently labeled cells in a flow [6, 7]. They are typically targeted to only one or very few molecules, but are highly specific and sensitive. Moreover, the data are collected only at a single time point, which prohibit dynamic monitoring of cell *responses*.

The recent development in microfluidic techniques has exhibited a powerful tool for single-cell analysis [8]. Compared to conventional methods, microfluidics with micro-sized channels has the advantages to handle mass-limited analytes, control the local microenvironment, integrate multiple functions into a single system and analysis in a parallel mode. The automatic analytical ability through high integration of multifunction units like sample preparation, separation, and detection can greatly reduce measurement errors generated from human operations. For single-cell analysis, miniaturized microfluidic systems are compatible to the size of a single cell ($\sim 10\ \mu\text{m}$ in size), and they manipulate picoliter to nanoliter volumes of solution that help reduce sample loss and decrease dilution, resulting in highly sensitive assays. Moreover, microfluidics can combine with many detection techniques for online and real-time analysis, and different detection methods are allowed to be combined together for multiple types of targets detection. Sample handling is a critical procedure for single-cell analysis, and most protocols involve highly efficient manipulation of single cells. Up to now, various microfluidic-based strategies have been developed for single-cell capture, such as microwells [9, 10], microtraps [11], microvalves [12], flow cytometric methods [13], droplet-based

methods [14, 15], and optical tweezers [16]. And many detection techniques including fluorometry [17] and spectroscopy [18] can be combined with microfluidic systems for online single-cell analysis. The fluorescence microscope technique needs to pre-label the selected molecules by molecular probes or reporters, but the types of detected molecules are limited to labeling reagents. Recently developed approaches tend to label-free analytical methods, such as mass spectrometry (MS), Raman spectroscopy, and impedance measurements. These strategies do not require any tedious labeling, and cells can be observed without any intervention.

MS is becoming a powerful and well-accepted analytical approach for single-cell analysis due to its outstanding characteristics such as information-rich, high sensitivity, excellent specificity, and so on [19]. As the development of MS technology, two “soft” ionization methods, electrospray ionization (ESI) and matrix-assisted laser desorption/ionization (MALDI), are the most popular. In both methods, molecules are ionized with minimal fragmentation, so that highly accurate intact molecule weight can be provided, making identification of molecules easier. In addition, their corresponding fragment ions can be further generated through collision-induced dissociation (CID) for structure identification. ESI produces charged ions directly from a liquid, which made it convenient to online couple of chromatographic separations with mass spectrometry. However, it is tedious because sample pretreatment and chromatographic separation steps are time-consuming. For MALDI-MS analysis, the requirement of vacuum operation condition restricts its application in live single-cell analysis. In recent years, secondary ion mass spectrometry (SIMS), an advanced technology for surface analysis, is also reported for the analysis of chemicals in single cell with high sensitivity, high throughput, and spatial resolution. However, high vacuum condition is also needed during secondary ions on their way to the detector. With the invention of ambient ionization techniques, ambient MS has attracted an increasing interest since the beginning of twenty-first century [20, 21]. Samples can be directly and straightforwardly analyzed in an open-air under ambient conditions without or minimal sample pretreatment. Up until now, different kinds of ambient MS techniques have been explored for single-cell analysis, which open a new way for rapid, direct, in situ, and real-time study of the complexity and heterogeneity in single cells.

Coupling of microfluidics to MS has the advantages of flexible sample manipulation, fast analysis time, high throughput, and enhanced sensitivity. The development of coupling microfluidic chips with MS in the early stages mainly focused on the MS interface. With the maturation of microfluidic fabrication techniques, microfluidics has evolved from simple infusion tools interfacing to MS to sophisticated functions that integrated with many sample pretreatment units, such as sample extraction, derivatization, and separation. A few reviews have been published about the microfluidics and MS combination systems for various applications in life science [22–24]. In this chapter, we review the advances in the field of microfluidics and MS combination systems for single-cell analysis that have been published in recent years. We firstly describe various function units integrated on

microfluidic chips, such as single-cell capture, automated sample preparation, and MS analysis. Secondly, we highlight the advances in the coupling of microfluidics to the MS interfaces with different ionization techniques. Recent applications of microfluidics-MS in nucleic acid, proteins, small molecules, and pharmaceutical analysis are reviewed and commented. Finally, we also discuss the future directions in the improvement of microfluidic techniques and ambient MS for automatic and highly sensitive single-cell analysis.

7.2 On-Chip Sample Preparation

The first step in single-cell analysis on microfluidic devices is sample preparation, including isolation of individual cells from bulk cells and docking them into a desired location for further treatment. For free cells like yeast, bacterial, or blood cells, they can be manipulated easily. But for the cells from tissue samples, they should be firstly released by chemical reagents or enzymes or by micromechanical forces [25]. With the rapid advances in micro-electro-mechanical systems (MEMS) technology, the microchannel size can be fabricated downscale to several micrometers so that the single cells can be precisely manipulated [26–28]. We highlight the most commonly used single-cell manipulation techniques and recent developments to improve efficiency and sensitivity.

7.2.1 Microwells

The microwell structures provide a convenient way to isolate and trap single cells using physical boundaries. The geometry, size, depth, and material properties of the microwells can be easily changed to capture *cells of interest* [29]. There are a few reviews reporting single-cell isolation using microwells in detail [30, 31]. One common method to achieve this goal is to design cell-sized microwells to dock them through gravity-dependent sedimentation. The excess cells outside the wells are then flushed away. The general methods to fabricate microwell arrays is based on poly(dimethylsiloxane) through soft lithography. But the process is time-consuming, and expensive chrome photomasks are needed for photolithography when the well size is less than 20 μm for single-cell capture. To overcome this limitation, Liu et al. developed a simple and cheap approach to fabricate masters for microwell generation [32]. As shown in Fig. 7.1a, a master was formed by self-assembling polystyrene microspheres on a *glass slide* and then partially melted the microspheres. The master could be used for the formation of 10- to 20- μm microwells for single-cell capture. Recently, another easy-to-use method called digital micromirror approach was developed by Yang et al. to fabricate a poly(ethylene glycol) diacrylate (PEGDA) hydrogel microwell chip [33]. As shown in Fig. 7.1b, a digital mask based on shadowed light instead of conventional physical

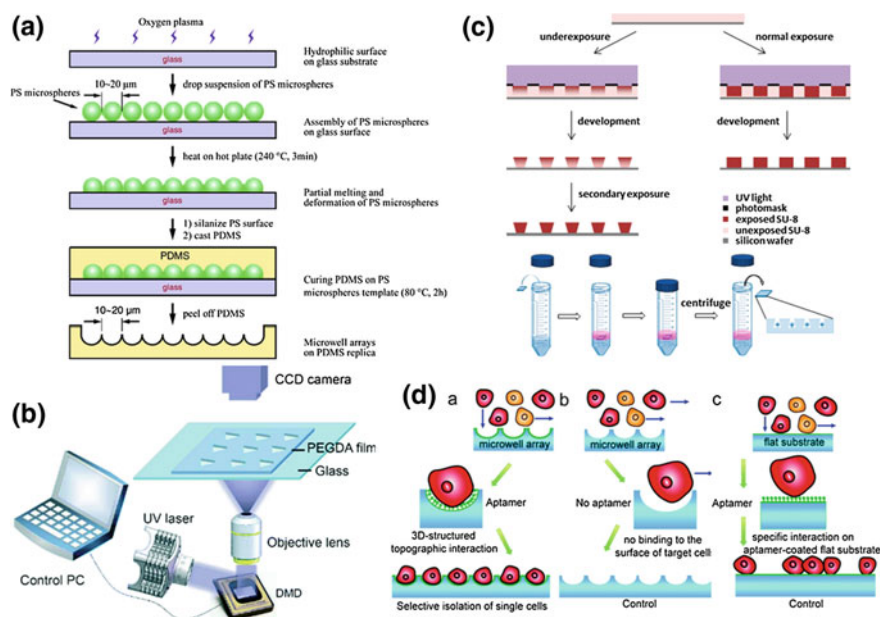


Fig. 7.1 Single-cell capture in microwell arrays. **a** Schematic illustration for the fabrication of PDMS microwell arrays and captured cell arrays on the microwells. Reprinted with permission from Ref. [32]. Copyright © 2010 American Chemical Society. **b** A schematic representation of microwell fabrication and single-cell analysis via a *digital micromirror device (DMD)*-based modulating projection printing system. Reprinted with permission from Ref. [33]. Copyright © 2017 Royal Society of Chemistry. **c** The fabrication of inverse truncated cone-shaped microposts (left) and normal columnar microposts (right) and single-cell trapping in truncated cone-shaped microwell array was realized by centrifugation assistance. Reprinted with permission from Ref. [37]. Copyright © 2010 American Chemical Society. **d** Microwells modified with DNA-aptamer for single target cell isolation. Reprinted with permission from Ref. [42]. Copyright © 2012 Royal Society of Chemistry

mask was used during the microwell fabrication process. Moreover, the constraining hydrogel film could be peeled off from glass slide for further cell analysis.

One main drawback of microwell-based microfluidic devices is that single-cell occupation rate is a bit low, ranging from 2.6 to 39% [34]. To improve the capture efficiency, external operations like aided by vacuum or centrifugation [35] are applied instead of passive gravity drive. For example, Terstappen et al. designed a self-seeding microwell chip with a single 5-μm pore in the bottom of each microwell, so that single cells can be fast and easily dragged into the pore of the microwells under a negative pressure of 10 mbar generated by degassing in a vacuum chamber [36]. The single-cell capture efficiency could finally improve to 67% with this slight structural improvement. Wu's research group designed a truncated cone-shaped microwell array to trap single cells, and the single-cell capture efficiency was increased to approximately 90% with the assistance of centrifugation [37]. As shown in Fig. 7.1c, the truncated cone-shaped microwell

structure also greatly prevented significant cell loss during cell treatment. However, majority of the reported platforms have only one fluid channel on top of the microwell arrays, which allow paracrine communication between cells, making it impossible for accurate multi-parameter detection in single cells. Recently, Garcia-Cordero et al. designed a microvalve channel on top of the microwells to create an independent microenvironment for each well [38]. During the experiments, a less than 0.02 Pa of shear stress was generated inside the wells which could keep biological behaviors of cells.

The above physical structure-based single-cell capture has the challenge in selectively isolating specific single cells, such as target tumor cells in blood. To overcome this limitation, microfabricated physical structures modified with bio-recognizable molecules will be a powerful strategy and open up a new opportunity to analysis cells of interest. Moreover, surface modification without complicated cell-sized microwell fabrication is also a good way for unique cell trapping. The commonly used molecules with specific recognition function for the isolation of specific single cells are aptamer [39], antibody [40], and protein [41]. Lin's research group used DNA-aptamer to modify microwells to bio-selectively isolate target tumor cells (Fig. 7.1d) [42]. The single-cell occupancy rate was significantly enhanced from 0.5 to 88.2%.

7.2.2 *Micropatterns*

Micropatterning of surface is another frequently used technique for spatial arrangement of single cells by fabricating cell-adhesive spots surrounded by cell-repellent surfaces. These contact-based single-cell trapping is an easy and cheap way for high-throughput studies. Commonly used biomimetic materials and cell adhesion molecules for adhesive regions are fibronectin [43], laminin, collagen [44], vitronectin, and poly-L-lysine [45]. However, hydrophilic polymers for cell-repellent surface modification are polyethylene glycol (PEG) [46, 47], poly-vinyl alcohol (PVA) [48], and alkanethiol [49], and so on. Different strategies including microcontact printing [45], ink-jet printing [50], and photopatterning [51] have been developed to produce chemical surface patterns. However, there are still some difficulties in the homogeneous distribution of cells on the patterned area because of the nonspecific absorption of cells on the cell-repellent area. Whitesides et al. have reviewed the patterning of proteins and cells using three soft lithography techniques, microcontact printing, patterning using microfluidic channels, and laminar flow patterning [52].

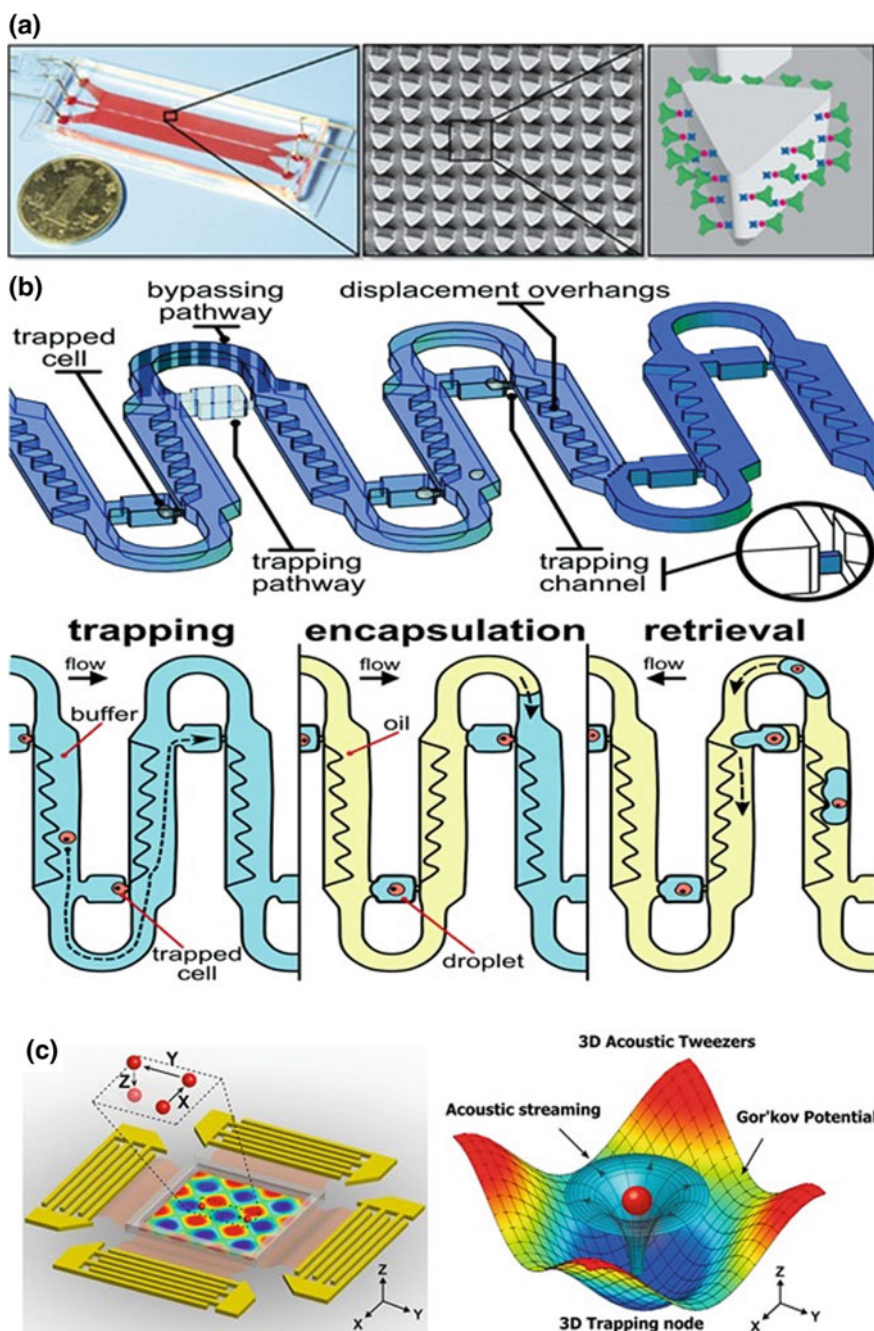
Micropatterning cells on different-shaped chemical surfaces have been widely used for cell behaviors and cell-material interaction studies, such as cell shape, division, migration, and invasion [53, 54]. Recently, Zhao et al. presented a new patterning fabrication method using tape-assisted photolithographic-free microfluidic chip for tumor migration study [55]. This technique did not need the use of microfabricated laboratory to fabricate the chip, which could be easily accessible in

routine biological lab for biological mechanism studies. Isolating specific cell subtypes of certain disease is extremely important for early disease diagnosis with no clinical symptoms. Referring to cancer disease, circulating tumor cells (CTCs) play a key role in metastatic procedure through hematopoietic dissemination [56]. The isolation of rare CTCs from peripheral blood sample can help doctor guide cancer care, but it faces some technical challenges. Micropatterning the surface of the microchannel or micropillars with chemical linkers like aptamer *or* antibody is an effective strategy to solve this problem. Yang et al. functionalized micropillars with anti-epithelial cell adhesion molecule (anti-EpCAM) antibody to capture CTCs from blood samples (Fig. 7.2a) [57]. The shape and location of the micropillars were optimized hydrodynamically to provide lower shear stress so that contact time between CTCs cells and immunodecorated micropillars would be increased to improve the capture efficiency. The retrieve of captured cells from initial capture site is also important for downstream biological analysis. A microfluidic device incorporated with a photodegradable hydrogel functionalized with leukocyte-specific antibodies was recently reported by Revzin et al. to capture and release target cells [58]. Human CD4 or CD8 T-cells from a peripheral blood sample were captured by the modified antibodies, and then the desired cells were released by UV-induced photo-degradation for the following flow cytometry analysis.

7.2.3 Traps

Similar to well- and pattern-based cell capture approaches, trapping of single cells at fixed positions by active or passive capture strategies in microfluidic systems has benefit for cell biological analysis which needs the maintenance of cells for a longer period. The related techniques *include* hydrodynamic, mechanical, magnetic, optical, electrical, and acoustic traps. Laurell and colleagues have previously reviewed both the contact and non-contact mode trapping techniques in detail [59]. Here, we will focus on the recent advances in the most commonly used microfluidic-based single-cell trapping methods.

Cells trapped by hydrodynamic flow are the most commonly used mechanism. In general, cells are stopped and trapped from the flow of a cell suspension by microscale structures (such as U-shaped *structures* [60–62]) or by bypass-channel traps [63]. Referring to bypass-channel traps, the bypass channels were usually perpendicular to the main flow channel, *and* the cells can be suctioned into the small side channel through focusing flow. Various shapes like dams, weirs, and holes can be designed for the trap structures. For example, Sauzade et al. developed a serpentine-shaped microchannel with a linear array of hydrodynamic trapping sites and filtering structures to isolate, capture, and retrieve individual cells [64]. As shown in Fig. 7.2b, incoming cells initially displaced toward the unoccupied trapping site by focusing structures. Additional cells were then diverted the flow through bypass pathway and occupied the downstream traps. The trapping scheme



◀**Fig. 7.2** Single-cell trapping by micropatterns and trap methods. **a** Simulated and experimental results demonstrated the size-dictated interaction of particles in *Size-Dictated Immunocapture Chip*. Reprinted with permission from Ref. [57]. Copyright © 2017 Wiley-VCH Verlag GmbH & Co. KGaA, Weinheim. **b** Schematics of the microfluidic circuit and work flow for true single-cell encapsulation. Reprinted with permission from Ref. [64]. Copyright © 2017 Royal Society of Chemistry. **c** Illustration of 3D acoustic tweezers for particle or cell trapping. Reprinted with permission from Ref. [67]. Copyright © 2016 National Academy of Sciences

can improve the single-cell capture efficiency to a near-perfect rate. However, the hydrodynamic trapping technique usually generates mechanical stress on cells, which will have negative effects on physiological function of cells. Recently, a mechanical trap array with four optical transparent optical arms was developed by Gracias et al. to capture and encapsulate single cells [65]. The four arms consisted of SiO and SiO₂ on a quartz substrate can fold by tailoring a thin film stress to encapsulate cells without any perturbation.

Except to those passive techniques, some non-contact and active trapping techniques like dielectrophoretic (DEP) and acoustic-driven traps are also reported in recent years to manipulate individual cells with high precision. For DEP traps, cells can be moved by forces generated in a non-uniform electric field. The key point for DEP trapping is to control a scalable array individually to increase the number of cells available for analysis. To solve this problem, Zhang et al. combined an alternative pause-and-sort Raman-activated cell sorting on microfluidic device with positive DEP for single-cell trap and release [66]. This method allowed the single-cell trapping, sequence position and separation, and individual detection by Raman in a high-speed flow. Acoustic actuation, like ultrasonic standing waves, offers dynamic control of cell environment for short-term analysis. Cells or particles can be pushed toward pressure nodes by the acoustic radiation force generated by acoustic waves. Huang's research group has focused on the surface acoustic waves driven for many years, and they have received many excellent achievements. Recently, they integrated surface acoustic waves into the microfluidic device to generate an array of 3D trapping nodes for trapping and *manipulating single cells* and particles (Fig. 7.2c) [67]. The operating frequency of acoustic waves has significant effect on cell viability and behavior. Neild's research group systematically investigated the relationship between acoustic power and cell viability [68]. They found that the critical acoustic power for lymphocytes was less than 570 mW, and the lysis threshold power was different to different cell types. However, one main shortcoming for acoustic cell trapping is *the disability to keep cell viable for long-term analysis*.

7.2.4 Droplets

Droplet-based microfluidics has emerged as a new forerunner for massive parallelized single-cell analysis in recent years. The fact can be attributed to the

following reasons. Firstly, single cells and reagents can be isolated and encapsulated in monodisperse picoliter liquid droplets at a throughput of thousands per second. Secondly, droplets provide an isolated compartment so that the risk of cross-contamination can be largely reduced. Thirdly, small-sized droplets facilitate rapid mixing of encapsulated solution, thereby minimizing sample dilution. Joensson's research group have reviewed the technical advances on the droplet microfluidic field for single-cell analysis and the application of these technical developments to further biological understanding [69]. Later, Dittrich et al. discussed the advantages and limitations of the droplet microfluidic approach for single-cell analysis [70].

Typically, T-junction and flow-focusing geometries' microfluidic channels were designed for the generation of highly monodisperse droplets. Water-in-oil or oil-in-water emulsions as well as complex multiple-phase emulsions can be generated (Fig. 7.3a) [71]. The size and rate of droplet formation can be regulated by a series of parameters, such as channel dimensions, flow rates, viscosities, and interfacial tension [72, 73]. Compared to other techniques, droplet microfluidics allows for high-throughput and massively parallelized studies on single cells due to the generation of droplets with high frequency from Hz to kHz. Currently, droplet microfluidics has been widely used in cell biology, clinical research, materials science, and drug discovery. Different from conventional microfluidic-based droplet generation approach, Chen et al. developed an ink-jet printing-based droplet system for single-cell encapsulation, and the single-cell lipids can be directly analyzed by probe electrospray ionization mass spectrometry [74]. As shown in Fig. 7.3b, the droplet volume can be precisely controlled by adjusting the voltage and pulse time exerted on the ink-jet head. The position of the generated droplets from the ink-jet could be adjusted by an automatic X-Y stage. In order to keep the homogeneous distribution of cells in liquid, a homemade magnetic stirring device was applied to the cell suspension reservoir. Although single cells can be encapsulated in independent aqueous microdroplets, large different sizes between cells (about 1 pL) and droplet volumes (ranged from nanoliter to microliter), and the matrix effects from cell culture medium or intercellular matrix will affect the following detection sensitivity. To address this problem, a droplet-based extraction capillary was developed by Zhang et al. to combine with ESI MS for cellular metabolites detection [75]. As shown in Fig. 7.3c, a pulled glass capillary containing extraction solvent at the tip of the capillary, manipulated by a three-dimensional manipulator, could be placed close to the surface of a single cell for cellular component extraction. Different desired metabolites could be easily extracted by using specific extraction solvent. *Although* most of the microfluidic-based droplet systems have been successfully applied in single-cell analysis, *they* still face the challenges of adding reagents into the generated droplets. Fang's group developed a solid pin-based droplet system to dip and deposit liquids on a two-dimensional and movable oil-covered hydrophilic pillars for liquid-liquid reactions and assays [76]. As shown in Fig. 7.3d, by using solid pin-based liquid "dipping-depositing-moving" manipulation strategies, they could *easily realize additional reagents adding* to the sample droplet. However, this technique still suffers from

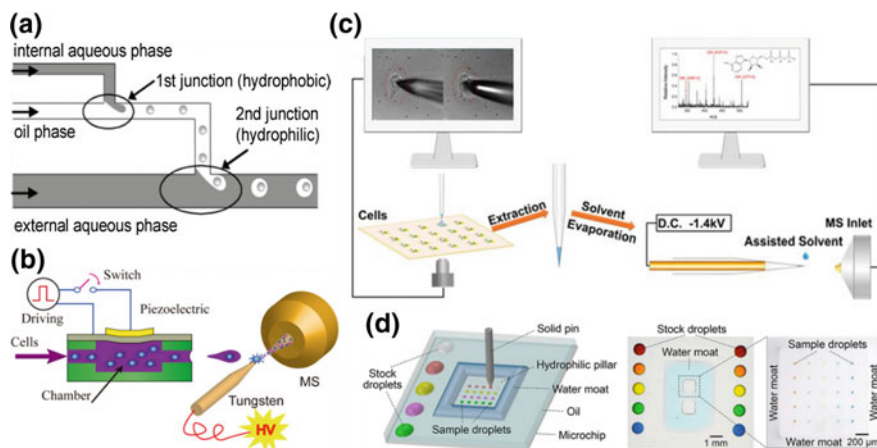


Fig. 7.3 Single-cell capture by microdroplets. **a** Basic concept for preparing double emulsions (W/O/W) using T-shaped microchannels. Reprinted with permission from Ref. [71]. Copyright © 2004 American Chemical Society. **b** The novel method for single-cell analysis and lipid profiling by combining drop-on-demand ink-jet cell printing and probe electro spray ionization mass spectrometry (PESI-MS). Reprinted with permission from Ref. [74]. Copyright © 2016 American Chemical Society. **c** A method that integrated droplet-based microextraction with single-cell mass spectrometry. Reprinted with permission from Ref. [75]. Copyright © 2016 Springer Nature Limited. **d** Setup of the solid pin-based droplet system. Reprinted with permission from Ref. [76]. Copyright © 2018 American Chemical Society

limited sample pretreatment procedures. Later, they developed a nanoliter-scale oil-air-droplet microfluidic system for single-cell proteomic analysis [77]. Multistep complex sample pretreatment and injection procedures could be realized on the established platform with minimum sample loss; thus, the analytical sensitivity was significantly increased for single-cell samples.

7.3 Chip-MS Interface Development

As we all known, a single cell contains small amount of biomolecules with a wide range distribution, which brings huge challenges for single-cell component analysis. Therefore, there is an urgent need of detection methods with high sensitivity. Fluorescence, electrochemical, PCR-based detection, and mass spectrometry are the most commonly used techniques for microfluidic-based single-cell analysis. Among these detection methods, mass spectrometry receives extensive attention due to its high sensitivity and capability to identify unknown molecules without *pre-labeling*. Different types of ablation and ionization methods can be coupled to a mass spectrometer, such as ESI, laser ablation/laser desorption ionization (LA/LDI), secondary ionization (SI), inductively coupled plasma (ICP), and ambient

ionization. The development of technologies and applications in microfluidics and mass spectrometry combination systems have been previously discussed from the year 2008 to 2013. Lin's research group has reviewed the progress made in the techniques about the *microchip-MS* and related applications in proteomics and cell analysis [22.77-79]. Over the past two years, a few reviews have been published in high-impact journals, such as *Angewandte Chemie* [78], *Journal of the American Chemical Society* [79], and *Trends in Analytical Chemistry* [80], to thoroughly overview recent advances in mass spectrometry-based single-cell analysis. Mass spectroscopy types have been developed from those requiring high pressure and a vacuum to transport the ionized molecules to the MS with ambient ionization techniques. The most important *issue* for coupling of microfluidics to MS is to *develop* stable and effective interfaces.

7.3.1 ESI-MS

ESI was firstly introduced by Dole et al. in the late 1960s [81] and later applied in the ionization of proteins by Fenn et al. in the late 1980s [82]. In ESI, molecules in sample solutions are ionized through an electrospray emitter, which is usually a needle-shaped structure. According to the requirement, the earliest miniaturization of emitters includes microspray and nanospray ionization formats mainly using pulled glass capillaries. Referring to microfluidic chip-ESI-MS interfaces, there are two categories of miniaturized emitters, capillaries and microchip emitters. With the advances in the microfabrication techniques, the microchip emitters have developed from one ESI emitter to multi-ESI emitters [83], which greatly increased the analytical throughput. For online ESI-MS detection, salts and buffers should be firstly removed to eliminate ion suppression. Micro-solid-phase extraction (micro-SPE) is the most commonly used approaches for sample pretreatment and cleanup interferences from analytical samples. For the analysis of complex samples by MS, the interference by the background and ion suppression between molecules are required to be considered [84]. In order to overcome these drawbacks, some on-chip separation strategies like capillary electrophoresis (CE) or liquid chromatography (LC) [85] to MS can be adopted. Recently, tremendous efforts have been focused on the integration of related sample pretreatment units, such as enzymatic digestion, extraction, desalting, and preconcentration on microfluidic devices for directly MS detection [86–88].

Our group [89–91] has engaged in the coupling of microfluidics with MS for chemical and cell biology studies for nearly ten years. Due to the powerful and integration abilities of microfluidic devices to mimic the physiological system of interest, various related functional parts, including cell culture, metabolism generation or cell secretion, sample pretreatment, and MS detection, can be integrated on one microfluidic platform. For example, Gao et al. [92] firstly coupled the microfluidics to ESI-Q-TOF-MS directly through a silica-fused capillary. As shown in Fig. 7.4a, by integrating cell culture and micro-SPE functions on one

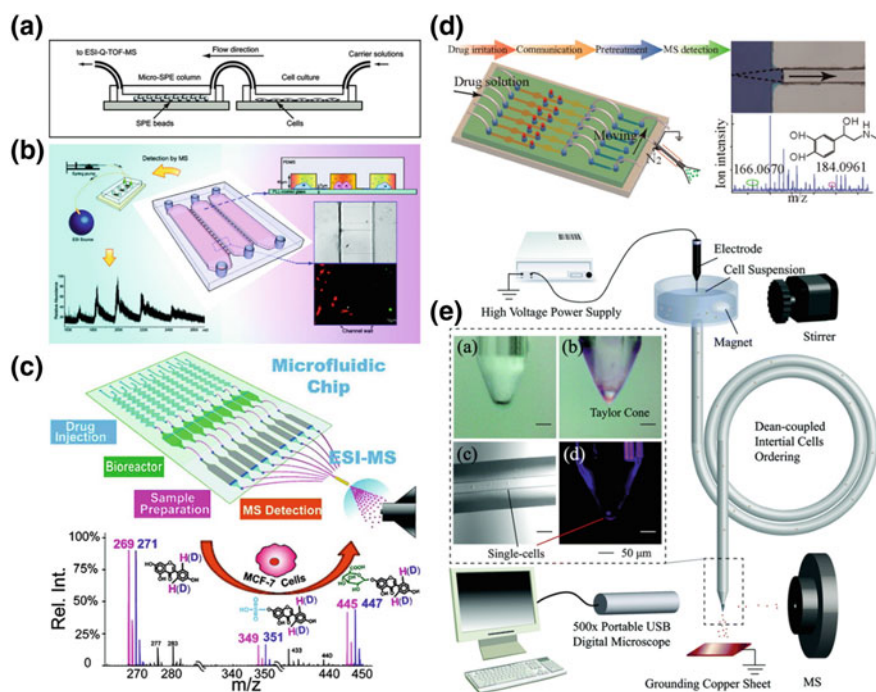


Fig. 7.4 Microfluidic-based single-cell analysis with ESI-MS detection. **a** Schematics of one unit for cell culture and sample pretreatment prior to ESI-Q-TOF-MS detection. Reprinted with permission from Ref. [92]. Copyright © 2010 American Chemical Society. **b** Schematic illustration of the microfluidic device integrated in a controlled co-culture system for detection of secreted proteins. Reprinted with permission from Ref. [89]. Copyright © 2011 American Chemical Society. **c** A stable isotope labeling-assisted microfluidic chip electro spray ionization mass spectrometry (SIL-chip-ESI-MS) platform. Reprinted with permission from Ref. [94]. Copyright © 2012 American Chemical Society. **d** A novel method for cell-to-cell communication study on an integrated microdevice. Reprinted with permission from Ref. [96]. Copyright © 2013 American Chemical Society. **e** Experimental setup of Dean flow-induced cell sorting and Taylor cone-induced electro spray for single-cell analysis. Reprinted with permission from Ref. [97]. Copyright © Royal Society of Chemistry 2018

microfluidic device, metabolism of vitamin E in human lung epithelial A549 cells can be easily studied. Compared with conventional methods, our method provides short analysis time (less than 10 min), low sample and reagent consumption (less than 100 μ L). Our established platform opens up a new approach for direct, fast, and semi-automated cell-based analysis. Based on this combination technique, Lin's group later successfully detected glutamate release from neuronal PC12 cells using online ESI-Q-TOF-MS [89]. As shown in Fig. 7.4b, Wei et al. also mimicked biological bioreactions generated from the interaction between PC12 and GH3 cells on a microfluidic device, and the regulation of growth hormone secretion by PC12 cells was demonstrated by ESI-Q-TOF-MS detection [93]. In

order to realize more accurate quantitative analysis by the chip-MS combination system, Chen et al. introduced a stable isotope labeling-assisted technique for quantitation in metabolic studies (Fig. 7.4c) [94]. In the drug discovery process, prediction of drug and metabolism toxicity is extremely important to screen drug candidates during the preclinical stage. Mao et al. developed a microfluidic device to simultaneously *evaluate* drug metabolism in human liver by online ESI-Q-TOF-MS and its cytotoxicity on HepG2 cells [95]. Cell-to-cell communication plays a critical role in living tissues and *has* attracted much attention to biologists. Mao et al. later developed a “Surface Tension Plug” on a microfluidic chip for cell-to-cell communication study, and signal molecules like epinephrine and glucose secreted from 293 and L-02 cells separately were successfully detected by online ESI-Q-TOF-MS after on-chip SPE treatment (Fig. 7.4d) [96]. However, all the above systems lack automatic analytical capability, because a silica-fused capillary for the connection of microfluidics to MS should be manually moved from one channel to another for multiple cell experiments’ analysis. To overcome this drawback, Huang et al. from Lin’s group recently developed a novel Dean flow-assisted cell ordering system to generate single cells rapidly for high-throughput ESI-MS analysis (Fig. 7.4e) [97]. Based on the principle of Dean flow, the agglomeration and uneven distribution of cells in the cell suspension could be greatly reduced, which significantly improved the efficiency of single-cell MS analysis. In this platform, a spiral capillary was installed for rapid cell ordering and with the capillary tip polished and silanized for the generation of *Taylor cone* to induce ESI and *flow* in the capillary. They distinguished the cell subpopulations of several human tumor cells and confirmed a slightly different amount of phospholipids between various tumor cells.

7.3.2 MALDI-MS

MALDI is another common soft ionization method, which was firstly proposed by Karas and Hillenkamp [98] and Tanaka et al. [99] in late 1980s. MALDI is generally used for large molecules analysis, such as proteins, carbohydrates, peptides, and polymers [100]. In MALDI, a laser is used to irradiate co-crystallized film of target analytes and a matrix. During the ionization process, the matrix firstly absorbs laser energy and then transfers parts of its charge to analytes to ionize them [101]. Compared with other ionization techniques, a specific characteristic of MALDI-MS is the ability to provide both chemical and spatial information. Moreover, MALDI-MS has higher tolerance to buffers, salts, and impurities in samples. However, the main factors of MALDI that limit the spatial resolution down near to the single-cell level are matrix crystal size and laser beam size. Recently, several technological and methodological advances have been made to overcome these difficulties, and some of them have been reviewed by Trouillon et al. [102]. For example, (1) the usage of the smartbeam II laser instead of standard nitrogen or solid-state laser with Gaussian beam to obtain higher spectral quality;

(2) employment of a commercial matrix application device (e.g., Imageprep) to obtain optimal extraction with minimal crystal sizes [103]; (3) stretch cell sample to compensate for the limited spatial resolution of MALDI imaging [104].

Microfluidic-based MALDI analysis is usually performed using an offline format because a MALDI target is under vacuum while the microfluidic operations are at ambient condition. Samples are usually deposited directly on a sample target by dropping, spraying, or spotting for the sequential analysis. There are a few researches about the direct analysis of cellular biomolecules at single-cell level by MALDI-MS [105, 106]. However, the cells should be manually selected which significantly reduce the throughput. To improve it, our group developed a microwell-array-based microfluidic chip to combine with MALDI-MS for automatic and high-throughput single-cell phospholipid analysis [107]. As shown in Fig. 7.5a, a high-density PDMS microwell array was fabricated to assist the formation of a cell array on an indium tin oxide (ITO)-coated glass slide. After matrix deposition, MALDI-MS imaging analysis could be automatically performed in a

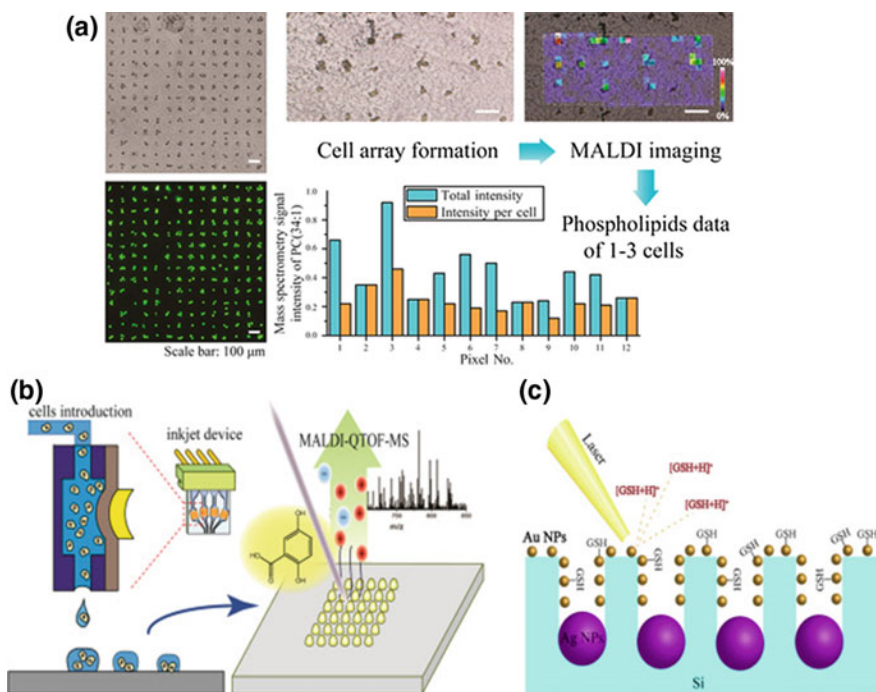


Fig. 7.5 Microfluidic-based single-cell analysis with LDI MS detection. **a** The combination of microfluidic chip and MALDI-MS for high-throughput and automatic single-cell phospholipids analysis. Reprinted with permission from Ref. [107]. Copyright © 2015 American Chemical Society. **b** Ink-jet cell introduction for MALDI-MS analysis. Reprinted with permission from Ref. [50]. Copyright © 2017 Elsevier B.V. **c** Schematic of cell analysis on a silicon chip with in situ synthesis of Ag and Au NPs. Reprinted with permission from Ref. [108]. Copyright © 2017 Elsevier B.V. (C)

high-throughput mode by setting a matched distance between cell spacing and step size of the sample stage. However, the single-cell capture efficiency is a little low, about 30%. Korenaga et al. developed an ink-jet automatic single cells and matrices printing system to directly print sample onto a ITO glass substrate for single-cell MALDI-MS analysis (Fig. 7.5b) [50]. This technique shows controllable high-throughput analytical capabilities. Unfortunately, the most commonly used chemical matrix has strong background signals in low-mass region (< 600 Da), which makes spectral analysis more difficult. The developed surface-assisted laser desorption ionization MS (SALDI MS) offers a matrix-free way to reduce low-mass range background noise. Wang et al. in Lin's Lab developed a porous silicon chip modified with gold nanoparticles for the capture of Caco-2 cells, and intercellular glutathione was detected by SALDI MS [108]. As shown in Fig. 7.5c, the silicon chip was array-patterned for high efficient cell capture and high-throughput automatic SALDI MS detection. This method showed great potential for more efficient analysis of small thiol biomarkers in complex biological samples.

7.3.3 Secondary Ion Mass Spectroscopy (SIMS)

A large number of single-cell-based works have been carried out with SIMS due to its high spatial resolution. For single-cell analysis, time-of-flight SIMS (TOF-SIMS) uses a pulsed ion beam desorb secondary ions from the very outermost surface of a single cell. The technique has the ability to detect biological molecules with molecular weight lower than 1000 Da, such as lipids, metabolites, and the resolution can downscale to subcellular level. Sample preparation is a key step in biological mass spectrometric analysis, especially for those methods requiring a vacuum environment. Probably due to this reason, microfluidic-based single-cell analysis scarcely uses the SIMS as the detection technique. Recently, inspired by our previous work [107], Wu's group developed a micropatterning PDMS stencil film to capture and form single-cell microarray with the assistance of centrifugation, and they studied drug-induced cellular phenotypic alterations by TOF-SIMS for the first time [109]. The facile single-cell patterning method exhibited higher than 90% of site occupancy and more than 97% of single-cell resolution. Most work in this field can be done to help better understand the molecular biology for many diseases and discover potential biomarkers for early diagnosis of disease.

7.3.4 Chromatographic Techniques Coupled to MS

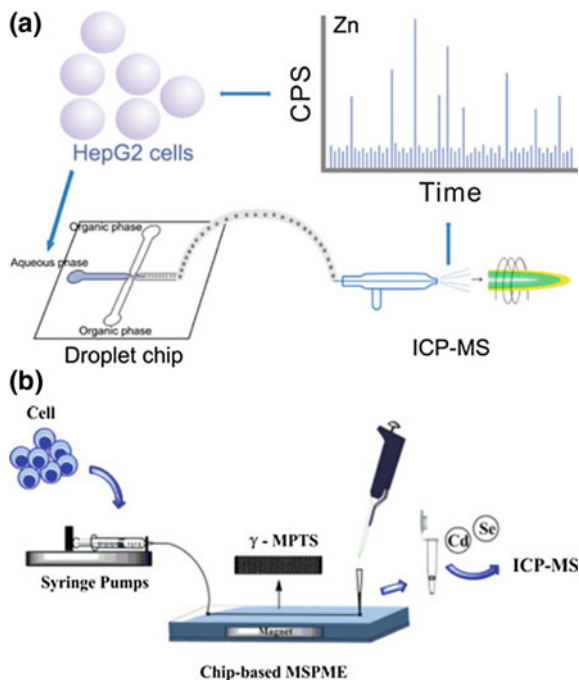
Due to the tiny concentrations of biomolecules with a wide range of distribution in single cells, the coupling of chromatographic techniques to MS will significantly enhance separation and identification of intercellular compounds. Capillary

electrophoresis (CE) represents the most popularly used separation techniques for this purpose because of its strong abilities for separation of cellular metabolites in miniaturized sample volume. Since the development of CE coupling to MS has been reviewed recently by Fritzsche et al. [110], Kleparnik et al. [111], Zhong et al. [112], and Tycova et al. [101], we only focus on the major progress in this field for single-cell analysis. Ramsey's group integrated cell lysis, electrophoresis separation, and an integrated electrospray emitter on a crossed microfluidic device for online separation of intracellular molecules and direct analysis using ESI-MS [113]. Onijko et al. presented a CE-ESI-MS approach for metabolites identification in single embryonic cells from the South African clawed frog [114]. By *microextraction* of their metabolomes, they could identify 40 metabolites that have relationship with central metabolic networks. The differences in activities between different cell types in the wild-type, unperturbed embryos could be revealed by relative quantitation analysis.

7.3.5 ICP MS

The application of ICP MS for trace elemental analysis in single cells has attracted an increasing interest in recent years [115]. The ion source of ICP MS uses high-temperature plasma to transform the atomic or molecular ion of a sample into a charged ion [116, 117]. ICP MS has several distinct advantages as follows: (1) ICP MS can be injected at ambient pressure, enabling combining with other injection technique easily; (2) ICP MS has low detection limit, fast analysis speed, and simple spectrum; (3) the low initial ion energy made it compatible with many simple mass analyzers. Many researches have reported about the combination of droplet microfluidics with ICP MS for ultra-trace elements analysis in single cells. For example, Hu et al. presented a cross-channel droplet chip to directly sampling to time-resolved ICP MS via a miniaturized nebulization system for the quantification of Zn in single HepG2 cells (Fig. 7.6a) [118]. To match each ICP MS spike with one cell, the cells should be spatially and temporally separated. By optimizing the dimensions of the droplet generation channels and sampling flow rate, an average diameter of 25 μm droplets was formed with the droplet generation frequency of $3\text{--}6 \times 10^6$ droplets per minute, which could be applied for *high-throughput* single-cell analysis. However, the direct quantification of trace elements in cells by ICP MS still faces a large bottleneck. One reason is caused by the serious matrix effect from complex intracellular components. To alleviate this disadvantage, an appropriate sample pretreatment technique can be taken. Yu et al. in Hu's Lab integrated a magnetic solid-phase microextraction (MSMPE) column on a chip to extract the released Cd and Se from single cells after treated with CdSe QDs and directly detected by ICP MS (Fig. 7.6b) [119]. Under the optimized extraction conditions, the limits of detection (LOD) of the developed platform are 2.2 and 21 ng L^{-1} for Cd and Se, separately.

Fig. 7.6 Microfluidic-based single-cell analysis with ICP MS detection. **a** Schematic diagrams of single-cell analysis on the combination of facile droplet chip and ICP MS. Reprinted with permission from Ref. [118]. Copyright © 2017 American Chemical Society. **b** Schematic illustration of chip-based magnetic solid-phase microextraction coupled with ICP MS for the determination of Cd and Se in single cells. Reprinted with permission from Ref. [119]. Copyright © 2018 Elsevier B.V



7.3.6 Paper Spray Ionization MS

As discussed above, the vacuum operating conditions of some ionization techniques (e.g., MALDI and SIMS) limit their applications in living cell analysis. The recently developed ambient ionization techniques, which allow the direct analysis of complex samples under ambient condition, are good selective for living cell analysis. Since the invention of ambient ionization techniques, many efforts have been made to apply ambient MS for single-cell analysis. A series of ambient MS have been explored to analyze various compounds at cellular/subcellular level, such as desorption electrospray ionization (DESI) [120], probe-ESI [121], easy ambient sonic-spray ionization (EASI) [122]. Paper spray ionization, possessing both the characteristics of ESI and ambient ionization techniques, has made some significant progress.

To improve the efficiency and capability for live cell analysis, automatic multi-channel paper-based chip-MS was developed for direct MS cell analysis by Lin's group [123, 124]. As shown in Fig. 7.7a, Liu et al. developed a microdialysis-paper spray ionization as the interface to MS for online chemical monitoring of cell culture [123]. A homemade microdialysis hollow fiber module was constructed to selectively dialysis molecules of interest from cell culture medium. Microdroplets were then generated with controllable size and frequency through a syringe pump and were directly dropped on the paper substrate for online

MS detection. They further developed a multi-channel paper-based chip for cell metabolism study by ESI MS under ambient condition [125]. As shown in Fig. 7.7b, a multi-channel microfluidic device with the functions of a concentration gradient generator and cell culture chambers was used to generate samples with different stimulation conditions. Paper spray ionization was simultaneously employed for microsampling these samples and as the interface for direct MS analysis without any sample pretreatment. On this platform, they investigated the effects of hypoxia on lactate efflux from normal and cancer cells and the differential inhibitory effects and dose–response information of α -cyano-4-hydroxycinnamate on different types of cancer cells. Instead of using paper as the substrate for ionization spray, Wu et al. developed a glass spray-MS platform for direct cell-based drug assay under ambient pressure (Fig. 7.7c) [126]. The authors later developed a multi-channel glass spray chip-MS platform, in which cell co-culture, cell apoptosis assay, and MS detection could be simultaneously performed [127]. Chen et al. later developed a cell-compatible polycarbonate paper chip for in situ live cell components detection by paper spray MS [124]. However, this method is well suitable for large amount of cell analysis, but not appropriate for single-cell analysis. To perform in situ single-cell analysis, a Live Single-Cell Extractor (LSCE) was presented

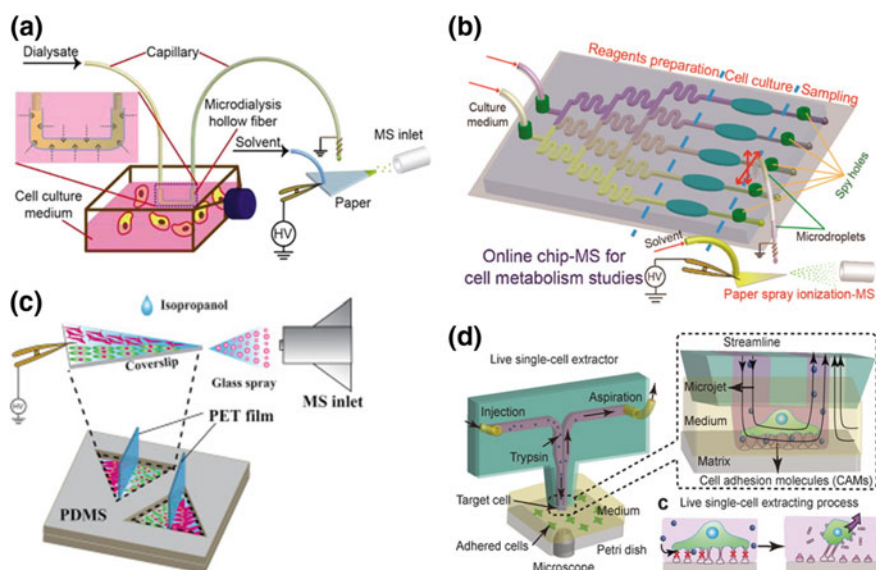


Fig. 7.7 Living single-cell analysis on microfluidic device. **a** Schematics of a microdialysis-paper spray ionization-MS system for online chemical monitoring of cell culture. Reprinted with permission from Ref. [123]. Copyright © 2014 American Chemical Society. **b** Schematic illustration of the online multi-channel microfluidic chip-MS platform for cell metabolism study. Reprinted with permission from Ref. [125]. Copyright © 2016 American Chemical Society. **c** A versatile glass spray-MS platform for direct drug assay. Reprinted with permission from Ref. [126]. Copyright © 2015 Elsevier B.V. **d** Microfluidic chip-based LSCE. Reprinted with permission from Ref. [128]. Copyright © 2018 John Wiley & Sons, Inc.

by Mao et al. for single-cell extraction, *cell adhesion, and cell heterogeneity analysis* (Fig. 7.7d) [128]. The tip of the LSCE was placed perpendicular to a petri dish with cell samples, and a stable microjet could be formed underneath the tip of the LSCE when the ratio between aspiration and injection flow rates is sufficiently high. They employed trypsin molecules as the injection liquid to selectively digest the adhered cell of interest. The collected cells can be further analyzed by mass spectrometry and other detection techniques.

The rapid assays of illicit drugs *are* becoming more urgent in Europe and North America. Espy et al. presented the determination of eight drugs of abuse in blood using paper spray or extraction spray MS in less than 2 min *of* minimal sample preparation [129]. Compared with conventional blood sampling methodologies, this method showed the potential for rapid, high-throughput, and quantitative assays of multi-abused drugs.

7.3.7 Mass Cytometry

Single cell mass cytometry, a technique of coupling flow cytometry with ICP MS, is firstly proposed by Garry Nolan's group at Stanford University [130]. In this technique, cells are labeled with epitope-specific antibodies conjugated to transition element isotope reporters. In contrast to the fluorophores used in conventional flow cytometry, the stained individual cells are ionized and sensitively detected with cytometry and time-of-flight ICP MS. Up to 34 parameters could be simultaneously detected by this mass cytometry technique. Later, Nolan's group applied this technique to other applications, such as delineating cell cycle stages [131] and identifying *in vivo* skeletal muscle stem cell [132]. However, the combination of mass cytometry with microfluidics has not been reported yet. Due to the multi-parameter analytical ability for cells as well as the flexible manipulation property for single cells, their advantages may promote the development of their combination system for the application in biological research field.

7.4 Applications in MS-Based Single-Cell Analysis

7.4.1 Nucleic Acids

Single-cell genetic analysis plays a critical role in the study of disease diagnosis, embryonic development, microbe detection, and so on. With the development of highly sensitive technologies, nucleic acid detection can be realized at single-molecule resolution. Recently, whole-genome evaluation is becoming increasingly popular at the single-cell level. Reverse transcriptase polymerase chain reaction (RT-PCR)-based approach is probably the most widely used technique to

amplify the transcribed target RNA strands, and the amplification steps were generally monitored by optical methods such as imaging via chemiluminescence or fluorescent labeling, aiming to reveal the heterogeneity of different cell types. For single-cell gene analysis, microfluidic-based RT-PCR *enabled* high-throughput sequencing applications and parallel analysis of multiple single cells. Microfluidic approaches also provide a flexible platform for sensitive detection of gene *with the measurement precision better than* conventional methods [133, 134]. For example, sample pretreatment procedures can be integrated on the microfluidics to remove some PCR inhibitors to reduce false-negative results [135].

7.4.2 Proteins

Single-cell-based qualitative and quantitative analysis of proteins play an essential role in *the* understanding of cellular functions and revealing protein heterogeneity, which is extremely important in biomarker discovery, disease diagnostics, pathology, and therapy [136]. Protein analysis at the single-cell level is challenging due to the low abundance of proteins in single cells, the large dynamic range of many protein constituents, and the temporary existence of cellular proteins responding to external stimulation [137, 138]. Microfluidic-based MS analysis *provides* an effective approach for multi-parameter, specific, high-throughput, and automated proteins studies. Many essential functions for protein identification, such as enzymatic digestion, separation, and sample infusion, can be integrated on the microfluidic device. For example, Zhu et al. developed a microfluidic-based approach termed nanoPOTS (nano-droplet processing in one-pot for trace samples) to increase sample processing efficiency for single-cell analysis (Fig. 7.8a) [139]. nanoPOTS uses robotic nanoliter liquid handling to dispense cells and reagents *into nanowell*s on a standard microscope slide. Cell suspension, MS-compatible surfactant, reducing reagent, alkylating agent, and multiple proteases were subsequently added into each nanowell with the total volume of 200 nL. To minimize evaporation during reaction incubation procedures, a layer of 30 μm PDMS was reversibly sealed to the nanowell chip. By combination with ultrasensitive nanoLC-MS, over 3000 proteins were confidently identified from just 10 HeLa cells.

Quantitative analysis of specific proteins is helpful for the diagnosis of early disease more accurately like cancer. Isobaric tags for relative and absolute quantitation (iTRAQ) is a widely used isobaric labeling method for quantitative proteomics by MS analysis. Recently, Ros et al. presented a reversible PDMS microfluidic system for relative and absolute quantification of targeted proteins by MALDI-MS/MS [140]. As shown in Fig. 7.8b, a two-layer device contained a fluid layer and a control layer *forming* a set of defined wells. An ITO-coated glass slide was reversible sealing with the two *layers* for fluid treatment and also served as the conductive MALDI-MS sample plate. In order to realize quantification analysis, the authors used iTRAQ labeling strategy to label proteins on *the* microfluidic device

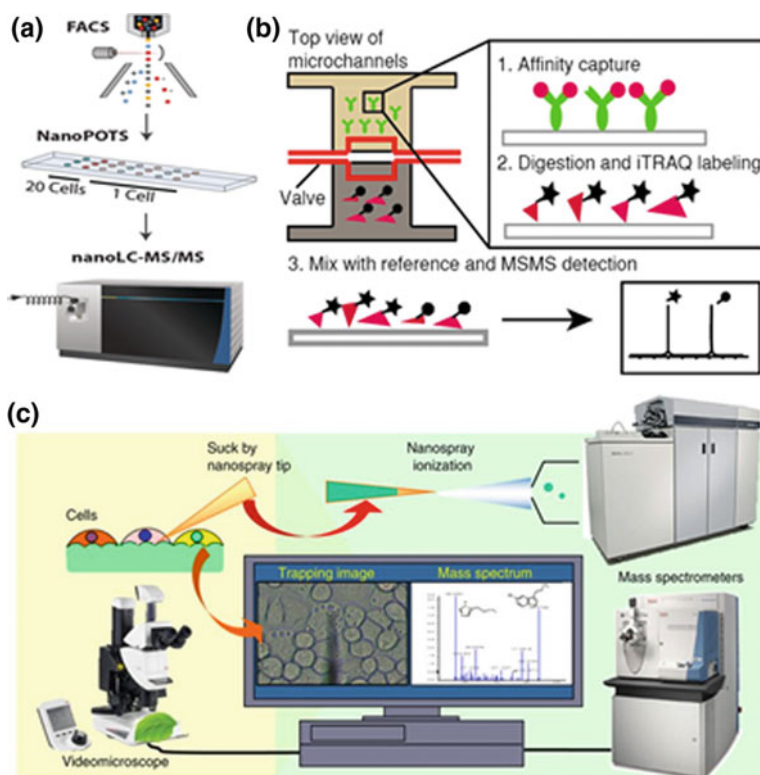


Fig. 7.8 Protein and small molecules analysis in single cells on microfluidic device. **a** Schematic of FACS–nanoPOTS coupling for quantitative proteomic analysis in single mammalian cells. Reprinted with permission from Ref. [139]. Copyright © 2018 John Wiley & Sons, Inc. **b** A quantitative approach employing isobaric tags with *MALDI-MS* realized with a microfluidic platform. Reprinted with permission from Ref. [140]. Copyright © 2016 American Chemical Society. **c** Schematic principle of live plant single-cell MS. Reprinted with permission from Ref. [144]. Copyright © 2015 Springer Nature Limited

for the first time. They also integrated all the necessary manipulation procedures on the chip, such as protein digestion, labeling, as well the matrix delivery. After finishing all liquid handling steps, the PDMS layer was removed, remaining analyte-matrix co-crystallized on the ITO glass surface for *MALDI-MS* detection. The apoptosis-related protein Bcl-2 was successfully detected, and the number of Bcl-2 molecules was quantitatively assessed.

Among proteins analysis, proteomics has attracted an increasing interest, with the aim to study the complete or subset of proteins present in a species under a certain condition. It is very useful for the investigation of the relationship between diseases and clinical diagnostics [141]. However, to develop a high-throughput method for single-cell proteomics by mass spectrometry, two major challenges should be resolved. Firstly, protein losses had to be minimized when delivering the

proteome of a single cell into a MS instrument. Secondly, peptides from single-cell samples *need* to be identified and quantified simultaneously. To overcome the above difficulties, Slavov et al. developed a single cell Proteomics by MS (SCoPE-MS) to identify distinct human cancer cell types based on their proteomes [142]. In this method, they manually picked live single cells under a microscope and lysed them mechanically which could obviate significant protein losses during LC/MS analysis. Besides, they used tandem mass tags (TMT) to quantify the levels of each TMT-labeled peptide and to increase analytical throughput. However, the single-cell processing is still done manually, and the introduction of microfluidic techniques into this system will greatly enhance the analytical capabilities for single cells.

7.4.3 *Small Molecules/Metabolomics*

The analysis of intercellular small molecules like metabolites and small molecule intermediates is extremely important. They are widely involved in signal pathways and have a close relationship with physiological and pathological processes. For example, glutathione (GSH) is one of the most important and potent antioxidants in our body. Wang et al. developed a Ag-Au nanoparticle-modified porous silicon chip with the surface as matrix to assist ionization LDI MS and could specially capture and analysis of thiol compounds through Au-S binding [108]. The array-patterned silicon chip showed high-throughput analytical ability and also had great potential for more efficient analysis of small thiol biomarkers in complex biological samples.

Single-cell metabolomics analysis is of great interest to biochemistry and clinical medicine scientists. It helps address fundamental biological questions and allows for the observation of metabolic phenomenon-related phenotypic heterogeneity in single cells. However, metabolomics analysis at the single-cell level is still a challenge because of its complex microenvironment and low content. Sensitive and high-throughput methods for single-cell metabolomics analysis are still in urgent need. Microfluidic techniques provide a promising platform for single-cell metabolomics. MS, a label-free and *having the ability* to provide structural information of chemicals, has become a key enabling tool in the field of metabolomics [143, 144]. Many studies have presented the combination system of microfluidics and MS for single-cell metabolites analysis. For example, Korenaga et al. developed an ink-jet automated single cells and matrices printing system to directly positioning of single cells at defined sites of ITO glass substrate for MALDI-MS analysis, and intercellular phospholipids from single or several cells were successfully detected [50]. In this work, microarrays of cells *through* the developed ink-jet printing system is extremely important because it provides the ability for imaging and automatic analysis, which opens the way to higher-throughput measurements. Masujima and his colleagues developed a live single-cell MS platform for single plant and animal cell analysis, especially for embryo cells [145–147]. In this technology, they used microspray tips or other microcapillary tips to insert into a

single cell to sample a small amount of cell's contents [144] (Fig. 7.8c). A microliter of ionization solvent was then added to the opposite end of the tip, and the trapped intercellular metabolites were finally sprayed into the mass spectrometer by applying a high voltage between the tip and the inlet of the MS.

7.4.4 Pharmacological Analysis

Tumor–endothelial cell interaction plays an important role in many physiological and pathological processes, such as cancer metastasis, angiogenesis, and colonization. Majority of researches have showed that crosstalk between tumor cells and endothelial cells via paracrine/juxtacrine action has a significant impact on tumor growth, progression, and drug efficiency. To better understand their interaction, Lin et al. developed an integrated microfluidic device to probe the interaction between tumor and endothelial cells and its application in drug screening, in which all the necessary procedures including cell co-culture, protein detection, micro-solid-phase extraction unit for drug metabolites, and online MS detection could be performed [148]. Cervical carcinoma cells (CaSki cells) and human umbilical vein endothelial cells (HUVECs) were co-cultured in the cell co-culture component, which allowed for real-time monitoring of paclitaxel-induced apoptosis, the contents of intercellular ROS and GSH. After stimulation with paclitaxel, cell culture medium was introduced into the specific aptamer-precoated reaction chamber through a connecting tube for cell-secreted proteins detection by fluorescent. Whereas for cell metabolites detection, cell co-culture and the pretreatment components were connected for desalting and purification of paclitaxel metabolites and *then online* detected by ESI MS. This integrated microfluidic platform *provides* a promising tool for drug screening using the *in vitro* cell co-culture model.

7.5 Conclusion and Outlook

Coupling of microfluidics with MS takes advantages of both technologies, with the purpose to improve efficiency, sensitivity, and throughput. In this chapter, we documented the significant improvements in microfluidic technologies for single-cell analysis with mass spectrometry detection over the past few years, covering the recent development in microfluidic manipulation techniques for single cells, innovations in the coupling of microfluidic chips with different types of MS, and their applications in biological research and drug development. The microfluidics has become increasingly integrated which contained multiple necessary functional units for single-cell capture, separation, and detection. Several approaches have been reported for single-cell generation, including microwells, micropatterns, traps, and droplets. Their applications have tended to multi-targets or even omics components. Although some advances have been made in single-cell

analysis by microfluidics and MS combination system, there are still some demands needed to be improved like more efficient single-cell manipulation and sample pretreatment abilities to compatible with the requirement of MS detector. With the increasing requirement of analytical throughput for single cells, computational methods with powerful data processing abilities *are* also needed to be simultaneously improved. Because of the complexity of cellular process and the detection limitation of one MS technique, two or more types of MS detectors can be used together to detect more intercellular components, which will be helpful for more comprehensive understanding of the function and regulation mechanism of intercellular molecules in biological processes. Moreover, developing a new methodology to maintain the single-cell viability is a significant and essential issue in the future to perform single-cell analysis in its original state. With the development of integrated microfluidics and MS combination systems for automated single-cell manipulation, sample pretreatment, and MS detection, more applications of microfluidics-MS systems in clinical diagnosis can be expected in the near future.

References

1. Buettner F, Natarajan KN, Casale FP, Proserpio V, Scialdone A, Theis FJ, Teichmann SA, Marioni JC, Stegle O (2015) Computational analysis of cell-to-cell heterogeneity in single-cell RNA-sequencing data reveals hidden subpopulations of cells. *Nat Biotechnol* 33 (2):155–160. <https://doi.org/10.1038/nbt.3102>
2. Junker JP, van Oudenaarden A (2014) Every cell is special: genome-wide studies add a new dimension to single-cell biology. *Cell* 157(1):8–11. <https://doi.org/10.1016/j.cell.2014.02.010>
3. Zenobi R (2013) Single-cell metabolomics: analytical and biological perspectives. *Science* 342(6163):1243259. <https://doi.org/10.1126/science.1243259>
4. Rubakhin SS, Romanova EV, Nemes P, Sweedler JV (2011) Profiling metabolites and peptides in single cells. *Nat Methods* 8(4 Suppl):S20–S29. <https://doi.org/10.1038/nmeth.1549>
5. Armbrrecht L, Dittrich PS (2017) Recent advances in the analysis of single cells. *Anal Chem* 89(1):2–21. <https://doi.org/10.1021/acs.analchem.6b04255>
6. Krutzik PO, Crane JM, Clutter MR, Nolan GP (2008) High-content single-cell drug screening with phosphospecific flow cytometry. *Nat Chem Biol* 4(2):132–142. <https://doi.org/10.1038/nchembio.2007.59>
7. Krutzik PO, Nolan GP (2006) Fluorescent cell barcoding in flow cytometry allows high-throughput drug screening and signaling profiling. *Nat Methods* 3(5):361–368. <https://doi.org/10.1038/nmeth872>
8. Whitesides GM (2006) The origins and the future of microfluidics. *Nature* 442(7101):368–373. <https://doi.org/10.1038/nature05058>
9. Park MC, Hur JY, Cho HS, Park SH, Suh KY (2011) High-throughput single-cell quantification using simple microwell-based cell docking and programmable time-course live-cell imaging. *Lab Chip* 11(1):79–86. <https://doi.org/10.1039/c0lc00114g>
10. Guan Z, Jia S, Zhu Z, Zhang M, Yang CJ (2014) Facile and rapid generation of large-scale microcollagen gel array for long-term single-cell 3D culture and cell proliferation heterogeneity analysis. *Anal Chem* 86(5):2789–2797. <https://doi.org/10.1021/ac500088m>

11. Weng L, Ellett F, Edd J, Wong KHK, Uygun K, Irimia D, Stott SL, Toner M (2017) A highly-occupied, single-cell trapping microarray for determination of cell membrane permeability. *Lab Chip* 17(23):4077–4088. <https://doi.org/10.1039/c7lc00883j>
12. Wu H, Wheeler A, Zare RN (2009) Chemical cytometry on a picoliter-scale integrated microfluidic chip. *Proc Natl Acad Sci U S A* 101:12809–12813. <https://doi.org/10.1073/pnas.0405299101>
13. Yang RJ, Fu LM, Hou HH (2018) Review and perspectives on microfluidic flow cytometers. *Sens Actuators B Chem* 266:26–45. <https://doi.org/10.1016/j.snb.2018.03.091>
14. Brouzes E, Medkova M, Savenelli N, Marran D, Twardowski M, Hutchison JB, Rothberg JM, Link DR, Perrimon N, Samuels ML (2009) Droplet microfluidic technology for single-cell high-throughput screening. *Proc Natl Acad Sci U S A* 106:14195–14200. <https://doi.org/10.1073/pnas.0903542106>
15. Huebner A, Srisa-Art M, Holt D, Abell C, Hollfelder F, deMello AJ, Edel JB (2007) Quantitative detection of protein expression in single cells using droplet microfluidics. *Chem Commun (Camb)* 12:1218–1220. <https://doi.org/10.1039/b618570c>
16. Zhang H, Liu KK (2008) Optical tweezers for single cells. *J R Soc Interface* 5(24):671–690. <https://doi.org/10.1098/rsif.2008.0052>
17. Amann R, Fuchs BM (2008) Single-cell identification in microbial communities by improved fluorescence in situ hybridization techniques. *Nat Rev Microbiol* 6(5):339–348. <https://doi.org/10.1038/nrmicro1888>
18. Wu H, Volponi JV, Oliver AE, Parikh AN, Simmons BA, Singh S (2011) In vivo lipidomics using single-cell Raman spectroscopy. *Proc Natl Acad Sci U S A* 108(9):3809–3814. <https://doi.org/10.1073/pnas.1009043108>
19. Walker BN, Antonakos C, Retterer ST, Vertes A (2013) Metabolic differences in microbial cell populations revealed by nanophotonic ionization. *Angew Chem Int Ed Engl* 52(13):3650–3653. <https://doi.org/10.1002/anie.201207348>
20. Venter A, Nefliu M, Cooks GR (2008) Ambient desorption ionization mass spectrometry. *Trends Anal Chem* 27(4):284–290. <https://doi.org/10.1016/j.trac.2008.01.010>
21. Yang Y, Deng J (2016) Analysis of pharmaceutical products and herbal medicines using ambient mass spectrometry. *Trends Anal Chem* 82:68–88. <https://doi.org/10.1016/j.trac.2016.04.011>
22. Gao D, Liu H, Jiang Y, Lin JM (2013) Recent advances in microfluidics combined with mass spectrometry: technologies and applications. *Lab Chip* 13(17):3309–3322. <https://doi.org/10.1039/c3lc50449b>
23. Chattopadhyay PK, Gierahn TM, Roederer M, Love JC (2014) Single-cell technologies for monitoring immune systems. *Nat Immunol* 15(2):128–135. <https://doi.org/10.1038/ni.2796>
24. Li Y, Chen D, Zhang Y, Liu C, Chen P, Wang Y, Feng X, Du W, Liu BF (2016) High-throughput single cell multidrug resistance analysis with multifunctional gradients-customizing microfluidic device. *Sens Actuators B Chem* 225:563–571. <https://doi.org/10.1016/j.snb.2015.11.097>
25. Espina V, Heiby M, Pierobon M, Liotta LA (2007) Laser capture microdissection technology. *Expert Rev Mol Diagn* 7:647–657. <https://doi.org/10.1586/14737159.7.5.647>
26. Wheeler AR, Thronset WR, Whelan RJ, Leach AM, Zare RN, Liao YH, Farrell K, Manger ID, Daridon A (2003) Microfluidic device for single-cell analysis. *Anal Chem* 75:3581–3586. <https://doi.org/10.1021/ac0340758>
27. Gao J, Yin XF, Fang ZL (2004) Integration of single cell injection, cell lysis, separation and detection of intracellular constituents on a microfluidic chip. *Lab Chip* 4(1):47–52. <https://doi.org/10.1039/b310552k>
28. Zare RN, Kim S (2010) Microfluidic platforms for single-cell analysis. *Annu Rev Biomed Eng* 12:187–201. <https://doi.org/10.1146/annurev-bioeng-070909-105238>
29. Wang Y, Shah P, Phillips C, Sims CE, Allbritton NL (2012) Trapping cells on a stretchable microwell array for single-cell analysis. *Anal Bioanal Chem* 402(3):1065–1072. <https://doi.org/10.1007/s00216-011-5535-9>

30. Hosis S, Murthy SK, Koppes AN (2016) Microfluidic sample preparation for single cell analysis. *Anal Chem* 88(1):354–380. <https://doi.org/10.1021/acs.analchem.5b04077>
31. Konry T, Sarkar S, Sabhachandani P, Cohen N (2016) Innovative tools and technology for analysis of single cells and cell-cell interaction. *Annu Rev Biomed Eng* 18:259–284. <https://doi.org/10.1146/annurev-bioeng-090215-112735>
32. Liu CS, Liu J, Gao D, Ding MY, Lin JM (2010) Fabrication of microwell arrays based on two-dimensional ordered polystyrene microspheres for high-throughput single-cell analysis. *Anal Chem* 82:9418–9424. <https://doi.org/10.1021/ac102094r>
33. Yang W, Yu H, Li G, Wei F, Wang Y, Liu L (2017) Mask-free fabrication of a versatile microwell chip for multidimensional cellular analysis and drug screening. *Lab Chip* 17(24):4243–4252. <https://doi.org/10.1039/c7lc01101f>
34. Nguyen A, Khoo WH, Moran I, Croucher PI, Phan TG (2018) Single cell RNA sequencing of rare immune cell populations. *Front Immunol* 9:1553. <https://doi.org/10.3389/fimmu.2018.01553>
35. Park SM, Lee JY, Hong S, Lee SH, Dimov IK, Lee H, Suh S, Pan Q, Li K, Wu AM, Mumenthaler SM, Mallick P, Lee LP (2016) Dual transcript and protein quantification in a massive single cell array. *Lab Chip* 16(19):3682–3688. <https://doi.org/10.1039/c6lc00762g>
36. Swennenhuis JF, Tibbe AG, Stevens M, Katika MR, van Dalum J, Tong HD, van Rijn CJ, Terstappen LW (2015) Self-seeding microwell chip for the isolation and characterization of single cells. *Lab Chip* 15(14):3039–3046. <https://doi.org/10.1039/c5lc00304k>
37. Huang L, Chen Y, Chen Y, Wu H (2015) Centrifugation-assisted single-cell trapping in a truncated cone-shaped microwell array chip for the real-time observation of cellular apoptosis. *Anal Chem* 87(24):12169–12176. <https://doi.org/10.1021/acs.analchem.5b03031>
38. Jimenez-Valdes RJ, Rodriguez-Moncayo R, Cedillo-Alcantar DF, Garcia-Cordero JL (2017) Massive parallel analysis of single cells in an integrated microfluidic platform. *Anal Chem* 89(10):5210–5220. <https://doi.org/10.1021/acs.analchem.6b04485>
39. Liu W, Wei H, Lin Z, Mao S, Lin JM (2011) Rare cell chemiluminescence detection based on aptamer-specific capture in microfluidic channels. *Biosens Bioelectron* 28(1):438–442. <https://doi.org/10.1016/j.bios.2011.07.067>
40. Revzin A, Sekine K, Sin A, Tompkins RG, Toner M (2005) Development of a microfabricated cytometry platform for characterization and sorting of individual leukocytes. *Lab Chip* 5(1):30–37. <https://doi.org/10.1039/b405557h>
41. Lin L, Chu YS, Thiery JP, Lim CT, Rodriguez I (2013) Microfluidic cell trap array for controlled positioning of single cells on adhesive micropatterns. *Lab Chip* 13(4):714–721. <https://doi.org/10.1039/c2lc41070b>
42. Chen Q, Wu J, Zhang Y, Lin Z, Lin JM (2012) Targeted isolation and analysis of single tumor cells with aptamer-encoded microwell array on microfluidic device. *Lab Chip* 12(24):5180–5185. <https://doi.org/10.1039/c2lc40858a>
43. Ruiz A, Zychowicz M, Ceriotti L, Mehn D, Sirghi L, Rauscher H, Mannelli I, Colpo P, Buzanska L, Rossi F (2013) Microcontact printing and microspotting as methods for direct protein patterning on plasma deposited polyethylene oxide: application to stem cell patterning. *Biomed Microdevices* 15:495–507. <https://doi.org/10.1007/s10544-013-9749-9>
44. Priest DG, Tanaka N, Tanaka Y, Taniguchi Y (2017) Micro-patterned agarose gel devices for single-cell high-throughput microscopy of *E. coli* cells. *Sci Rep* 7:17750. <https://doi.org/10.1038/s41598-017-17544-2>
45. Yang T, Gao D, Jin F, Jiang Y, Liu H (2016) Surface-printed microdot array chips coupled with matrix-assisted laser desorption/ionization mass spectrometry for high-throughput single-cell patterning and phospholipid analysis. *Rapid Commun Mass Spectrom* 30(Suppl 1):73–79. <https://doi.org/10.1002/rcm.7628>
46. Ren D, Xia Y, Wang J, You Z (2013) Micropatterning of single cell arrays using the PEG-Silane and biotin-(strept)avidin system with photolithography and chemical vapor deposition. *Sens Actuators B Chem* 188:340–346. <https://doi.org/10.1016/j.snb.2013.07.037>

47. Wang Z, Zhang P, Kirkland B, Liu Y, Guan J (2012) Microcontact printing of polyelectrolytes on PEG using an unmodified PDMS stamp for micropatterning nanoparticles, DNA, proteins and cells. *Soft Matter* 8(29):7630. <https://doi.org/10.1039/c2sm25835h>
48. Beckwith KM, Sikorski P (2013) Patterned cell arrays and patterned co-cultures on polydopamine-modified poly(vinyl alcohol) hydrogels. *Biofabrication* 5(4):045009. <https://doi.org/10.1088/1758-5082/5/4/045009>
49. Chen Z, Li Y, Liu W, Zhang D, Zhao Y, Yuan B, Jiang X (2009) Patterning mammalian cells for modeling three types of naturally occurring cell-cell interactions. *Angew Chem Int Ed Engl* 48(44):8303–8305. <https://doi.org/10.1002/anie.200902708>
50. Korenaga A, Chen F, Li H, Uchiyama K, Lin JM (2017) Inkjet automated single cells and matrices printing system for matrix-assisted laser desorption/ionization mass spectrometry. *Talanta* 162:474–478. <https://doi.org/10.1016/j.talanta.2016.10.055>
51. Custodio CA, Miguel-Arranz VS, Gropeanu RA, Gropeanu M, Wirkner M, Reis RL, Mano JF, del Campo A (2014) Photopatterned antibodies for selective cell attachment. *Langmuir* 30(33):10066–10071. <https://doi.org/10.1021/la502688h>
52. Kane RS, Takayama S, Ostuni E, Ingber DE, Whitesides GM (1999) Patterning proteins and cells using soft lithography. *Biomaterials* 20(23–24):2363–2376. [https://doi.org/10.1016/S0142-9612\(99\)00165-9](https://doi.org/10.1016/S0142-9612(99)00165-9)
53. Jiang X, Bruzewicz DA, Wong AP, Piel M, Whitesides GM (2005) Directing cell migration with asymmetric micropatterns. *Proc Natl Acad Sci U S A* 102:975–978. <https://doi.org/10.1073/pnas.0408954102>
54. Thery M, Racine V, Pepin A, Piel M, Chen Y, Sibarita JB, Bornens M (2005) The extracellular matrix guides the orientation of the cell division axis. *Nat Cell Biol* 7(10):947–953. <https://doi.org/10.1038/ncb1307>
55. Zhao L, Guo T, Wang L, Liu Y, Chen G, Zhou H, Zhang M (2018) Tape-assisted photolithographic-free microfluidic chip cell patterning for tumor metastasis study. *Anal Chem* 90(1):777–784. <https://doi.org/10.1021/acs.analchem.7b03225>
56. Chaffer CL, Weinberg RA (2011) A perspective on cancer cell metastasis. *Science* 331(6024):1559–1564. <https://doi.org/10.1126/science.1203543>
57. Ahmed MG, Abate MF, Song Y, Zhu Z, Yan F, Xu Y, Wang X, Li Q, Yang C (2017) Isolation, detection, and antigen-based profiling of circulating tumor cells using a size-dictated immunocapture chip. *Angew Chem Int Ed Engl* 56(36):10681–10685. <https://doi.org/10.1002/anie.201702675>
58. Shin DS, You J, Rahimian A, Vu T, Siltanen C, Ehsanipour A, Stybayeva G, Sutcliffe J, Revzin A (2014) Photodegradable hydrogels for capture, detection, and release of live cells. *Angew Chem Int Ed Engl* 53(31):8221–8224. <https://doi.org/10.1002/anie.201404323>
59. Nilsson J, Evander M, Hammarstrom B, Laurell T (2009) Review of cell and particle trapping in microfluidic systems. *Anal Chim Acta* 649(2):141–157. <https://doi.org/10.1016/j.aca.2009.07.017>
60. Chen H, Sun J, Wolvetang E, Cooper-White J (2015) High-throughput, deterministic single cell trapping and long-term clonal cell culture in microfluidic devices. *Lab Chip* 15(4):1072–1083. <https://doi.org/10.1039/c4lc01176g>
61. Zhu J, Shang J, Olsen T, Liu K, Brenner D, Lin Q (2014) A mechanically tunable microfluidic cell-trapping device. *Sens Actuators A Phys* 215:197–203. <https://doi.org/10.1016/j.sna.2013.10.016>
62. Skelley AM, Kirak O, Suh H, Jaenisch R, Voldman J (2009) Microfluidic control of cell pairing and fusion. *Nat Methods* 6(2):147–152. <https://doi.org/10.1038/nmeth.1290>
63. Yamaguchi Y, Arakawa T, Takeda N, Edagawa Y, Shoji S (2009) Development of a poly-dimethylsiloxane microfluidic device for single cell isolation and incubation. *Sens Actuators B Chem* 136(2):555–561. <https://doi.org/10.1016/j.snb.2008.11.052>
64. Sauzade M, Brouzes E (2017) Deterministic trapping, encapsulation and retrieval of single-cells. *Lab Chip* 17(13):2186–2192. <https://doi.org/10.1039/c7lc00283a>

65. Jin Q, Li M, Polat B, Paidi SK, Dai A, Zhang A, Pagaduan JV, Barman I, Gracias DH (2017) Mechanical trap surface-enhanced raman spectroscopy for three-dimensional surface molecular imaging of single live cells. *Angew Chem Int Ed Engl* 56(14):3822–3826. <https://doi.org/10.1002/anie.201700695>
66. Zhang P, Ren L, Zhang X, Shan Y, Wang Y, Ji Y, Yin H, Huang WE, Xu J, Ma B (2015) Raman-activated cell sorting based on dielectrophoretic single-cell trap and release. *Anal Chem* 87(4):2282–2289. <https://doi.org/10.1021/ac503974e>
67. Guo F, Chen Y, Xie Z, Lata JP, Li P, Ren L, Liu J, Yang J, Dao M, Sureshd S, Huang TJ (2016) Three-dimensional manipulation of single cells using surface acoustic waves. *Proc Natl Acad Sci U S A* 113:1522–1527. <https://doi.org/10.1073/pnas.1524813113>
68. Collins DJ, Morahan B, Garcia-Bustos J, Doerig C, Plebanski M, Neild A (2015) Two-dimensional single-cell patterning with one cell per well driven by surface acoustic waves. *Nat Commun* 6:8686. <https://doi.org/10.1038/ncomms9686>
69. Joensson HN, Andersson SH (2012) Droplet microfluidics—a tool for single-cell analysis. *Angew Chem Int Ed Engl* 51(49):12176–12192. <https://doi.org/10.1002/anie.201200460>
70. Hummer D, Kurth F, Naredi-Rainer N, Dittrich PS (2016) Single cells in confined volumes: microchambers and microdroplets. *Lab Chip* 16(3):447–458. <https://doi.org/10.1039/c5lc01314c>
71. Okushima S, Nisisako T, Torii T, Higuchi T (2004) Controlled production of monodisperse double emulsions by two-step droplet breakup in microfluidic devices. *Langmuir* 20:9905–9908. <https://doi.org/10.1021/la0480336>
72. Teh SY, Lin R, Hung LH, Lee AP (2008) Droplet microfluidics. *Lab Chip* 8(2):198–220. <https://doi.org/10.1039/b715524g>
73. Lagus TP, Edd JF (2013) A review of the theory, methods and recent applications of high-throughput single-cell droplet microfluidics. *J Phys D Appl Phys* 46(11):114005. <https://doi.org/10.1088/0022-3727/46/11/114005>
74. Chen F, Lin L, Zhang J, He Z, Uchiyama K, Lin JM (2016) Single-cell analysis using drop-on-demand inkjet printing and probe electrospray ionization mass spectrometry. *Anal Chem* 88(8):4354–4360. <https://doi.org/10.1021/acs.analchem.5b04749>
75. Zhang XC, Wei ZW, Gong XY, Si XY, Zhao YY, Yang CD, Zhang SC, Zhang XR (2016) Integrated droplet-based microextraction with ESI-MS for removal of matrix interference in single-cell analysis. *Sci Rep* 6:24730. <https://doi.org/10.1038/srep24730>
76. Guo XL, Wei Y, Lou Q, Zhu Y, Fang Q (2018) Manipulating femtoliter to picoliter droplets by pins for single cell analysis and quantitative biological assay. *Anal Chem* 90(9):5810–5817. <https://doi.org/10.1021/acs.analchem.8b00343>
77. Li ZY, Huang M, Wang XK, Zhu Y, Li JS, Wong CCL, Fang Q (2018) Nanoliter-scale oil-air-droplet chip-based single cell proteomic analysis. *Anal Chem* 90(8):5430–5438. <https://doi.org/10.1021/acs.analchem.8b00661>
78. Zhang L, Vertes A (2018) Single-cell mass spectrometry approaches to explore cellular heterogeneity. *Angew Chem Int Ed Engl* 57(17):4466–4477. <https://doi.org/10.1002/anie.201709719>
79. Comi TJ, Do TD, Rubakhin SS, Sweedler JV (2017) Categorizing cells on the basis of their chemical profiles: progress in single-cell mass spectrometry. *J Am Chem Soc* 139(11):3920–3929. <https://doi.org/10.1021/jacs.6b12822>
80. Yang Y, Huang Y, Wu J, Liu N, Deng J, Luan T (2017) Single-cell analysis by ambient mass spectrometry. *Trends Anal Chem* 90:14–26. <https://doi.org/10.1016/j.trac.2017.02.009>
81. Dole M, Mack LL, Hines RL, Mobley RC, Ferguson LD, Alice MB (1968) Molecular beams of macroions. *J Chem Phys* 49(5):2240–2249. <https://doi.org/10.1063/1.1670391>
82. John B, Fenn MM, Meng CK, Wong SF, Whitehouse GM (1989) Electrospray ionization for mass spectrometry of large molecules. *Science* 246(4926):64–71. <https://doi.org/10.1126/science.2675315>
83. Mao P, Wang HT, Yang P, Wang D (2011) Multinozzle emitter arrays for nanoelectrospray mass spectrometry. *Anal Chem* 83(15):6082–6089. <https://doi.org/10.1021/ac2011813>

84. Oleschuk RD, Harrison DJ (2000) Analytical microdevices for mass spectrometry. *Trends Anal Chem* 19:379–388. [https://doi.org/10.1016/S0165-9936\(00\)00013-3](https://doi.org/10.1016/S0165-9936(00)00013-3)
85. Polat AN, Ozlu N (2014) Towards single-cell LC-MS phosphoproteomics. *Analyst* 139 (19):4733–4749. <https://doi.org/10.1039/c4an00463a>
86. Ramos Payan MD, Jensen H, Petersen NJ, Hansen SH, Pedersen-Bjergaard S (2012) Liquid-phase microextraction in a microfluidic-chip–high enrichment and sample clean-up from small sample volumes based on three-phase extraction. *Anal Chim Acta* 735:46–53. <https://doi.org/10.1016/j.aca.2012.05.023>
87. Ji J, Nie L, Qiao L, Li Y, Guo L, Liu B, Yang P, Girault HH (2012) Proteolysis in microfluidic droplets: an approach to interface protein separation and peptide mass spectrometry. *Lab Chip* 12(15):2625–2629. <https://doi.org/10.1039/c2lc40206h>
88. Dietze C, Schulze S, Ohla S, Gilmore K, Seeberger PH, Belder D (2016) Integrated on-chip mass spectrometry reaction monitoring in microfluidic devices containing porous polymer monolithic columns. *Analyst* 141(18):5412–5416. <http://doi.org/10.1039/c6an01467d>
89. Wei H, Li H, Gao D, Lin JM (2010) Multi-channel microfluidic devices combined with electrospray ionization quadrupole time-of-flight mass spectrometry applied to the monitoring of glutamate release from neuronal cells. *Analyst* 135(8):2043–2050. <https://doi.org/10.1039/c0an00162g>
90. Jie M, Mao S, Li H, Lin JM (2017) Multi-channel microfluidic chip-mass spectrometry platform for cell analysis. *Chin Chem Lett* 28(8):1625–1630. <https://doi.org/10.1016/j.ccl.2017.05.024>
91. Jie M, Mao S, Liu H, He Z, Li HF, Lin JM (2017) Evaluation of drug combination for glioblastoma based on an intestine-liver metabolic model on microchip. *Analyst* 142 (19):3629–3638. <https://doi.org/10.1039/c7an00453b>
92. Gao D, Wei H, Guo GS, Lin JM (2010) Microfluidic cell culture and metabolism detection with electrospray ionization quadrupole time-of-flight mass spectrometer. *Anal Chem* 82:5679–5685. <https://doi.org/10.1021/ac101370p>
93. Wei H, Li H, Mao S, Lin JM (2011) Cell signaling analysis by mass spectrometry under coculture conditions on an integrated microfluidic device. *Anal Chem* 83(24):9306–9313. <https://doi.org/10.1021/ac201709f>
94. Chen Q, Wu J, Zhang Y, Lin JM (2012) Qualitative and quantitative analysis of tumor cell metabolism via stable isotope labeling assisted microfluidic chip electrospray ionization mass spectrometry. *Anal Chem* 84(3):1695–1701. <https://doi.org/10.1021/ac300003k>
95. Mao S, Gao D, Liu W, Wei H, Lin JM (2012) Imitation of drug metabolism in human liver and cytotoxicity assay using a microfluidic device coupled to mass spectrometric detection. *Lab Chip* 12(1):219–226. <https://doi.org/10.1039/c1lc20678h>
96. Mao S, Zhang J, Li H, Lin JM (2013) Strategy for signaling molecule detection by using an integrated microfluidic device coupled with mass spectrometry to study cell-to-cell communication. *Anal Chem* 85(2):868–876. <https://doi.org/10.1021/ac303164b>
97. Huang Q, Mao S, Khan M, Zhou L, Lin JM (2018) Dean flow assisted cell ordering system for lipid profiling in single-cells using mass spectrometry. *Chem Commun* 54(21):2595–2598. <https://doi.org/10.1039/c7cc09608a>
98. Karas M, Hillenkamp F (1988) Laser desorption ionization of proteins with molecular masses exceeding 10,000 daltons. *Anal Chem* 60(20):2299–2301. <https://doi.org/10.1021/ac00171a028>
99. Tanaka K, Waki H, Ido Y, Akita S, Yoshida Y, Yoshida T, Matsuo T (1988) Protein and polymer analyses up to m/z 100,000 by laser ionization time-of-flight mass spectrometry. *Rapid Commun Mass Spectrom* 2:151–153. <https://doi.org/10.1002/rcm.1290020802>
100. Lin Z, Cai Z (2018) Negative ion laser desorption/ionization time-of-flight mass spectrometric analysis of small molecules by using nanostructured substrate as matrices. *Mass Spectrom Rev* 37:681–696. <https://doi.org/10.1002/mas.21558>
101. Tycova A, Ledvina V, Kleparnik K (2017) Recent advances in CE-MS coupling: instrumentation, methodology, and applications. *Electrophoresis* 38(1):115–134. <https://doi.org/10.1002/elps.201600366>

102. Trouillon R, Passarelli MK, Wang J, Kurczy ME, Ewing AG (2013) Chemical analysis of single cells. *Anal Chem* 85(2):522–542. <https://doi.org/10.1021/ac303290s>
103. Lagarrigue M, Becker M, Lavigne R, Deininger SO, Walch A, Aubry F, Suckau D, Pineau C (2011) Revisiting rat spermatogenesis with MALDI imaging at 20- μ m resolution. *Mol Cell Proteomics* 10(3):M110-005991. <https://doi.org/10.1074/mcp.m110.005991>
104. Zimmerman TA, Rubakhin SS, Sweedler JV (2011) MALDI mass spectrometry imaging of neuronal cell cultures. *J Am Soc Mass Spectrom* 22:828–836. <https://doi.org/10.1007/s13361-011-0111-2>
105. Ibanez AJ, Fagerer SR, Schmidt AM, Urban PL, Jefimovs K, Geiger P, Dechant R, Heinemann M, Zenobi R (2013) Mass spectrometry-based metabolomics of single yeast cells. *Proc Natl Acad Sci U S A* 110(22):8790–8794. <https://doi.org/10.1073/pnas.1209302110>
106. Neupert S, Rubakhin SS, Sweedler JV (2012) Targeted single-cell microchemical analysis: MS-based peptidomics of individual paraformaldehyde-fixed and immunolabeled neurons. *Chem Biol* 19(8):1010–1019. <https://doi.org/10.1016/j.chembiol.2012.05.023>
107. Xie W, Gao D, Jin F, Jiang Y, Liu H (2015) Study of phospholipids in single cells using an integrated microfluidic device combined with matrix-assisted laser desorption/ionization mass spectrometry. *Anal Chem* 87(14):7052–7059. <https://doi.org/10.1021/acs.analchem.5b00010>
108. Wang J, Jie M, Li H, Lin L, He Z, Wang S, Lin JM (2017) Gold nanoparticles modified porous silicon chip for SALDI-MS determination of glutathione in cells. *Talanta* 168:222–229. <https://doi.org/10.1016/j.talanta.2017.02.041>
109. Huang L, Chen Y, Weng LT, Leung M, Xing X, Fan Z, Wu H (2016) Fast single-cell patterning for study of drug-induced phenotypic alterations of HeLa cells using time-of-flight secondary ion mass spectrometry. *Anal Chem* 88(24):12196–12203. <https://doi.org/10.1021/acs.analchem.6b03170>
110. Fritzsche FS, Dusny C, Frick O, Schmid A (2012) Single-cell analysis in biotechnology, systems biology, and biocatalysis. *Annu Rev Chem Biomol Eng* 3:129–155. <https://doi.org/10.1146/annurev-chembioeng-062011-081056>
111. Kleparnik K (2013) Recent advances in the combination of capillary electrophoresis with mass spectrometry: from element to single-cell analysis. *Electrophoresis* 34(1):70–85. <https://doi.org/10.1002/elps.201200488>
112. Zhong X, Zhang Z, Jiang S, Li L (2014) Recent advances in coupling capillary electrophoresis-based separation techniques to ESI and MALDI-MS. *Electrophoresis* 35(9):1214–1225. <https://doi.org/10.1002/elps.201300451>
113. Mellors JS, Jorabchi K, Smith L, Ramsey JM (2010) Integrated microfluidic device for automated single cell analysis using electrophoretic separation and electrospray ionization mass spectrometry. *Anal Chem* 82:967–973. <https://doi.org/10.1021/ac902218y>
114. Onjiko RM, Moody SA, Nemes P (2015) Single-cell mass spectrometry reveals small molecules that affect cell fates in the 16-cell embryo. *Proc Natl Acad Sci U S A* 112(21):6545–6550. <https://doi.org/10.1073/pnas.1423682112>
115. Wei X, Hu LL, Chen ML, Yang T, Wang JH (2016) Analysis of the distribution pattern of chromium species in single cells. *Anal Chem* 88(24):12437–12444. <https://doi.org/10.1021/acs.analchem.6b03810>
116. Flores SE, Day AS, Keenan JI (2015) Measurement of total iron in *Helicobacter pylori*-infected gastric epithelial cells. *Biometals* 28(1):143–150. <https://doi.org/10.1007/s10534-014-9810-z>
117. Wang M, Zhang Z, Meng J, Wang H, He M, Zhang F, Liu Y, Hu B, He Z, Hu Q, Wang H (2015) In vivo study of immunogenicity and kinetic characteristics of a quantum dot-labelled baculovirus. *Biomaterials* 64:78–87. <https://doi.org/10.1016/j.biomaterials.2015.06.030>
118. Wang H, Chen B, He M, Hu B (2017) A facile droplet-chip-time-resolved inductively coupled plasma mass spectrometry online system for determination of zinc in single cell. *Anal Chem* 89(9):4931–4938. <https://doi.org/10.1021/acs.analchem.7b00134>

119. Yu X, Chen B, He M, Wang H, Hu B (2018) Chip-based magnetic solid phase microextraction coupled with ICP-MS for the determination of Cd and Se in HepG2 cells incubated with CdSe quantum dots. *Talanta* 179:279–284. <https://doi.org/10.1016/j.talanta.2017.11.013>
120. Ferreira CR, Eberlin LS, Hallett JE, Cooks RG (2012) Single oocyte and single embryo lipid analysis by desorption electrospray ionization mass spectrometry. *J Mass Spectrom* 47(1):29–33. <https://doi.org/10.1002/jms.2022>
121. Nakashima T, Wada H, Morita S, Erra-Balsells R, Hiraoka K, Nonami H (2016) Single-cell metabolite profiling of stalk and glandular cells of intact trichomes with internal electrode capillary pressure probe electrospray ionization mass spectrometry. *Anal Chem* 88(6):3049–3057. <https://doi.org/10.1021/acs.analchem.5b03366>
122. Liu Y, Zhang J, Nie H, Dong C, Li Z, Zheng Z, Bai Y, Liu H, Zhao J (2014) Study on variation of lipids during different growth phases of living cyanobacteria using easy ambient sonic-spray ionization mass spectrometry. *Anal Chem* 86(14):7096–7102. <https://doi.org/10.1021/ac501596v>
123. Liu W, Wang N, Lin X, Ma Y, Lin JM (2014) Interfacing microsampling droplets and mass spectrometry by paper spray ionization for online chemical monitoring of cell culture. *Anal Chem* 86(14):7128–7134. <https://doi.org/10.1021/ac501678q>
124. Chen Q, He Z, Liu W, Lin X, Wu J, Li H, Lin JM (2015) Engineering cell-compatible paper chips for cell culturing, drug screening, and mass spectrometric sensing. *Adv Healthc Mater* 4(15):2291–2296. <https://doi.org/10.1002/adhm.201500383>
125. Liu W, Lin JM (2016) Online monitoring of lactate efflux by multi-channel microfluidic chip-mass spectrometry for rapid drug evaluation. *ACS Sens* 1(4):344–347. <https://doi.org/10.1021/acssensors.5b00221>
126. Wu J, Wang S, Chen Q, Jiang H, Liang S, Lin JM (2015) Cell-patterned glass spray for direct drug assay using mass spectrometry. *Anal Chim Acta* 892:132–139. <https://doi.org/10.1016/j.aca.2015.08.020>
127. Wu J, Jie M, Dong X, Qi H, Lin JM (2016) Multi-channel cell co-culture for drug development based on glass microfluidic chip-mass spectrometry coupled platform. *Rapid Commun Mass Spectrom* 30(Suppl 1):80–86. <https://doi.org/10.1002/rcm.7643>
128. Mao S, Zhang W, Huang Q, Khan M, Li H, Uchiyama K, Lin JM (2018) In situ scatheless cell detachment reveals correlation between adhesion strength and viability at single-cell resolution. *Angew Chem Int Ed Engl* 57(1):236–240. <https://doi.org/10.1002/anie.201710273>
129. Espy RD, Teunissen SF, Manicke NE, Ren Y, Ouyang Z, van Asten A, Cooks RG (2014) Paper spray and extraction spray mass spectrometry for the direct and simultaneous quantification of eight drugs of abuse in whole blood. *Anal Chem* 86(15):7712–7718. <https://doi.org/10.1021/ac5016408>
130. Bendall SC, Simonds EF, Qiu P, Amir ED, Krutzik PO, Finck R, Brugner RV, Melamed R, Trejo A, Ornatsky OI, Balderas RS, Plevritis SK, Sachs K, Pe'er D, Tanner SD, Nolan GP (2011) Single-cell mass cytometry of differential immune and drug responses across a human hematopoietic continuum. *Science* 332:687–696. <https://doi.org/10.1126/science.1198704>
131. Behbehani GK, Bendall SC, Clutter MR, Fantl WJ, Nolan GP (2012) Single-cell mass cytometry adapted to measurements of the cell cycle. *Cytometry A* 81(7):552–566. <https://doi.org/10.1002/cyto.a.22075>
132. Porpiglia E, Samusik N, Ho ATV, Cosgrove BD, Mai T, Davis KL, Jager A, Nolan GP, Bendall SC, Fantl WJ, Blau HM (2017) High-resolution myogenic lineage mapping by single-cell mass cytometry. *Nat Cell Biol* 19(5):558–567. <https://doi.org/10.1038/ncb3507>
133. Tang F, Barbacioru C, Wang Y, Nordman E, Lee C, Xu N, Wang X, Bodeau J, Tuch BB, Siddiqui A, Lao K, Surani MA (2009) mRNA-Seq whole-transcriptome analysis of a single cell. *Nat Methods* 6:377. <https://doi.org/10.1038/nmeth.1315>

134. Streets AM, Zhang X, Cao C, Pang Y, Wu X, Xiong L, Yang L, Fu Y, Zhao L, Tang F, Huang Y (2014) Microfluidic single-cell whole-transcriptome sequencing. *Proc Natl Acad Sci U S A* 111(19):7048–7053. <https://doi.org/10.1073/pnas.1402030111>
135. Geng T, Mathies RA (2015) Minimizing inhibition of PCR-STR typing using digital agarose droplet microfluidics. *Forensic Sci Int Genet* 14:203–209. <https://doi.org/10.1016/j.fsigen.2014.10.007>
136. Majewski IJ, Bernards R (2011) Taming the dragon: genomic biomarkers to individualize the treatment of cancer. *Nat Med* 17(3):304–312. <https://doi.org/10.1038/nm.2311>
137. Beulig RJ, Warias R, Heiland JJ, Ohla S, Zeitler K, Belder D (2017) A droplet-chip/mass spectrometry approach to study organic synthesis at nanoliter scale. *Lab Chip* 17(11):1996–2002. <https://doi.org/10.1039/c7lc00313g>
138. Nolan GP, Fiering S, Nicolas JF, Herzenberg LA (1988) Fluorescence-activated cell analysis and sorting of viable mammalian cells based on beta-D-galactosidase activity after transduction of *Escherichia coli* lacZ. *Proc Natl Acad Sci U S A* 95:2603–2607. <https://doi.org/10.1073/pnas.95.5.2603>
139. Zhu Y, Clair G, Chrisler WB, Shen Y, Zhao R, Shukla AK, Moore RJ, Misra RS, Pryhuber GS, Smith RD, Ansong C, Kelly RT (2018) Proteomic analysis of single mammalian cells enabled by microfluidic nanodroplet sample preparation and ultrasensitive nanoLC-MS. *Angew Chem Int Ed Engl* 57(38):12370–12374. <https://doi.org/10.1002/anie.201802843>
140. Yang M, Nelson R, Ros A (2016) Toward analysis of proteins in single cells: a quantitative approach employing isobaric tags with MALDI mass spectrometry realized with a microfluidic platform. *Anal Chem* 88(13):6672–6679. <https://doi.org/10.1021/acs.analchem.5b03419>
141. Haynes PA, Roberts TH (2007) Subcellular shotgun proteomics in plants: looking beyond the usual suspects. *Proteomics* 7(16):2963–2975. <https://doi.org/10.1002/pmic.200700216>
142. Budnik B, Levy E, Harmange G, Slavov N (2018) Mass-spectrometry of single mammalian cells quantifies proteome heterogeneity during cell differentiation. *bioRxiv* 19:161. <https://doi.org/10.1101/102681>
143. Dettmer K, Aronov PA, Hammock BD (2007) Mass spectrometry-based metabolomics. *Mass Spectrom Rev* 26(1):51–78. <https://doi.org/10.1002/mas.20108>
144. Han J, Datla R, Chan S, Borchers CH (2009) Mass spectrometry-based technologies for high-throughput metabolomics. *Bioanalysis* 1(9):1665–1684
145. Fujii T, Matsuda S, Tejedor ML, Esaki T, Sakane I, Mizuno H, Tsuyama N, Masujima T (2015) Direct metabolomics for plant cells by live single-cell mass spectrometry. *Nat Protocols* 10:1445. <https://doi.org/10.1038/nprot.2015.084>
146. Hiyama E, Ali A, Amer S, Harada T, Shimamoto K, Furushima R, Abouleila Y, Emara S, Masujima T (2015) Direct lipidomics of single floating cells for analysis of circulating tumor cells by live single-cell mass spectrometry. *Anal Sci* 31(12):1215–1217. <https://doi.org/10.2116/analsci.31.1215>
147. Tejedor LM, Mizuno H, Tsuyama N, Harada T, Masujima T (2012) In situ molecular analysis of plant tissues by live single-cell mass spectrometry. *Anal Chem* 84(12):5221–5228. <https://doi.org/10.1021/ac202447t>
148. Lin L, Lin X, Lin L, Feng Q, Kitamori T, Lin JM, Sun J (2017) Integrated microfluidic platform with multiple functions to probe tumor-endothelial cell interaction. *Anal Chem* 89(18):10037–10044. <https://doi.org/10.1021/acs.analchem.7b02593>

Chapter 8

Micro/Nano fluidics Enabled Single-Cell Biochemical Analysis



Ling Lin

Abstract In the last 20 years, micro-fluidic technique has emerged as an important enabling tool for single-cell chemical analysis, owing to the miniaturization of the fluidic environment. These methodologies made various applications in single-cell analysis fields, and their superior performances such as rapid, simple, and high-efficient processing have been proved. Recently, the space is further down-scaling to the 10–1000 nm scale (nano-space). The nano-space is located between conventional nanotechnology (10–1000 nm) and microtechnology (>1 mm), and the research tools are not well established. For these purposes, a new research field is now being created which are quite different from those in micro-space. In this chapter, we focus on the basic researches in nano-fluidic space and survey the fundamental technologies for nano-fluidic space. Then, recent developments of nano-fluidic technologies for single-cell analysis are reported. Finally, the potential of nano-fluidics-based single-cell analysis is discussed.

Keywords Nano-fluidic · Micro-fluidic · Single-cell analysis · Biochemical analysis



8.1 Introduction

Cell is one of the fundamental units of life. Individual cells are heterogeneous in terms of gene expression, metabolite levels, ion concentrations, or patterns of response to a specified stimulus [1–6]. Many investigations have demonstrated that individual cells, even for those identical in appearance, show cell-to-cell variability caused by genetic or microenvironment variations [7–10]. Recent investigations enumerate the cell heterogeneity as a characteristic of progress in cell biology and tissue engineering, highlighting the necessity to probe individual cells in a cell

L. Lin (✉)

National Center for Nanoscience and Technology, Chinese Academy of Sciences,
Beijing 100190, People's Republic of China
e-mail: linling@nanoctr.cn

Table 8.1 Requirement of single-cell analysis [14]

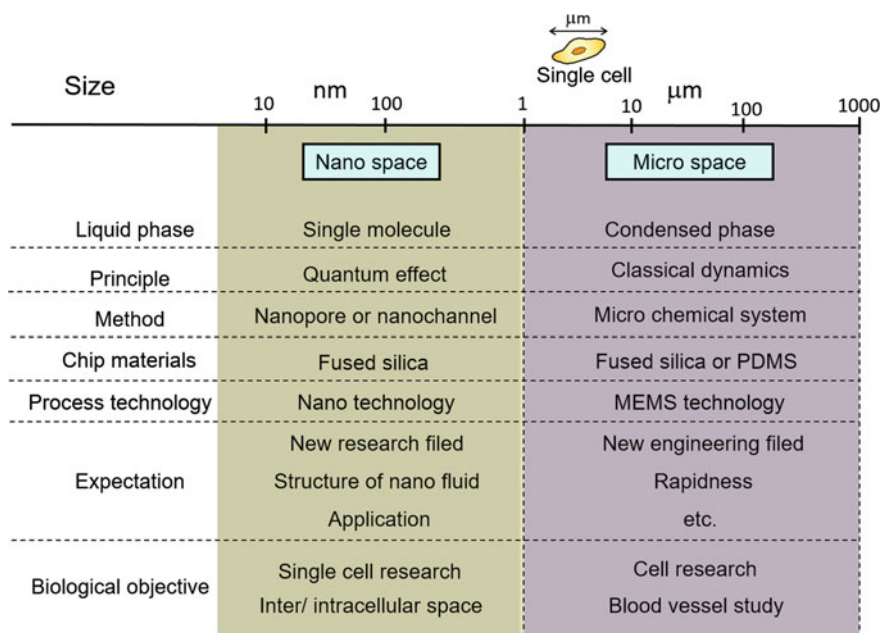
	Traditional cell analysis	Requirement
Number of cells	~10 ⁶ cells 	Single cell 
Sample volume	μL – mL	aL~ fL
Detection limit	pM × mL = 10 ⁶ molecule	pM × pL = 10 ⁰ molecule

population [11, 12]. Single-cell analysis provides a new venue to capture the cellular heterogeneity in extracellular circumstances as well as intracellular conditions at the single-cell level [13].

Single-cell analysis requires the capacity to manipulate a small sample volume down to picoliter (pL) in order to interrogate individual cells. Generally, cell analysis is performed in microtubes or micro-wells with the sample volume on a microliter (μL) scale, which is much larger (six orders or magnitude) than the single-cell volume of pL. Table 8.1 presents the conventional methods for cell analysis (~10⁶ cells) and the requirement for single-cell analysis. The reduced sample volume of single-cell analysis directly results in the improved detection limit. Assuming that a pM concentration of typical analytical targets is available, single-cell analysis tools could detect very few targeted molecules, while the number of detectable molecules is in the order of 10⁶ by conventional cell analysis methods. Therefore, there is an urgent need to develop sophisticated tools for manipulation of single cells.

For these purposes, designing tools of micro-chemical processes and reliable fluidic devices will be important technologies. Micro-total analysis systems (μ-TAS) have shown great advantage for the analysis of single cells [15–18]. In addition, nanometer-scale chemical experiment is opening new horizon of single-cell study tool. Recently, the advances in nano-fabrication technologies enable the biochemical analysis within a “nano-space,” which is defined by the length scale between the 10 nm and 1000 nm [19, 20] as shown in Table 8.2. The major advantage of nano-space is the use of extremely small sample volumes: the femtoliter (fL) or attoliter (aL) scale [21, 22]. It is noted that the sample volume in nano-space is 10⁴–10³ times smaller than that of single cell, thus allowing for real-time analysis of a minute sample volume from living single cells [23, 24].

In this chapter, we focus on the methodologies and new application for single-cell analysis in nano-space. Firstly, nano-channel fabrication, the surface modification,

Table 8.2 Comparison of micro-fluidics and nano-fluidics technologies for single-cell analysis [14]


Size	10 nm	100 nm	1 μm	10 μm	100 μm	1000 μm
	Nano space			Micro space		
Liquid phase	Single molecule			Condensed phase		
Principle	Quantum effect			Classical dynamics		
Method	Nanopore or nanochannel			Micro chemical system		
Chip materials	Fused silica			Fused silica or PDMS		
Process technology	Nano technology			MEMS technology		
Expectation	New research filed			New engineering filed		
	Structure of nano fluid Application			Rapidness etc.		
Biological objective	Single cell research			Cell research		
	Inter/ intracellular space			Blood vessel study		

and fluidic control methods as basic research tools for nano-space are reported. Secondly, nano-fluidic technology approaches for single-cell manipulation, single-cell treatment, and detection for samples from single-cell are reviewed. Thirdly, future perspectives and problems to be solved are briefly illustrated.

8.2 Nanofluidic Devices

Nanoscale devices can be used to manipulate single cells or deliver chemicals into cells in a controlled fashion. In the nano-fluidic chip, the nano-space can be used to characterize the behavior of individual molecules. There is much of the relevant literature cites the potential and especially the high-throughput operation for enveloping analytical methods to observe, manipulate, and explore single cell in the nano-space.

8.2.1 Fabrication Methods

There are many fabrication methods for nanoscale structures, and their methods can be divided into two categories. One is top-down processes in which the nano-structures are directly prepared on bulk substrates by cutting or milling the substrates. The other is a bottom-up process that manipulates and self-assembles atoms and molecules to prepare nano-structures on substrates. Microchips with nano-channels were fabricated using fused silica substrates via nano-channels fabrication (electron-beam lithography), micro-channel fabrication (UV lithography), dry etching, drilling holes, and substrate bonding.

8.2.1.1 Nano-channel Fabrication (Electron-Beam Lithography and Dry Etching)

The substrates for fabrication of the nano-channel were 1-mm-thick fused silica rectangle plates. The substrates were mechanically polished and thermally annealed to obtain an optically flat surface and washed in acetone, ethanol, and pure water and cleaned in an O₂ plasma reactor. First, the substrate was covered with electron-beam resist and conductive polymer layers by spin coater (Fig. 8.1a). Then, it was placed in the vacuum chamber of an electron-beam lithography system. A computer-controlled electron-beam scanner was used to draw a nanometer-sized channel pattern (Fig. 8.1b). After the exposure, the conductive polymer layer was removed in pure water, and the electron-beam resist layer was developed in xylene. After the drawn nano-patterns were etched due to inductively coupled plasma (ICP) etching with a mixture of SF₆/CHF₃ gases, plasma etching with CHF₃/O₂ gases, or a fast atom beam (FAB) etching with CHF₃ gas, 2-D nano-space channels could be obtained onto the substrate. After FAB etching, the resist layer was removed in the O₂ plasma chamber (Fig. 8.1c). The fabricated nano-spaces were connected with micro-channels that were fabricated by either plasma etching process. The inlet holes were pierced through the fabricated substrate using a diamond coated drill. The substrate was washed repeatedly in pure water and piranha solution, and the nano-in-micro structures on the substrate were sealed by thermal bonding or sodium silicate layer with pressing [25]. An example of the fabrication procedure for a glass chip with nano-in-micro structures is shown in Fig. 8.1d.

8.2.1.2 Micro-channel Fabrication

To introduce liquid samples into the nano-channels, we need fabricated micro-channels on the substrate to connect nano-channels. Micro-channels in fused silica rectangle plates were fabricated by laser-beam patterning and sand-blast processing. First, the positive photo-resist material was coated by spin onto the Au/

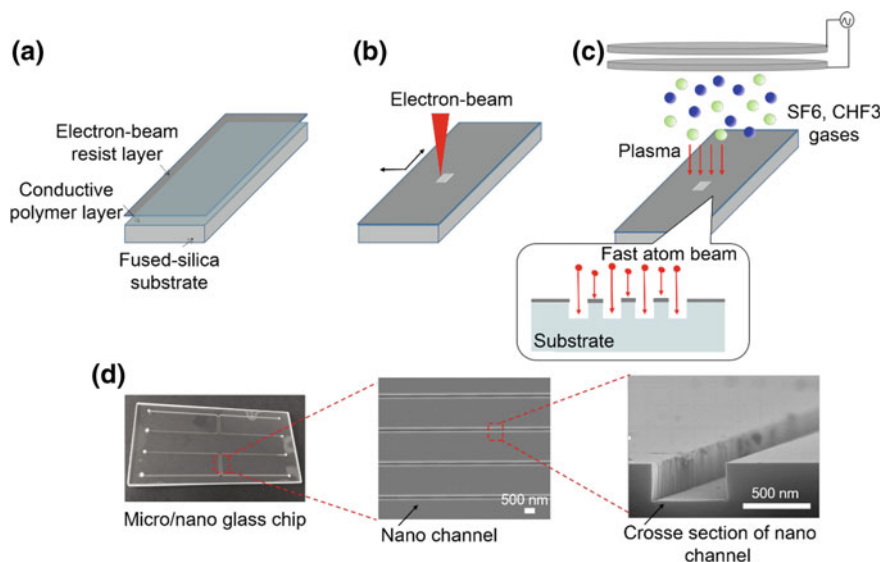


Fig. 8.1 Fabrication scheme: **a** Spin coating of electron-beam resist and conductive polymer layers on fused silica substrate. **b** Electron-beam lithography of nanometer-sized channels. **c** Fast atom beam etching of nanometer-sized channels. **d** Photograph of a glass chip invoking nano-in-micro structures and SEM image of nano-channels

Cr glass and UV (ultraviolet) light was irradiated by a photomask (polyimide sheet) for transferring the channel pattern onto the photo-resist material. The UV-exposed photo-resist material was etched by the pattern. Then, the micro-channel was etched into a patterned substrate by plasma etching technique and the remaining photo-resist material and metal layers were removed completely. After the dry etching process, a 0.4-mm-diameter hole was drilled at the end of each channel.

8.2.1.3 Cover Plate Bonding

To cover the nano-channels and micro-channels, a fused silica plate (nano-channel) should bond to the substrate (micro-channel). In the traditional methods [26, 27], the fused silica plates were laminated by a thermally bonding method at the softening point of fused silica (1150 °C) for 24 h. However, too high a temperature cause glass to deform, we chose low-temperature bonding method by using hydrofluoric acid. Low-temperature (25–100 °C) bonding methods recently developed by Kitamori group [28, 29] avoid thermal destruction because the principle is based on chemical bonding between silanol groups without heat. Next, the substrates were laminated with the fused silica plate by low-temperature (25–100 °C) bonding methods. The substrate and fused silica plate were successively washed in acetone, ethanol, pure water, a mixed solution of sulfuric acid and

hydrogen peroxide (2:1), 1 M NaOH solution, and pure water. Then, the clean silica substrate with channels was placed in the plasma chamber and treated with fluorine-containing oxygen plasma (60 Pa O_2 , 250 W power) for 40 s. The substrate was removed from the plasma chamber and brought into contact with each other. In order to increase the strength of substrate bonding, the plates were pressurized for 2 h at 5000 N and 100 °C using a bonding machine (Bondtech Co., Ltd., Japan). The bonded device was kept at room temperature (25 °C) for 24 h before use. Finally, completeness of the bonding was confirmed by sight and a leakage test observed under an optical microscope. If the bonding had failed, an optical interference ring pattern was observed.

8.2.2 Surface Modification Methods

On the surface modification methods, there were so many reports in micro-space utilizing light, electron beam, contact printing, ink-jet so on. However, a closed geometry of the nano-channel limits significantly the use of conventional methods for channel modification. Therefore, for closed nano-space, local surface modification with light will be one candidate. So far, there were only a few reports on the local surface modification in nano-space utilizing light.

Here, an example of local immunoassays in nano-space using a photolithographic technique with vacuum ultraviolet light and low-temperature (100 °C) bonding method is shown in Fig. 8.2 [30]. In order to introduce functional groups for antibody immobilization, the entire surface of a fused silica substrate was modified with aminopropyltriethoxysilane (APTES) in the gas phase to achieve uniform APTES layering. Upon irradiation with VUV light through a chromium photomask, reactive

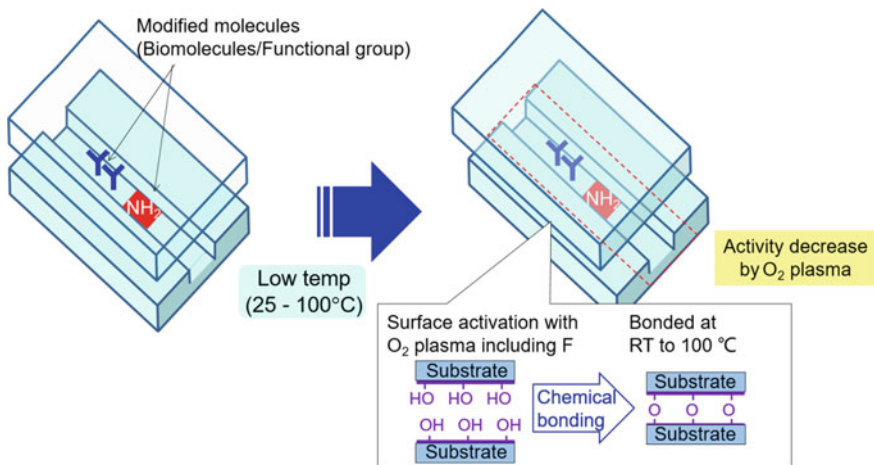


Fig. 8.2 Example of local immunoassays in nano-space [30]

oxygen species generated from oxygen gas molecules absorbing the high-energy VUV light oxidatively decompose the APTES. Because the glass surface become super-hydrophilic and activated after decomposition of APTES, it was able to achieve strong glass bonding, which is critical for nano-fluidic control using a high-pressure flow system. For designing and regulating the size and position of the antibody immobilized region, a partially modified APTES layer was formed by masking part of the substrate area from VUV light irradiation with the photomask. The advantage of using VUV light is that both pattern formation and surface activation can be achieved simultaneously. The APTES-patterned substrate was then brought into contact with the upper glass substrate containing micro- and nano-channels, and the substrate was activated by fluorine-containing oxygen plasma. Then, substrates were bound by low-temperature bonding methods. After bonding, to reduce the potential for non-specific protein adsorption to the nano-channel surfaces, the surfaces were chemically modified with trimethoxysilane-poly(ethyleneglycol) (PEG) for reducing the potential non-specific protein adsorption in the nano-channel surfaces [31, 32]. Capture antibodies were chemically immobilized by crosslinking the amino groups of APTES molecules and antibodies using glutaraldehyde. Residual reactive groups were blocked with ethanolamine. As an important subject, modification in nano-space will be an essential problem to detect single-molecule using ELISA for single-cell analyst. In the future, this ultralow-volume molecular capture method could be developed into a nano-fluidics-based ELISA for quantification at the single-molecule level by integrating chemical amplification with the enzymatic reaction and high-sensitivity detection of colorimetric products with differential interference contrast thermal lens microscopy [21].

8.2.3 *Detection Methods*

Ultrasensitive detection methods in nano-channel are very important for miniaturization. In nano-space, the volume of the sample is usually aL-fL level. Therefore, single-molecule sensitivity is required. So far, single-molecule sensitivity detection methods have reported which are mainly on optical and electrochemistry methods. Recently, nano-pores were increasingly utilized for sensitive detection and have been reported to successfully detect single porphyrin molecules. The experimental principle is based on conductivity measurements that apply a constant voltage to the nano-pore to detect changes in conductivity that occur as molecules pass through the nano-pore. However, the combination with nano-channels is relatively difficult because of the complex structure of the nano-channels. On the other hand, optical methods can also be used for sensitive detection in nano-channels. For example, the now popular laser-induced fluorescence method can be used not only for detecting samples but also for observing imaging fluid movement. However, most of the molecules in a single cell are non-fluorescent (non-fluorescent proteins or DNAs), and we need sensitive detection methods for non-fluorescent molecules.

Thermal lens microscope (TLM) is one of the candidates for these purposes. Here, an ultrasensitive method for detection on the nanoscale was developed based on a differential interference contrast thermal lens microscope (DIC-TLM) [21, 33], our original and ultrasensitive detection method for non-fluorescent molecules in aL detection volumes. Thermal lens microscopy (TLM) is a kind of photothermal spectroscopy that measures absorption and thermal relaxation and has been reported to be more sensitive than absorption spectrometry. Although conventional TLM offers a very high sensitivity to determine concentration of single-molecule level in micro-channels, it is not applicable to nano-channel, because its working principle is based on “geometrical optics.” In this case, as the size of nano-channel is smaller than the beam spot diameter ($\sim \mu\text{m}$) and the confocal length ($\sim 1 \mu\text{m}$), the refractive index distribution of the thermal lens might be too small to be detected.

Recently, Kitamori group has introduced the interferometry principle into TLM, which is referred as differential interference contrast TLM (DIC-TLM) and succeeded in TLM detection in $\sim 10^2 \text{ nm}$ space [21, 33]. The principle is shown in Fig. 8.3. The probe beam is separated by a DIC prism into two beams with perpendicular polarization. On the other hand, the excitation beam is not separated, as its polarization plane is rotated at an angle of 45° . The excitation beam is absorbed

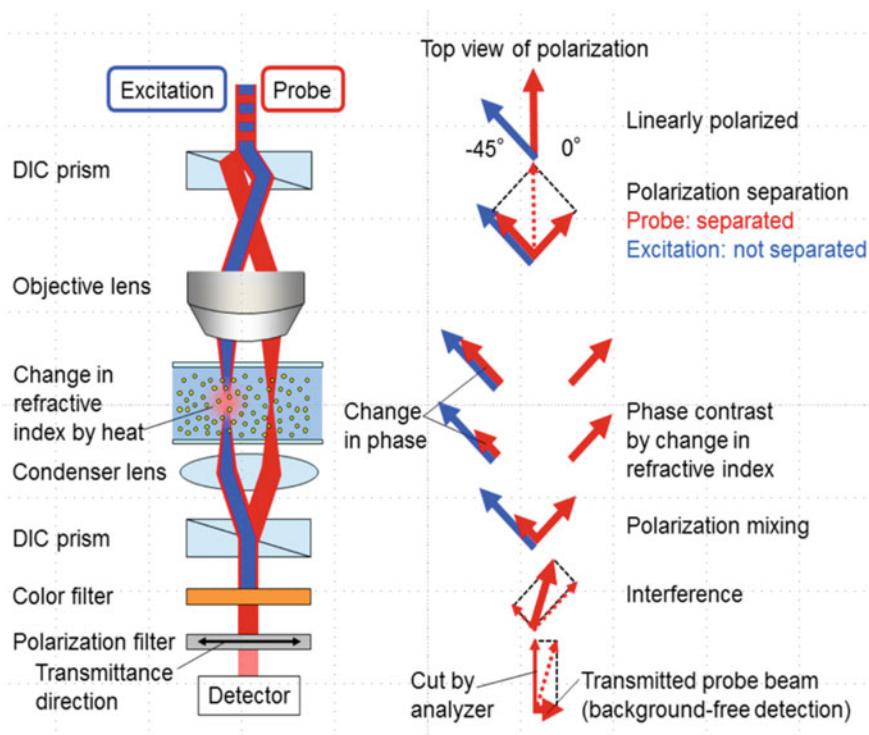


Fig. 8.3 Principle of differential interference contrast thermal lens microscopy [33]

by an analyte, and a thermal lens effect is induced. Then, phase contrast appears between the two probe beams due to the difference in refractive index. In the next step, the probe beams are combined again by another DIC prism, which results in a new polarization component. Finally, only this new component is detected as signal by removing the initial polarization component using a polarization filter. DIC-TLM extracts only the information of phase shift of probe beam caused by the change of refractive index. The principle is based on not geometric optics but wave optics, and therefore, DIC-TLM can measure molecules in the nano-space which is smaller than the wavelength of the light. In addition, DIC-TLM realizes background-free detection of thermal lens effects because the intensity of the transmitted probe beam is zero when no analyte is in the focus area of the excitation beam.

8.3 Fluidic Control Methods

Fluid control of nano-channels is generally divided into electroosmotic flow and pressure-driven flow. Electroosmotic flow has been recognized as a most popular fluid control method for micro-fluidic chips. A number of research groups have reported the integration of electrophoretic systems in nano-channels for the analysis of DNA and proteins. However, the pressure-driven flow is more suitable for the analysis of single cells in nano-channels. Therefore, it is essential to develop the pressure-driven nano-fluidic control system for nano-spaces and to evaluate the fluidic behavior in them.

In order to control the behavior of the fluid in the nano-channel, high pressure and low volume flow are required, because of its quite large pressure drop in nano-spaces. Because nano-space requires very strong and stable pressure, commercial syringe pumps cannot be utilized to drive a liquid in nano-channels. Therefore, Tamaki et al. developed a backpressure-based nano-fluid control system, in which was consisting of a backpressure regulator and an HPLC pump with flow rate detection [20, 34]. In the experiment, the aqueous solution of the benzenediol probe molecule was introduced into a U-shaped micro-channel by HPLC pump, and then the flow rate was detected after entering the nano-channels. The results show that the measured flow rate is linear with the pressure applied, and the measured flow rate is lower than the flow rate expected by Hagen–Poiseuille’s law. However, this method depended on the response times of backpressure regulators, such as backward flow in the nano-space channel. Tsukahara et al. improved a backpressure-based system to an air-pressure-based nano-fluidic control system (Fig. 8.4), and evaluated its performance [35]. This fluidic system allows a high pressure of MPa and a low flow rate of pL min^{-1} to control the nano-fluidics.

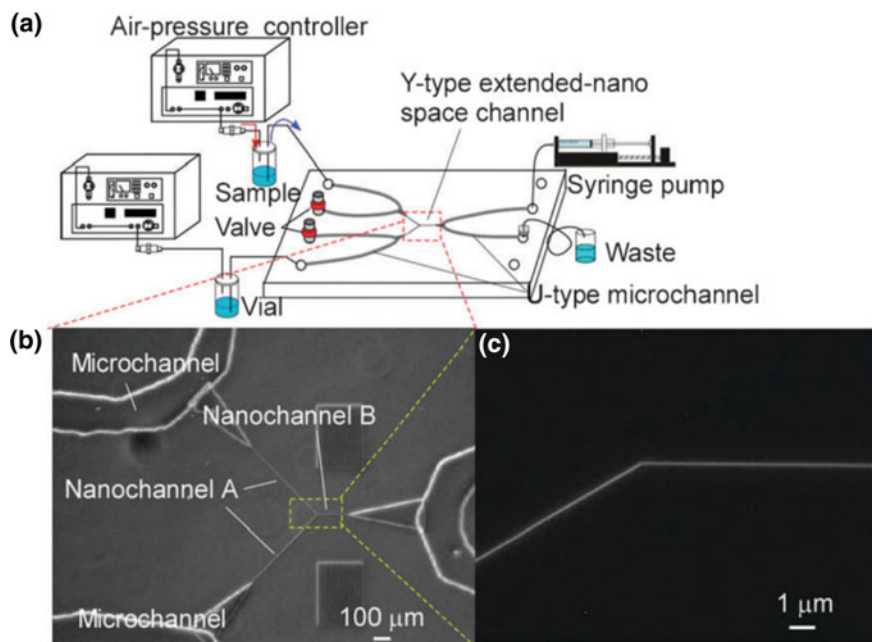


Fig. 8.4 Overview of experimental setup for nano-channel fluidic control. **a** Schematic illustration of air-pressure-based nano-fluidic control system. **b** Enlarged view of the fabricated microchip with U-shaped micro-channels and the Y-shaped nano-channels A and B. **c** A fluorescence image by mixing two different solutions; a fluorescein solution and a buffer solution flowing into the Y-shaped nano-channel [35]

8.4 Single Analysis on Nano/Microfluidic

8.4.1 Sampling from Single Cell

Single-cell analysis is of increasing importance in many fields, but is challenging due to the ultrasmall volumes (pL) of single cells. A single cell is typically $10^1 \mu\text{m}$ in diameter and has a volume of several pL, and so analysis of a specific analyte might require the analysis of a single molecule or several molecules. Consequently, single-cell analysis is quite challenging. Analytical processes typically include three steps: (1) sampling, (2) chemical processing, and (3) detection. Among them, many papers reported the chemical processing and detection methods [36–40]. However, sampling for pL single cells is still challenging due to the difficulty of volume control at fL level and maintaining the viability. Sampling is an essential process for general analytical chemistry.

Development of a sampling interface would permit determination of controlling sample volume and keeping cell viability for living single-cell analysis. Although there are many studies that focus on nanotechnology for single-cell analysis

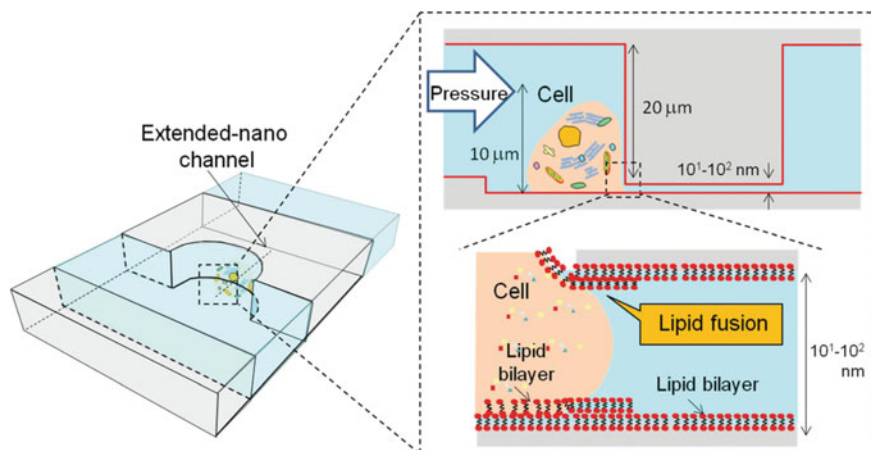


Fig. 8.5 Concept of micro-/nano-sampling interface. A lipid bilayer was modified on the nano-channel by vesicle. When the pressure was increased, the lipid bilayers on the cell and nano-channel contact and form a new lipid bilayer after the fusion. As a result, a hole with same size with the nano-channel is formed, and the proteins inside the single cell can be sampled by applying pressure without leakage [44]

[41, 42], their usage was limited to observation of cellular activities or morphologies. Sampling from living single cell would expand the study of intracellular biomolecules, that are expected to be present in low numbers of around a few tens of thousands [43].

However, a key technical challenge that must be overcome to realize sampling interface is how to achieve fL sampling volume from living single cell. The critical issue in developing a sampling interface of exploring the nano-space is to ensure that formed nano-order hole on cell membrane and tight connection between cell and nano-channel. Here, Lin et al. developed a micro-/extended-nano-sampling interface from living single cell [44]. A single-cell chamber and a micro-fluidic channel were used to handle and isolate single cells by micro-fluidic control. The nano-channel worked as a femtoliter pipette for sampling. The major technical challenge was to connect the single cell with the extended-nano-pipette, and a micro-/extended-nano-sampling interface was developed utilizing lipid fusion (Fig. 8.5). With these technical advancements, they demonstrated fL level sampling of the cytoplasm of a living single human aortic endothelial cell (HAEC).

8.4.2 Separation of Sample

Miniaturization of liquid chromatography separation columns is a key trend in chemical and biochemical areas, particularly in single-cell analysis. This separation method relies on a novel analytical platform that can separate much smaller sample

volumes than cells. A basic experimental setup of extended-nano-chromatography is shown in Fig. 8.6 [45]. In order to realize a separation mode of the sample in the micro/nano-chip, a pressure-driven and fluid control system is required. As shown in Fig. 8.7, pressures are applied from the top and left and right sides to fill the sample solution in a loading channel and the mobile phase in a separation channel (Fig. 8.7a). Then, the pressure from the right side is turned off to leak a small volume of sample into the separation channel (Fig. 8.7b). After a time lag, the pressure from the top side is turned off to cut off the sample in the separation channel (Fig. 8.7c). The injected sample is detected downstream of the separation channel (Fig. 8.7d). Based on this principle, a liquid chromatography system providing pressure-driven flow in nano-channels in a micro/nano-fluidic chip permits highly efficient separation of molecules in attoliter-volume samples [20, 46–48].

Recently, Smirnova et al. reported step-mixing generation and reversed phase chromatographic separation were implemented on a chip with nano-channels, which was tested for use in amino acids analysis. As shown in Fig. 8.8, this on-chip nano-chromatography platform completed 17 amino acids separation and analyses in 50 s. It was the first demonstration of liquid chromatography separation of complex mixtures on an open tubular nano-channel. Such unique characteristics of separation in extended-nano-space can be applied for the separation of proteins and

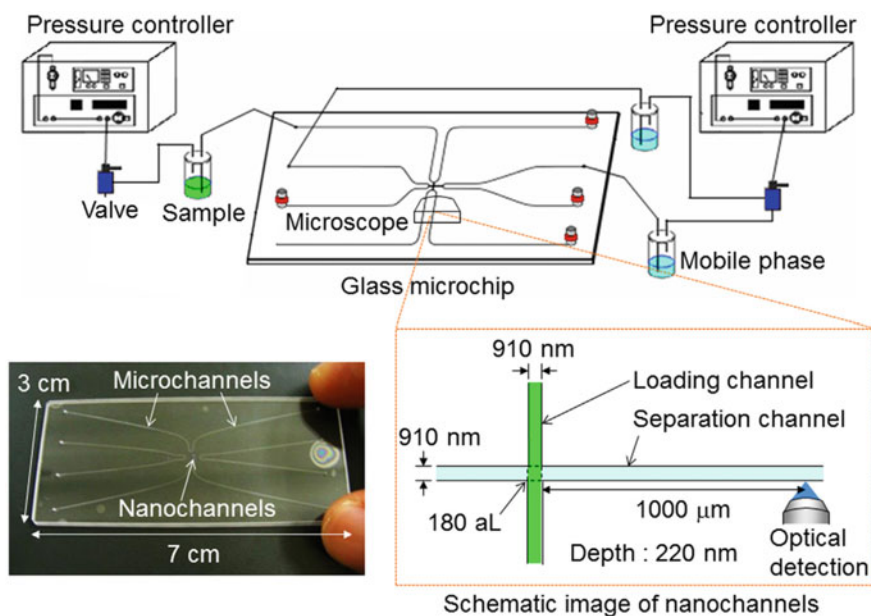


Fig. 8.6 Overview of experimental setup for extended-nano-chromatography. Two pressure controllers are used to push solutions of the sample and mobile phase in vials. The vials are connected to a glass microchip, which has micro-channels for introduction and nano-channels. Two nano-channels, the loading and separation channels, cross orthogonally at the center of the microchip [45]

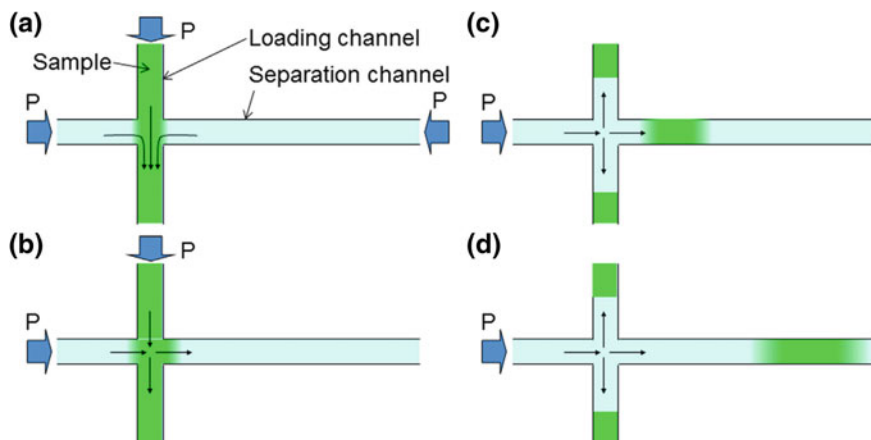


Fig. 8.7 Flow control of sample injection by pressure switching. **a** Sample is loaded from the loading channel. Pressures from the top, left, and right sides are balanced at the intersection of nano-channels. **b** Sample is injected from the loading channel to the separation channel by switching off the pressure from the right side. **c** Sample is cut off by switching off the pressure from the top side after a time lag. **d** Sample diffuses in the separation channel [45]

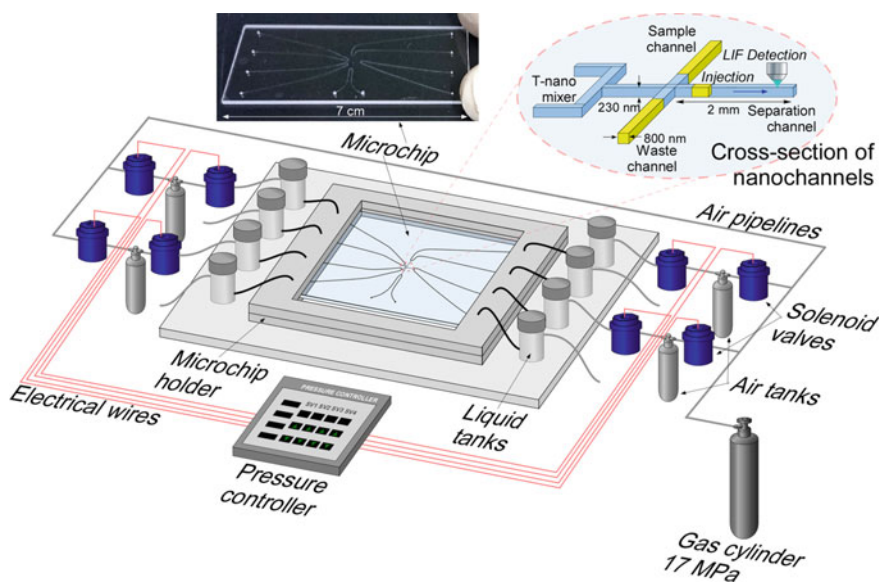


Fig. 8.8 Extended-nano-fluidic device for handling and sorting samples at aL [49]

large molecules and for applications to biological samples, especially for living single-cell analysis [49]. This study demonstrates that this method has the potential for analysis of the intracellular contents, to elucidate the transmembrane transport, and to study protein synthesis in cells.

8.4.3 *Detection of Sample*

Sample volumes used in single-cell research are becoming smaller and concentrations [50]. Therefore, ultrasmall volume sample should be precisely processed and detected for analysis. Here, Shirai et al. reported a single-molecule ELISA (enzyme-linked immunosorbent assay) device utilizing micro-/nano-fluidic technology. Both chemical processing [51] and detection [52] were integrated into nano-channels, and the integration allowed precise processing and detection of a specific single molecule (protein) for the first time.

In chemical processing part, they developed nano-fluidic immunoassay device that has highly-efficient (near 100%) immunochemical reactions on a seconds timescale. In this study, the technical challenge was to ensure proper antibody patterning on the inner surface of nano-channels. They developed a chemical method employing a photolithographic technique with VUV light with low-temperature bonding that allows for patterning prior to bonding. They developed a chemical method employing a photolithographic technique with VUV light and low-temperature bonding that allows for patterning prior to bonding. As shown in Fig. 8.9, the nano-fluidic immunoassay device requires pressure-driven fluid control to introduce and capture targeted molecules through regulation of liquid volume and liquid exchange. In the chemical processing part, high-efficient antigen-antibody reaction in the nano-space was developed. Extremely small amount of analyte can be captured without loss. However, the limit of detection did not reach to single or countable molecules region.

In detection part, Shirai et al. improved the limit of detection to single-molecule level using combination of chemical amplification by enzymatic reaction and ultrahigh-sensitive detection by DIC-TLM. This device allowed both the chemical processing and detection of a specific single molecule, capabilities that are essential for single-molecule analytical chemistry (Fig. 8.10). The experimental conditions were designed for enabling single analyte molecule detection including optimal channel size for DIC-TLM detection and enzymatic reaction time. Then, the signal of ELISA in the extended-nano-channel was successfully obtained. Moreover, the developed device had the performance for the analysis of countable number of molecules. This methodology would be applied to the analysis of ultrasmall volume sample such as single cell and single bacteria. In addition, the antigen-antibody reaction timescale would enable ultrafast immunoassay which has the potential to shorten clinical assay time dramatically.

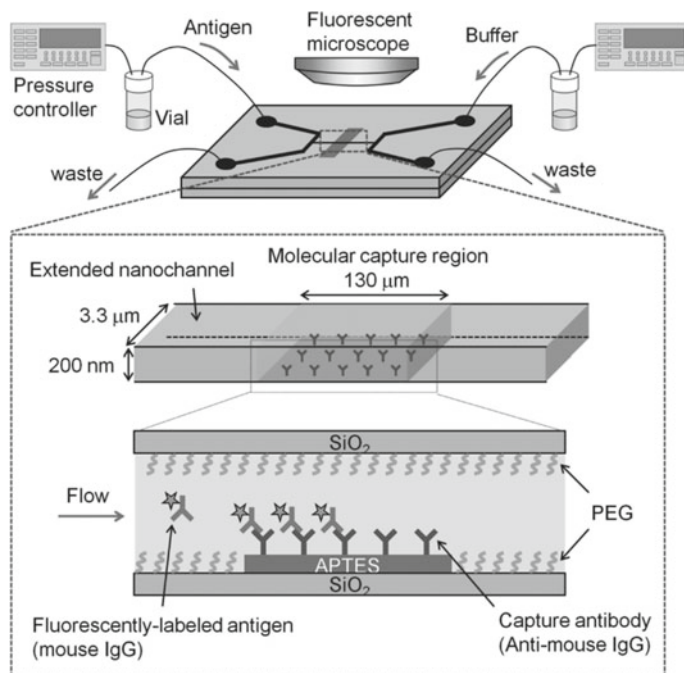


Fig. 8.9 Schematic illustrating fluidic control and the immunochemical reaction in the molecular capture region [51]

8.4.4 Other Applications

The nano-space has drawn great attention regarding device engineering due to its effective use of a unique property and small scale. The volume of the nano-channel (aL-fL) is much smaller than single-cell volumes (pL), and the nano-space will be promising for living single-cell analysis by analyzing small volumes of sample from single cells in nano-space. However, a large size gap exists between a single cell and the nano-channel. A basic platform is required to bridge the cell and the nano-channel. A novel micro-fluidic platform was developed by integrating a single-cell chamber and an extended-nano-channel (Fig. 8.11a) [53]. A single cell was isolated and cultured for more than 12 h by pressure-driven flow control. In addition, an electric resistance measurement method was developed to monitor the cell viability without fluorescence labeling. This platform will provide a new method for living single-cell analysis by utilizing the novel analytical functions of the extended-nano-space. Additionally, the living single-cell sampling was first proposed using a micro/extended-nano-sampling interface [54]. After fL sampling, single cells were analyzed while maintaining cell viability. This method would work as a connection for single cell and nano-space. A connection with a mass spectrometer (MS) is important for single-cell analysis. For this purpose, a nano-pillar

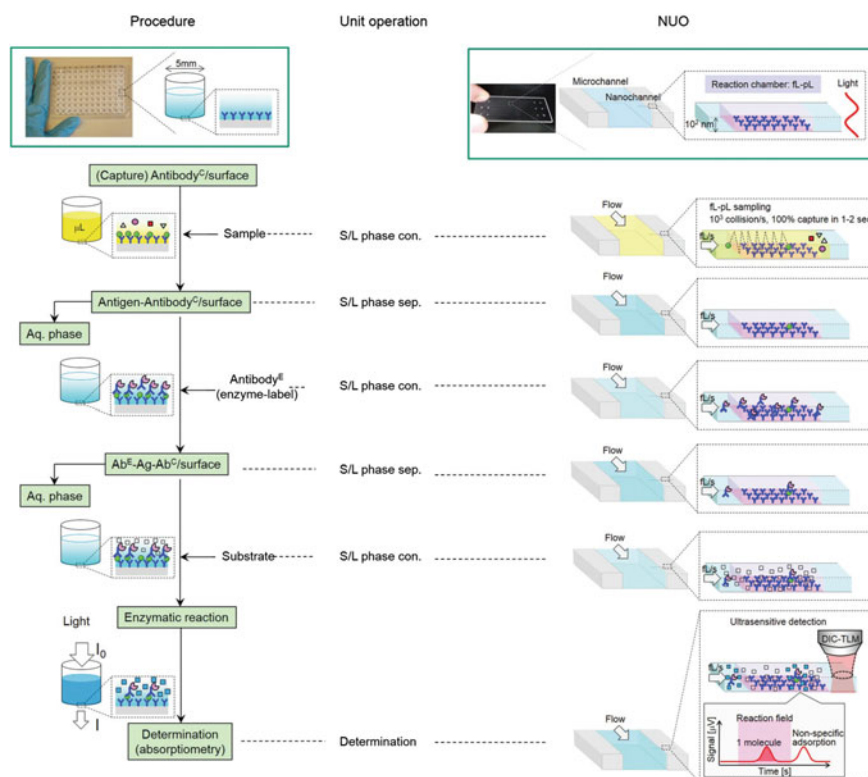


Fig. 8.10 Concept of single-molecule ELISA based on micro/nano-fluidic technology [52]

array was embedded in a nano-channel using two-step electron beam lithography and dry-etching process. The basic principle of the Laplace nano-valve was verified, and a 1.7 fL droplet was successfully generated and handled (Fig. 8.11b) [55]. Furthermore, the fL-valve made of glass and other rigid materials (such as plastic) was developed. An fL-valve based on an analytical material deformation model was designed and developed a valve fabrication process (Fig. 8.11c). Then, using 308 fL-valve chamber test valve open/close state, the nano-valve has a four-stepped nano-structure fitting an arc-shape of deflected glass, confirmed its stability and durability over 50 open/close operations, and successfully stopping/flowing an aqueous solution under 209 fL s^{-1} under 100 kPa pressure in nano-channel, quick response with $\sim 0.65 \text{ s}$ [56]. Moreover, a valve system was developed in the nano-space for sample injection control. They replaced the open/closed pressure control system (Fig. 8.11d). This method can be achieved by integrating a valve in the nano-channel [57]. In the future, nano-channels are expected to contribute to living single-cell analysis and ultrasensitive detection with small volume. Moreover, basic measurement methods for the nano-space including flow velocimetry would explain the molecular behavior in the nano-channels [58, 59].

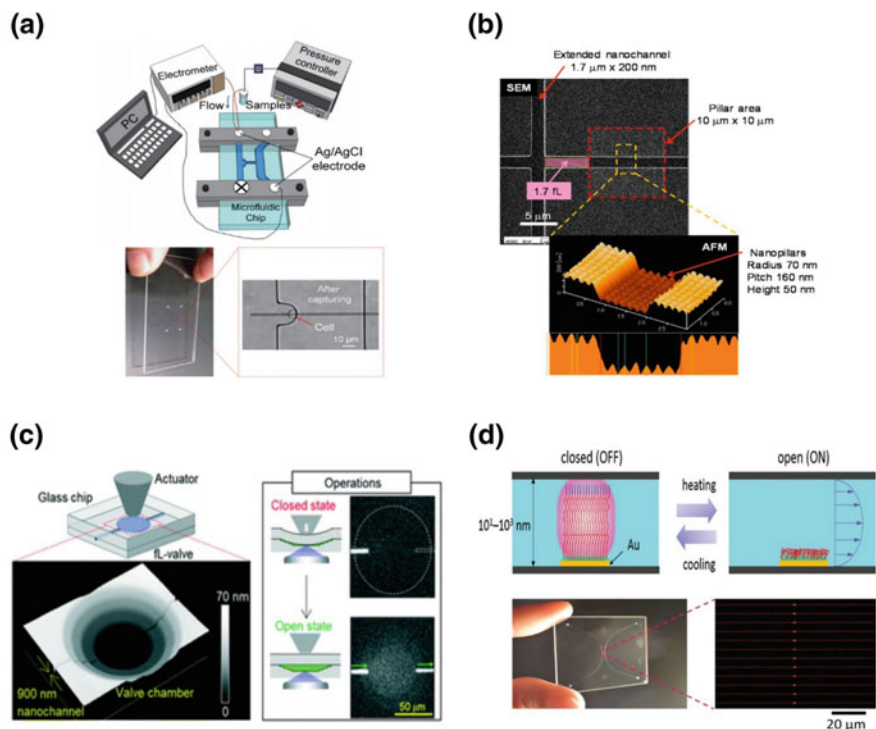


Fig. 8.11 Nano-fluidic for single-cell analysis. **a** Living single-cell electric resistance measurement method utilizing micro-/nano-fluidic technology [49]. **b** SEM and AFM images of the nano-valve and nano-pillar array [50]. **c** Schematic illustration of a nano-channel open/close valve. Image below shows the valve chamber with the four-stepped nano-structure, which is connected to the nano-channels, observed by an optical profiler [56]. **d** Nano-valve system in nano-space for sample injection control [51]

8.5 Concluding Remarks and Future Perspectives

In the future, various biochemistry applications will be opened by utilizing the advantages of micro/nano-channel chip platform. In this chapter, we documented the advances in coupling micro/nano-chips for single-cell analysis in the past decade, covering both fabrication of micro/nano-chip and their applications in single-cell research, for example, single-cell sampling, chemical processing and detection, while complex and precise fluidic controls are required. Artificial and size-controlled nano-channels will be the appropriate platform for this purpose compared with porous materials and carbon nanotube. As a preliminary research, micro/nano-sampling interface, nano-ELISA, and nano-chromatograph were integrated into nano-channel, and the basic principles were reported. These features will provide new tools for single-cell research because the volume of single cell is picoliter and larger than the volume of the nano-space. Therefore, concept and

methodologies for designing tool of the chemical processes and realization of single-cell analysis devices will also be important subjects. By using these new methods and combining with micro-chemical processes, new bioanalytical tools will be possible which are difficult by conventional microtechnologies.

References

1. Spudich JL, Koshland DE (1976) Non-genetic individuality chance in single cell. *Nature* 262:467–471
2. Spiller DG, Wood CD, Rand DA, White MRF (2010) Measurement of single-cell dynamics. *Nature* 465:736–745
3. Rubaknin SS, Romanova EV, Nemas P, Sweedler JV (2011) Profiling metabolites and peptides in single cells. *Nat Methods* 8:20–29
4. Frei AP, Bava F-A, Zunder ER, Hsieh EWY, Chen SY, Nolan GP, Gherardini PF (2016) Highly multiplexed simultaneous detection of RNAs and proteins in single cells. *Nat Methods* 13:269–275
5. Sassolas A, Leca-Bouvier BD, Blum LJ (2008) DNA biosensors and microarrays. *Chem Rev* 108:109–139
6. Mao S, Zhang W, Huang Q, Khan M, Li H, Uchiyama K, Lin JM (2018) In situ scatheless cell detachment reveals connections between adhesion strength and viability at single-cell resolution. *Angew Chem Int Ed* 57(1):236–240
7. Levsky JM, Shenoy SM, Pezo RC, Singer RH (2002) Single-cell gene expression profiling. *Science* 279:836–840
8. Zhuang Q, Wang S, Zhang J, He Z, Li H, Ma Y, Lin JM (2016) Nephrocyte-neurocyte interaction and cellular metabolic analysis on membrane-integrated microfluidic device. *Sci China Chem* 59:243–250
9. Yu X, Gong J, Zhang Z, Zhao Z, Zhang X, Tan W (2017) Nanocarrier based on the assembly of protein and antisense oligonucleotide to combat multidrug resistance in tumor cells. *Sci China Chem* 60:1318–1323
10. Chang HH, Hemberg M, Barahona M, Ingber DE, Huang S (2008) Transcriptome-wide noise controls lineage choice in mammalian progenitor cells. *Nature* 453:544–547
11. Tanihuchi Y, Choi PJ, Li GW, Chen H, Bahu M, Hearn J, Emili A, Xie XS (2010) Quantifying *E. coli* proteome and transcriptome with single-molecule sensitivity in single cells. *Science* 329:533–538
12. Sims CE, Allbritton NL (2007) Analysis of single mammalian cells on chip. *Lab Chip* 7:423–440
13. Huang Y, Cai D, Chen P (2011) Micro-and nanotechnologies for study of cell secretion. *Anal Chem* 83:4393–4406
14. Lin L, Chen Q, Sun J (2018) Micro/nanofluidics-enabled single-cell biochemical analysis. *TrAC-Trends Anal Chem* 99:66–74
15. Reyes DR, Iossifidis D, Auroux PA, Manz A (2002) Micro total analysis systems. 1. Introduction, theory, and technology. *Anal Chem* 74:2623–2636
16. Reyes DR, Iossifidis D, Auroux PA, Manz A (2002) Micro total analysis systems. 2. Analytical standard operations and applications. *Anal Chem* 74:2637–2652
17. Vilkner T, Janasek D, Manz A (2002) Micro total analysis systems. 3. Recent developments. *Anal Chem* 74:3373–3385
18. Lin L, Lin X, Lin L, Feng Q, Kitamori T, Lin JM, Sun J (2017) Intergrated microfluidic platform with multiple functions to probe the tumor-endothelial cell interaction. *Anal Chem* 89:10037–10044

19. Hibara A, Saito T, Kim H-B, Tokeshi M, Ooi T, Nakao M, Kitamori T (2002) Nanochannels on a fused-silica microchip and liquid properties investigation by time-resolved fluorescence measurements. *Anal Chem* 74:6170–6176
20. Tsukahara T, Mawatari K, Hibara A, Kitamori T (2008) Development of a pressure-driven nanofluidic control system and its application to an enzymatic reaction. *Anal Bioanal Chem* 391:2745–2752
21. Shimizu H, Mawatari K, Kitamori T (2010) Sensitive determination of concentration of nonfluorescent species in an extended-nano channel by differential interference contrast thermal lens microscope. *Anal Chem* 82:7479–7484
22. Zhou J, Jiang D, Chen H-Y (2017) Nanoelectrochemical architectures for high-spatial-resolution single cell analysis. *Sci China Chem.* 60:1277–1284
23. Haywood DG, Saha-Shah A, Baker LA, Jacobson SC (2015) Fundamental studies of nanofluidics: nanopores, nanochannels, and nanopipets. *Anal Chem* 87:172–187
24. Napoli M, Eijkel JC, Pennathur S (2010) Nanofluidic technology for biomolecule applications: a critical review. *Lab Chip* 10:957–985
25. Tsukahara T, Mizutani W, Mawatari K, Kitamori T (2009) NMR studies of structure and dynamics of liquid molecules confined in extended nanospaces. *J Phys Chem B* 113:10808–10816
26. Sato K, Kawanishi H, Tokeshi M, Kitamori T, Sawada T (1999) Sub-zeptomole detection in a microfabricated glass channel by thermal-lens microscopy. *Anal Sci* 15:525–529
27. Ng HC, Uddayasankar U, Wheeler AR (2010) Immunoassays in microfluidic systems. *Anal Bioanal Chem* 397(3):991–1007
28. Xu Y, Wang C, Dong Y, Li L, Jang K, Mawatari K, Suga T, Kitamori T (2012) Low-temperature direct bonding of glass nanofluidic chips using a two-step plasma surface activation process. *Anal Bioanal Chem* 402(3):1011–1018
29. Xu Y, Wang C, Li L, Matsumoto N, Jang K, Dong Y, Mawatari K, Suga T, Kitamori T (2013) Bonding of glass nanofluidic chips at room temperature by a one-step surface activation using an O₂/CF₄ plasma treatment. *Lab Chip* 13(6):1048–1052
30. Otha R, Mawatari K, Takeuchi T, Morikawa K, Kitamori T (2019) Detachable glass micro/nanofluidic device. *Biomicrofluidics* 13:024104
31. Heyes CD, Kobitski AY, Amirgoulova EV, Nienhaus GU (2004) Biocompatible surfaces for specific tethering of individual protein molecules. *J Phys Chem B* 108:13387–13394
32. Tessler LA, Reifenberger JG, Mitra RD (2009) Protein quantification in complex mixtures by solid phase single-molecule counting. *Anal Chem* 81:7141–7148
33. Shimizu H, Mawatari K, Takehiko T (2009) Development of differential interference contrast thermal lens microscope (DIC-TLM) for sensitive individual nanoparticle detection in liquid. *Anal Chem* 81:9802–9806
34. Tamaki E, Sato K, Tokeshi M, Sato K, Aihara M, Kitamori K (2002) Single cell analysis by a scanning thermal lens microscope with a microchip: direct monitoring of cytochrome-c distribution during apoptosis process. *Anal Chem* 74:1560–1564
35. Tamaki E, Hibara A, Tokeshi M, Kitamori T (2003) Microchannel-assisted thermal-lens spectrometry for microchip analysis. *J Chromatogr A* 987:197–204
36. Huh D, Matthews BD, Mammoto A, Montoya-Zavala M, Hsin HY, Ingber DE (2010) Reconstituting organ-level lung functions on a chip. *Science* 328:1662–1668
37. Khademhosseini A, Langer R, Borenstein J, Vacanyi JP (2006) Microscale technologies for tissue engineering and biology. *Proc Natl Acad Sci USA* 103:2480–2487
38. Gobaa S, Hoehnel S, Roccio M, Negro A, Kobel S, Lutolf MP (2011) Artificial niche microarrays for probing single stem cell fate in high throughput. *Nat Methods* 8:581–593
39. Lee H, Sun E, Ham D, Weissleder R (2008) Chip–NMR biosensor for detection and molecular analysis of cells. *Nat Med* 14:869–874
40. Neuzil P, Giselbrecht S, Lange K, Huang TJ, Manz A (2012) Revisiting lab-on-a-chip technology for drug discovery. *Drug Discov* 11:620–632
41. Yan R, Park J-H, Choi Y, Heo C-J, Yang S-M, Lee LP, Yang P (2012) Nanowire-based single-cell endoscopy. *Nat Nano* 7:191–196

42. Zheng XT, Li CM (2013) Single cell analysis at the nanoscale. *Chem Soc Rev* 41:2061–2071
43. Schwanhauser B, Busse D, Li N, Dittmar G, Schuchhardt J, Wolf J, Chen W, Selbach M (2013) Corrigendum: global quantification of mammalian gene expression control. *Nature* 495:126–127
44. Lin L, Mawatari K, Morikawa K, Pihosh Y, Yoshizaki A, Kitamori T (2017) Micro/extended-nano sampling interface from living single cell. *Analyst* 142:1689–1696
45. Shimizu H, Smirnova A, Mawatari K, Kitamori T (2017) Extended-nano chromatography. *J Chromatogr A* 1490:11–20
46. Ishibashi R, Mawatari K, Kitamori T (2012) Highly efficient and ultra small volume separation by pressure driven liquid chromatography in extended nanochannels. *Small* 8:1237–1242
47. Ishibashi R, Mawatari K, Kitamori T (2012) Development of a pressure-driven injection system for precisely time controlled attoliter sample injection into extended nanochannels. *J Chromatogr A* 1228:51–56
48. Shimizu H, Toyoda K, Mawatari K, Terabe S, Kitamori T (2019) Femtoliter gradient elution system for liquid chromatography utilizing extended-nano fluidics. *Anal Chem* 91(4):3009–3014
49. Smirnova A, Shimizu H, Pihosh Y, Mawatari K, Kitamori T (2016) On-chip step-mixing in a t-nanomixer for liquid chromatography in extended-nanochannels. *Anal Chem* 88:10059–10064
50. Ferreira J, Santos MJL, Rahman MM, Brolo AG, Gordon R, Sinton D, Girotto EM (2009) Attomolar protein detection using in-hole surface plasmon resonance. *J Am Chem Soc* 131:436–437
51. Shirai K, Mawatari K, Kitamori T (2014) Extended nanofluidic immunochemical reaction with femtoliter sample volumes. *Small* 10(8):1514–1522
52. Shirai K, Mawatari K, Kitamori T (2018) Single-molecule ELISA device utilizing nanofluidics. *Analyst* 143:943–948
53. Lin L, Mawatari K, Morikawa K, Kitamori T (2016) Living single cell analysis platform utilizing microchannel, single cell chamber, and extended-nano channel. *Anal Sci* 32:75–78
54. Lin L, Mawatari K, Morikawa K, Kitamori T (2015) Femtoliter sampling method from living single cell by extended-nano/micro interface. *Proc MicroTAS* 1:54–56
55. Mawatari K, Kubota S, Xu Y, Priest C, Sedev R, Ralston J, Kitamori T (2012) Femtoliter droplet handling in nanofluidic channels: a laplace nanovalve. *Anal Chem* 84:10812–10816
56. Kazoe Y, Pihosh Y, Takahashi H, Ohyama T, Sano H, Morikawa K, Mawatari K, Kitamori T (2019) Femto-liter nanofluidic valve utilizing glass deformation. *Lab Chip* 19:1686–1694
57. Xu Y, Shinomiya M, Harada A (2016) Soft matter-regulated active nanovalves locally self-assembled in femtoliter nanofluidic channels. *Adv Mater* 28:2209–2216
58. Kazoe Y, Mawatari K, Kitamori T (2015) Behavior of nanoparticles in extended nanospace measured by evanescent wave-based particle velocimetry. *Anal Chem* 87:4087–4091
59. Kazoe Y, Iseki K, Mawatari K, Kitamori T (2013) Evanescent wave-based particle tracking velocimetry for nanochannel flows. *Anal Chem* 85:10780–10786

Chapter 9

Microfluidic Chip-Based Live Single-Cell Probes



Sifeng Mao and Jin-Ming Lin

Abstract Single-cell analysis provides critical information to understand key disease processes and disease diagnosis. However, nearly all of the current methods carry out single-cell analysis in suspension, which not only destroy extracellular context but also may perturb the intracellular metabolites. It is essential to develop new methods to meet the requirements of understanding individual cell behaviors and their relations in adherent tissue culture. Advances in single-cell methodologies have highlighted the single-cell biology and are opening new vistas for scientists to explore. How to realize precise operation of single cells and subcellular molecule infusion is a critical question that researchers face. And, as the technologies to study single cells expand, sophisticated analytical tools are required to make sense of various behaviors and components of single cells as well as their relations in adherent tissue culture. Microfluidic chip has been proved an outstanding approach for single-cell analysis. Recently, the developments of single-cell probes open up new avenues to operate open microfluidics to perform single-cell extraction, single-cell mass spectrometric analysis, single-cell adhesion analysis, and subcellular operations.

Keywords Microfluidics · Single-cell analysis · Cell adhesion · Subcellular operations · Subcellular molecular infusion · Cell-cell adhesion · Metastasis · Single-cell mass spectrometry

9.1 Introduction

As the basic unit of life, cell has been widely studied for biological behaviors, drug metabolism, and nerve conduction. Samples were usually prepared from a large number of cells in certain condition in order to get sufficient amounts of molecules

S. Mao · J.-M. Lin (✉)
Department of Chemistry, Tsinghua University,
Beijing 100084, People's Republic of China
e-mail: jmlin@mail.tsinghua.edu.cn

© Springer Nature Singapore Pte Ltd. 2019
J.-M. Lin (ed.), *Microfluidics for Single-Cell Analysis*,
Integrated Analytical Systems, https://doi.org/10.1007/978-981-32-9729-6_9

to meet the sensitivity of different methodologies in traditional methods for biochemical analyses [1, 2]. Those results were “average” ones. However, we frequently found that the behaviors of isogenic cells were not identical even in the same culture dish [3, 4]. The “averaged” results should be insufficient and sometimes incorrect when under consideration of individual cell behaviors.

Single-cell analysis provides critical information to enhance the understanding toward cell behaviors and mechanism of cell metabolism [5, 6]. A large number of methods on single-cell array [7, 8], single-cell droplet [9–11] were combined with fluorescence analysis [12, 13], electrophoresis [14], and mass spectrometry [15, 16]. Unfortunately, most of the current methods carried out single-cell measurement in suspension, which not only destroyed extracellular context but also may perturb the intracellular metabolites. Thus, a new approach to obtain multiple information in a cell in adherent culture, and ideally clarify the connections between information and phenotype for a particular cell while knowing its external context, is desirable. Nowadays, more and more scientists are jumping into single-cell analysis [17].

It is well known that cell adhesions are crucial for the assembly of individual cells of identical type and cells of different types into three-dimensional tissue [18, 19]. This phenomenon, as one of the most important characteristics, is related to cell spreading area, cell size, cell activity, and intercellular metabolites [20–22]. Nowadays, there are many methods for cell adhesion measurement, including protein staining [23], isotope-labeling [24], fluorescein labeling [25, 26], and intracellular enzyme release assay [27, 28]. They characterized the cell adherence ability by counting cell number. However, the results belonged to statistical results that cannot represent the cell adherence ability of a particular single cell. Thus, it is a vital issue to measure single-cell adherence ability and connect it to cell viability.

Cell theory is a cornerstone of biology, where cell functions as the basic unit of life [29–31]. Cell biology promotes us well dissecting life’s mysteries and provides insights into some of the most fundamental processes in biology [32–34]. In human body, most types of cells are adherent cells that are closely networked with the matrix [35–37]. The cell matrix and microenvironment are very important to cell behavior in both *in vivo* and *in vitro* cell researches [38–40]. Tissues were jointly constructed by cells and matrix [21, 41]. Usually, adherent cells in suspension will function different from that in adherent state [42, 43]. In prediction, different biomaterials and modified substrates as matrix will affect cell functions and cell behaviors [1, 44, 45], such as metabolism, migration, proliferation, and apoptosis.

Much effort has been made on the development of biomaterials to reconstitute cell matrix and cell microenvironment precisely *in vitro* [46, 47]. Advances in biomaterials have contributed much to *in vitro* tissue construction and cell behavior studies [48, 49]. When they are utilized in cell studies, the biocompatibility and the interaction of the biomaterials with cultured cells are the most important characterizations [23]. Biocompatibilities of different biomaterials were studied by measurement of cell viability and cell morphology with current methods [50–52]. Those approaches concern about the status of cells themselves, but they are incapable for evaluating the influence of biomaterials on the interaction between adhered cells and matrix. In the previous researches, cells with good viability and large spreading

area did not always hold strong interaction with the matrix [53, 54]. Thus, the development of new biotechnologies for precisely evaluating the interaction between cells and biomaterials is still a vital issue.

Among different methods for cell researches, single-cell analysis has become the outstanding one [55–57]. Single-cell researches focus on cell-to-cell interaction [58, 59], single-cell metabolism [60, 61], whole-genome sequencing analysis [62] from single cells and cell-cycle dynamics of single cells [63]. More and more scientists have jumped and are jumping into single-cell analysis and development of biomaterials for single-cell analysis. Collection of single cell from tissue samples while keeping their viability becomes an essential issue. Moreover, evaluating the functions of new biomaterials for cell adherence and cell activities is essential for scientists in materials science. Thus, a new methodology to meet those requirements in single-cell biology and materials science is required.

Essential cellular processes such as survival, spreading, migration, proliferation, and differentiation were closely related to cell adhesion [64]. Cell adhesion is of prime importance on cell biology and medicine and plays a key role in several biological processes such as tumor metastasis [65, 66], stem-cell fate [67], and cell death [68]. Deviant adhesion behaviors usually lead to diseases including cancer [40], atherosclerosis [69], and arthritis [70]. Deeper insight into cell adhesion is helpful to solve those physiological problems. Cell-to-cell adhesions play an important role in the processes including tumor metastasis, tissue regeneration, and immune response [5].

In tumor metastasis, CTCs have been demonstrated one of the key roles that account for the majority of cancer-associated deaths, though the complex process remains the least aspect of cancer biology [71]. CTCs mutating from normal cells or arising from primary tumor invade into the vasculature of adjacent normal tissues. The intravasation supplies an avenue for CTCs to travel to distant positions, where they seed new tumors [72]. In this process, most of the CTCs rapidly cleared, while few of them would be physically trapped to the vascular internal wall for only seconds or minutes after their initial entry to the vasculature [73]. Adherent CTCs are capable for maneuvering through the capillary-sized vessels to a new site where a single CTC acts as a seed for new tumors. The conventional therapies focus more on induction of cancer cell apoptosis and interdiction cancer cell proliferation. In principle, blocking cell adherence to vessels will be a new tumor therapy stagey.

Benefit from technical advances in the isolation of CTCs from blood of cancer patients, single-cell analysis has been extensively studied in recent years [74, 75]. Detections of CTCs allow precancerous diagnosis, and apoptosis analysis *in vitro* can be utilized to profile genetic mutations and drug sensitivities [76, 77]. Deeper understandings on metastasis indicated that CTC adhesion is essential in tumor metastasis [78]. In particular, a better comprehension of the adhesion between cancer cells and endothelial cells will contribute to understand how the cancer cells leave the original tumor, adhere to vascular internal wall, and invade tissue from vessels [79]. Till now, rare methods work on adhesion analysis of single CTC, though there are many methods for adhesion measurement of cell population, including cell counting [80, 81] and quartz crystal microbalance (QCM) sensor [82]

that only revealed statistical properties. Based on AFM [83] and micropipette [84], some methods performed well on this issue, but they caused severe damage to the cellular functions or even kill the cells. It is vital to develop a gentle approach for adhesion strength analysis of natural cell at single-cell resolution which contributes to the understanding of tumor metastasis.

Complex organisms are built from one, then two, then four seemingly identical cells of an embryo [10, 54]. Research on the diversity of cell type and activity is confirmed much greater than conventional studies on populations of cells [8, 85, 86]. Single-cell biology has attracted more and more attention in recent years. Advances in new tools allow biologists to explore the characteristics of an individual cell. Single-cell biology promotes scientists to dissect life's mysteries, one cell at a time [87].

Scientists have made massive efforts on new approaches for single-cell analysis [47], including optical tweezers [88, 89], microfluidic chip [74], dual capillary probe [90], and microfluidic probe [91]. The developments on technologies have greatly promoted single-cell researches, such as single-cell metabolism [69–71], whole-genome sequencing analysis [92, 93] from single cells, and cell-cycle dynamics of single cells [63]. In fact, the cell itself is not homogeneous; more efforts should be made for developing new tools for subcellular studies to understand the regional difference of a single cell. Additionally, operation on portion of a cell is vital in unfolding cell wound repair, signal transduction, and molecule transfer in cell.

New methods have been developed for sampling cellular contents, such as microsampling methods [94–96] and Fluidic Force Microscopy [97–99]. The requirements in those technologies of inserting operation into the cell were harmful to live cell. Physical operations of tissues and cells by knife or needle suffered from low spatial resolution. Nowadays, microdissection [100] has become the best choice for tissue and cell separation with high resolution. However, it is still difficult to operate portion of a cell, because its resolution is not high enough. Developed by Whitesides group, laminar flow in microfluidic chip [101, 102] was demonstrated a powerful tool for subcellular positioning and microenvironment controlling. Yet, the reported laminar flow in microchannels was not convenient to treat different cell or a cell in the tissue, which seriously limited its applications. Recently, microfluidic probe [103, 104] and chemical pen [105–107] have been reported as promising approaches for fluid and laminar flow control in open space. Precise operation and treatment of portions of a cell in situ are still of vital importance for subcellular studies.

9.2 Live Single-Cell Extractor (LSCE)

A live single-cell extractor (LSCE) was described in this section for extracting single cell in adherent tissue culture for understanding cell heterogeneity and the connections of various single-cell behaviors [54]. U87-MG cells (U87) and human

hepatoma (HepG2) cells cultured in dish were locally extracted by the LSCE in non-touch mode. The morphology and stained metabolites of individual cells were recorded simultaneously. The connections between cell adhesion strength and cell morphologies were studied. The correlation between cell adhesion strength and intracellular metabolites was also uncovered.

9.2.1 Principle and Design

The design of the LSCE is detailed in Fig. 9.1a. In experimental process, a petri dish with cell samples was placed on the XY stage of an inverted microscope (Fig. 9.1a). The tip of the LSCE was placed perpendicular to the sample surface, while both were immersed in the surrounding medium (Fig. 9.1b). The “gap” was defined as the clearance between the LSCE tip and sample surface. When the ratio between aspiration and injection flow rates is sufficiently high, a stable microjet of injected liquid will form underneath the tip of LSCE (Fig. 9.1b). In later experiments, trypsin solution was used as the injection for digesting adherent cultured cells. The cell adhesion molecules (CAMs) connecting the adhered cell and extracellular matrix will be digested by trypsin molecules in the microjet.

9.2.2 Numeric Simulation

To comprehensively understand the microjet existing between the LSCE and the substrate, a simulation was carried out using the Comsol Multiphysics software

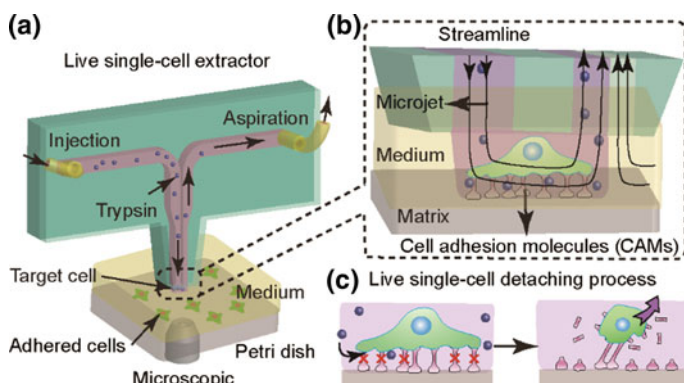


Fig. 9.1 Microfluidic chip-based live single-cell extractor (LSCE). **a** Illustration of LSCE and single-cell extraction system. **b** Illustration of microjet applying on live single cell. **c** Live single-cell detaching process. Mao et al. [54]. Copyright 2018. Reproduced with permission of Wiley-VCH Verlag GmbH & Co. KGaA, Weinheim

simulation program. Navier–Stoke equations and convection–diffusion equation were used in the simulation. The gap was set as $50\ \mu\text{m}$, injection flow rate was set as $2\ \mu\text{L}\ \text{min}^{-1}$, and they were kept constant in all simulations and experiments. Geometry of the LSCE in computer simulation was identical to that in the experiment. The flow ratio between aspiration and injection flow rates was initially set as 5. Fluorescein solution with a concentration of $1\ \mu\text{g}\ \text{mL}^{-1}$ (equals to $3\ \mu\text{M}$) as a diffusive species indicated the microjet region. The diffusion coefficient of fluorescein is $500\ \mu\text{m}^2\ \text{s}^{-1}$ [103]. Figure 9.2a shows the bottom view of streamlines. Negative pressure relative to atmospheric pressure existed between the two apertures at the substrate (Fig. 9.2b). Along the positive direction of z-axis, pressure increased underneath the outlet of the injection channel and decreased underneath the inlet of the aspiration channel. Shear stress at the substrate surface is shown in Fig. 9.2c and reached a maximum ($1.27\ \text{Pa}$) at the inner edge of the aspiration aperture. Such low shear stress was friendly for use in conjunction with live cells and tissues. The concentration distributions of fluorescein at the plane of symmetry (Fig. 9.2d) and at the substrate pane (Fig. 9.2e) were simultaneously obtained. The concentration gradients resulted from diffusion were observed. Points with concentrations higher than 10% of the original diffusive species concentration were defined as the boundary of the efficient microjet (Fig. 9.2e). The boundary (red boundary in Fig. 9.2e) was observed when considering 10% of the original concentration of diffusive species as a boundary. Inside it, the diffusive species concentration was higher than 10% of its original concentration. The length and width of the red boundary at the substrate were defined and calculated (Fig. 9.2e).

In the experiments, boundaries of microjet were confirmed by using a solution containing fluorescein as injected solution. And, the leakage from the microjet was evaluated. A microjet with stable boundaries was obtained when the aspiration flow rate of $10\ \mu\text{L}\ \text{min}^{-1}$ was first applied (Fig. 9.2f). The fraction of integrated fluorescent intensity in the area besides microjet was calculated to evaluate the leakage. Different flow ratios were applied both in simulations and in experiments. The leakage from the microjet is at most 0.1% and even less under high aspiration flow rates. With the increase of flow ratio, the microjet shrunk gradually. The experimental results were consistent with the analytical results data (Fig. 9.2g, h). When flow ratio increased from 2.5 to 10, the length of microjet could be ranged from 260 to $130\ \mu\text{m}$ (Fig. 9.2g). Meanwhile, the width of the microjet could be ranged from 220 to $80\ \mu\text{m}$ (Fig. 9.2h). The dimensions of cells (U87 cells as an example) in adherent culture could reach to $100\ \mu\text{m}$; thus, their dimensions were comparable to the dimensions of a cell. The gap of $50\ \mu\text{m}$ was optimized. Both the trypsin concentration in microjet and the size of microjet decreased, and larger diffusion region was observed with the gap increased. The trypsin concentration was close to the initial one, and the boundary of the microjet was clear. As too small gap would sometimes cause physical damage to cell when moving the sample substrate, gap of $50\ \mu\text{m}$ was an appropriate condition for cell extraction.

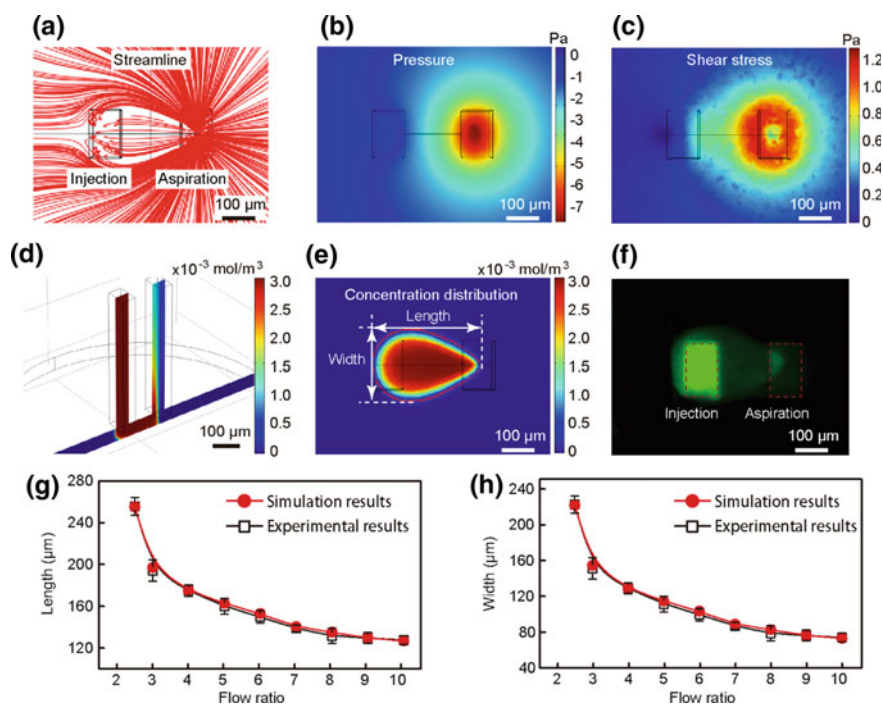


Fig. 9.2 Microjet underneath the LSCE. **a** Flow streamline fields. **b** Pressure near the substrate. **c** Calculated shear stress at the substrate surface. **d** Concentration distributions of diffusive species at the plane of symmetry. **e** Concentration distributions of diffusive species at the substrate. **f** Fluorescent image of microjet underneath the LSCE in the experimental results. **g** Length of microjet for varying flow ratio in experimental results and analytical results. **h** Width of microjet for varying flow ratio in experimental results and analytical results. Mao et al. [54]. Copyright 2018. Reproduced with permission of Wiley-VCH Verlag GmbH & Co. KGaA, Weinheim

9.2.3 Analysis of Cell Heterogeneity

An XYZ stage was functioned as a positioner to adjust the position of the petri dish to make a specified single cell right at the clearance between the two apertures (Fig. 9.3a). At the same time, the extraction of a single cell started. CAMs located on the cell surface [24] involved in binding with other cells or with the extracellular matrix (ECM). They were digested by trypsin. The live single cell was gradually detached from the bottom of petri dish (Fig. 9.3b) under the effect of negative pressure (Fig. 9.2b). The selected cell was successfully extracted and aspirated into the right aperture at time passed 4.5 min (Fig. 9.3c). The LSCE was demonstrated to be capable of local live single-cell extraction. The temperature was kept at 30 °C during all the experiments. The U87 cell would be extracted within ten to several ten seconds when temperature was controlled at 37 °C. It would be difficult to reveal cell heterogeneity in the latter case. In the case of samples with high cell

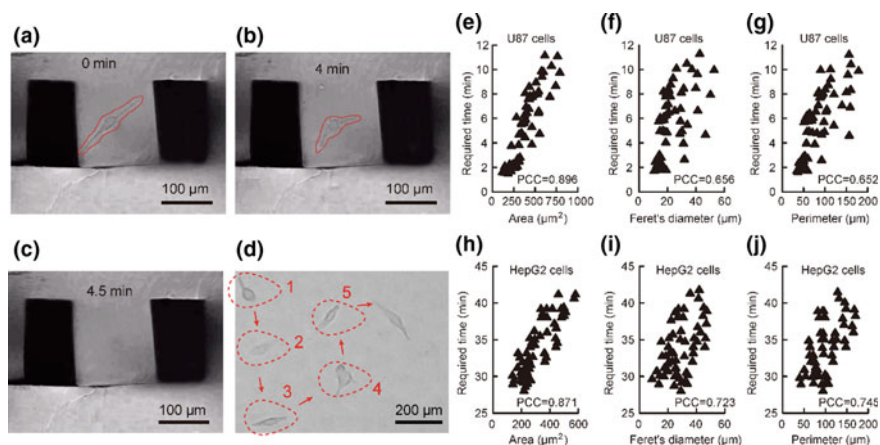


Fig. 9.3 In situ scatheless live single-cell detachment and connections between cell adhesion strength and cell morphology. The bright-field images during the cell extraction with different treating time—a 0 min, b 4 min, and c 4.5 min. d Localized extraction of particular single cells. Required time for extraction of each U87 cell relative to it, e area, f Feret's diameter, and g perimeter, and required time for extraction of each HepG2 cell relative to it's, h area, i Feret's diameter, and j Perimeter. Mao et al. [54]. Copyright 2018. Reproduced with permission of Wiley-VCH Verlag GmbH & Co. KGaA, Weinheim

density, cells still could be extracted on by one as different cells required different treating time. The extracting time for U87 cell could be shortened below 30 s through increasing trypsin concentration and optimizing temperature. If the cell samples were treated with trypsin with 20 s, we U87 cells could be extracted one by one in 5 s. This means the tool has potential of high-throughput analysis. When short extracting time was benefit to high-throughput analysis, long extracting time would be benefit to the cell heterogeneity.

There were several approaches for cell adhesion measurement [22, 24, 25, 108], but rare of them were capable for the measurement at single-cell resolution and the distinction of the individual differences between different cells. Single cells at different positions in the petri dish were extracted one by one (Fig. 9.3d), and the required time for extraction was recorded at the same time. The area, Feret's diameter, and perimeter of each single cell were analyzed using Image-Pro plus software (Media Cybernetics Inc., Bethesda, MD, USA). Pearson correlation coefficient (PCC) was calculated using IBM SPSS Statistics software 22.0 (SPSS Inc., Chicago, IL, USA). The results showed that a high PCC (0.896) revealed that the cell adhesion strength of each single U87 cell was closely relative to its area (Fig. 9.3e) at single-cell resolution. Also, the cell adhesion strength of each single U87 cell was relative to its Feret's diameter (Fig. 9.3f, PCC = 0.656) and perimeter (Fig. 9.3g, PCC = 0.652). The cell adhesion strength of particular cell was directly proportional to its area, Feret's diameter, and perimeter at single-cell resolution.

Moreover, the connection between cell adhesion strength of HepG2 cells and their morphologies was also investigated under the same experimental conditions as for U87. The results indicated that the required time of each single cell was different. The area, Feret's diameter, and perimeter of each single cell were related to its extraction time. The cell adhesion strength of each U87 cell showed positive correlations with cell area (Fig. 9.3h, PCC = 0.871), Feret's diameter (Fig. 9.3i, PCC = 0.723), and perimeter (Fig. 9.3j, PCC = 0.745). Similarly, cell adhesion strength of each single HepG2 cell was closely related to its area, Feret's diameter, and perimeter. The cell differences on morphology as well as the connections between cell adhesion strength and cell morphology at single-cell resolution were demonstrated.

9.2.4 Correlation Between Adhesion Strength and Viability at Single-Cell Resolution

Cells themselves not only have individual cell morphologies, but also have individual intracellular contents, such as metabolites and organelles. The differences have been reported through several approaches [109, 110]. Yet, correlations between multiple parameters are still vital issues. Adherent cultured cells were co-stained by 2,3-Naphthalenedicarboxaldehyde (NDA, 10 μ M), Dihydroethium (DHE, 25 μ M, Sigma), MitoTracker Red (1 μ M), and HOE (1 μ M) in phosphate buffer (PBS, 0.01 M, pH 7.4) to represent reduced glutathione (GSH), oxidized glutathione (GSSG), mitochondrion, and state of nucleus in cells, respectively. The normalized fluorescent intensity (NFI) with a high value corresponds to a high amount of stained target intracellular content. U87 cells in adherent tissue culture stained by NDA and DHE are shown in Fig. 9.4a. Different cells were remarked with a Cell No under the observation by confocal microscope. The numbered cell was then extracted by the LSCE to measure the cell adhesion strength. Thus, the cell adhesion strength of an individual cell was conveniently related to the amount of different intracellular contents.

The cell adhesion strength of each U87 cell showed good positive correlations with the NFI of NDA (Fig. 9.4b, PCC = 0.928), which represented the content of GSH, and had negative correlations with the NFI of DHE (Fig. 9.4c, PCC = -0.916) which represented the contents of GSSG in cell. U87 cells in adherent tissue culture co-stained by MitoTracker Red and HOE are shown in Fig. 9.4d. The cell adhesion strength of each U87 cell showed good positive correlations with the NFI of MitoTracker (Fig. 9.4e, PCC = 0.964) which represented the content of mitochondrion in cell. Otherwise, the cell adhesion strength of each U87 cell had low negative correlation with the NFI of HOE which represented the content of nucleus in cell (Fig. 9.4f, PCC = -0.768).

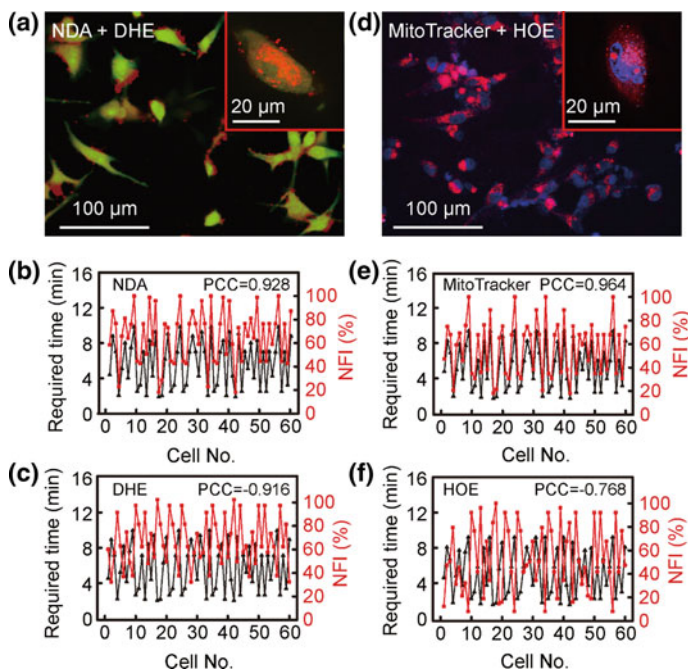


Fig. 9.4 Cell heterogeneity analysis and the connections between cell adhesion strength and its viability in individual U87 cells at single-cell resolution. **a** A merged fluorescent image of U87 cells stained by NDA (in green) and DHE (in red). **b** A merged fluorescent image of U87 cell stained by MitoTracker (in red) and HOE (in blue). Required time for extraction of each U87 cell relative to the NFI of **c** NDA, **d** MitoTracker, **e** DHE, and **f** HOE. Mao et al. [54]. Copyright 2018. Reproduced with permission of Wiley-VCH Verlag GmbH & Co. KGaA, Weinheim

Co-stained HepG2 cells with NDA and DHE in the same manner are shown in Fig. 9.5a. The co-stained HepG2 cells with MitoTracker Red and HOE are shown in Fig. 9.5b. The adhesion strength of HepG2 revealed positive correlations with amount of GSH (Fig. 9.5c, $PCC = 0.806$) and mitochondrion (Fig. 9.5d, $PCC = 0.824$). Additionally, it revealed negative correlations with amount of GSSG (Fig. 9.5e, $PCC = -0.738$) and state of nucleus (Fig. 9.5f, $PCC = -0.862$) at single-cell resolution. Those results suggested that a particular cell with high adhesion strength usually possessed high cell viability. Moreover, the cell with high viability might have a high amount of GSH, ATP (corresponding to amount of mitochondrion) and a low amount of GSSG. The LSCE was demonstrated to be capable for uncovering the correlations between the cell adhesion strength and its multiple intracellular content levels at single-cell resolution. Single-cell studies will continue to illuminate the inner life of the cell itself. Thus, the presented methodology will contribute to tissue research at single-cell resolution.

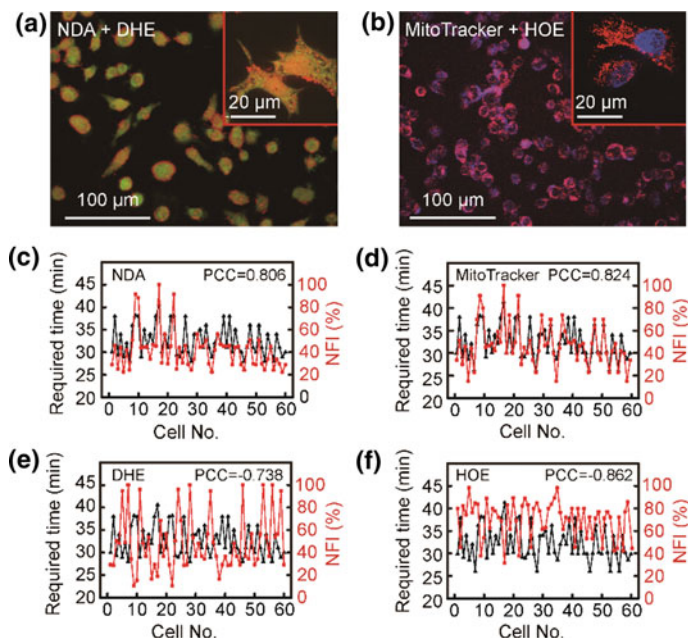


Fig. 9.5 Cell heterogeneity analysis and the connections between cell adhesion strength and cell viability in individual HepG2 cells at single-cell resolution. **a** A merged fluorescent image of HepG2 cells stained by NDA (in green) and DHE (in red). **b** A merged fluorescent image of HepG2 cell stained by MitoTracker (in red) and HOE (in blue). Required time for extraction of each HepG2 cell relative to the NFI of **c** NDA, **d** MitoTracker, **e** DHE, and **f** HOE. Mao et al. [54]. Copyright 2018. Reproduced with permission of Wiley-VCH Verlag GmbH & Co. KGaA, Weinheim

9.3 Measurement of Cell-Matrix Adhesion at Single-Cell Resolution

In this section, a novel strategy was described for measuring cell-matrix adhesion at single-cell resolution and for precisely evaluating of functions of biomaterials for adherent cell culture [111]. Different biomaterials were prepared using chemical modifications or physical modifications. The method was applied for measurement of cell-matrix adhesion and evaluation of biomaterials on their compatibilities. The effects of those biomaterial substrates on the cells cultured on them were uncovered at single-cell resolution.

9.3.1 Operation System and Flow Confinement

The operation system contained the LSCE, pump system, temperature controller, position holder, and the microscope (Fig. 9.6a). The designed LSCE consists of a channel for trypsin solution injection and another channel for solution aspiration (Fig. 9.6b). The bottom end of the pen was placed parallel to the sample surface while both were immersed in solution. The sample was placed on a hotplate to preserve a steady temperature (37 °C as an example), while the temperature was controlled by a temperature controller (Pecon, Wetzlar, Germany). Simultaneous aspiration flow and injection flow of trypsin solution were controlled by syringe pumps. The tip part contains two parallel microchannels used to create a stable zone of trypsin solution by hydrodynamic confinement for single-cell extraction to measure cell-matrix adhesion. A clearance existed between the bottom end of the pen and the sample surface, which was defined as “gap.” An XYZ stage was utilized as a LSCE holder for adjusting the gap. Convection would be fast enough to prevent diffusion of molecules of interest out of the region when the gap was sufficiently small and the aspiration flow rate (Q_A) is sufficiently larger than the injection flow rate (Q_I). This was demonstrated in the experiment using fluorescein solution ($1 \mu\text{g mL}^{-1}$) (Fig. 9.6c; where $Q_I = 10 \mu\text{L/min}$, $Q_A = 50 \mu\text{L/min}$, gap = 50 μm). Leakage from the working region was investigated by using a solution containing 0.25% trypsin and 0.02% EDTA, as well as 1 $\mu\text{g/ml}$ fluorescein for visualization. The leakage was evaluated by calculating ratio between the

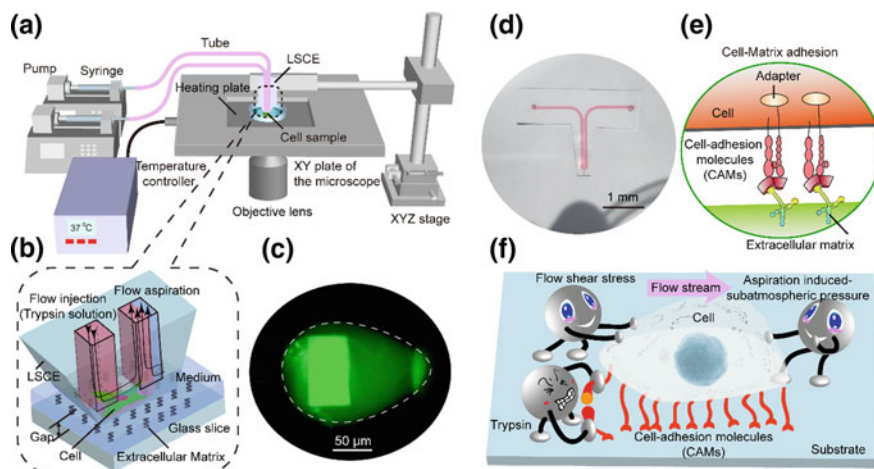


Fig. 9.6 Single cell-matrix adhesion measurement for precise evaluating functions of biomaterials. **a** The operation system for cell adhesion measurement. **b** LSCE device for single-cell extraction. **c** The zone of fluorescein solution at the surface underneath the LSCE. **d** A photograph of the device filled with red dye. **e** Mechanism of cell-matrix adhesion. **f** The process of cell detachment and dominant impact factors. Mao et al. [111]. Copyright 2018. Reproduced with permission of American Chemical Society

fluorescent intensity in microjet and that in surrounding area. The leakage was evaluated under different gaps and aspiration flow rates. The upper bound of the region depended on the diffusivity of the molecule transported. In convenience, the zone size was adjusted to be slightly larger than the size of the cell (10–60 μm here) to allow extraction of only a single cell underneath the LSCE tip. The LSCE device filled with a red dye is shown in Fig. 9.6d.

Cells were usually cultured on biomaterials in cell researches in vitro. Cell-matrix adhesion will significantly affect the behaviors of cells, such as cell spreading, migration, division, metabolism, and interactions with other cells. In some cases, cell adhesion is fundamental to cell behaviors. Cell adhesion molecules (CAMs) on cell surface bound to various components of ECM after cells were loaded on biomaterials (Fig. 9.6e). Confinement of the trypsin solution to a zone ensures that neighboring cells are not disturbed, when allowing the target cell's capture back into the device (Fig. 9.6b). Trypsin digests the CAMs between cell and matrix gradually (Fig. 9.6f) [112]. Flow stream pushes the cell right at the same time, and the subatmospheric pressure near the aspiration aperture pulls the cell. The time for achieving cell detachment represents the cell-matrix adhesion strength.

9.3.2 Biomaterials Preparation and Adherent Cell Culture on Biomaterials

Glass slides were modified with hydroxyl group (OH) by immersing the glass into piranha solution for 1 h. OTS-Toluene (1% v/v, J&K, China) and APTES-Toluene (1%, v/v, J&K, China) were, respectively, poured onto the OH-modified glass and then shook incessantly for 1 h to convert OH to amino group (NH_2) and alkyl group (C18). The OH-modified glass slides were immersed into 0.01% PLL (Sigma, USA) solution and 250 $\mu\text{g}/\text{mL}$ FN solution (Invitrogen, USA), incubated for 1 h to prompt the adsorption of biomolecules to the glass, then washed with PBS for 3 times, and utilized immediately. All biomaterials surfaces were analyzed by X-ray photoelectron spectroscopy (XPS, PHI Quantera II, Ulvac-Phi Inc., Japan) and Atomic force microscope (AFM, Dimension, Bruker, German) before and after modifications.

Cells might lose some essential functions without appropriate cell matrix [40], which necessitates the search for proper biomaterials that are suitable for cell culture, especially for cell adhesion. For this aim, reliable methodologies should be established for sufficiently revealing the functions of biomaterials for cell adhesion. Various biomaterials were prepared by chemical and physical modifications, including piranha solution (*caution: piranha is corrosive and must be handled with care*)-treated glass slice (OH-glass) as the substrate. (3-Aminopropyl) triethoxysilane-coated glass slice (APTES-glass), octadecyltrichlorosilane-coated glass slice (OTS-glass), poly (*L*-polylysine)-coated glass slice (PLL-glass), and fibronectin-coated glass slice (FN-glass) were prepared for cell culture (Fig. 9.7a). Cell-matrix adhesion measurements on those biomaterials were implemented to

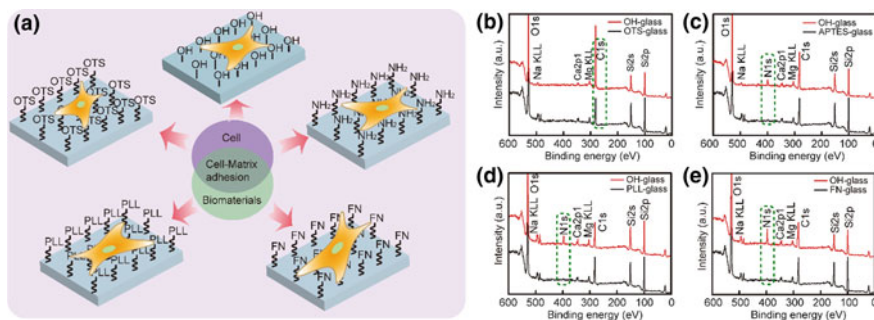


Fig. 9.7 Biomaterials preparation and characterizations. **a** Biomaterials preparation and scheme for cell-matrix adhesion. XPS analysis for **b** OTS, **c** APTES, **d** PLL, **e** FN-coated glass from OH-glass. Mao et al. [111]. Copyright 2018. Reproduced with permission of American Chemical Society

evaluate the functions of those biomaterials for cell culture. XPS analysis was utilized to investigate the surficial structure on various biomaterials and to demonstrate the successful modification. Compared to the XPS analysis of OH-glass, an obvious increase of the core level of C 1s belonging to carbon appeared on the OTS-glass (Fig. 9.7b), so that the successful immobilization of OTS was confirmed. After the OH-glass was treated by APTES solution, a remarkable N 1s belonging to nitrogen in XPS analysis indicated the successful immobilization of APTES (Fig. 9.7c). In the same manner, the successful modifications of PLL (Fig. 9.7d) and FN (Fig. 9.7e) were demonstrated, respectively.

U87 cells were purchased from Cancer Institute & Hospital of the Chinese Academy of Medical Science (Beijing, China). Cells were cultured in a humidified atmosphere of 95% air and 5% CO₂ at 37 °C. U87 cells were maintained in minimal essential medium (MEM, Corning, USA) with Earle's Salts and L-glutamine supplemented with 10% fetal bovine serum (FBS, Corning, USA), nonessential amino acids, 100 units/mL penicillin, and 100 units/mL streptomycin. Cells were maintained in petri dishes for 2–3 days prior to commencing the experiments. All the experiments were carried out when the cells were in the exponential growth phase. Cells were detached from the petri dishes with 0.25% trypsin, resuspended in cell culture medium, and seed onto various biomaterials at a final density of $\sim 1 \times 10^4$ cells/cm². Cells were maintained on the biomaterials for at least 6 h for cell adherence prior to cell-matrix adhesion measurement experiments.

9.3.3 Cell-Matrix Adhesion Measurement at Single-Cell Resolution

U87 cells with an appropriate cell density (about 1×10^4 cell/cm²) were cultured on the various biomaterials (APTES-glass for example). The sample was placed

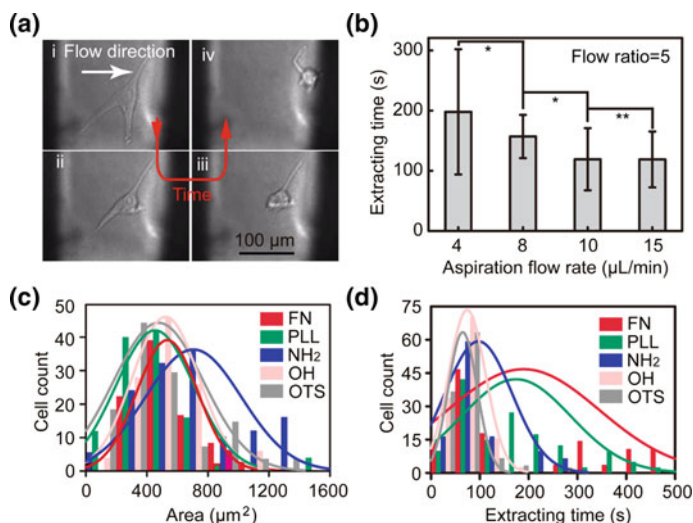


Fig. 9.8 Cell-matrix adhesion measurement for evaluating of biomaterials. **a** Cell-matrix adhesion measurement by extracting single-cell from the biomaterials surface. **b** The influence of flow rates on extracting time. * $P < 0.05$, ** $P > 0.05$, one-sided Student's t -test. **c** Distributions of single cells spreading area on various biomaterials. **d** Distribution of extracting time for single cells on various biomaterials. Mao et al. [111]. Copyright 2018. Reproduced with permission of American Chemical Society

underneath the LSCE after cell adhered on the biomaterials. Both the sample and LSCE were immersed in cell culture medium. By adjusting the XYZ stage, the gap was adjusted to be 50 μm . The injection flow rate of trypsin flow and aspiration flow rate were set as 10 and 50 $\mu\text{L}/\text{min}$, respectively. The cell sample was adjusted to make a target single cell right at the clearance between the two apertures using the XY stage on the microscope (Fig. 9.8a, part i). The measurement of cell-matrix adhesion started immediately. Working temperature was kept at 37 $^{\circ}\text{C}$ using the heating plate on the microscope in all the experiments. ECM and CAMs that located on cell surface were digested from the cell edge (Fig. 9.6b). As a result, cell gradually left the substrate and shrank simultaneously (Fig. 9.8a, part ii). Portions of the cell folded over the remaining part toward the flow direction as time passed (Fig. 9.8a, part iii). Finally, the cell-matrix adhesion was completely overcome and the whole cell left away from the substrate and was drawn back into the right aperture (Fig. 9.8a, part iv). The strength of the cell-matrix adhesion between this single cell and substrate was represented by the extracting time for the whole process. By repeating the process, the cell-matrix adhesion at different points was measured by extracting single cells one by one. As a result, the cell-matrix adhesion at single-cell resolution was clarified.

In further studies, flow shear stress also has remarkable influences on the extracting time (Fig. 9.8b). The extracting time revealed significant decreases (P -value below 0.05) when the injection flow rate increased from 4 to 8 $\mu\text{L}/\text{min}$

($P = 0.023$) and then to 10 $\mu\text{L}/\text{min}$ ($P = 0.001$), while no significance was found when the injection flow rate increased from 10 to 15 $\mu\text{L}/\text{min}$ ($P = 0.254$). The optimized conditions of $Q_I = 10 \mu\text{L}/\text{min}$, $Q_A = 50 \mu\text{L}/\text{min}$ were used to measure the cell-matrix adhesion strength between adherent U87 cells and various biomaterials. Aim to distinguish the differences between different cells, excessive decrease on extracting time does not benefit to observe these differences. In the future, the extracting time can be reduced by increasing the trypsin concentration to meet the requirements of high-throughput assay.

The cell spreading was reported a vital factor to evaluate the functions of biomaterials and their biocompatibilities [113]. Cell spreading areas on four of the five kinds of biomaterials showed little difference, while those on APTES-glass appeared significantly larger (Fig. 9.8c). Those results may indicate that APTES-glass owned the highest biocompatibility while the other four held comparable biocompatibilities. According to the cell spreading area, the order of compatibilities of various biomaterials was displayed as follows: APTES-glass > FN-glass > OH-glass > OTS-glass > PLL-glass (Fig. 9.8c). The cell spreading area on various biomaterials excepted APTES-glass showed slight difference. Surprisingly, the order was not consistent with reported compatibilities of those biomaterials [114–116]. Thus, it was difficult to determine which kind of biomaterial was better for adherent cell culture. In such case, the conventional methods became powerless to distinguish those biomaterials, and the results became insufficient and inaccurate.

By using the LSCE device to measure the cell-matrix adhesion, the results (Fig. 9.8d) showed that PLL-glass and FN-coated glass slice owned the best biocompatibility for adherent cell culture following by the APTES-glass. Those results were consistent with reported findings [114–116]. OH-glass slice and OTS-glass slice showed weak biocompatibilities (Fig. 9.8d). The LSCE in the section showed a more precise and reliable evaluation of biomaterials for adherent cell culture. Influences of biomaterials on cell heterogeneity were also a dominant parameter to evaluate their functions for cell researches. The coefficient of variation (CV) of extracting time was calculated to reveal the cell heterogeneity of cell-matrix adhesion. From the results, OTS modification weakened the heterogeneity while APTES, PLL, and FN modifications enhanced the heterogeneity comparing to the initial OH-glass (Fig. 9.8d). The ascending order of cell heterogeneity of cell-matrix adhesion was displayed as follows: FN-glass (CV = 0.82) > PLL-glass (CV = 0.70) > APTES-glass (CV = 0.64) > OH-glass (CV = 0.51) > OTS-glass (CV = 0.45). Although there are several approaches for cell adhesion measurement, none of them enabled the measurement at single-cell resolution and the estimation of the individual differences between different single cells. The LSCE described in this section was capable of uncovering not only the compatibility of the biomaterials, but also the influences of them on cell heterogeneity.

9.4 Adhesion Analysis of Single Circulating Tumor Cell on Base Layer of Endothelial Cells

A novel approach was described for measuring natural cell-to-cell adhesion strength of single CTC on base layer of ECs that would contribute to uncovering the mechanism of tumor metastasis[117]. Trypsin solution in confined zone was utilized to extract single adhered CTC from EC layer. The adhesion strength of multiple types of single CTCs as well as the drug influences on CTCs adhesion was investigated. The results indicated that different types of CTCs maintained different adhesion strength and very few single CTCs in each type held strong adhesion ability to HUVEC cell layer.

9.4.1 Work Principle for Cell-Cell Adhesion Analysis

Adherence of CTC to the vascular internal wall is a key step in tumor metastasis, (Fig. 9.9). At first, CTC suspension was loaded on EC layer in adherent culture (Fig. 9.10a, part i) and then CTCs adhered on EC layer (Fig. 9.10a, part ii) with or without the effect of drugs. A stable open microflow with distribution of trypsin was used to analyze single CTC for its adhesion strength (Fig. 9.10a, part iii). A commercially available solution containing 0.25% trypsin and 0.02% EDTA was used in all experiments. Trypsin solution (if not noted specially, its concentration was always 3 mmol/m^3) was injected into the system through the upper aperture of the left microchannel and flowed out through the lower aperture. The trypsin renewed ceaselessly, and the products could be eliminated in time. Target cell was always surrounded by fresh trypsin with stable concentration (Fig. 9.10a, part iii). The temperature was controlled at $37 \text{ }^\circ\text{C}$, and the pH also remained constant (pH 7.4) because of the buffering of culture medium.

The extracting time mainly depended on the adhesion strength of the target cell under the constant conditions. Convection and diffusion were the two fundamental modes of mass transfer. The effect of diffusion driven by concentration gradient should be as weak as possible to control the spatial distribution of trypsin. In the experiments, cell sample and LSCE were immersed in cell culture medium with 10% fetal bovine serum (FBS). Trypsin would be diluted by culture medium once the trypsin solution was aspirated back to the aspiration aperture. Therefore, the excess trypsin would be neutralized by sufficient FBS to prevent continued digestion of cellular proteins.

Cell-to-cell adhesion was mediated by cell adhesion molecules (CAMs) including Ig-superfamily, selectin and cadherin and integrin (Fig. 9.10b) [118]. ECM proteins were recruited to form tight connections between cells during the process of cell adherence under the regulation of enzymes including focal adhesion kinase. The peptide bonds formed by lysine and arginine were digested by trypsin. Then, single cells were detached gradually from adjacent cells. The time for the

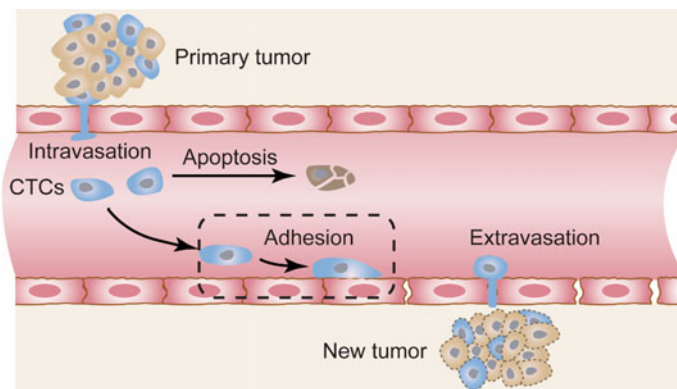


Fig. 9.9 CTCs adherence to the vascular internal wall in tumor metastasis

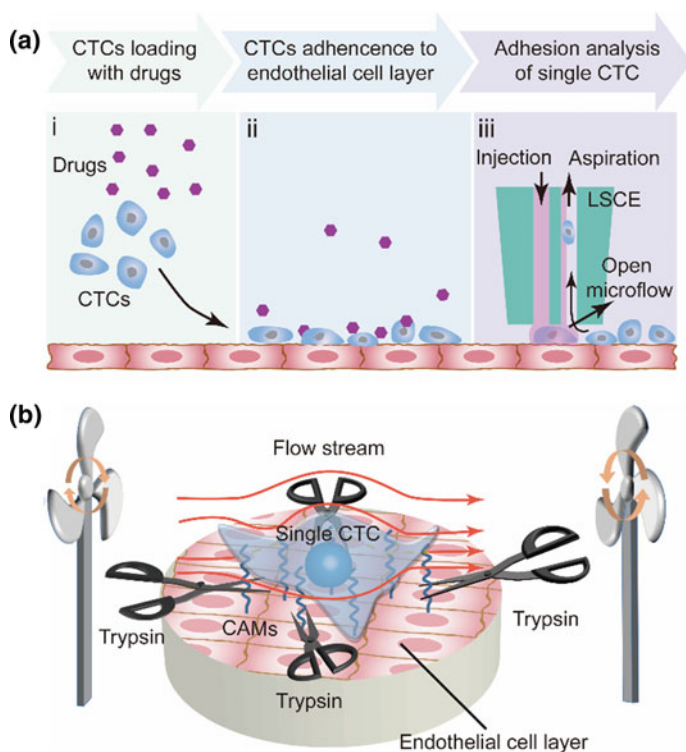


Fig. 9.10 Adhesion strength analysis of single CTC on EC layer. **a** Co-culture of CTCs on ECs and evaluation of drug influences of CTCs adhesion. **b** Adhesion strength measurement of single CTC by the time required for extracting the cell from EC layers. Mao et al. [117]. Copyright 2018. Reproduced with permission of Royal Society of Chemistry

detachment represented the cell adhesion strength when the operation conditions (trypsin concentration, flow rates, temperature, and pH) remained constant. The recorded adhesion strength measured by the LSCE represented the dynamic cell response during deadhesion, which was quite different from the protein analysis of focal adhesion [119].

9.4.2 Numeric Simulation

Simulated by COMSOL Multiphysics, the dynamic characteristics of fluid around the cell are shown in Fig. 9.11. In the model (Fig. 9.11a), the two cuboids represented the solution in both channels. The disk represented the solution between the bottom surface of the device and the substrate in the petri dish. The trypsin solution and surrounding medium were jointly aspirated back into the right microchannel through its lower aperture. Cell was modeled approximately to a bell-shaped rotator (Fig. 9.11a).

In the simulation, if not noted specially, the injection flow rate (R_i) = 10 $\mu\text{L}/\text{min}$, aspiration flow rate (R_a) = 50 $\mu\text{L}/\text{min}$, and gap = 50 μm . The zone of trypsin (Fig. 9.11b) was consistent with experiment results. By adjusting the gap between the tip of channels and the substrate surface, the 3D distribution of trypsin could be well controlled (Fig. 9.11c). The concentration of trypsin near the target cell became lower with an increased gap (100 μm) near the target cell. The results indicated that cells in the higher layer were covered with higher concentration of trypsin, resulting in a shorter digestion time. Then, different flow ratios were applied. The zone of trypsin decreased with the increase of flow ratio (Fig. 9.11d) when the boundaries of the zone were set at 10% (or 90%) of the maximum of trypsin concentration. Excessively low flow ratio would result in the leakage of trypsin, while too high flow ratio made the small diffusion region fail to cover the target cell completely. In order to confine trypsin in a small area with high concentration, flow ratio was further optimized.

9.4.3 Adhesion Analysis of CTCs on Cell Layer

Cells owned better adhesion ability (HUVEC cell as an example) were chosen as base, and the substrate in cell-to-cell adhesion experiments was pretreated to enhance the cell layer adhesion on substrate. As a result, the upper cells could be extracted before base cells were influenced obviously. HUVEC cells acted as ECs, and U87 cells acted as CTCs.

There were three single cells on the cell layer in the bright-field image of one observational micro-zone (Fig. 9.12a). Aim to distinguish U87 cells from HUVEC cells, the former ones were stained by 1,1'-dioctadecyl-3,3',3'-tetramethylindocarbocyanine Perchlorate (Dil) with red fluorescence for visualization of

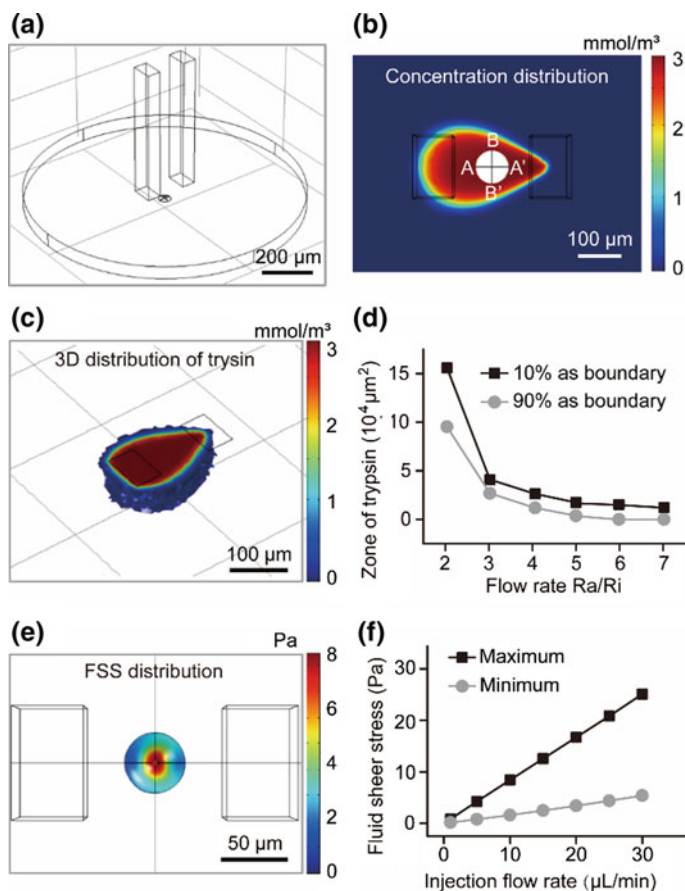


Fig. 9.11 A simulation of the physical quantity of the micro-zone by COMSOL Multiphysics. **a** Overall model. **b** Concentration distribution of trypsin on the surface of substrate. **c** 3D distribution of trypsin. **d** Zone of the trypsin on the surface of substrate under different Ra/Ri ratio. Injection flow rate was constant (10 $\mu\text{L}/\text{min}$). **e** Distribution of fluid shear stress on the surface of the cell mode. **f** Relationship of shear stress on the surface of the cell (maximum and minimum) and inflow rate under the same ratio Ra/Ri. Mao et al. [117]. Copyright 2018. Reproduced with permission of Royal Society of Chemistry

single U87 cell on HUVEC cell layer (Fig. 9.12b). No. 1 cell was confirmed as U87 cell by comparing the fluorescent image (Fig. 9.12b) with bright-field image (Fig. 9.12a). Then, extraction of single CTC from EC layer was demonstrated (Fig. 9.12c–f). Generally, single U87 cell would move and leave the HUVEC cell layer gradually after the proteins were digested by trypsin. The time required for finishing the extraction of the cell could reflect the adhesion strength of single U87 cell on HUVEC cell layer. As calculated, the translational speed of the U87 cell under the flow environment was almost constant (0.1 $\mu\text{m}/\text{s}$), which indicated that some single-U87 cells were only physically adsorbed on the HUVEC layer.

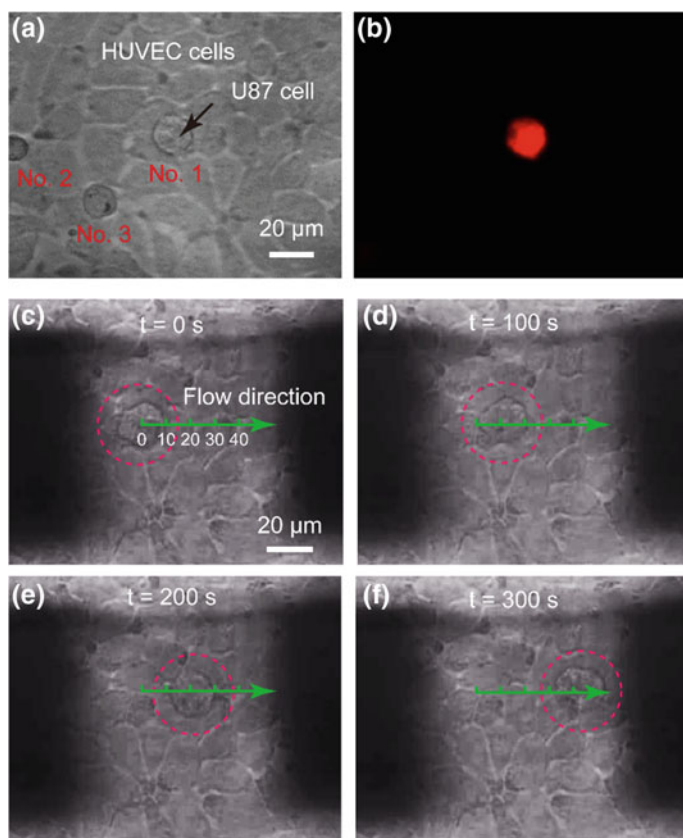


Fig. 9.12 U87 cells adherence on HUVEC cell layer and its extraction. **a** Bright-field image of U87 cell on HUVEC layer. **b** Fluorescent image of U87 cell on HUVEC cell layer. Bright-field images of the single U87 cell at different time on HUVEC cell layer **c** 0 s, **d** 100 s, **e** 200 s, **f** 300 s in the extracting process. Mao et al. [117]. Copyright 2018. Reproduced with permission of Royal Society of Chemistry

In principle, the concentration of trypsin, the fluid drag force (depending on flow velocity), and subatmospheric pressure jointly contributed to the extraction (Fig. 9.10b). The extracting time raised with the increase of Ri and related Ra under constant flow ratio (Fig. 9.13a). With the increase of flow rate, the concentration of trypsin near the cell edge (point A and point B in Fig. 9.11b) showed no significant change (Fig. 9.13b). On the contrary, the fluid drag force and subatmospheric pressure that rose with flow rates shortened the extracting time. The raising fluid drag force and subatmospheric pressure induced reduction of the extracting time (Fig. 9.13c) when flow ratio rose from 3 to 5, because the concentration of trypsin near cell edge showed no significance (Fig. 9.13d). Then, the extracting time increased because of the sharp decrease of trypsin concentration when flow ratio

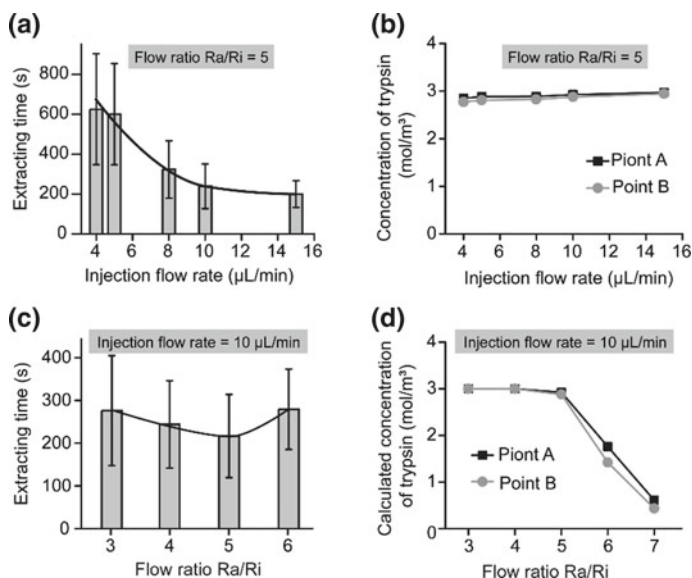


Fig. 9.13 Adhesion strength analysis of single-U87 cells on HUVEC cell layer. **a** Extracting time under different injection flow rates ($Ra/Ri = 5$) ($n = 100$). **b** Calculated trypsin concentration on the cell surface (points A and B in Fig. 2b) under different injection flow rates ($Ra/Ri = 5$). **c** Extracting time under different flow ratios Ra/Ri ($n = 100$). The injection flow rate was $10 \mu\text{L}/\text{min}$. **d** Calculated trypsin concentration on the cell surface (points A and B) under different flow ratios. Mao et al. [117]. Copyright 2018. Reproduced with permission of Royal Society of Chemistry

move to 6 (Fig. 9.13d). When the ratio was higher than 7, the U87 cells failed to leave the glass within 30 min because the trypsin couldn't reach the adhesion area. As a result, flow ratio ($Ra/Ri = 5$) was optimal.

9.4.4 Drug Influences on Cell-Cell Adhesion

U87 cells, Caco-2 cells, and HepG2 cells were analyzed when they were co-cultured and adhered to HUVECs that acted as ECs. The extracting time divided by cell contact surface area for normalization of the data represents the adhesion strength of the cell. Cell contact surface was calculated using Image-Pro plus software (Media Cybernetics Inc., Bethesda, MD, USA). Each type of CTCs showed significantly different adhesion strength on HUVEC cell layer (Fig. 9.14a). HepG2 cells appeared stronger adhesion ability, which indicated that they may be easier to adhere on vascular internal wall. The glycoprotein on plasma may be the dominant parameter. Yet, more effort should be made to uncover the mechanism for this strong adhesion by cell molecule biology. However, it should be noticed that

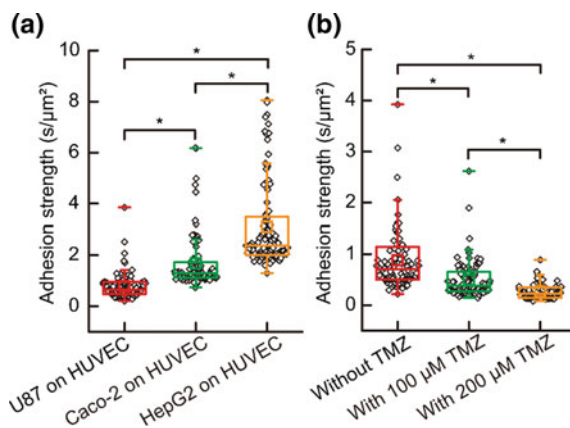


Fig. 9.14 Adhesion strength analysis of single CTC on EC layer. **a** Adhesion strength analysis of different types of CTCs on EC layer ($n = 100$ for each type of CTC). **b** Drug influence (TMZ) on adhesion strength of U87 cells on HUVEC cell layer ($n = 100$ for each group). Two-tailed Student's t -test was performed in A and B. $*P < 0.001$. Mao et al. [117]. Copyright 2018. Reproduced with permission of Royal Society of Chemistry

those results were far from concluding that this type of CTC (HepG2 cell) was much easier to occur tumor metastasis, because there were many other parameters. Those results were helpful for characterizing and understanding the process of CTCs adherence. The adhesions of single CTCs had heterogeneity, and rare cells possessed extremely high adhesion strength in each type of CTCs.

Prevention of the CTCs adherence to vascular internal wall might be an efficient way to prevent tumor metastasis. HUVEC cells cultured in a petri dish then formed a cell layer. The suspension of U87 cells containing antitumor drug (Temozolomide, TMZ) was added to the HUVEC cell layer in petri dish. After 3 h, the medium surrounding the cells was replaced by fresh cell culture medium without drug. Dead cells or non-adhered cells were removed. Adhesion of each U87 cell was carried out to evaluate the influence of TMZ and reveal its role in cancer therapy. The results indicated that TMZ significantly weakened the adhesions of single-U87 cells on HUVEC cell layer, and the adhesion strength further decreases with the increasing concentration of TMZ (Fig. 9.14b). TMZ led to apoptosis of tumor cells and would damage DNA, resulting in abnormal protein secretion. Thus, the adhesion was weakened. The results suggested that TMZ was effective not only for chemotherapy but also for preventing tumor metastasis. As adhesion of CTCs in blood vessels is a complex phenomenon, more factors should be considered in the future, such as influence of fluid shear stress and participation of immunocyte. This method offered a novel perspective to study single CTC adhesion and supply a potential avenue for evaluation and screening of antitumor drug. In the future, this tool was expected to be a new avenue for adhesion behaviors analysis of CTCs and provided new insights into prevention of tumor metastasis.

9.5 Fluidic Cell Knife (Fluid CK) for Chemical Surgery on Single Cells

The section discusses on a fluid cell knife [120], a highly flexible microfluidic methodology, which provides users with the ability to cut off a portion of a living single cell from precise position and treat portions of cells. The device was capable for local excision of a desirable single cell and microenvironment control of partial cell. In conventional method for generating confined flow in open space [121–123], the interface of the interested solution with the adjacent one had a remarkable positional fluctuation caused by the elasticity of pathway and vibration of pumps. Therefore, maintaining stable interface at a precise position was still difficult. The Fluid CK was designed with a symmetrical geometry, so the two solutions would confront each other to counteract the fluctuation. Benefiting from the symmetrical geometry, the interface of two adjacent solutions was extremely stable.

9.5.1 Fluid Cell Knife

The design of the Fluid CK with symmetrical geometry contained four identical apertures (Fig. 9.15a). In use, the tip of the Fluid CK and the cell samples were immersed in cell culture medium. The tip of Fluid CK was placed perpendicular to the cell sample surface, and a “gap” existed between the tip of the Fluid CK and the sample surface (Fig. 9.15a). Through two opposite apertures, the solution A (red) and solution B (green) were injected into the device using two individual gas-tight syringes driven by one pump (Fig. 9.15b). The other two apertures were for solution aspiration by connecting to two individual gas-tight syringes driven by another pump. As a result, a straight interface across the centers of two aspiration apertures generated. In experiments, cell was manipulated to make the interface at a desirable subcellular position, resulting in one portion of the cell immersed in solution A and the other portion in solution B (Fig. 9.15b). When solution A was cell culture medium and solution B was cell lysis buffer, the portion in solution B would be cut off while the other portion was well protected by the cell culture medium (Fig. 9.15c). The Fluid CK functioned as a lancet to operate a single cell. When solution A and solution B contained different species, different portions of the cell were infused with different types of molecules (Fig. 9.15d). Subcellular molecule infusions were achieved for partial cell staining and analysis of organelle transports.

9.5.2 Finite Element Analysis (FEA)

Fluid underneath the Fluid CK was simulated by Finite element analysis (FEA) using a commercially available software COMSOL Multiphysics 5.3 (Comsol).

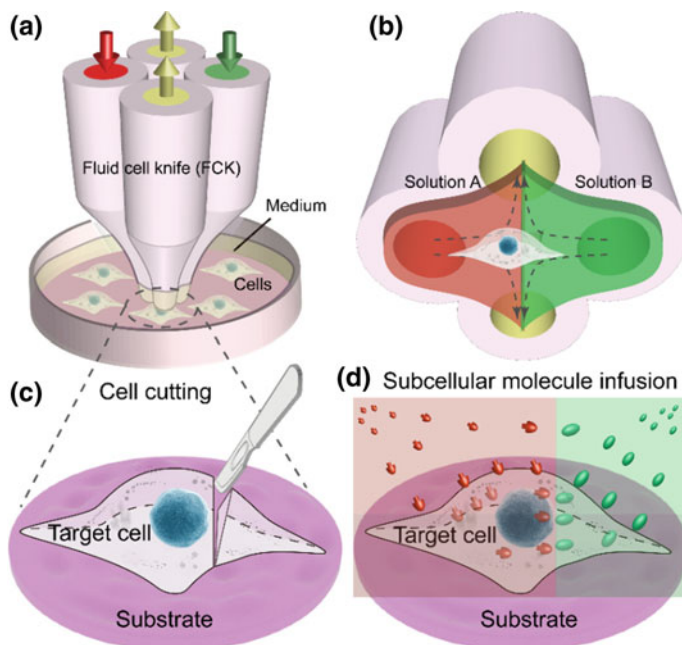


Fig. 9.15 Fluid cell knife (Fluid CK) for precise chemical surgery on single cells. **a** Design and operation of the Fluid CK. **b** Principle of fluid control for partial treatment. **c** Illustration of precise cutting of a single cell. **d** Subcellular molecule infusion to a single cell using the Fluid CK. Mao et al. [120]. Copyright 2019. Reproduced with permission of Royal Society of Chemistry

Navier–Stoke equations and convection–diffusion equation were coupled in the FEA. The geometry of the model was identical to the device in experiments (Fig. 9.16a). If not noted specially, the injection flow rate (R_i) = $1 \mu\text{L min}^{-1}$, aspiration flow rate (R_a) = $10 \mu\text{L min}^{-1}$, and gap = $50 \mu\text{m}$. The injected solution containing fluorescein ($1 \mu\text{g mL}^{-1}$, equals to $3 \mu\text{M}$) as a diffusive species indicated the microjet region. The diffusion coefficient of fluorescein is $500 \mu\text{m}^2 \text{s}^{-1}$ [102]. The bottom views of streamlines and the velocity field at the substrate are shown in Fig. 9.16b, c, respectively. Both appeared symmetrical distributions.

In the simulation results, the concentration distribution of the species (Fig. 9.16d) had a planar interface along line YY' . A concentration gradient existed along line XX' (Fig. 9.16e). Moreover, a uniform concentration was observed along line YY' near the center (Fig. 9.16f), which indicated the proper function of the laminar flow within this spatial range. FSS distributions near the substrate were calculated (Fig. 9.16g) as cells were sensitive to fluid shear stress (FSS) [124, 125]. The FSS at the point near the center (with a distance smaller than $50 \mu\text{m}$) was sufficiently lower than 0.1 Pa (Fig. 9.16h, i), which would not harm the cell [124]. Negative pressure relative to atmospheric pressure existed at the microregion. The maxima of FSS, velocity, and pressure were linear with the flow ratio as well as

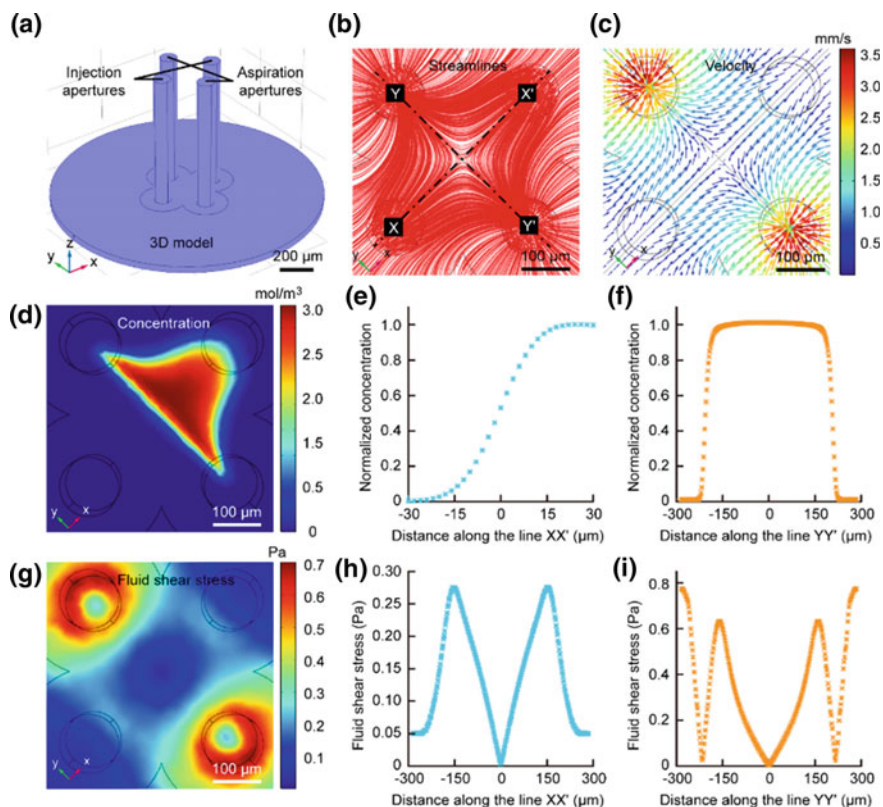


Fig. 9.16 Microjet underneath the Fluid CK in the FEA. **a** Geometry of the Fluid CK in the simulation. **b** Flow streamline fields. **c** Velocity distribution at the substrate. **d** Concentration distributions of the diffusive species at the substrate. **e** Concentration profile of the diffusive species at the substrate along the line XX' connecting the two injection apertures. **f** Concentration profile of the diffusive species at the substrate along the line YY' connecting the two aspiration apertures. **g** Calculated shear stress at the substrate surface. **h** Shear stress profile at the substrate along the line XX' connecting the two injection apertures. **i** Shear stress profile at the substrate along the line YY' connecting the two aspiration apertures. Mao et al. [120]. Copyright 2019. Reproduced with permission of Royal Society of Chemistry

the injection flow rate. We could adjust those elements conveniently to meet the further requirements in applications.

9.5.3 Cell Cutting Operation and Wound Repair

The structure of the Fluid CK (Fig. 9.17a, b). The flatness of the tip surface was characterized by a scanning electron microscope (SEM) (Fig. 9.17c). The zone of injected flow was confirmed using a fluorescein solution for visualization

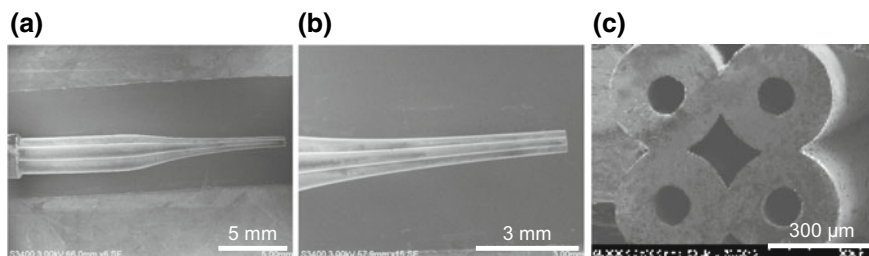


Fig. 9.17 SEM image of the Fluid CK. **a** SEM image of the Fluid CK. **b** SEM of the tip of the Fluid CK. **c** SEM image of the bottom surface of the tip. Mao et al. [120]. Copyright 2019. Reproduced with permission of Royal Society of Chemistry

(Fig. 9.18a). The boundaries were defined as 10% of the local maximum of fluorescent intensity. Fluctuation amplitude (A_y) of the boundaries at y -axis (point Q in Fig. 9.18a) was extremely large because of the flow fluctuations caused by the stepper motor in the pump and elasticity of the Fluid CK and connecting tube (Fig. 9.18b). In contrast, the flow fluctuation amplitude (A_x) at x -axis (point P) was extremely small because the symmetry of two injected solution offset the undesirable fluctuations (Fig. 9.18b), which suggested a stable interface. A_x showed excellent stability when the ratio was higher than 10 (Fig. 9.18b). Thus, the optimal ratio was selected as 10. A_x and A_y decreased with the increasing Ri when keeping a constant Ra/Ri . A_x was as small as $1 \mu\text{m}$ when Ri was $1 \mu\text{L min}^{-1}$. The resolution was suitable for subcellular analysis. The Fluid CK was capable to generate an extremely stable interface between two adjacent miscible solutions, reasoning from the symmetrical design.

A portion of a single cell was immersed in certain solution environment near the interface, so the molecule in this environmental solution would selectively treat the desired portion of the cell. In subcellular cutting operation, RIPA non-denatured tissue lysis buffer was injected into the upper right aperture, and cell culture medium was injected into the lower left aperture. The lysis buffer functioned for cutting portions of the cell, while the cell culture medium functioned for protecting other portions of the cell. The gap was $50 \mu\text{m}$. The injection and aspiration flow rates were 1 and $10 \mu\text{L/min}$, respectively. Laminar flows generated underneath the Fluid CK and a planar interface (the white dot line in Fig. 9.18e) existed. An adherent cultured U87 cell was positioned at the cell culture medium environment first and then moved toward and crossed the interface gradually. The portions of cell immersed in the lysis buffer environment were cut off rapidly (less than 20 s) (Fig. 9.18e). The lysis time is defined as the time from initially immersing a portion of cell in the lysis buffer zone (Fig. 9.18e, part i) to its entire cutting (Fig. 9.18e, part ii). The lysis time for individual U87 cells was various within the range from 10 to 20 s. Furthermore, four more types of adherent cells, including HUVEC, Caco-2, MCF-7, and HepG2 cells, were successfully cut from desired position. The results indicated that the Fluid CK were applicable to various types of adherent

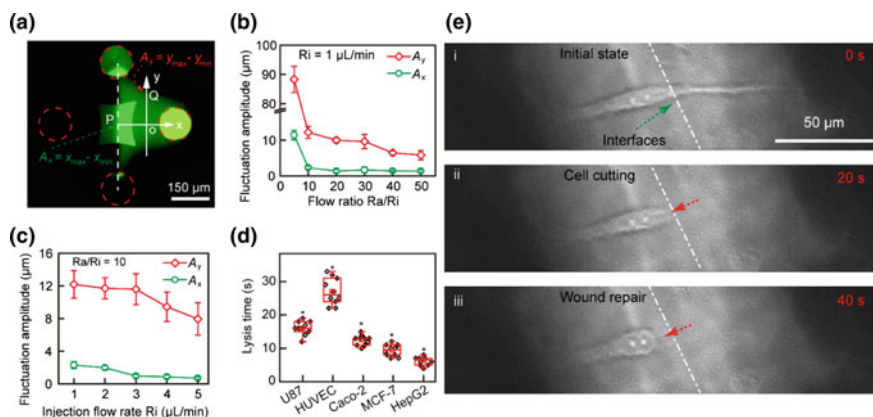


Fig. 9.18 Stability of the interface between two miscible solutions underneath the Fluid CK and cell cutting for wound repair studies. **a** Fluorescent image of the microjet underneath the Fluid CK in the experimental results. **b** Fluctuation amplitude at the point A on x -axis and point B on y -axis under different flow ratio Ra/Ri . The injection flow rate was constant ($1 \mu\text{L}/\text{min}$). **c** Fluctuation amplitude at the point A on x -axis and point B on y -axis under different injection flow rate Ri . The flow ratio Ra/Ri was constant (equal to 10). **d** The lysis time for different types of cells. Two-tailed Student's t -test was performed. $*P < 0.05$. **e** Single-cell cutting and wound repair processes, including (i) the initial state, (ii) the state of the target single-cell after precise cutting, and (iii) wound repair. Mao et al. [120]. Copyright 2019. Reproduced with permission of Royal Society of Chemistry

cells. The lysis time for any two different types of cells showed significant differences. In further research, mass spectrometric analysis and immunofluorescence analysis may be helpful to understand the differences.

At beginning, U87 cells were in adherent culture (Fig. 9.18e, part i). After the entire cutting (Fig. 9.18e, part ii), wound repair was observed (Fig. 9.18e, part iii). The incomplete plasma recovered by itself. Wound repair of cell plasma is a vital feature distinguishing living from non-living cells [126, 127]. Although microfluidic approaches have supplied important methods for wound repair studies of cell in suspension, they are usually not applicable to adherent cells [101, 127]. The method by Fluid CK in the section provides a new avenue for cell cutting and wound repair studies for adherent cells at single-cell resolution.

9.5.4 Subcellular Molecule Infusion and Organelle Transport Analysis

As the position of the interface was extremely stable, it was expected to perform well on subcellular molecule infusion. MitoTracker Green FM ($1 \mu\text{M}$) and MitoTracker Deep Red FM ($0.5 \mu\text{M}$) were prepared as the two injected solutions. A single U87 cell was positioned at the interface to carry out subcellular molecule

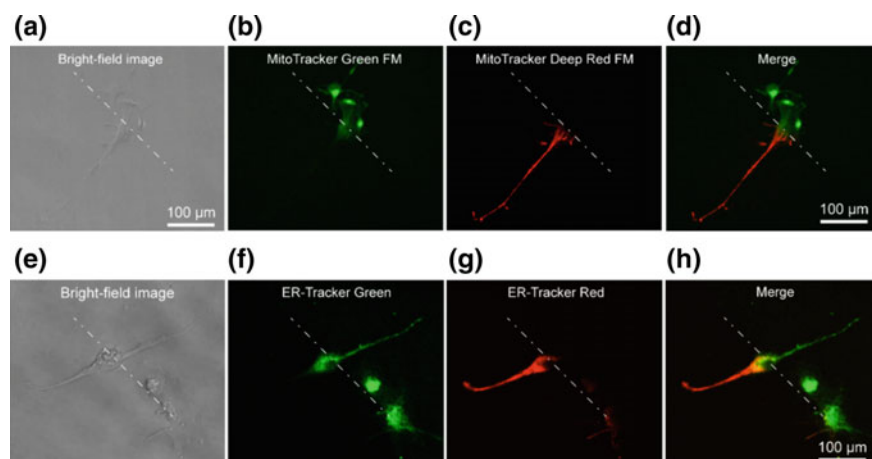


Fig. 9.19 Precise molecule infusion to portion of a cell for local staining of partial organelles. **a** Bright-field image of a U87 cell. **b** Fluorescent image of local staining of the mitochondria in the upper right portion of the cell by MitoTracker Green FM. **c** Fluorescent image of local staining of the mitochondria in the lower left portion of the cell by MitoTracker Deep Red FM. **d** Merged fluorescent image of the mitochondria in the cell co-stained by the MitoTracker Green FM and MitoTracker Deep Red FM. **e** Bright-field image of a U87 cell. **f** Fluorescent image of local staining of the ER in the upper right portion of the cell by ER-Tracker Green. **g** Fluorescent image of local staining of the ER in the lower left portion of the cell by ER-Tracker Red. **h** Merged fluorescent image of the ER in the cell co-stained by the ER-Tracker Green and ER-Tracker Red. Mao et al. [120]. Copyright 2019. Reproduced with permission of Royal Society of Chemistry

infusion (Fig. 9.19a). The upper right portion of the cell was stained with MitoTracker Green FM (Fig. 9.19b), while the other portion with MitoTracker Deep Red FM (Fig. 9.19c). After 3 min, the mitochondria in different portions were stained with different color. A clear planar interface was observed between the portion with green fluorescence and the other portion with red fluorescence in the merged fluorescent image the cell (Fig. 9.19d). In the same manner, ER-Tracker Green (1 μM) and ER-Tracker Red (1 μM) were used for partial staining of endoplasmic reticulum in a cell for 5 min (Fig. 9.19e–h). All the results demonstrated that the Fluid CK has excellent performances on subcellular molecule infusion.

The mitochondria were selected as a model of organelle. MitoTracker Deep Red FM (0.5 μM) and cell culture medium were the two injected solutions. The cell culture medium just functioned for protecting the portions of cell immersed in it. By adjusting the *XY* plate, the target U87 cell moved toward and then kept staying at the interface. After 3 min, the Fluid CK was moved always and the staining finished (Fig. 9.20a).

Because molecule adsorption on the device caused a big background that had remarkable influences on cell imaging, it would be difficult to record the cell from

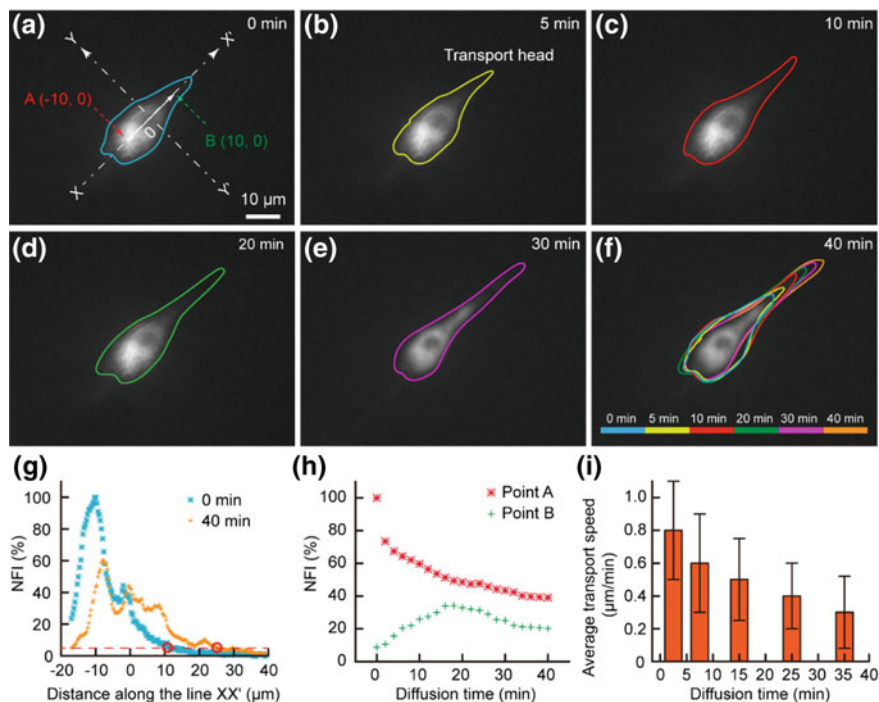


Fig. 9.20 Precise molecule infusion to portion of a cell for local staining of partial organelles. **a** Bright-field image of a U87 cell. **b** Fluorescent image of local staining of the mitochondria in the upper right portion of the cell by MitoTracker Green FM. **c** Fluorescent image of local staining of the mitochondria in the lower left portion of the cell by MitoTracker Deep Red FM. **d** Merged fluorescent image of the mitochondria in the cell co-stained by the MitoTracker Green FM and MitoTracker Deep Red FM. **e** Bright-field image of a U87 cell. **f** Fluorescent image of local staining of the ER in the upper right portion of the cell by ER-Tracker Green. **g** Fluorescent image of local staining of the ER in the lower left portion of the cell by ER-Tracker Red. **h** Merged fluorescent image of the ER in the cell co-stained by the ER-Tracker Green and ER-Tracker Red. **i** Measured transport speed at different time segments Mao et al. [120]. Copyright 2019. Reproduced with permission of Royal Society of Chemistry

the beginning. For convenience, the recording time for mitochondria transport was defined simply as Zero at the time of moving the device away (Fig. 9.20a). The outlines of the stained portion were set at the boundaries where the fluorescent intensity was high than three times of that at the background ($S/N = 3$). The fluorescent images across time with outlines of the stained mitochondria distribution zone are shown in Fig. 9.20a–f. Figure 9.20f shows a color overlay of those outlines, and significant transports of the stained mitochondria along line XX' was observed. The profiles of the normalized fluorescent intensity (NFI) at time of 0 min and time of 40 min appeared a significant spatial extension along line XX'

(Fig. 9.20g). The temporal changes of the fluorescent intensity at point A and point B were recorded (Fig. 9.20h). The NFI at point A decreased gradually, resulting from the transport of the stained mitochondria toward the upper right and the effect of fluorescent quenching. At the beginning, the NFI of point B increased gradually, and it decreased then under the effect of continuous fluorescent quenching and weakening transport of stained mitochondria to point B (Fig. 9.20h). The average transport speed (V) at different time segments was calculated by dividing the moving distance of the transport head (Fig. 9.20b) with the period time. The speed decreased gradually then because of the continuously decreasing labeled mitochondria at the transport head (Fig. 9.20i). All the results indicated that our method provided a new approach for subcellular studies and organelles behaviors analysis.

9.6 Concluding Remarks and Future Outlook

The LSCE presented in this chapter supplies a new avenue for operation of open microfluidics for single-cell analysis. Based on LSCE, a novel methodology was established for in situ live single-cell detachment that is capable of studying cell heterogeneity and clarifying the connections between cell adhesion strength and its viability at single-cell resolution. A new approach by LSCE was developed to understand the differences between individual isogenic cells. Cell adhesion strength was successfully related to its morphology and intracellular metabolites. This method was demonstrated to be a non-touch, flexible, and region-selective method for single-cell biology study, with particular relevance to situations where a few phenotypically distinct cells are of interest. Moreover, it was powerful for cell-matrix adhesion analysis and cell-cell adhesion analysis that were useful for biomaterials evaluation and drug influence analysis. Furthering, it could be a potential tool for single-cell extraction to combine with mass spectrometry, capillary electrophoresis, or liquid chromatography for single-cell analysis and tissue imaging. Furthermore, it is a potential tool for single-cell metabolism study in drug test and single-cell labeling in cell probe development.

As single-cell and subcellular analyses have become more and more important, advance in techniques development will greatly promote those researches. Wound repair is essential for cell viability. Signal transmission and mass transfer are very important in a cell for its behaviors. Techniques such as Fluid CK supply new approaches for chemical surgery on a living single cell. Cell wound repair and organelle transport were well studied by such method. Partial treatment using laminar flows in open space generated by the Fluid CK is an effective way to deliver small molecules to the selected domains inside a single mammalian cell. This technique opens up avenues for subcellular microenvironment controlling, precise cellular cutting, wound repair analysis, and subcellular molecule infusion.

References

1. Mao SF, Zhang J, Li HF, Lin JM (2013) Strategy for signaling molecule detection by using an integrated microfluidic device coupled with mass spectrometry to study cell-to-cell communication. *Anal Chem* 85(2):868–876. <https://doi.org/10.1021/ac303164b>
2. Green BJ, Safaei TS, Mephram A, Labib M, Mohamadi RM, Kelley SO (2016) Beyond the capture of circulating tumor cells: next-generation devices and materials. *Angew Chem Int Edit* 55(4):1252–1265. <https://doi.org/10.1002/anie.201505100>
3. Fukano Y, Tsuyama N, Mizuno H, Date S, Takano M, Masujima T (2012) Drug metabolite heterogeneity in cultured single cells profiled by pico-trapping direct mass spectrometry. *Nanomedicine* 7(9):1365–1374. <https://doi.org/10.2217/nnm.12.34>
4. Jiang Y, Zhao H, Lin YQ, Zhu NN, Ma YR, Mao LQ (2010) Colorimetric detection of glucose in rat brain using gold nanoparticles. *Angew Chem Int Ed* 49(28):4800–4804. <https://doi.org/10.1002/anie.201001057>
5. Gao PF, Gao MX, Zou HY, Li RS, Zhou J, Ma J, Wang Q, Liu F, Li N, Li YF, Huang CZ (2016) Plasmon-induced light concentration enhanced imaging visibility as observed by a composite-field microscopy imaging system. *Chem Sci* 7(8):5477–5483. <https://doi.org/10.1039/c6sc01055e>
6. Li CM, Zheng LL, Yang XX, Wan XY, Wu WB, Zhen SJ, Li YF, Luo LF, Huang CZ (2016) DNA-AuNP networks on cell membranes as a protective barrier to inhibit viral attachment, entry and budding. *Biomaterials* 77:216–226. <https://doi.org/10.1016/j.biomaterials.2015.11.008>
7. Qiao Y, An J, Ma L (2013) Single cell array based assay for in vitro genotoxicity study of nanomaterials. *Anal Chem* 85(8):4107–4112. <https://doi.org/10.1021/ac400242w>
8. Zare RN, Kim S (2010) Microfluidic platforms for single-cell analysis. *Annu Rev Biomed Eng* 12:187–201. <https://doi.org/10.1146/annurev-bioeng-070909-105238>
9. Gallina ME, Kim TJ, Shelor M, Vasquez J, Mongersun A, Kim M, Tang SKY, Abbyad P, Pratz G (2017) Toward a droplet-based single-cell radiometric assay. *Anal Chem* 89(12):6472–6481. <https://doi.org/10.1021/acs.analchem.7b00414>
10. Klein AM, Mazutis L, Akartuna I, Tallapragada N, Veres A, Li V, Peshkin L, Weitz DA, Kirschner MW (2015) Droplet barcoding for single-cell transcriptomics applied to embryonic stem cells. *Cell* 161(5):1187–1201. <https://doi.org/10.1016/j.cell.2015.04.044>
11. Mazutis L, Gilbert J, Ung WL, Weitz DA, Griffiths AD, Heyman JA (2013) Single-cell analysis and sorting using droplet-based microfluidics. *Nat Protoc* 8(5):870–891. <https://doi.org/10.1038/nprot.2013.046>
12. Ali A, Abouleila Y, Amer S, Furushima R, Emara S, Equis S, Cotte Y, Masujima T (2016) Quantitative live single-cell mass spectrometry with spatial evaluation by three-dimensional holographic and tomographic laser microscopy. *Anal Sci* 32(2):125–127. <https://doi.org/10.2116/analsci.32.125>
13. Mondal M, Liao R, Xiao L, Eno T, Guo J (2017) Highly multiplexed single-cell in situ protein analysis with cleavable fluorescent antibodies. *Angew Chem Int Ed* 56(10):2636–2639. <https://doi.org/10.1002/anie.201611641>
14. Xie H, Li YT, Lei YM, Liu YL, Xiao MM, Gao C, Pang DW, Huang WH, Zhang ZY, Zhang GJ (2016) Real-time monitoring of nitric oxide at single-cell level with porphyrin-functionalized graphene field-effect transistor biosensor. *Anal Chem* 88(22):11115–11122. <https://doi.org/10.1021/acs.analchem.6b03208>
15. Huang L, Chen Y, Weng LT, Leung M, Xing XX, Fan ZY, Wu HK (2016) Fast single-cell patterning for study of drug-induced phenotypic alterations of hela cells using time-of-flight secondary ion mass spectrometry. *Anal Chem* 88(24):12196–12203. <https://doi.org/10.1021/acs.analchem.6b03170>
16. Chen F, Lin L, Zhang J, He Z, Uchiyama K, Lin JM (2016) Single-cell analysis using drop-on-demand inkjet printing and probe electrospray ionization mass spectrometry. *Anal Chem* 88(8):4354–4360. <https://doi.org/10.1021/acs.analchem.5b04749>

17. Callaway E (2017) The trickiest family tree in biology. *Nature* 547(7661):20
18. Li J, Lei Y, Sun C-L, Zheng W, Jiang X, Zhang H-L (2015) Rationally designed peptide interface for potential modulated cell adhesion and migration. *Adv Mater Interfaces* 2 (15):1500335. <https://doi.org/10.1002/admi.201500335>
19. Edelman GM, Crossin KL (1991) Cell adhesion molecules: implications for a molecular histology. *Annu Rev Biochem* 60:155–190. <https://doi.org/10.1146/annurev.biochem.60.1.155>
20. Jie X, Yang H, Wang M, Zhang Y, Wei W, Xia Z (2017) A peroxisome-inspired chemiluminescent silica nanodevice for the intracellular detection of biomarkers and its application to insulin-sensitizer screening. *Angew Chem* 129(46):14788–14793. <https://doi.org/10.1002/ange.201708958>
21. Gumbiner BM (1996) Cell adhesion: the molecular basis of tissue architecture and morphogenesis. *Cell* 84(3):345–357. [https://doi.org/10.1016/s0092-8674\(00\)81279-9](https://doi.org/10.1016/s0092-8674(00)81279-9)
22. Yu H, Huang S, Chokhawala H, Sun M, Zheng H, Chen X (2006) Highly efficient chemoenzymatic synthesis of naturally occurring and non-natural α -2,6-linked sialosides: A *P. damsela* α -2,6-sialyltransferase with extremely flexible donor–substrate specificity. *Angew Chem Int Ed* 45(24):3938–3944. <https://doi.org/10.1002/anie.200600572>
23. Tan M, Yamaguchi S, Yamahira S, Nakamura M, Nagamune T (2017) Quantitative image cytometry for analyzing intracellular trafficking of G protein-coupled receptors on a chemical-trapping single cell array. *Lab Chip* 17(11):1933–1938. <https://doi.org/10.1039/c7lc00198c>
24. Howard RJ, Smith PM, Mitchell GF (1980) Characterization of surface-proteins and glycoproteins on red blood-cells from mice infected with haemosporidia—*Babesia-Rodhaini* infections of Balb-C mice. *Parasitology* 81(Oct):251–271. <https://doi.org/10.1017/s003118200005602x>
25. Ginis I, Faller DV (1994) Quantitative estimation of the degree of cell spreading on different surfaces and cell monolayers using a fluorescent plate scanner. *Anal Biochem* 219(2):288–296. <https://doi.org/10.1006/abio.1994.1268>
26. Nordstrom T, Knekt M, Nordstrom E, Lindqvist C (1999) A microplate-based fluorometric assay for monitoring human cancer cell attachment to cortical bone. *Anal Biochem* 267 (1):37–45. <https://doi.org/10.1006/abio.1998.2971>
27. Pagel M, Hassert R, John T, Braun K, Wiessler M, Abel B, Beck-Sickinge AG (2016) Multifunctional coating improves cell adhesion on titanium by using cooperatively acting peptides. *Angew Chem Int Ed* 55(15):4826–4830. <https://doi.org/10.1002/anie.201511781>
28. Loster K, Horstkorte R (2000) Enzymatic quantification of cell-matrix and cell-cell adhesion. *Micron* 31(1):41–53. [https://doi.org/10.1016/s0968-4328\(99\)00062-1](https://doi.org/10.1016/s0968-4328(99)00062-1)
29. Zhou W, Cao Y, Sui D, Lu C (2016) Radical pair-driven luminescence of quantum dots for specific detection of peroxynitrite in living cells. *Anal Chem* 88(5):2659–2665. <https://doi.org/10.1021/acs.analchem.5b03827>
30. Lan F, Demaree B, Ahmed N, Abate AR (2017) Single-cell genome sequencing at ultra-high-throughput with microfluidic droplet barcoding. *Nat Biotechnol* 35:640–646. <https://doi.org/10.1038/nbt.3880>
31. Zilionis R, Nainys J, Veres A, Savova V, Zemmour D, Klein AM, Mazutis L (2017) Single-cell barcoding and sequencing using droplet microfluidics. *Nat Protoc* 12(1):44–73. <https://doi.org/10.1038/nprot.2016.154>
32. Wu J, Chen Q, Liu W, He Z, Lin J-M (2017) Recent advances in microfluidic 3D cellular scaffolds for drug assays. *TrAC-Trends Anal Chem* 87:19–31. <https://doi.org/10.1016/j.trac.2016.11.009>
33. Wu J, Chen Q, Liu W, Lin J-M (2013) A simple and versatile microfluidic cell density gradient generator for quantum dot cytotoxicity assay. *Lab Chip* 13(10):1948–1954. <https://doi.org/10.1039/c3lc00041a>
34. Zhou W, Dong S, Lin Y, Lu C (2017) Insights into the role of nanostructure in the sensing properties of carbon nanodots for improved sensitivity to reactive oxygen species in living cells. *Chem Commun* 53(13):2122–2125. <https://doi.org/10.1039/c7cc00169j>

35. Li X, Valadez AV, Zuo P, Nie Z (2012) Microfluidic 3D cell culture: potential application for tissue-based bioassays. *Bioanalysis* 4(12):1509–1525. <https://doi.org/10.4155/bio.12.133>
36. Wei WL, Xu C, Gao N, Ren JS, Qu XG (2014) Opposing enantiomers of tartaric acid anchored on a surface generate different insulin assemblies and hence contrasting cellular responses. *Chem Sci* 5(11):4367–4374. <https://doi.org/10.1039/c4sc01386g>
37. Jie MS, Mao SF, Li HF, Lin JM (2017) Multi-channel microfluidic chip-mass spectrometry platform for cell analysis. *Chin Chem Lett* 28(8):1625–1630. <https://doi.org/10.1016/j.ccllet.2017.05.024>
38. Dou MW, Sanjay ST, Benhabib M, Xu F, Li XJ (2015) Low-cost bioanalysis on paper-based and its hybrid microfluidic platforms. *Talanta* 145:43–54. <https://doi.org/10.1016/j.talanta.2015.04.068>
39. Kurokawa YK, George SC (2016) Tissue engineering the cardiac microenvironment: multicellular microphysiological systems for drug screening. *Adv Drug Deliv Rev* 96:225–233. <https://doi.org/10.1016/j.addr.2015.07.004>
40. Qi H, Huang G, Han YL, Lin W, Li X, Wang S, Lu TJ, Xu F (2016) In vitro spatially organizing the differentiation in individual multicellular stem cell aggregates. *Crit Rev Biotechnol* 36(1):20–31. <https://doi.org/10.3109/07388551.2014.922917>
41. Xia M-C, Cai L, Zhang S, Zhang X (2017) Cell-penetrating peptide spirolactam derivative as a reversible fluorescent pH probe for live cell imaging. *Anal Chem* 89(2):1238–1243. <https://doi.org/10.1021/acs.analchem.6b03813>
42. Sarkar A, Kowitz S, Lauffenburger DA, Han J (2014) Microfluidic probe for single-cell analysis in adherent tissue culture. *Nat Commun* 5:3421–3429. <https://doi.org/10.1038/Ncomms4421>
43. Kadem LF, Suana KG, Holz M, Wang W, Westerhaus H, Herges R, Selhuber-Unkel C (2017) High-frequency mechanostimulation of cell adhesion. *Angew Chem Int Ed* 56(1):225–229. <https://doi.org/10.1002/anie.201609483>
44. Zhao S-P, Ma Y, Lou Q, Zhu H, Yang B, Fang Q (2017) Three-dimensional cell culture and drug testing in a microfluidic sidewall-attached droplet array. *Anal Chem* 89(19):10153–10157. <https://doi.org/10.1021/acs.analchem.7b02267>
45. Huh D, Hamilton GA, Ingber DE (2011) From 3D cell culture to organs-on-chips. *Trends Cell Biol* 21(12):745–754. <https://doi.org/10.1016/j.tcb.2011.09.005>
46. Si X, Xiong X, Zhang S, Fang X, Zhang X (2017) Detecting low-abundance molecules at single-cell level by repeated ion accumulation in ion trap mass spectrometer. *Anal Chem* 89(4):2275–2281. <https://doi.org/10.1021/acs.analchem.6b03390>
47. Fu X, Shang WJ, Wang SS, Liu YP, Qu JY, Chen X, Wang PG, Fang JQ (2017) A general strategy for the synthesis of homogeneous hyaluronan conjugates and their biological applications. *Chem Commun* 53(25):3555–3558. <https://doi.org/10.1039/c6cc09431g>
48. Verneti LA, Senutovitch N, Boltz R, DeBiasio R, Shun TY, Gough A, Taylor DL (2016) A human liver microphysiology platform for investigating physiology, drug safety, and disease models. *Exp Biol Med* 241(1):101–114. <https://doi.org/10.1177/1535370215592121>
49. Zhou W, Cao Y, Sui D, Lu C (2016) Turn-on luminescent probes for the real-time monitoring of endogenous hydroxyl radicals in living cells. *Angew Chem Int Ed* 55(13):4236–4241. <https://doi.org/10.1002/anie.201511868>
50. Brandenburg N, Lutolf MP (2016) In Situ patterning of microfluidic networks in 3d cell-laden hydrogels. *Adv Mater* 28(34):7450–7456. <https://doi.org/10.1002/adma.201601099>
51. Chen Q, Utech S, Chen D, Prodanovic R, Lin J-M, Weitz DA (2016) Controlled assembly of heterotypic cells in a core-shell scaffold: organ in a droplet. *Lab Chip* 16(8):1346–1349. <https://doi.org/10.1039/c6lc00231e>
52. Smith S, Grima R (2018) Single-cell variability in multicellular organisms. *Nat Commun* 9:345–352. <https://doi.org/10.1038/s41467-017-02710-x>
53. Wu J, Chen Q, Lin J-M (2017) Microfluidic technologies in cell isolation and analysis for biomedical applications. *Analyst* 142(3):421–441. <https://doi.org/10.1039/c6an01939k>

54. Mao SF, Zhang WL, Huang QS, Khan M, Li HF, Uchiyama K, Lin JM (2018) In situ scatheless cell detachment reveals correlation between adhesion strength and viability at single-cell resolution. *Angew Chem Int Ed* 57(1):236–240. <https://doi.org/10.1002/anie.201710273>
55. Li X, Ling V, Li PC (2008) Same-single-cell analysis for the study of drug efflux modulation of multidrug resistant cells using a microfluidic chip. *Anal Chem* 80(11):4095–4102. <https://doi.org/10.1021/ac800231k>
56. Li X, Li PCH (2005) Microfluidic selection and retention of a single cardiac myocyte, on-chip dye loading, cell contraction by chemical stimulation, and quantitative fluorescent analysis of intracellular calcium. *Anal Chem* 77(14):4315–4322. <https://doi.org/10.1021/ac048240a>
57. Liu P, Li X, Greenspoon SA, Scherer JR, Mathies RA (2011) Integrated DNA purification, PCR, sample cleanup, and capillary electrophoresis microchip for forensic human identification. *Lab Chip* 11(6):1041–1048. <https://doi.org/10.1039/c0lc00533a>
58. Lin L, Lin XX, Lin LY, Feng Q, Kitamori T, Lin JM, Sun JS (2017) Integrated microfluidic platform with multiple functions to probe tumor-endothelial cell interaction. *Anal Chem* 89(18):10037–10044. <https://doi.org/10.1021/acs.analchem.7b02593>
59. Kelly C, Flatt PR, McClenaghan NH (2010) Cell-to-cell communication and cellular environment alter the somatostatin status of delta cells. *Biochem Biophys Res Commun* 399(2):162–166. <https://doi.org/10.1016/j.bbrc.2010.07.036>
60. Qian R-C, Cao Y, Zhao L-J, Gu Z, Long Y-T (2017) A Two-stage dissociation system for multilayer imaging of cancer biomarker-synergic networks in single cells. *Angew Chem Int Ed* 56(17):4802–4805. <https://doi.org/10.1002/anie.201702415>
61. Tian H, Sun Y, Liu C, Duan X, Tang W, Li Z (2016) Precise quantitation of microrna in a single cell with droplet digital per based on ligation reaction. *Anal Chem* 88(23):11384–11389. <https://doi.org/10.1021/acs.analchem.6b01225>
62. Athanasiadis EI, Bothof JG, Andres H, Ferreira L, Lio P, Cvejic A (2017) Single-cell RNA-sequencing uncovers transcriptional states and fate decisions in haematopoiesis. *Nat Commun* 8:2045–2055. <https://doi.org/10.1038/s41467-017-02305-6>
63. Nagano T, Lubling Y, Vaarnai C, Dudley C, Leung W, Baran Y, Cohen NM, Wingett S, Fraser P, Tanay A (2017) Cell-cycle dynamics of chromosomal organization at single-cell resolution. *Nature* 547(7661):61–68. <https://doi.org/10.1038/nature23001>
64. Craig SEL, Brady-Kalnay SM (2011) Cancer cells cut homophilic cell adhesion molecules and run. *Cancer Res* 71(2):303–309. <https://doi.org/10.1158/0008-5472.can-10-2301>
65. Weis SM, Cheresh DA (2011) Tumor angiogenesis: molecular pathways and therapeutic targets. *Nat Med* 17(11):1359–1370. <https://doi.org/10.1038/nm.2537>
66. Malanchi I, Santamaria-Martinez A, Susanto E, Peng H, Lehr HA, Delaloye JF, Huelsken J (2012) Interactions between cancer stem cells and their niche govern metastatic colonization. *Nature* 481(7379):85–95. <https://doi.org/10.1038/nature10694>
67. Trappmann B, Gautrot JE, Connelly JT, Strange DGT, Li Y, Oyen ML, Stuart MAC, Boehm H, Li BJ, Vogel V, Spatz JP, Watt FM, Huck WTS (2012) Extracellular-matrix tethering regulates stem-cell fate. *Nat Mater* 11(8):742. <https://doi.org/10.1038/nmat3339>
68. Kang HJ, Cui Y, Yin H, Scheid A, Hendricks WPD, Schmidt J, Sekulic A, Kong D, Trent JM, Gokhale V, Mao H, Hurley LH (2016) A Pharmacological chaperone molecule induces cancer cell death by restoring tertiary DNA structures in mutant hTERT promoters. *J Am Chem Soc* 138(41):13673–13692. <https://doi.org/10.1021/jacs.6b07598>
69. Ding YY, Huang LZ, Xian XD, Yuhanna IS, Wasser CR, Frotscher M, Mineo C, Shaul PW, Herz J (2016) Loss of Reelin protects against atherosclerosis by reducing leukocyte-endothelial cell adhesion and lesion macrophage accumulation. *Sci Signal* 9(419):ra29. <https://doi.org/10.1126/scisignal.aad5578>
70. Umar S, Hedaya O, Singh AK, Ahmed S (2015) Thymoquinone inhibits TNF-alpha-induced inflammation and cell adhesion in rheumatoid arthritis synovial fibroblasts by ASK1 regulation. *Toxicol Appl Pharmacol* 287(3):299–305. <https://doi.org/10.1016/j.taap.2015.06.017>

71. Poudineh M, Labib M, Ahmed S, Nguyen LNM, Kermanshah L, Mohamadi RM, Sargent EH, Kelley SO (2017) Profiling functional and biochemical phenotypes of circulating tumor cells using a two-dimensional sorting device. *Angew Chem Int Ed* 56 (1):163–168. <https://doi.org/10.1002/anie.201608983>
72. Song Y, Tian T, Shi Y, Liu W, Zou Y, Khajvand T, Wang S, Zhu Z, Yang C (2017) Enrichment and single-cell analysis of circulating tumor cells. *Chem Sci* 8(3):1736–1751. <https://doi.org/10.1039/c6sc04671a>
73. Au SH, Storey BD, Moore JC, Tang Q, Chen Y-L, Javaid S, Sarioglu AF, Sullivan R, Madden MW, O’Keefe R, Haber DA, Maheswaran S, Langenau DM, Stott SL, Toner M (2016) Clusters of circulating tumor cells traverse capillary-sized vessels. *Proc Natl Acad Sci U S A* 113(18):4947–4952. <https://doi.org/10.1073/pnas.1524448113>
74. Wheeler AR, Thronset WR, Whelan RJ, Leach AM, Zare RN, Liao YH, Farrell K, Manger ID, Daridon A (2003) Microfluidic device for single-cell analysis. *Anal Chem* 75 (14):3581–3586. <https://doi.org/10.1021/ac0340758>
75. Labib M, Mohamadi RM, Poudineh M, Ahmed SU, Ivanov I, Huang CL, Moosavi M, Sargent EH, Kelley SO (2018) Single-cell mRNA cytometry via sequence-specific nanoparticle clustering and trapping. *Nat Chem* 10(5):489–495. <https://doi.org/10.1038/s41557-018-0025-8>
76. Jing T, Ramji R, Warkiani ME, Han J, Lim CT, Chen CH (2015) Jetting microfluidics with size-sorting capability for single-cell protease detection. *Biosens Bioelectron* 66:19–23. <https://doi.org/10.1016/j.bios.2014.11.001>
77. Khoo BL, Grecni G, Jing T, Lim YB, Lee SC, Thiery JP, Han J, Lim CT (2016) Liquid biopsy and therapeutic response: circulating tumor cell cultures for evaluation of anticancer treatment. *Sci Adv* 2(7):e1600274. <https://doi.org/10.1126/sciadv.1600274>
78. Zhu Z, Yang CJ (2017) Hydrogel droplet microfluidics for high-throughput single molecule/cell analysis. *Acc Chem Res* 50(1):22–31. <https://doi.org/10.1021/acs.accounts.6b00370>
79. Giladi A, Amit I (2017) Immunology, one cell at a time. *Nature* 547(7661):27. <https://doi.org/10.1038/547027a>
80. Christ KV, Turner KT (2010) Methods to measure the strength of cell adhesion to substrates. *J Adhes Sci Technol* 24(13–14):2027–2058. <https://doi.org/10.1163/016942410x507911>
81. Lykotrafitis G (2015) Human red blood cell adhesion to laminin measured by atomic force microscopy. *Biophys J* 108(2):167a. <https://doi.org/10.1016/j.bpj.2014.11.923>
82. Chen JY, Penn LS, Xi J (2018) Quartz crystal microbalance: Sensing cell-substrate adhesion and beyond. *Biosens Bioelectron* 99:593–602. <https://doi.org/10.1016/j.bios.2017.08.032>
83. Friedrichs J, Helenius J, Muller DJ (2010) Quantifying cellular adhesion to extracellular matrix components by single-cell force spectroscopy. *Nat Protoc* 5(7):1353–1361. <https://doi.org/10.1038/nprot.2010.89>
84. Hogan B, Babataheri A, Hwang YY, Barakat AI, Husson J (2015) Characterizing cell adhesion by using micropipette aspiration. *Biophys J* 109(2):209–219. <https://doi.org/10.1016/j.bpj.2015.06.015>
85. Lu J, Zhong X, Liu H, Hao L, Huang CT-L, Sherafat MA, Jones J, Ayala M, Li L, Zhang S-C (2016) Generation of serotonin neurons from human pluripotent stem cells. *Nat Biotechnol* 34(1):89–94. <https://doi.org/10.1038/nbt.3435>
86. Hao L, Johnson J, Lietz CB, Buchberger A, Frost D, Kao WJ, Li L (2017) Mass defect-based N,N-Dimethyl Leucine labels for quantitative proteomics and amine metabolomics of pancreatic cancer cells. *Anal Chem* 89(2):1138–1146. <https://doi.org/10.1021/acs.analchem.6b03482>
87. Li XT, Zhao SL, Hu HK, Liu YM (2016) A microchip electrophoresis-mass spectrometric platform with double cell lysis nano-electrodes for automated single cell analysis. *J Chromatogr A* 1451:156–163. <https://doi.org/10.1016/j.chroma.2016.05.015>
88. MacDonald MP, Spalding GC, Dholakia K (2003) Microfluidic sorting in an optical lattice. *Nature* 426(6965):421–424. <https://doi.org/10.1038/nature02144>
89. Kotlyar VV, Kovalev AA, Porfirev AP (2016) An optical tweezer in asymmetrical vortex Bessel-Gaussian beams. *J Appl Phys* 120(2). <https://doi.org/10.1063/1.4958309>

90. Ainla A, Jansson ET, Stepanyants N, Orwar O, Jesorka A (2010) A microfluidic pipette for single-cell pharmacology. *Anal Chem* 82(11):4529–4536. <https://doi.org/10.1021/ac100480f>
91. Juncker D, Schmid H, Delamarque E (2005) Multipurpose microfluidic probe. *Nat Mater* 4(8):622–628. <https://doi.org/10.1038/nmat1435>
92. Fu Y, Chen H, Liu L, Huang Y (2016) Single cell total RNA sequencing through isothermal amplification in picoliter-droplet emulsion. *Anal Chem* 88(22):10795–10799. <https://doi.org/10.1021/acs.analchem.6b02581>
93. Kaiser M, Jug F, Julou T, Deshpande S, Pfohl T, Silander OK, Myers G, van Nimwegen E (2018) Monitoring single-cell gene regulation under dynamically controllable conditions with integrated microfluidics and software. *Nat Commun* 9:212–227. <https://doi.org/10.1038/s41467-017-02505-0>
94. Fujii T, Matsuda S, Tejedor ML, Esaki T, Sakane I, Mizuno H, Tsuyama N, Masujima T (2015) Direct metabolomics for plant cells by live single-cell mass spectrometry. *Nat Protoc* 10(9):1445–1456. <https://doi.org/10.1038/nprot.2015.084>
95. Mizuno H, Tsuyama N, Harada T, Masujima T (2008) Live single-cell video-mass spectrometry for cellular and subcellular molecular detection and cell classification. *J Mass Spectrom* 43(12):1692–1700. <https://doi.org/10.1002/jms.1460>
96. Gong XY, Zhao YY, Cai SQ, Fu SJ, Yang CD, Zhang SC, Zhang XR (2014) Single cell analysis with probe ESI-mass spectrometry: detection of metabolites at cellular and subcellular levels. *Anal Chem* 86(8):3809–3816. <https://doi.org/10.1021/ac500882e>
97. Guillaume-Gentil O, Rey T, Kiefer P, Ibáñez AJ, Steinhoff R, Brönnimann R, Dorwling-Carter L, Zambelli T, Zenobi R, Vorholt JA (2017) Single-cell mass spectrometry of metabolites extracted from live cells by fluidic force microscopy. *Anal Chem* 89(9):5017–5023. <https://doi.org/10.1021/acs.analchem.7b00367>
98. Guillaume-gentil O, Grindberg RV, Kooger R, Dorwlingcarter L, Martínez V, Ossola D, Pilhofer M, Zambelli T, Vorholt JA (2016) Tunable single-cell extraction for molecular analyses. *Cell* 166(2):506–516. <https://doi.org/10.1016/j.cell.2016.06.025>
99. Tang SKY, Marshall WF (2017) Self-repairing cells: how single cells heal membrane ruptures and restore lost structures. *Science* 356(6342):1022–1025. <https://doi.org/10.1126/science.aam6496>
100. Moffitt RA, Marayati R, Flate EL, Volmar KE, Loeza SG, Hoadley KA, Rashid NU, Williams LA, Eaton SC, Chung AH, Smyla JK, Anderson JM, Kim HJ, Bentrem DJ, Talamonti MS, Iacobuzio-Donahue CA, Hollingsworth MA, Yeh JJ (2015) Virtual microdissection identifies distinct tumor- and stroma-specific subtypes of pancreatic ductal adenocarcinoma. *Nat Genet* 47(10):1168–1178. <https://doi.org/10.1038/ng.3398>
101. Takayama S, Ostuni E, LeDuc P, Naruse K, Ingber DE, Whitesides GM (2001) Subcellular positioning of small molecules. *Nature* 411(6841):1016. <https://doi.org/10.1038/35082637>
102. Atencia J, Beebe DJ (2005) Controlled microfluidic interfaces. *Nature* 437(7059):648–655. <https://doi.org/10.1038/nature04163>
103. Qasaimeh MA, Gervais T, Juncker D (2011) Microfluidic quadrupole and floating concentration gradient. *Nat Commun* 2:464–471. <https://doi.org/10.1038/ncomms1471>
104. Kaigala GV, Lovchik RD, Delamarque E (2012) Microfluidics in the “open space” for performing localized chemistry on biological interfaces. *Angew Chem Int Ed* 51(45):11224–11240. <https://doi.org/10.1002/anie.201201798>
105. Zhang Y, Mao S, Suzuki Y, Tanaka Y, Kawaguchi M, Zhang W, Zeng H, Nakajima H, Yang M, Uchiyama K (2018) Elaborately programmed nanowires fabricated using a tapered push-pull nozzle system. *Chem Commun* 54(7):719–722. <https://doi.org/10.1039/c7cc07873k>
106. Mao S, Sato C, Suzuki Y, Yang J, Zeng H, Nakajima H, Yang M, Lin J-M, Uchiyama K (2016) Microchemical pen: an open microreactor for region-selective surface modification. *ChemPhysChem* 17(20):3155–3159. <https://doi.org/10.1002/cphc.201600857>
107. Mao SF, Zhang Y, Li HF, Zeng HL, Lin JM, Uchiyama K (2017) Writing of nanowires via high viscosity-induced nano diffusive layer. *J Mater Chem C* 5(45):11666–11671. <https://doi.org/10.1039/c7tc03962j>

108. Doura T, Kamiya M, Obata F, Yamaguchi Y, Hiyama TY, Matsuda T, Fukamizu A, Noda M, Miura M, Urano Y (2016) Detection of lacZ-positive cells in living tissue with single-cell resolution. *Angew Chem Int Ed* 55(33):9620–9624. <https://doi.org/10.1002/anie.201603328>
109. Liu CS, Liu JJ, Gao D, Ding MY, Lin JM (2010) Fabrication of microwell arrays based on two-dimensional ordered polystyrene microspheres for high-throughput single-cell analysis. *Anal Chem* 82(22):9418–9424. <https://doi.org/10.1021/ac102094r>
110. Lombard-Banek C, Moody SA, Nemes P (2016) Single-cell mass spectrometry for discovery proteomics: quantifying translational cell heterogeneity in the 16-cell frog (*xenopus*) embryo. *Angew Chem Int Ed* 55(7):2454–2458. <https://doi.org/10.1002/anie.201510411>
111. Mao S, Zhang Q, Li H, Huang Q, Khan M, Uchiyama K, Lin J-M (2018) Measurement of cell–matrix adhesion at single-cell resolution for revealing the functions of biomaterials for adherent cell culture. *Anal Chem* 90(15):9637–9643. <https://doi.org/10.1021/acs.analchem.8b02653>
112. Lodish H, Berk A, Zipursky SL, Matsudaira P, Baltimore D, Darnell J (2004) *Molecular cell biology*, vol 22. W.H. Freeman and Company, New York
113. Zhang B, Montgomery M, Chamberlain MD, Ogawa S, Korolj A, Pahnke A, Wells LA, Masse S, Kim J, Reis L, Momen A, Nunes SS, Wheeler AR, Nanthakumar K, Keller G, Sefton MV, Radisic M (2016) Biodegradable scaffold with built-in vasculature for organ-on-a-chip engineering and direct surgical anastomosis. *Nat Mater* 15(6):669–678. <https://doi.org/10.1038/nmat4570>
114. Sunyer R, Jin AJ, Nossal R, Sackett DL (2012) Fabrication of hydrogels with steep stiffness gradients for studying cell mechanical response. *PLoS ONE* 7(10):e46107. <https://doi.org/10.1371/journal.pone.0046107>
115. Gao D, Li HF, Wang NJ, Lin JM (2012) Evaluation of the absorption of methotrexate on cells and its cytotoxicity assay by using an integrated microfluidic device coupled to a mass spectrometer. *Anal Chem* 84(21):9230–9237. <https://doi.org/10.1021/ac301966c>
116. Hong Y, Koh I, Park K, Kim P (2017) On-chip fabrication of a cell-derived extracellular matrix sheet. *ACS Biomater Sci Eng* 3(12):3546–3552. <https://doi.org/10.1021/acsbiomaterials.7b00613>
117. Mao S, Zhang Q, Li H, Zhang W, Huang Q, Khan M, Lin J-M (2018) Adhesion analysis of single circulating tumor cells on a base layer of endothelial cells using open microfluidics. *Chem Sci* 9(39):7694–7699. <https://doi.org/10.1039/C8SC03027H>
118. Anselme K (2000) Osteoblast adhesion on biomaterials. *Biomaterials* 21(7):667–681. [https://doi.org/10.1016/S0142-9612\(99\)00242-2](https://doi.org/10.1016/S0142-9612(99)00242-2)
119. Kanchanawong P, Shtengel G, Pasapera AM, Ramko EB, Davidson MW, Hess HF, Waterman CM (2010) Nanoscale architecture of integrin-based cell adhesions. *Nature* 468(7323):580–584. <https://doi.org/10.1038/nature09621>
120. Mao S, Zhang Q, Liu W, Huang Q, Khan M, Zhang W, Lin C, Uchiyama K, Lin J-M (2019) Chemical operations on a living single cell by open microfluidics for wound repair studies and organelle transport analysis. *Chem Sci* 10(7):2081–2087. <https://doi.org/10.1039/C8SC05104F>
121. Queval A, Ghattamaneni NR, Perrault CM, Gill R, Mirzaei M, McKinney RA, Juncker D (2010) Chamber and microfluidic probe for microperfusion of organotypic brain slices. *Lab Chip* 10(3):326–334. <https://doi.org/10.1039/B916669F>
122. Autebert J, Kashyap A, Lovchik RD, Delamarche E, Kaigala GV (2014) Hierarchical hydrodynamic flow confinement: efficient use and retrieval of chemicals for microscale chemistry on surfaces. *Langmuir* 30(12):3640–3645. <https://doi.org/10.1021/la500875m>
123. Feinerman O, Moses E (2003) A picoliter ‘fountain-pen’ using co-axial dual pipettes. *J Neurosci Methods* 127(1):75–84. [https://doi.org/10.1016/S0165-0270\(03\)00099-2](https://doi.org/10.1016/S0165-0270(03)00099-2)
124. Abadier M, Pramod AB, McArdle S, Marki A, Fan ZC, Gutierrez E, Groisman A, Ley K (2017) Effector and regulatory t cells roll at high shear stress by inducible tether and sling formation. *Cell Rep* 21(13):3885–3899. <https://doi.org/10.1016/j.celrep.2017.11.099>

125. He Z, Zhang W, Mao S, Li N, Li H, Lin J-M (2018) Shear stress-enhanced internalization of cell membrane proteins indicated by a hairpin-type DNA Probe. *Anal Chem* 90(9):5540–5545. <https://doi.org/10.1021/acs.analchem.8b00755>
126. Griffin DR, Weaver WM, Scumpia PO, Di Carlo D, Segura T (2015) Accelerated wound healing by injectable microporous gel scaffolds assembled from annealed building blocks. *Nat Mater* 14(7):737–744. <https://doi.org/10.1038/nmat4294>
127. Blauch LR, Gai Y, Khor JW, Sood P, Marshall WF, Tang SKY (2017) Microfluidic guillotine for single-cell wound repair studies. *Proc Natl Acad Sci U S A* 114(28):7283. <https://doi.org/10.1073/pnas.1705059114>

Index

A

- Acoustic waves
 - standing surface acoustic waves (SSAWs), 9, 11, 32, 33, 101, 104
 - surface acoustic waves (SAWs), 32, 45, 102, 171
 - travelling surface acoustic waves (TSAWs), 32, 33
- Acute myeloid leukemia, 155
- Adaptor, 150
- Algorithm, 41, 150, 151
- Allele, 147
- Alternating Current (AC), 31
- Aminopropyltriethoxysilane (APTES), 202, 203, 229, 230, 232
- Arg-Gly-Asp (RGD), 60, 66, 126
- Arrays, 4, 6, 7, 13, 16, 29, 30, 34, 36–40, 42, 58, 61, 64, 66, 68–71, 73, 87, 88, 98, 100, 104, 105, 144, 147, 149, 151, 166–169, 171, 177, 178, 185, 212, 213, 218
- Atomic Force Microscope (AFM), 213, 220, 229
- Attoliter (aL), 198, 203, 204, 209, 211
- Augmentation bias, 155
- Autosomal chromosomes, 150

B

- Biochemical microfluidic approaches
 - aptamer-based approaches, 28, 41
 - immunoaffinity, 39–41
- Bond number (Bo), 86
- Bulk standing waves, 11, 101, 103, 104

C

- Cancer Genome Atlas (CGA), 144
- Capillary Electrophoresis (CE), 5, 90, 174, 179
- Capillary number (Ca), 86, 87, 92, 122
- Capillary Zone Electrophoresis (CZE), 5
- Cell adhesion, 9, 20, 43, 64, 66, 72, 153, 168, 169, 182, 217–219, 224, 228, 229, 232, 233, 235, 238, 247
- Cell adhesion measurement
 - fluorescein labeling, 218
 - intracellular enzyme release assay, 218
 - isotope labeling, 218
 - protein staining, 218
- Cell Adhesion Molecules (CAMs), 221, 223, 229, 231, 233
- Cell adhesion strength, 7, 59, 221, 224–227, 233, 235, 247
- Cell aggregation, 34
- Cell-cycle dynamics, 219, 220
- Cell death, 56, 62, 127, 219
- Cell heterogeneity, 2, 3, 7, 42, 59, 77, 132, 135, 164, 182, 197, 220, 223, 224, 226, 227, 232, 247
- Cell lysis, 1, 8, 17–20, 106–110, 130, 154, 179, 240
- Cell manipulation
 - acoustic manipulation, 101, 103
 - electrical manipulation, 95, 96
 - magnetic manipulation, 100
 - mechanical manipulation, 104
 - microstructures manipulation, 95
 - optical manipulation, 12, 99, 101
- Cell-matrix adhesion, 42, 44, 59, 227–232, 247

- Cell sorting, 1, 6, 8–14, 20, 30, 34, 54–56, 60, 76, 99, 104, 171, 175
- Cell-suspension, 152
- Cell types
- A549 cells, 175
 - breast cells, 67
 - BT-474 cell line, 75
 - caco-2 cells, 178, 238
 - CaSki cells, 186
 - CD4 T-cells, 169
 - CD8 T-cells, 169
 - circulating tumor cells (CTCs), 35, 36, 95, 132, 135, 153, 219, 233, 234, 236, 239
 - endothelial cells (ECs), 4, 43, 44, 59, 156, 186, 219, 233–236, 238, 239
 - GH3 cells, 175
 - HeLa cells, 31, 61, 183
 - hematopoietic stem cell (HSC), 57, 62, 95
 - human hepatoma (HepG2), 59, 176, 179, 221, 224–227, 238, 239, 243
 - human umbilical vein endothelial cells (HUVECs), 156, 186, 233, 235–239, 243
 - lymphoblastic lymphoma T-cells, 73
 - mammalian cells, 5, 62, 90, 95, 97, 100, 127, 128, 154, 184, 247
 - mammalian neurons, 73
 - MCF-7 cells, 34, 243
 - MDA-MB-231 cells, 34
 - mesenchymal stem cells, 66
 - PC12 cells, 71, 74, 175
 - prostatic cells, 67
 - THP-1 cells, 34
 - thymocytes, 73
 - U87-MG cells (U87), 59, 220, 222–226, 230, 232, 235–239, 243–246
- Cellular population, 5, 143, 151, 153
- Chromosome, 143, 147, 151, 152, 156, 157
- Circulating Tumor Cells (CTCs), 37, 41, 43, 44, 59, 74, 101, 153, 169, 219, 233–235, 238, 239
- Clausius-Mossotti (CM), 97
- Coflow, 88
- Convection–diffusion equation, 222, 241
- Copy number, 147, 149–151
- Copy Number Variations (CNV), 150, 151
- Cross-flow, 88, 89
- D**
- Dean flow, 13, 14, 36, 71, 74, 135, 175, 176
- Deoxyribonucleic Acid (DNA), 7, 19, 42, 57, 64, 70, 72, 91, 107, 119, 129–132, 143–156, 167, 168, 203, 205, 239
- Dielectrophoresis (DEP), 9, 10, 16, 28, 30, 31, 45, 95–99, 110, 171
- Differential Interference Contrast Thermal Lens Microscope (DIC-TLM), 203–205, 210
- Digital Polymerase Chain Reaction (dPCR), 90, 148, 157
- Dimensionless number, 86
- Direct Current (DC), 31, 91, 92, 97
- Direct Deterministic Phasing (DDP), 151
- DNA nanostructure scaffold-supported aptamer pull-down (DNAPull), 42, 43
- Droplet-based microfluidics, 57, 110, 119, 120, 132, 135, 171
- Droplet generation, 17, 85–93, 121–123, 133, 179
- Dual capillary probe, 220
- E**
- Electroactive double-Well Array (EdWA), 30, 31
- Electrochemical detector, 146
- Electroosmotic Flow (EOF), 9, 10, 99
- Electrophoresis (EP), 9, 10, 96, 99, 145, 247
- Electrospray Ionization Mass Spectrometry (ESI-MS), 71, 74, 75, 91, 175
- Electrowetting-On-Dielectric (EWOD), 91
- Enzyme Linked Immunosorbent Assay (ELISA), 203, 210, 212, 213
- Epigenetic, 2, 27, 156
- ER-Tracker Green, 245, 246
- ER-Tracker Red, 245, 246
- Ethylenediaminetetraacetic (EDTA), 66, 67, 128, 149, 228, 233
- Extracellular Matrix (ECM), 42, 62, 70, 221, 223, 229, 231, 233
- F**
- Fast Atom Beam (FAB), 200
- Feret's diameter, 224, 225
- Fetal Bovine Serum (FBS), 230, 233
- Finite Element Analysis (FEA), 240–242
- Flow-focusing, 37, 67, 88, 89, 91, 93, 122, 128
- Flow Shear Stress (FSS), 231, 241
- Flow streamline, 223, 242
- Fluid Cell Knife (Fluid CK), 241
- Fluidic Force Microscopy (Fluid FM), 220
- Fluidigm C1, 153

Fluorescence Resonance Energy Transfer (FRET), 40, 70, 71

G

Gas Chromatography-Mass Spectrometry (GC-MS), 4

GC bias, 151

Genes, 2, 6, 69–71, 85, 108, 120, 129, 130, 143, 144, 150, 153, 155, 156, 183, 197

Genetic materials, 110, 144, 145, 147, 149, 151, 153–157

Genomics

amplification, 57, 147, 157

annealing, 147, 150

genotyping, 151, 154

haplotyping, 146

replication, 147, 151

whole-genome amplification (WGA), 57, 147–150, 152–157

Germline, 147

Glutathione (GSH), 185, 186, 225, 226

H

Hairpin (HP), 42

Hemagglutinin, 155

High-Performance Liquid Chromatography (HPLC), 4, 205

Human Aortic Endothelial Cell (HAEC), 207

Human Genome Project (HGP), 143, 144

I

ICELL8, 153

Inductively Coupled Plasma (ICP), 163, 173, 179, 180, 182, 200

Ink-jet, 90, 91, 123, 133–135, 148, 168, 172, 173, 177, 178, 185

Interdigital Transducers (IDTs), 9, 11, 32, 33, 102

Interferon (IFN γ), 42

Interleukin-8 (IL-8), 41

K

Kilopascal (kPa), 212

L

Laser-Induced Fluorescence (LIF), 5

Laser Tweezers Raman Spectroscopy (LTRS), 29, 71, 72

Live Single-Cell Extractor (LSCE), 42–44, 55, 56, 59, 109, 181, 182, 220–223, 225, 226, 228, 229, 231–233, 235, 247

Locus, 150, 151

Lysate, 14, 16, 17, 74, 107, 109, 143, 145, 154

M

Mass Spectrometer (MS), 4, 5, 14, 71, 74, 75, 90, 91, 163, 165, 166, 172–187, 211

Metalloproteinases (MMPs), 70

Metaphase, 152

Microliter (μ L), 6, 155, 172, 186, 198, 222, 228, 231, 232, 235, 236, 238, 241, 243, 244

Micromagnet Arrays (MMAs), 34

Micromolding In Capillaries (MIMIC), 66

Micro-Thin Layer Chromatography (mTLC), 4

Micro Total Analysis Systems (μ -TAS), 198

Microwell Displacement Amplification System (MIDAS), 154

Mitotracker Deep Red FM, 244–246

Mitotracker Green FM, 244–246

Multiple Annealing And Looping-Based Amplification Cycles (MALBAC), 147, 149, 150, 156, 157

Multiple Displacement Amplification (MDA), 34, 147–149, 153, 154, 157

N

Navier–Stoke equations, 222

Negative dielectrophoresis (nDEP), 10, 30, 60

Normalized Fluorescent Intensity (NFI), 225–227, 246, 247

O

Optical tweezers, 11, 12, 28–30, 44, 45, 72, 99, 100, 145, 220

Oxidized glutathione (GSSG), 225, 226

P

Pathogen, 155

Pearson Correlation Coefficient (PCC), 224–226

Perimeter, 224, 225

Physical microfluidic techniques

acoustic waves, 9, 28, 171

Dielectrophoresis (DEP), 30, 31

hydrodynamic traps, 36–38, 45, 61, 105, 169, 171

magnetic traps, 28, 34–36, 45

optical tweezers, 12, 28–30, 44, 45, 72, 99, 100, 145, 165, 220

optoelectronic tweezers, 29, 60

thermophoresis, 30

Picoliter (pL), 34, 39, 42, 43, 86, 90, 93, 120, 123, 127, 156, 164, 172, 198, 205, 206, 211

Pico Mol/L (pM), 198

Pneumatic microvalve arrays (P μ VAs), 37

- Poly(acrylamide) (PAA), 127
 Poly (acrylic acid) (PAA), 126, 127
 Poly (dimethylsiloxane) (PDMS), 58
 Poly(ethylene glycol) diacrylate (PEG-DA), 28, 67, 166
 Polyethylene Glycol (PEG), 64, 67, 68, 126, 127, 155, 166, 168, 203
 Polymerase, 129, 135, 147, 148, 155, 182
 Polymerase chain reaction (PCR), 19, 57, 91, 107–109, 120, 129–131, 135, 147–150, 154, 155, 157, 173, 183
 Polystyrene (PS), 6, 30, 36, 58, 65, 166
 Poly (vinyl alcohol) (PVA), 126, 127, 168
 Positive counting, 148
 Positive dielectrophoresis (pDEP), 10, 30
 Probe electrospray ionization mass spectrometry, 90, 172, 173
- Q**
 Quantum dot (QD), 36, 179
 Quartz crystal microbalance (QCM), 219
- R**
 Rayleigh-Plateau, 93
 Reactive Oxygen Species (ROS), 73, 186, 203
 Reads, 150
 Reverse-transcription PCR (RT-PCR), 130, 182, 183
 Reynolds number (Re), 87, 97
 Rolling Circle Amplification (RCA), 132, 135
- S**
 Scanning Electron Microscope (SEM), 71, 201, 213, 242, 243
 Sequencing errors, 151
 Single-cell analysis
 capillary electrophoresis (CE-ESI), 174, 178
 cyclic voltammetry (CV), 74
 dual capillary probe, 220
 electrochemical analysis, 73, 76
 electrospray ionization(ESI), 71, 74, 84, 163, 165, 172–175, 180, 181, 186
 electrospray/nano-electrospray ionization (ESI/Nano-ESI), 74
 fluorescence, 165, 173, 211
 fluorescence in situ hybridization (FISH), 71
 fluorescence resonance energy transfer (FRET), 71
 fluorescent super-resolution microscopy (SRM), 71, 72
 interferometric scattering microscopy (iSCAT), 71, 72
 label-free optical methods, 70, 72
 laser ablation/laser desorption ionization (LA/LDI), 173
 laser tweezers raman spectroscopy (LTRS), 60, 71, 72
 mass cytometry, 182
 mass spectrometric analysis, 74, 76, 178, 217
 matrix-assisted laser desorption/ionization MS (MALDI-MS), 71, 75, 165, 177
 microfluidic chip, 10, 11, 34, 109, 110, 120, 166, 175, 177, 186
 microfluidic probe, 220
 optical characterization, 69, 70, 76
 optical tweezers, 165
 paper spray ionization MS (PSI-MS), 180
 scanning electrochemical microscopy (SECM), 74
 secondary ionization mass spectrometry (SIMS), 74, 165, 178, 180
 surface-assisted laser desorption ionization MS (SALDI-MS), 178
 surface plasmon resonance imaging (SPRi), 71, 72
 time of flight secondary ion mass spectrometry (TOF-SIMS), 75, 178
 vertical nanowire electrode array (VNEA), 71, 73
- Single-cell capture
 biochemical microfluidic approaches, 39
 dielectrophoresis (DEP), 59, 60
 droplet, 55, 57, 58
 electrical trap, 55, 56, 59
 electrophoresis (EP), 59
 flow cytometric methods, 164
 fluorescence activated cell sorting (FACS), 54–57
 hydrodynamic trap, 55, 58, 59
 laser capture microdissection (LCM), 54–56
 laser tweezers Raman spectroscopy (LTRS), 60
 live single-cell extractor (LSCE), 55, 56, 59
 micro-manipulation, 54–56
 microwell, 55, 58
 optical trap, 55, 56, 60
 physical microfluidic techniques, 31, 36, 38, 39
 Raman-activated cell sorting (RACS), 60
- Single cell culture
 2D single-cell culture, 60, 61, 66
 3D single-cell culture, 60, 66–69
 cell proliferation, 66, 68
 chemically micropatterned surface, 65

- closed microfluidic systems, 61, 62
 - microcollagen gel array (μ CGA), 68, 69
 - microgel, 66–68
 - open microfluidic systems, 61, 63–65
 - Single-cell encapsulation, 120, 124, 135
 - Single cell encapsulation, 66, 85, 93, 94
 - Single-cell isolation, 166
 - Single cell lysis, 69, 86, 106–109
 - Single cell manipulation, 85, 95, 97, 100, 104, 105, 110, 163, 187
 - Single-Cell-Master-Mix, 148
 - Single-cell probes, 217
 - Single Copy Genetic Amplification (SSGA), 154
 - Single-molecule, 29, 145, 182, 203, 210
 - Single Nucleotide Polymorphism (SNP), 147, 151, 152
 - Single strands of DNA (ssDNA), 147
 - Standing Surface Acoustic Waves (SSAW), 11, 33, 102
 - Stem cell, 2, 54, 57, 60, 62, 66, 95, 110, 127, 129, 182
 - Superparamagnetic (SPM), 34
 - Surface-Enhanced Raman Spectroscopy (SERS), 41
- T**
- Temozolomide (TMZ), 239
 - Thermal Lens Microscope (TLM), 204, 205, 210
 - Traveling waves, 11, 12, 101, 104
 - Trypsin, 42, 59, 182, 221–224, 228–233, 235–238
 - Tumor metastasis, 219, 220, 233, 234, 239
- U**
- Ultravioletray (UV), 40, 68, 70, 126, 169, 200, 201
- V**
- Vacuum Ultraviolet (VUV), 202, 203, 210
- W**
- Weber number, 86
 - Wound repair, 37, 220, 242, 244, 247
- Z**
- Zygote, 156